HUMERAL TORSION AND ACTIVITY-RELATED CHANGE IN THE HUMAN UPPER LIMB AND PECTORAL GIRDLE

A Biomechanical Investigation and Social Implications

Jill Anne RHODES BSc (Hons), MSc

Submitted for the degree of
Doctor of Philosophy

Department of Archaeological Sciences

University of Bradford

2004

ABSTRACT

This project investigates humeral torsion and activity-related change in the human upper limb. Increased humeral torsion angles have been identified in the professional throwing athlete and may be associated with strenuous activity. The nature of humeral torsion as an osteogenic response to the strain environment is investigated to identify its role in the behavioural morphology of the upper limb. These physical manifestations of strenuous physical activity provide an insight into the make-up of medieval armies prior to the establishment of standing armies.

Populations analysed include two blade-injured samples, Towton and a sub-sample of blade-injured men from the Priory of St. Andrew, Fishergate, York. The men from the *Mary Rose,* a Tudor warship are also investigated. Other samples analysed include the rural sites of Wharram Percy and Hickleton, the urban cemeteries from the Priory of St. Andrew, Fishergate, York and the *leprosarium* of Sts. James and Mary Magdalene, Chichester, the modern cadaver-based Terry collection and non-human-primates, *Gorilla sp., Pan sp., Pongo sp.,* and *Macaca sp.*. Measurement of the humeral torsion angle and external measurements and indices of architecture, articulations and robusticity are employed. Cross-sectional geometric properties are investigated using CT imaging of the paired humeri from a sub-sample of blade-injured individuals and a comparative sample of those who were not. Bilateral asymmetry is investigated to identify the role of plasticity within the humerus and to reveal aspects of limb dominance. The results are compared with non-human primate species to obtain insight into inter-species differences.

Results indicate the humeral torsion is not ontogenetically constrained, but is highly variable between and within populations, individuals and even between sides. Biomechanical analyses indicate that in the Towton population, humeral torsion may serve as part of a two-stage adaptation, in which the architecture is modified to enable greater biomechanical efficiency in distributing strain, reducing the need of increased cortical thickness. Changes in humeral torsion related to strenuous activity have been identified, although in the blade-injured samples it is decreased torsion angles, while in the comparative sample it is increased torsion angles that significantly correlate with limb hypertrophy. Humeral torsion appears to be influenced by other measurements of humeral architecture, specifically, the amount of anterior bowing and anterior curvature to the distal humeral shaft.

This work demonstrates the need for individual rather than population-based analyses, as the heterogeneity within population samples obscures individual variation in activity patterns. This analysis provides baseline data for typical populations of the Middle Ages. From this, it is then possible to investigate the individual within this baseline, to identify those who stand out from their samples through habitual, strenuous activity patterns. Movement patterns identified related to warfare include those consistent with the use of the longbow in the Towton sample and the use of a sword in the Fishergate blade-injured sample. These men, and those of the *Mary Rose*, appear to have either been selected for combat based on size, or benefited from a more nutritious diet during growth.

Key Words: Humerus, behavioural morphology, humeral torsion, activity-related change, biomechanical analysis, robusticity, Towton, Fishergate, Mary Rose

TABLE OF CONTENTS

LIST OF FIGURES

LIST OF TABLES

LIST OF ABBREVIATIONS

ANTCV: Anterior curvature, a measurement of humeral architecture

ARTEPI: Articular / epicondylar index, an index of articular size

BMC: Bone mineral content

BMD: Bone mineral density

BMU: Basic multicellular units

CA: Cortical area

CAPIT: Capitular index, an index of articular size

CH: Chichester

DAB: Distal articular breadth, a measure of articular size

DELT: Deltoid index characterizing the robusticity of the humeral deltoid tuberosity, an index of humeral robusticity

DIAPFLAT: Diaphyseal flattening, an index of humeral architecture

DISH: Diffuse idiopathic skeletal hyperostosis

EPIC: Epicondylar index of the humerus, an index of humeral robusticity

FG: Fishergate

FG BI: Fishergate blade-injured

HC: Minimum humeral circumference

HDBW: Distal bowing of the humeral diaphysis, a measurement of humeral architecture

HEAD: Humeral head index, a measurement of articular size

HEB: Epicondylar breadth of the humerus

HGBDST: Greatest breadth at the deltoid tuberosity (standardized by maximum humeral length), a measurement of humeral robusticity

HGT(ST): Greater tuberosity breadth of the humerus (standardized by maximum humeral length), a measurement of humeral robusticity

HK: Hickleton

HL: Maximum humeral length, a measurement of humeral robusticity

HML: Medio-lateral bowing of the humeral diaphysis, a measurement of humeral architecture

HPBW: Proximal bowing of the humeral diaphysis, a measurement of humeral architecture

HROB: Humeral robusticity index

HTBST: Trochlear breadth (standardised by humeral articular length), a measurement of articular size

Imax: Maximum second moment of area perpendicular to the neutral axis

Imin: Minimum second moment of area perpendicular to the neutral axis

Ix/Iy: The second moment of area measured parallel to the x axis divided by the second moment of area measured parallel to the y axis

J: A measure of diaphyseal robusticity calculated as Ix + Iy

MCL: Medial collateral ligament

MDSHFT: Midshaft index, a measurement of humeral robusticity

MES: Minimum effective strain

MGL: Middle glenohumeral ligament

MR: Mary Rose

MXCB: Maximum cubital angle, a measurement of humeral architecture

PCA: Percent cortical area

SGL: Superior glenohumeral ligament

SMA: Second moment of area

T: Towton

TA: Total area

TR: Terry collection

WP: Wharram Percy

ACKNOWLEDGEMENTS

I would like to offer my sincerest thanks to a number of people who have helped and supported me during this endeavor. First and foremost, I have to thank my husband, Brian, who has tolerated my absence on research visits, listened to my problems, offered advice and never complained, or at least not much! Without his support, I am certain I would not have succeeded. I would also like to thank my daughter, Jessie, for sitting relatively quietly in a baby swing for the first 4 months of her life and not complaining too much while her mother finished writing. I also want to thank my parents, Gene and Kathy Breitenstein, without their encouragement and support I would not have reached this stage.

Christopher Knüsel has served as my supervisor throughout this project and has been extremely helpful, giving generously of his time. Without his sage advice and guidance, this project would not have reached fruition. Special thanks also go to the Arts and Humanities Research Board (AHRB) who funded this project. Additional financial support has come from the Francis Raymond Hudson Fund and the Andy Jagger Fund, both operated by the University of Bradford. I would also like to thank my academic committee, Mike Richards.

I would like to thank all the people who have assisted me in the data collection phase, Darlene Weston at the Biological Anthropology Research Centre, University of Bradford; Christine McDonnell, Annie Jowett and Bev Shaw at the Archaeological Resource Centre, York Archaeological Trust, for providing access to the Fishergate collection; Andrew Elkerton for providing access to the Mary Rose skeletal remains; the Mammal curation group, Zoology department, Natural History Museum, London for providing access to the non-human primate material; Simon Mays, English Heritage for

providing access to the Wharram Percy skeletal assemblage; and, finally, David Hunt of the National Museum of Natural History, Smithsonian Institution, Washington DC for providing access to the Terry collection.

I have benefited along the way from advice, discussions and the odd computer program (NIH program for analysing biomechanical properties) from Holger Schutkowski, University of Bradford; Gabrielle Macho, University of Liverpool; Chris Ruff at Johns Hopkins University; and Richard Lazenby, University of Northern British Columbia. Statistics advice has come from Dave Jerwood, University of Bradford.

CHAPTER ONE

INTRODUCTION

Repetitive movement of the upper limb during growth and development leads to soft tissue and skeletal adaptation (Lieberman, 1996; Lanyon, 1987; Jones *et al.,* 1977, King *et al.,* 1969). These adaptations take the form of element robusticity, intracortical remodelling and changes in bone architecture. Variations in humeral torsion, one aspect of bone architecture, have previously been identified clinically in professional handball players (Pieper, 1998), as well as archaeologically, in a group of robust, blade-injured individuals from the Battle of Towton (1461 AD) (Knüsel, 2000a; Rhodes, 2002). This project investigates humeral torsion as a measure of shape and its potential as an osteogenic response to mechanical loading, as well as to identify its role in the behavioural morphology of the upper limb. This is conducted through analysis of external measurements characterising humeral morphology, its architecture, articular size, as well as its robusticity. Biomechanical analysis of the internal cross-sectional geometric properties is conducted on a sub-sample of blade-injured individuals from the Towton site, a mass grave from the Battle of Towton (1461 AD) dating to the Wars of the Roses (1455 – 1487 AD), and a medieval group of males from the church and priory of St. Andrew, Fishergate, York. These two blade-injured samples are evaluated against a comparative sample of non blade-injured individuals also from the Fishergate site.

The humerus is the ideal skeletal element for identifying activity pattern differences. The proximal ball and socket joint means this is the most mobile limb, capable of extended abduction, adduction, extension, flexion and medial and lateral rotation. The upper limb is used exclusively for voluntary actions, unlike the femur, so any pattern differences between populations will not be obscured by an underlying

locomotor function. Thus humeral morphological alterations may be seen to more often reflect differences in habitual behaviour.

By integrating the biological data with what is known about the social conditions, this study aims to identify differences in the humeral torsion angle and other activity-related variables in medieval populations that relate to differences in inferred lifestyles.

1.1 Historical Background

Historically, much is known about medieval society. This enables interpretations of activity differences through a well-developed contextual and socio-economic knowledge of the population samples. Sharp distinctions were made between the orders, or estates, of people in the Middle Ages. The Middle Ages saw the rise of three orders, those who prayed, the clergy; those who fought (the secular aristocrats) and, finally, those commoners who worked. Parts of the clergy were made up of individuals from aristocratic families, but sharp distinctions were made between the clergy and the warriors, as the clergy were responsible for spiritual functions. However, the early lives of such individuals may have been more similar with regard to physical activity, as they will both have been trained in weaponry and hunting. Financial support of the clergy was derived from benefices, landed estates or the provision of fixed capital assets. The aristocracy had the responsibility for providing administrative and military services. This landed class and the lesser nobles (gentry) made up a high proportion of royal armies, even after a formal obligation of knight service lapsed in the thirteenth and fourteenth centuries. By the end of the Middle Ages, the clergy and gentry were very similar in their standard of living and lifestyle. However, not all clergy were from the aristocracy and not all benefices provided comfortable incomes. Additionally, skilled

wage-earners would have been part of the ecclesiastical community, providing clerical services (Dyer, 1989).

The third order, or estate, comprised the largest proportion of medieval society and was made up of rural and urban labourers who provided the support for the other two estates. The term 'peasant' may be applied to the rural workers, small-scale cultivators, who were able to produce crops using their own manual labour to provide for their households. Permanent full-time wage earning was not common, and all peasants were involved in agricultural practices. By the High Middle Ages, the townsman, or urban labourer, made up about 15% of this order. The larger towns such as York would have had an upper rank of mercantile elite, as well as individuals who derived their incomes from holding office, legal practice or property rents. Below the merchants in the social order were the master craftsmen, their journeymen, unskilled labourers and servants (Dyer, 1989).

These social differences are reflected in the spatial patterning of burials dating to the Later Middle Ages. Burial location was a matter of honour, prestige and money. The church gained honour and nobility from high status burials, as did the individual gain status from his burial location. The most sought after, and hence, most expensive burial location was the area nearest to the high altar, in the chancel. This was followed by the rest of the chancel and the nave. The chapter house was the burial place of the abbots or members of the laity accorded special devotion. The east end of the churchyard was generally the burial location of the monks and canons, such as at St. Andrew's, Fishergate. Those individuals with little money, and therefore little influence, were buried outside in the churchyard (Daniell, 1998).

This study examines a broad range of human skeletal remains from a number of medieval sites, from a battle-related mass grave (Towton), to the remains from a sunken Tudor warship (The *Mary Rose*). The skeletal remains from cemeteries related to an urban priory (Fishergate, York), two rural villages (Wharram Percy and Hickleton, both in Yorkshire) and a *leprosarium* and later almshouse (Chichester, West Sussex) are also examined. A modern, cadaver-based sample (The Terry collection) and a group of non-human primates form comparative samples. The Towton sample is a group of battlefield casualties found in a mass grave and associated with the Wars of the Roses Battle of Towton (1461 AD). This conflict, which began in 1455 and lasted until 1487 AD, is well documented. The battle at Towton took place on Palm Sunday, in the midst of a spring snow storm. Historic documents of the period indicate a possible number of up to 50,000 combatants, with around 20,000 to 28,000 casualties recorded in contemporary documents (Boardman, 2000).

Armies such as those that took part at Towton were formed through a Commission of Array. In 1285, the Statute of Winchester called for all able-bodied men between sixteen and sixty years of age to serve for forty days a year. Commissioners, generally knights, travelled through towns and shires to muster men and inspect their readiness. In times of war, commissioners and noblemen received orders from the King to provide troops. These bodies of armed men would be formed partially through the use of livery soldiers. These men were 'retained' by the noble, acting as his bodyguard and supporting him as he fulfilled his duties. While being trained in arms, they would serve as pages, yeomen or grooms. On the battlefield, though, these men would form only a small percentage. Mercenaries and foreign allies provided additional ranks, but the majority of men would have been conscripted through the Commission of Array (Boardman, 1998). By the time of the Battle of Towton, the government had the ability

to muster increasingly substantial troop numbers and to maintain a number of them on a permanent basis, indicating the emergence of the professional soldier (Keen, 1999).

Typical weapons used on the battlefield may be indicated from the Bridport Muster Roll, a contemporary document from the Wars of the Roses (1457 AD). The Bridport Muster Roll is an itemisation of the men reporting for duty and the weapons they carried. Longbows were carried by 114 of the 201 men listed, while swords were the second most common weapon listed. The sword was traditionally the symbol of knighthood, and their weapons were long and slender, as opposed to the swords used by the foot soldiers, which were shorter. Daggers were carried by 64 of the men listed on the muster roll. Staff weapons included a lance, which was a spear around 10 feet long. A bill, originally an agricultural tool, had a long hooked blade on a six foot long shaft. It often had a stabbing spike at the end. This weapon is considered typical of the English infantryman. The glaive was a long, broad knife-like blade also attached to a long staff. The poleaxe, also on a long staff, had a blade, spike and hammer on each face. This was the preferred staff weapon of the noble class (Waller, 2000b), although it was used by the foot soldier as well. Axes and spears were also listed, as well as maces. These were used by the knight if his sword was broken in combat (Rimer, 2000).

The Mary Rose sample is comprised of the men who went down with King Henry VIII's flagship during a skirmish with the French in Portsmouth harbour in 1545 AD. The same muster laws applied to these men as with the men from the Wars of the Roses and according to records, 200 sailors, 185 soldiers and 30 gunners would have been on board. Due to a shortage of mariners at the time, a number of men would have been recruited through the use of impressments whereby men were forced to serve. A large number of longbows found at the wreck indicate the presence of archers on board

the ship, although they are not specifically detailed in the surviving records, referred to as the Anthony Roll (Stirland, 2000).

The Fishergate sample originates from an urban context, the city of York. In 1066, York would have had a population of 10,000, although this would decrease later in the Middle Ages (Dyer, 2002). The 1334 tax assessment indicates that York was the third wealthiest town in England, behind only London and Bristol. The prominent industry in the fourteenth century involved cloth-making. Weavers, fullers, dyers and others engaged in this industry were prominent in York at this time. The intramural cemetery area at Fishergate would have been reserved for the high status townspeople, either gentry who maintained town homes or merchants, while the demography of the southern cemetery at the site would largely include the lower orders, some craftsmen, workers and servants. Urban craftsmen were responsible for manufacturing, training apprentices and employing workers. Workers included both males and females engaged in retail trade. Women would have been involved in brewing and weaving, while those of the lower classes would have worked as spinsters, hucksters or second-hand clothiers. The lowest class would have worked as servants, or have resorted to begging or prostitution (Waugh, 1991).

Life inside a typical Gilbertine priory for the canons would have involved worship and reading. They were responsible for the administration of the property and would not have worked with the lay brethren, except possibly during haymaking and harvest times, when all hands were needed. Servants would be kept, although the lay brethren preformed most of the hard work while being instructed in the matters of religion (Graham, 1901). Entry to the priory would include some type of entry grant in the form of land or animals. St. Andrew's priory at York was founded by a royal clerk

and justice, Hugh Murdac, and this original foundation included an existing church and its adjoining lands, as well as rents paid on properties in York and the surrounding region (Golding, 1995).

The earlier burials from the rural villages of Wharram Percy and Hickleton date to the origins of the medieval nucleated village. In England, villages were largely formed in the eleventh century as the density of farms increased, established around a nucleus of the lord's house, the church and serf and peasant cottages. Each household had its own plot of land to harvest according to common law. A portion of the fields were left fallow every year to rejuvenate the soil. Livestock were grazed on these fields while the remaining plots were cultivated. Additionally, peasants were also expected to provide the labour on the lord's manor, the number of days worked owed were calculated according to the size of the peasant's holding (Dyer, 2002). The harvest itself was labour intensive and included both men and women. All crops were harvested at the same time, at the end of the summer, leaving the fields available for pasturing animals. Barley and oats were harvested with a scythe, while wheat was harvested with a sickle (Keen, 1990). Apart from the harvest, labour was divided by sex with typical male tasks including ploughing, carting and land clearance. Men also performed specialised crafts such as carpentry, masonry, thatching and smithing. The women would have been responsible for sewing and spinning flax, but would also have worked in the fields, planting and weeding and assisting in the harvest. They would also tend to the family croft, a garden close to the family home. Supplemental income would be generated through dairying, spinning or brewing (Waugh, 1991). While most villagers were involved in cultivation, there were also a number of specialist craftsmen. These would have included millers, bakers, smiths, carpenters and tailors (Keen, 1990).

The peasantry were not an economically homogenous class. A survey dated to the late thirteenth century found that only half of this population held seven to ten acres or less. Only a small number of families from each village would have held more than thirty acres. In the English Midlands, it has been estimated that a holding of ten acres would be required for a bare subsistence. Those who could not support themselves through their land holdings were forced to do extra wage earning work, such as brewing, wood-cutting, collecting underbrush or peat or hunting, among other things (Waugh, 1991). The plague (1348 – 1350 AD) brought labour shortages, as an estimated half of the English population died. There was less demand for land and a downturn in tillage. Land was now rented out by the lords, replacing the old manorial system involving bond tenants (Keen, 1990).

Social welfare was one of the responsibilities of the clerical order. Thus hospitals for the sick and almshouses for the poor were often ecclesiastical foundations. In addition to caring for the sick, hospitals in the fourteenth and fifteenth centuries also catered for pilgrims and travellers (Waugh, 1990). The leper hospital of St. James and St. Mary Magdalene, Chichester, was one such establishment. The earliest leper hospitals originate from the twelfth century, although their original purpose was not necessarily to isolate the sick and curb the spread of the contagion, but rather to offer prayers for its founder and benefactors. In many medieval *leprosaria*, it was common to gain admittance through payment, with some healthy, wealthy people admitted to what would have served as a form of sheltered accommodation. Administrative records from the hospital do not survive, although it is referred to in other documents, including listings of the inmates and their ailments (Magilton and Lee, 1989).

The Terry collection, a modern skeletal sample, does not have detailed historical records, however, there are morgue records detailing known age, sex, ethnic origin, cause of death and any pathological conditions identified. These individuals were largely indigent, from the lower classes of society of St. Louis, Missouri. St. Louis was established as a fur-trading centre in the mid-1700's and, by 1849, was considered a major city that provided a gateway or starting-off point to the west. There are numerous occupations listed in the records of the Terry collection. These men, born between 1841 and 1943 AD, performed physical jobs including working as labourers, odd job men, mechanics, farm workers, painters and wallpaper hangers. There is a furniture maker, a watchmaker, a tailor, a bricklayer, a vulcanizer (working with rubber products), a fireman, a paper cutter, a porter and numerous cooks and bakers. Less physically demanding jobs include a chauffeur, a railroad engineer (train driver), a barber, a restaurateur and numerous salesmen. A number of men may have originated from higher social classes, but fell victim to the great economic depression that followed the US stock market crash in 1929.

1.2 Project Aims

This study is important in its integration of historical and biological data. It seeks to identify the nature of morphological variation in humeral form in the context of activity and movement patterns. This project also investigates the physical results of participation in medieval warfare and the development of full-time soldiering in the period immediately before the historically recorded advent of standing armies in the Late Medieval period. There are a number of primary aims behind this research, each of which is addressed in the following chapters.

Aim 1: To examine skeletal tissue dynamics and establish plasticity as an active phenomenon adapting shape and size of skeletal elements (Chapter Two: Skeletal Tissue Dynamics). It is the objective of this chapter to discuss how both external and internal skeletal morphology is influenced by activity patterns. Thus what is being measured in this project are changes between populations and individuals resulting from differences in functional morphology brought about by differences in the individual's skeletal loading history. Specific questions include how the skeleton adapts to various loading and movement patterns at different developmental stages; the validity of Wolff's Law of Bone Remodelling in bioarchaeological research; and whether functional inferences from adult human bone variation reflect patterns established in childhood, or if the skeletal loading history may be modified in adulthood.

Aim 2: To examine variability and asymmetry in humeral torsion and identify any patterns in the torsional angle related to inferred habitual movement patterns (Chapter 5: Humeral Torsion). The primary hypothesis is that the humeral torsion angle is modified during the individual's lifetime by mechanical forces. The sports medicine literature links increased humeral torsion angles in the professional athlete to throwing. The hypothesis, then, is that an increased humeral torsion angle will be positively connected with other indicators of increased activity in the same limb. Specific issues regarding humeral torsion include its relationship to robusticity. If an increased torsion angle is related to higher levels of activity in the humerus, are increased angles found in the dominant or more robust limb? Does the humeral torsion angle relate to ontogenetic change or is it influenced by mechanical processes as indicated by the clinical literature? Further analysis addresses the nature of the torsional process and seeks to explain the level of variation in human populations. Early anatomists believed the torsional process to be limited to the proximal humeral diaphysis. However, if humeral torsion is related

to the functional use of the limb, there is no reason to assume that it relates exclusively to the proximal humeral diaphysis, as both the proximal and distal axes may undergo modification due to biomechanical forces.

More general questions about the humeral torsion angle include whether there are differences between archaeological samples and how the humeral torsion angle and the levels of bilateral asymmetry found between limbs compares between the archaeological samples and the Terry collection and the non-human primate species groups. Are there differences between sex and between right and left limbs? Is the size of the humeral torsion angle reflected in the spiral angle, a measure of the extension of the bicipital groove?

Aim 3: To examine variations in diaphyseal robusticity, diaphyseal shape and bilateral asymmetry through analysis of humeral cross-sectional geometric properties (Chapter 6: Biomechanics). This involves examination of a subset of data from two blade-injured samples (Towton and Fishergate samples) and a comparative sample chosen to represent the normal range of variation found in the Medieval period. The specific research question addresses the identification of movement patterns repeatedly performed during training for and involvement in armed conflict. A further goal is to identify what role architectural adaptations play in mechanical competence.

Aim 4: To identify and examine any differences in humeral morphology within and between population groups (Chapter 7: Analysis of Skeletal Variation). This is conducted through external measurements of architecture, articular size and robusticity, as well as analyses of bilateral asymmetry in these measurements. An objective of this chapter is to examine external measurements of robusticity and compare them with the

internal measurements obtained through cross-sectional properties. A further goal is to identify limb dominance through analysis of maximum humeral length asymmetry. Specific questions include defining the relationship between humeral torsion and other measurements of architecture, such as diaphyseal bowing.

CHAPTER TWO

SKELETAL TISSUE DYNAMICS

How does the skeleton adapt to loading and movement patterns? The interaction between morphology and the physiological mechanisms that influence it must be understood on both a macroscopic and microscopic level to interpret behaviour from the skeleton. To interpret the form, function and adaptive significance of skeletal elements requires detailed knowledge of skeletal tissue response to various mechanical and non-mechanical factors, as well as what initiates and controls the processes of bone modelling and remodelling (Burr, 1985). The purpose of the following discussion is to highlight how bone adapts to functional demands.

This chapter will encompass aspects of skeletal form and function, including adaptive bone response through modelling and remodelling, the mechanical adaptability of the skeleton, its architectural development, and the nature of bone plasticity. It will also review experimental work that has established functional adaptation of the skeleton through the study of bone modification in sports medicine and other fields and discuss the principles of biomechanical analyses.

2.1 The Determinants of Bone Form

The human skeleton serves many purposes. It gives the body its basic structure and serves as an anchoring point for non-osseous elements such as the tendinous attachment of muscles, ligaments and cartilage. It also protects internal organs and plays an important role in the basic metabolism of the human body (Carter and Beaupré, 2001). Prior to the 1960's skeletal research was focused on the biochemistry of the skeleton, concentrating especially on aspects of mineral metabolism. Bone was discovered to serve as a mineral reservoir for the rest of the body, storing calcium and phosphorus.

Therefore, skeletal tissue function was seen as a process of transferring mineral to and from the skeleton. This was thought to be carried out by the action of osteoclasts and osteoblasts. The osteoclasts functioned to remove bone mineral through a process of resorption; whereas, osteoblasts laid down new bone and thus replenished the mineral levels in bone. These cells were thought to be both separately controlled and to work independently of each other (Martin *et al.,* 1998). This view held that form and function were unrelated and that the skeletal tissue dynamics worked under the control of non-mechanical agents to maintain tissue homeostasis. Physiology was thus unrelated to general anatomy, muscle function, biomechanics or other tissue-level processes (Frost, 2001).

The basic concepts of biological adaptation were developed between 1859 and 1920, during a time when accepted wisdom dictated that morphology was a study of pure form divorced from function. Biological structures were considered in isolation and morphological features of the skeletal system were thought to alter ontogenetically and phylogenetically according to rigid mathematical laws. Again, biological structures were not seen to be part of a larger biological system that functions as a whole. The concept of skeletal alterations during ontogeny or phylogeny resulting from alterations in the relationship between the form-function complex and the environment was unknown (Bock and Von Wahlert, 1965).

Research conducted in the 1960's created the basis of what may be termed the 'new physiology' and identified the form-function complex. This work redefined the role played by osteoclasts and osteoblasts in the skeleton. It was discovered that these cells worked in tandem, with osteoblasts following osteoclasts and laying down new bone to replace that which was removed. These teams of cells were termed basic

multicellular units, or BMU's. This knowledge helped redefine the role of osteoclasts and osteoblasts within the skeletal system and demonstrated their role in maintaining mechanical integrity of skeletal elements. This integrity is maintained through a process of modelling and remodelling (Martin *et al.*, 1998). Thus tissue-level mechanisms, including biomechanical properties and the role of muscle development, were highlighted as key features to bone physiology with the role of homeostasis ranking below mechanical usage as a skeletal feature (Frost, 2001).

2.1.1 The Modelling and Remodelling Processes

Modelling is a basic function that shapes growing organs, including the skeleton. Its purpose is to adapt the size and shape of intact bones and their cortical area to meet the needs of typical peak mechanical loads. Modelling responds first to the growth process, secondarily to increases in body mass and muscle development during growth and, lastly, to mechanical pressures placed upon the growing skeleton while engaged in physical activity (Frost, 1985). Osteoclasts and osteoblasts work in sequenced actions that occur as a continuous or prolonged process and may be either resorptive or formative. This action is greatest during the growth phases of life and is greatly reduced after skeletal maturity (Martin *et al.*, 1998). Modelling can effectively move bone surfaces through formation drifts to build up a surface or through resorption drifts to remove bone from a surface (Figure 2.1). The actions of these drifts determine the cross-sectional size and shape of a bone, as well as the longitudinal shape of trabeculae and bone. In adults, modelling can increase trabecular strength and thickness throughout life, but is largely ineffectual on cortical bone. The process of modelling serves to increase bone strength and would seldom, if ever, decrease a bone's strength (Frost, 1999; 2001).

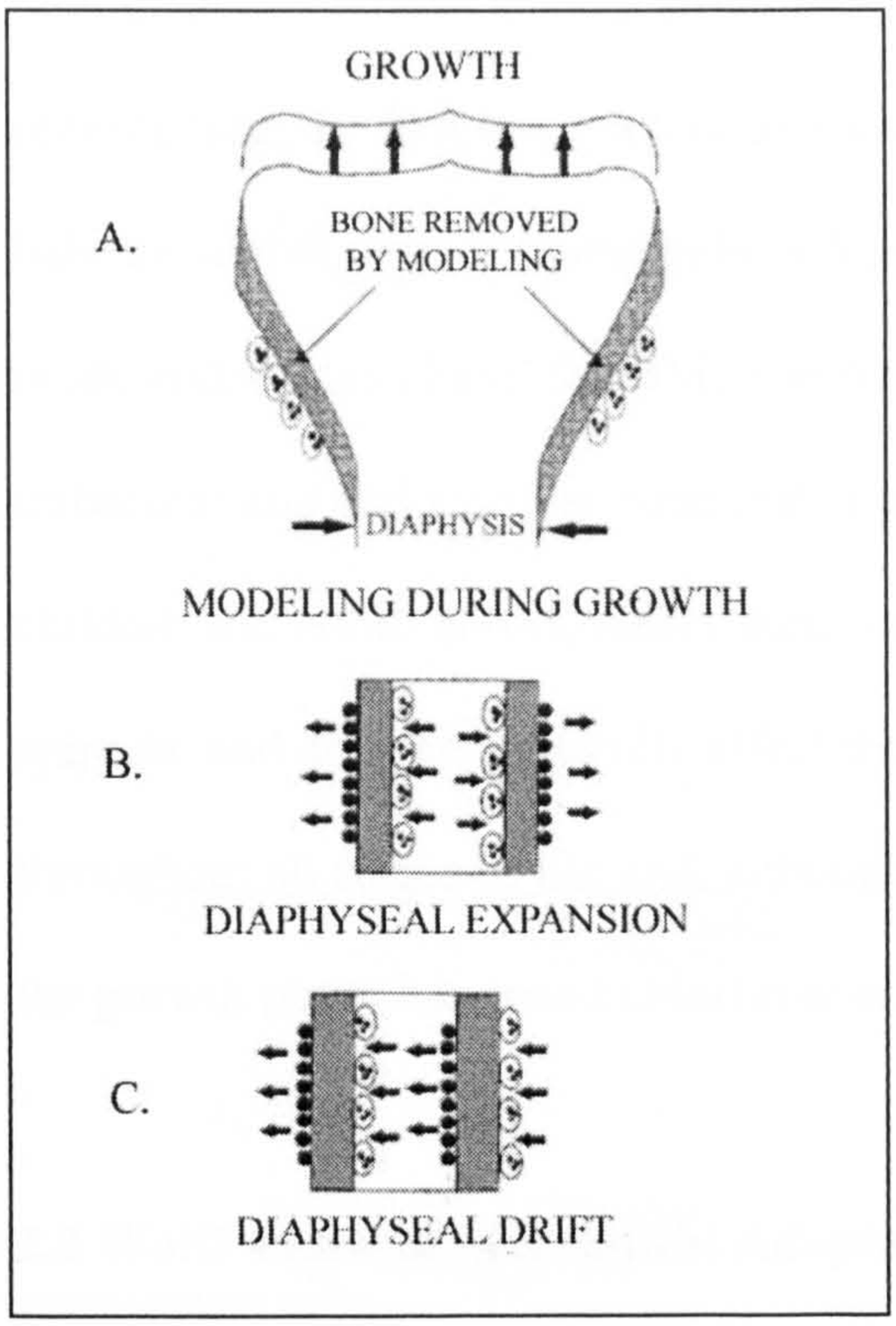

Figure 2.1: Modelling Drifts. A: Demonstrates resorptive modelling during growth to maintain diaphyseal shape. B: Demonstrates modelling drifts in diaphyseal expansion. The periosteal surfaces undergo bone formation while the endosteal surfaces undergo bone resorption. C: Demonstrates diaphyseal drift to maintain or alter diaphyseal curvature. The periosteal and endosteal surfaces each go through an opposing process of formation and resorption to alter curvature. The grey areas represent bone removal through modelling, the dark solid circles represent formation zones and the ovals with small circles inside represent resorption zones (After Martin *et al.*, 1998).

Remodelling is a basic function that signifies a turnover of hard tissue. An activation process triggers basic multicellular units (BMUs) to turn over bone in small packets. Osteoclasts resorb an area of bone while osteoblasts follow to fill in the resulting excavation, forming new bone in its place. Remodelling occurs in three forms, all of which can respond to mechanical usage (Frost, 2001). The primary form of remodelling is lamellar remodelling. Lamellar remodelling repairs mechanical microdamage and fractures. It also functions to control homeostasis, bone balance and turnover and mean skeletal age. A second form of remodelling resorbs mineralised cartilage to form primary spongiosa within growth plates, while the remaining form of remodelling finishes this process by removing the primary spongiosa and forming permanent, secondary spongiosa (Frost, 1985).

The overall purpose of the remodelling processes is replacement of bone or tissue with one set of biological and biomechanical properties with tissue of a different

biological and biomechanical structure. There appear to be at least two modes to remodelling, the first being a 'conservation mode'. In this process the BMUs work in a balance so that there is no net gain or loss of the bone. The second mode is a disuse mode and, in this phase, the BMUs make less bone than is resorbed, however it is only trabecular and endocortical bone that is preferentially resorbed. This occurs in both children and adults (Frost, 2001). Remodelling, as opposed to modelling, may be seen as episodic and does not generally affect the shape or size of the bone. Remodelling occurs throughout all stages of life and, although similar to modelling, the process slows after the growth phase has ended (Martin *et al.*, 1998).

2.2 Wolff's Law of Mechanical Adaptability in the Human Skeleton

Skeletal tissue can be seen as a dynamic entity with capability to adapt in response to the physiological and mechanical environment. In effect, skeletal elements have the ability to sense mechanical loading and, subsequently, modify their structure to adapt to changes in these loads. This premise is known as Wolff's Law of Bone Remodelling (Martin *et al.* 1998). Wolff's law states that:

> *Every change in the form and function of...bone[s] or of their function alone is followed by certain definite changes in their internal architecture, and equally definite secondary alterations in their external conformation, in accordance with mathematical laws* (J. Wolff, 1892 as quoted by Keith (1918) In: Martin *et al.*, 1998).

Today, Wolff's Law incorporates other nineteenth century concepts not specifically discussed by Wolff in his original treatise. The first of these is the optimisation of strength in respect to weight. Bone tissue is twice as dense as other tissues in the body. Therefore, it is important in bone to maximize strength in relation to its weight, as the metabolic cost of carrying about extra bone is very high. The second key concept relates

to trabecular alignment and directional stress. Wolff specifically referred to this relationship between trabecular architecture and principal stress trajectories, as noted in Figure 2.2. The last concept regards the self-regulatory aspect of bone in response to mechanical stimulus. This refers to the ability of the trabecular bone to orient itself in a pattern aligned with the stress trajectories according to changes in a functional stimulus (Martin *et al.* 1998). Martin and colleagues have restated Wolff's Law as the mechanical adaptability hypothesis. This states, "*bone structure is regulated so as to minimize fracture risk and bone mass while simultaneously optimising stiffness*" (1998: 230).

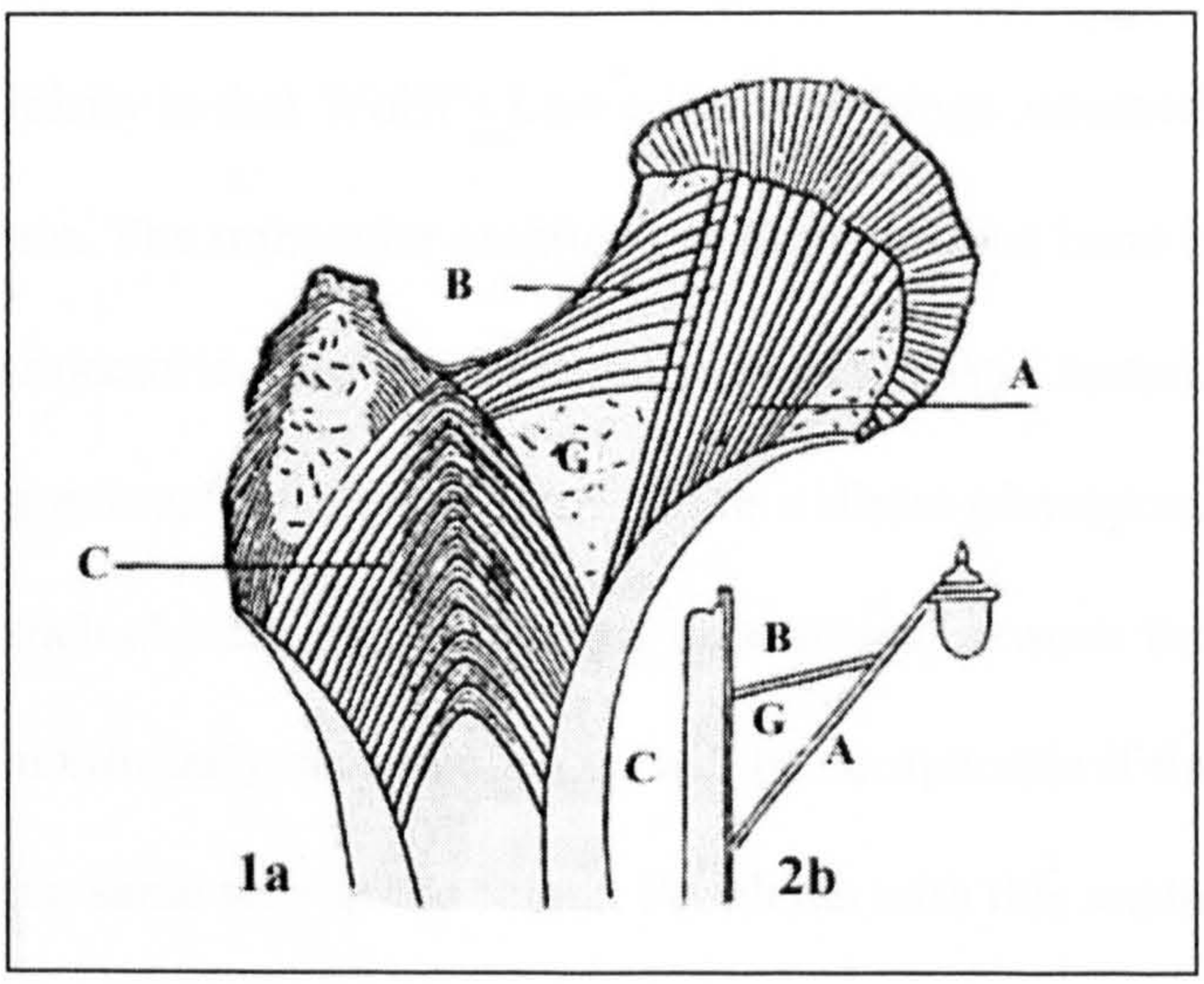

Figure 2.2: These images demonstrate trajectorial design. The trabeculae in the human femur (1a) appear to be aligned along principal strain gradients when compared to the image in 2b, a street lamp bracket. The femoral head in image 1a and the globe of the street lamp are supported by two beams (A, B) whose function is to distribute compressive stress into the principal support structure (C). Ward's triangle (G) forms the central 'opening' in this bracket (modified from Martin *et al.*, 1998).

Frost has proposed the "Utah paradigm", a still-evolving series of propositions designed to supplement previous ideas regarding the control of bone strength and mass under varying conditions of health, disease, gravitational surroundings, and as a function of physical activity (Frost, 2000). The first proposition of the paradigm states, "*healthy, postnatal load-bearing bones are designed to have only enough strength to keep chronically subnormal, normal or above normal voluntary loads (not injuries) from causing spontaneous fractures*" (2001:399). The second proposition states that tissue-level biological mechanisms require nonmechanical factors and effector cells (osteoblasts and osteoclasts) to achieve mechanical competence. Additionally, the

biological mechanisms are guided by bone loading and strains. Although most nonmechanical factors can help or modulate this process, they cannot replace mechanical loading (*ibid.*).

As may be ascertained, there are still a number of issues regarding the strength of Wolff's Law as a biological principle. The premise known as Wolff's Law has been restated and redesigned in modern literature as demonstrated above by Martin and colleagues (1998) and Frost (2000; 2001). Cowin (2001) maintains that there is a false premise in Wolff's Law relating to stress trajectories and trabecular architecture. The falsity is that Wolff's Law compares things assumed to be similar which, in practice, are not. The trabecular architecture of cancellous bone is compared with the stress trajectories in a homogenous isotropic elastic material, such as the street lamp seen previously in Figure 2.2. There is a direct correspondence assumed by Wolff between such objects. Thus the stress trajectories between the street lamp and the femoral head, as similarly shaped objects, will be comparable if the elastic model is statically loaded in the same way as the femur. Problems with this analogy lie in that trabecular bone is neither homogenous nor isotropic, nor are bones subjected to static loading.

Additional flaws in Wolff's Law, as cited by Cowin, include the 'mathematical' form of the law of trabecular architecture. This is considered invalid and has largely been rejected or ignored by students of functional adaptation, who instead employ a set of rules that regulate bone form to mechanical loading. Additionally, Wolff's Law does not compare with other laws or tenants of physiology when considering the scientific standard of the work. Interestingly, Wolff rejected the idea of bone resorption, instead believing that bone growth was identical to soft tissue growth, consisting solely of cell division and intracellular accumulation. He also erroneously believed compact bone

consisted of condensed trabeculae and the operational definition of 'function', a term that is strongly associated with Wolff's Law, was actually used to refer to the static rather than dynamic role of the bone. This does not mean, however, that Wolff's Law should be disregarded. It has become synonymous with the functional adaptation of osseous tissue despite a generally accepted physiological model and the best course of action would be to either downgrade it from being a physiological 'law' or rename the principles it supports (Cowin, 2001).

Bertram and Schwartz (1991), while also not advocating a total disregard for the premise of Wolff's Law, do raise many points regarding its principles. While recognizing the importance of mechanical loading in determining bone form, they are critical of the modern interpretation of Wolff's Law and feel it is weakly supported and suffers from a lack of control for other potentially important factors. Bertram and Swartz (*ibid.*) also question the fundamental tenant of the principles of trajectorial design, however, they believe the issue is that trabecular bone only appears adaptable as part of the fracture repair process. Trabeculae, they feel, are formed naturally in a mechanically appropriate design from its formation, rather than adapting to stress trajectories. Regarding the issue of atrophy, whether decreased loading does indeed lead to decreased mass, they feel the bone's sensitivity depends upon developmental maturation, as mature and immature bone react differently, and due to differences in anatomical locations, as distal elements are subjected to greater atrophy than are the proximal elements. These two points are certainly valid, as there is a different response between adult and juvenile bone to remodelling, as well as differences between the proximal and distal element. This will be discussed in greater depth later in this chapter.

The question of bone hypertrophy is perhaps easier to address. Experimental work, in the studies cited by Bertram and Swartz (1991), relied upon one of two different methods for creating increased mechanical loads. The first method involves an osteotomy, or removal of one of a pair of elements in the distal limb segment. The other technique involves planting pins in the element to apply loads directly. Based upon early work, Bertram and Swartz (*ibid.*) came to the conclusion that surgical intervention seems to create osteogenesis and that this irritation may be responsible for differences in bone formation. For support, they cite cases of increased bone formation in the absence of mechanical loading, but in the presence of injury. Current research in this area, such as that conducted by Pearson and Lieberman (2002), has a different methodological approach, one that does not involve any form of surgical intervention and would indicate a different conclusion. Sheep, divided into three age categories, were exercised on a treadmill for an hour a day and compared with sheep that were not. Fluorescent dyes were used to measure bone change and the bones were analysed directly. A similar study was conducted on one-month-old pigs and genetically identical armadillo twins. These animals were divided into exercised and non-exercised groups and longitudinal bone growth was monitored through intraperitoneal injections of fluorescent dyes that are incorporated into the bone mineral. Strain gauges were surgically implanted only towards the end of the experiment, minimising any reactive bone formation (Lieberman, 1996). These methods mean there is little or no osteogenic response from a surgical irritant and as the bone was analysed directly, if there was, it would have been visible as periostitis.

The idea proposed by Bertram and Swartz (1991) that bone response increases in relation to an irritant or injury is taken farther when considering the case of bone hypertrophy in athletes. Many of the early studies in this field report injuries, in addition

to bone hypertrophy, resulting from the high levels of activity required to participate in professional athletics. Unfortunately, the authors cannot seem to separate injury from hypertrophy and do not recognise this as it now is, part of a suite of changes that will occur with habitual, strenuous activity. In a summary statement regarding Wolff's Law, they feel that:

> *It has yet to be established whether the load applied to an element during growth determines its morphology, or acts as an enabling factor in the acquisition of a genetically controlled shape, in much the same way as the necessary calcium regulating hormones are known to act* (Bertram and Swartz, 1991: 251)

This is a valid point, and aptly sums up the nature vs. nurture debate in functional adaptation. This research project endeavours to answer some of these questions regarding increased bone formation from an irritant or injury. In skeletonised remains, it is possible to examine the cortical bone surface for new bone formation in the form of woven bone, signalling a 'pathological' periosteal reaction, rather than increased cortical bone thickness. Certainly, examination and identification of bilateral asymmetry in skeletal morphology would help demonstrate the role of functional loading, as it is unlikely that a genetically controlled shape would vary from one side to the other.

2.2.1 Mechanical Controls of Modelling and Remodelling

Mechanical loading deforms or strains bone, the larger the load, the bigger the strain. A strain may be defined as "*the deformation or change in dimensions and/or shape caused by a load on any structure or structural material*" (Frost, 2001:419). There are three types of strains caused by mechanical loading: compression, tension and shear. These strains are expressed in terms of microstrain units. One thousand microstrain in compression relates to a 0.1% shortening of bone length, while 10,000 microstrain

would shorten bone length by 1%. Strength and architecture in load-bearing bones are strongly influenced by strains, with the largest voluntary loading and strains originating from muscle action (*ibid.*). While diaphyses are exposed to axial compression, the greatest contribution to diaphyseal strains is from the bending and torsion moments that are created. The maximum compressive strains on the bone surface are generally 50% greater than tensile strains. This is because of the superposition of axial and bending loads (Carter & Beaupré, 2001).

Table 2.1 Physical activities and strains engendered in various animal bones (after Carter and Beaupré, 2001). The relative similarity in peak strain levels indicates that bone acts in a similar fashion irregardless to species.

Animal / Bone	**Activity**	**Peak Strain**
Horse tibia	Galloping	-3,200
Horse metacarpal	Accelerating	-3,000
Horse radius	Trotting	-2,800
Fish hypural	Swimming	-3,000
Goose humerus	Flying	-2,800
Pig radius	Trotting	-2,400
Monkey mandible	Biting	-2,400
Dog radius	Trotting	-2,400
Dog tibia	Galloping	-2,100
Turkey tibia	Running	-2,350
Sheep radius	Galloping	-2,300
Sheep femur	Trotting	-2,200
Sheep humerus	Trotting	-2,200

The strain magnitudes generated during extreme physical activities are great enough to introduce fatigue damage to the skeletal tissue. Cortical bone exposed to a single heavy loading event in the direction of the diaphyseal axis yields at a strain of about 6,000 microstrain in tension and 9,000 microstrain in compression. In cyclical loading *ex vivo*, damage occurs at a threshold of about 2,500 microstrain in tension and 4,000 microstrain in compression. The strain levels recorded in various animals implies that the bone hypertrophies to a level that accommodates *in vivo* strains, thus reducing the level at which significant damage occurs. It is, however, important to note that the strain magnitudes do not appear to change during development and are similar in immature and adult bone (Carter and Beaupré, 2001). A level of 2000-3000 microstrain

appears to be the peak level of periosteal strains in the long bones of various animals as seen in Table 2.1 (Martin *et al.*, 1998).

This introduces the concept of thresholds in bone modelling and remodelling. Modelling increases bone strength to reduce high-level strains and to maintain bone strength to accommodate typical peak strains and keep them from exceeding the bone's threshold. This is activated when strains exceed a modelling threshold range and has the effect of creating a bone stronger than required for peak voluntary loads. The modelling threshold may be defined as "*the genetically-determined Minimum Effective Strain range (MES) for mechanically controlled bone modeling*" (Frost 2001: 418). Modelling is inhibited while strains remain below the MES, while strains in excess of the MES activate the modelling process. Similarly, the remodelling threshold is "*the genetically-determined MES that helps control the switching of BMU-based remodelling between its conservation and disuse modes*" (Frost, 2001: 419). Completed BMUs make and resorb bone when strains exceed the MES, thus activating conservation-mode remodelling. In disuse-mode, strains fall below the MES and trigger the BMUs located near the endosteal surface to make less bone than is resorbed. This creates a disuse pattern osteopenia, which is characterised by endosteal expansion, thinned cortical bone but no reduction in external cortical diameter (*ibid*).

Mechanically-induced modelling remains dormant when strains fall below the range of 1,500 microstrain. However, strains in the range of 1,500 – 2,500 microstrain increase cortical bone mass. Therefore, the range of 1,500 – 2,500 would appear to be the set-point for the minimum effective strain for bone modelling in response to mechanical usage. One function of mechanically controlled bone modelling seems to be to keep typical peak strains below this threshold range. Smaller peak strains in the range of 100 – 300 microstrain appear to trigger mechanically induced remodelling. At this

level, new BMUs are recruited actively, yet when strains exceed this range, remodelling declines. It would appear that the remodelling process is more delicate, as a high MES set-point or range would accelerate removal of the endosteal surface while a MES set-point or range that is too low would conserve bone (Frost, 1987a).

Table 2.2: The effect of mechanical usage on bone growth, modelling, remodelling and mass (after Frost, 1987a).

Cumulative Activity		
Mechanical usage	**Growth and modelling**	**Remodelling**
Increased	Increased	Decreases
Decreased	Decreased	Increased
Compact Bone Mass		
Mechanical usage	**Mass**	**Mass**
Increased	Increase in children	Conservation in adults
Decreased	Growth retarded in children	Decrease through endosteal expansion in adults
Trabecular Bone Mass		
Mechanical usage	**Spongiosa**	**Spongiosa**
Increased	Increased addition in children	Conservation in all ages
Decreased	Addition decreased in children	Increased loss in all ages
Bone Architecture		
Mechanical usage	**Changes in childhood**	**Changes in adulthood**
Increased	Thicker cortex, increased external diameter, densification of spongiosa, reduced marrow cavity, increased bone length	Conserved spongiosa, conserved cortical-endosteal bone
Decreased	Reduction in external bone diameter, osteopenic spongiosa, reduction in bone length	Increased marrow cavity (endosteal expansion), osteopenic spongiosa

When discussing activation ranges and bone response, it is important to note that modelling and remodelling will not occur at the same surface at the same time and that they have opposite responses to mechanical loading (Table 2.2). As seen above, the activation thresholds vary between the two processes. Strains below the lower threshold will activate remodelling, but inhibit modelling. Strains in excess of the threshold will stimulate modelling while inhibiting remodelling, although microdamage may ensue that will eventually activate the remodelling response (Burr and Martin, 1989). This forms the basis of Frost's Mechanostat Theory. This theory is based upon the principle

that bone mass is equivalent to typical mechanical usage and that the mass may be overadequate but never inadequate. Therefore, there must be some type of monitoring of mechanical usage that adjusts for misfits in mass and mechanical usage that acts in a manner analogous to a thermostat a to turn on and off as required by the physical loading (Frost, 1987a). The mechanostat theory thus attempts to explain when activation of BMUs will occur with the mechanostat acting as a regulatory mechanism that turns on and off modelling and remodelling.

In addition to mechanical usage, there are non-mechanical influences to skeletal adaptation. A summary of factors may be found in Table 2.3. Frost (2001) proposes that such factors actually may help or modulate mechanical control of modelling and remodelling processes, however, they cannot replace the mechanical control. Between 3% and 10% of postnatal strength in bones may be the result of the direct cellular action by hormones, calcium, vitamin D and genes. However, the direct effect of modelling and remodelling in accordance with mechanical loading accounts for over 40% of bone strength.

Table 2.3: Non-mechanical factors influencing bone adaptation to mechanical usage (after Frost, 2001).

Hormones
Paracrine effects
Autocrine effects
Cytokines
Cellular interactions
Disease processes
Vitamins and minerals
Amino acids
Lipids
Dietary calcium
Malnutrition
D metabolites
Gene expression
Sex
Age
Ethnic origin
Occupation
Medications

2.2.2 The Stimulus for Mechanical Adaptability

There are multiple theories regarding the stimulus to mechanical adaptability, although these may be condensed into two approaches. The first approach, which identifies the mechanical stimulus as a stress gradient, is represented by the flexural neutralization and the osteon alignment theories. The flexural neutralisation theory relates to the correction of abnormally curved bones while the osteon alignment theory relates to BMUs and their orientation with the principle compressive stress direction. The BMUs carry a positive stress gradient on the resorptive surface and a negative stress gradient on the refilling surface, bearing the same relationship as does the cellular activity remodelling for the external surfaces of abnormally curved bones in the flexural neutralisation theory. A positive strain gradient activates osteoclasts and a negative strain gradient activates osteoblasts. The second theoretical approach identifies the mechanical stimulus as being a scalar measure of stress magnitude and is defined by the bone density optimisation, trabecular alignment and adaptive elasticity theories. In both of these categories of theories, osteocytes function as mechanical sensors that communicate across the osteocytic network. These sense a stress gradient that is seen to drive fluid flow in the flexural neutralisation and osteon alignment theories, while the bone density optimisation, trabecular alignment and adaptive elasticity theories relate to signal averaging. Problems with these theories relate to the stress magnitude, which does not function as the mechanical stimulus in the flexural neutralisation and osteon alignment theories, and in the second category, it is not yet clear whether stress gradients, as opposed to strain, would not function as the stimulus of mechanical adaptability, in addition to stress magnitude (Martin *et al.*, 1998).

Lanyon (1996) has proposed the error strain distribution hypothesis to explain what stimulates adaptive response in bone. This theory is based upon experimental

studies which indicate that normal loading does not stimulate bone response, nor is it adequate to maintain architecture. Therefore there must be a missing component to the mechanical environment which maintains mass. Atypical strain distributions, high strains and high strain rates were observed to stimulate the greatest osteogenic response, as the skeleton adapts to maintain structural integrity and eliminate or reduce these perceived deviations, or errors, from the normal strain distributions. Thus, the missing component in the osteogenic response was judged to be these 'error' strains. Osteoblasts are assumed to be the primary strain-sensitive cells that are programmed with a strain set-point that may vary by location. These cells then make adjustments locally to restore strain levels, rather than across a network as is the case with osteocytes (Lanyon, 1996).

2.3 Architectural Development

Modelling may be seen as a process during growth whereby the skeleton is adapted to specific loading patterns of the individual while remodelling may be seen as a process of fine-tuning the skeletal element to the mechanical demands placed upon it (Martin *et al.*, 1998). These processes enable a causal relationship between skeletal architecture and functional loading. Different elements have different functional roles within the skeletal system. Where shape or protection is a key role, such as in the bones of the skull, the architecture will be more strongly genetically encoded, although this has never been tested. In limb bones, only the general form is developed in the absence of mechanical loading. The features of resistance to functional loading, such as breadth, cortical thickness, cross-sectional geometry, curvature, mass and trabecular orientation only develop as an adaptive response to normal physical load-bearing. Therefore, in limb bones, most architectural features will be related to functional loading (Lanyon, 1987).

Problems in the interpretation of functional loading in relation to bone architecture lie in how to differentiate between functional adaptation and genetically determined growth patterns. Most individuals use their skeletons for similar functions which lead to comparable patterns of functional loading (Lanyon, 1990). The stereotyped control over foetal skeletal, muscular and neurological anatomy and function led to a stereotyped skeletal morphology. Thus all skeletons appear similar isolated from the effects of physical activity. Consider the different morphological aspects of the human and canine femur, for example. In the human form, the adult femur, though not the infant femur is bowed, while in canines, it is straight. The differences in the femoral shaft between the human and the canine form lie not in the execution of specific genetic information, but are the consequences of bone and chondral modelling in response to different postnatal mechanical usage during growth (Frost, 1985.)

Genetically controlled processes of growth and development ensure the appropriate tissue type is present. This tissue is then capable of adaptive change that modifies its architecture in response to the individual demands of physical load-bearing (Lanyon, 1987). However, the relationship between architecture and functional adaptation also may be affected by a number of factors, including systemic influences on architecture such as disease, nutrition, hormones, and metabolic states (Lanyon, 1990).

2.3.1 Muscle Bone Interaction

The potential impact of muscle-bone interaction is immense. The inefficiency of muscle lever arms means that 2 kg of muscle force is needed to move 1 kg of body weight. Therefore, the largest voluntary bone loading and strains originate from muscular action

rather than body weight. In an extreme situation, the longitudinal forces on an athlete's femur during running can briefly exceed five times their body weight. It also takes more muscular activity to move an obese body than a slender one. Consequently, an obese individual will have greater muscular strength and bone mass if this was achieved before physiological maturity. Individual variation in muscle use then causes variable differences in strength and tissue dynamics of the skeletal elements (Frost, 1999; 2001).

Muscle forces are directly imposed on the periosteum, and it is this surface which houses the osteoprogenitor cells, making the periosteum key in the influence of muscle upon bone (Herring, 1994). In this manner, the muscle-bone interaction also influences bone morphology and operates as a form of functional adaptation. However, this mechanism differs from that responsible for distributing mechanical loading through the bone matrix (Lanyon, 1996).

There are several key points to recognise when discussing muscle-bone relationships. The first is that the presence of a muscle attachment alone is not enough to produce osteogenesis. Areas of muscle attachment can be either resorptive or appositional. Second, while periosteal pressure can retard bone growth, muscle traction can influence bone length. Third, adjustments in the loading regime will modify the muscle attachment site. Modifications in the periosteum occur at such locations. Anastomosis occurs between the blood vessels between muscles and periostea only at muscle attachment sites. Additionally, there appears to be a special adaptation for stress application through polarisation of cells and specialised junctions at muscle insertion sites. Lastly, it is important to realise that the dynamics of the muscle-bone interaction vary with growth development. In young animals, the muscles, tendons and ligaments are invested largely within periosteum and do not intrude into the bone. However, in

adults, the muscle fibres are incorporated into the bone through the process of mineralization (Herring, 1994).

Size and shape of bones are strongly influenced by muscle activity. A specific example shows how periosteal pressure from the contraction of muscle bellies resting on the bone surface can directly influence the rate of bone apposition. The functional pressures exerted through muscle action would, in some cases, inhibit periosteal expansion, creating a localised flattening of the diaphysis. Immobilisation of the femora of rats had the effect of inhibiting the shaft diameter and creating a more circular diaphysis (Carter and Beaupré, 2001). This circularity is most likely from the removal of functional pressures on the periosteum, as there is an absence of muscle activity, hence no development of muscle attachments to influence morphology. Although it is important to recognise that circularity in Neandertal femora occurs not from muscle atrophy, but from hypertrophy of the surrounding structures such that the *linea aspera* and pilaster 'sink' into the surrounding bone. Muscle activity, or its absence can then affect bone diameter, density and curvature. Its absence may retard development of these characteristics, while hyperactivity may increase them.

2.4 Plasticity and the Nature vs. Nurture Debate

Wolff's Law says that osseous elements place or displace themselves in the direction of functional pressure. They do this through direct pressure upon the periosteum from muscular forces and through modelling and remodelling driven adaptations to the internal matrix to distribute functional strain resulting from repetitive loading. However, the plasticity of skeletal form in response to environmental factors is not completely understood, leading to the nature vs. nurture debate. Is skeletal form unchanging and dependent upon genetic inheritance, or is more a product of environmental influences?

At the beginning of the 1900's, skeletal characteristics were considered to be inherited, with little or no consideration of how environmental influence contributed to bone shape. Although research in the early 1900's asked the question of whether people who lived differently would grow up differently, the effects had not been fully formulated and tested. In this time period, common ideology stated that traits such as stature and facial proportions were indicative of 'race', and thus unchanging. An early analysis conducted in 1905 by Walcher, a German obstetrician, however, did show that cranial shape could be influenced by different habitual sleep positioning in infants. Babies placed upon their backs displayed broader crania than those habitually placed upon their sides. Franz Boas, in the early 20th century, conducted a seminal study in this field. He examined stature and cephalic index in European immigrants and their American-born children in both Jewish and Sicilian ethnic groups. In both groups, stature increased in the American-born offspring, but cephalic indices decreased in the Jewish group while increasing in the Sicilian group (Lasker, 1969). Despite the different response in cranial shape between the two ethnic groups, there were differences identified between immigrant parents and their US-born offspring in a trait that was considered static. This study was only one of many migrant-sedente population studies that formed the basis of work that established plasticity as a biological phenomenon (Schell, 1995).

Current research, however, questions the plasticity of cranial form, with two different groups of researchers re-analysing Boas's data and coming to contradictory conclusions. A 2002 study by Sparks and Jantz found Boas's conclusions questionable, and felt any change in cranial form between populations was small and insignificant. The work by Gravlee and colleagues (2003a), on the other hand, supports Boas's conclusions and finds changes in cranial form due to environment small, but real. A key

point to this disagreement lies in the degree of phenotypic control in cranial form and a misunderstanding in what Boas was saying. There is a large genetic component to cranial shape as Boas himself recognised (Holloway, 2002), so Sparks and Jantz's debunking of the proposition that the cranium is shaped *primarily* by environmental forces is incorrect, as that was never one of Boas's assertions. As Gravlee and colleagues (2003b) point out, other key differences between the two re-analyses lie in the application of different statistical approaches and the different questions asked of the data. Boas focused upon maternal exposure to the US environment as a key variable in cranial variation, as did Gravlee and colleagues, whereas Sparks and Jantz focused instead upon the number of years or age since migration of the child. As for the key point in the history of plasticity analyses - that cephalic index, once considered a permanent characteristic of human race, was subject to environmental influences; all analyses do in fact agree that variation did occur between generations without genetic admixture.

It was only with the work of Dobzhansky (1941) that the relationship between phenotype and genotype was identified as being dynamic, with the phenotype being the product of interactions between genotype and environment (Hulse, 1981). Dobzhansky identified two modes of adaptation, direct change to the genome and phenotypic change through mechanisms of gene expression. These were later modified by Lasker (1969) to be (1) selection, or genetic change from natural selection; (2) developmental plasticity; and (3) acclimatization, or short-term behavioural and physiological responses. These adaptations vary in relative timescales, degree of permanence and allocation of cost. The shortest timescale of adaptation occurs with acclimatization, this can take anywhere from a few seconds to occur to a few weeks and the changes are reversible. An example would be changes in skin tone (a sunburn or a tan) from excessive sun exposure.

Developmental plasticity occurs throughout the individual's lifetime and is an irreversible change. The longest timescale in adaptation would be genetic change. These occur over a number of successive generations and displays the greatest degree of permanence (Eckhardt, 2000).

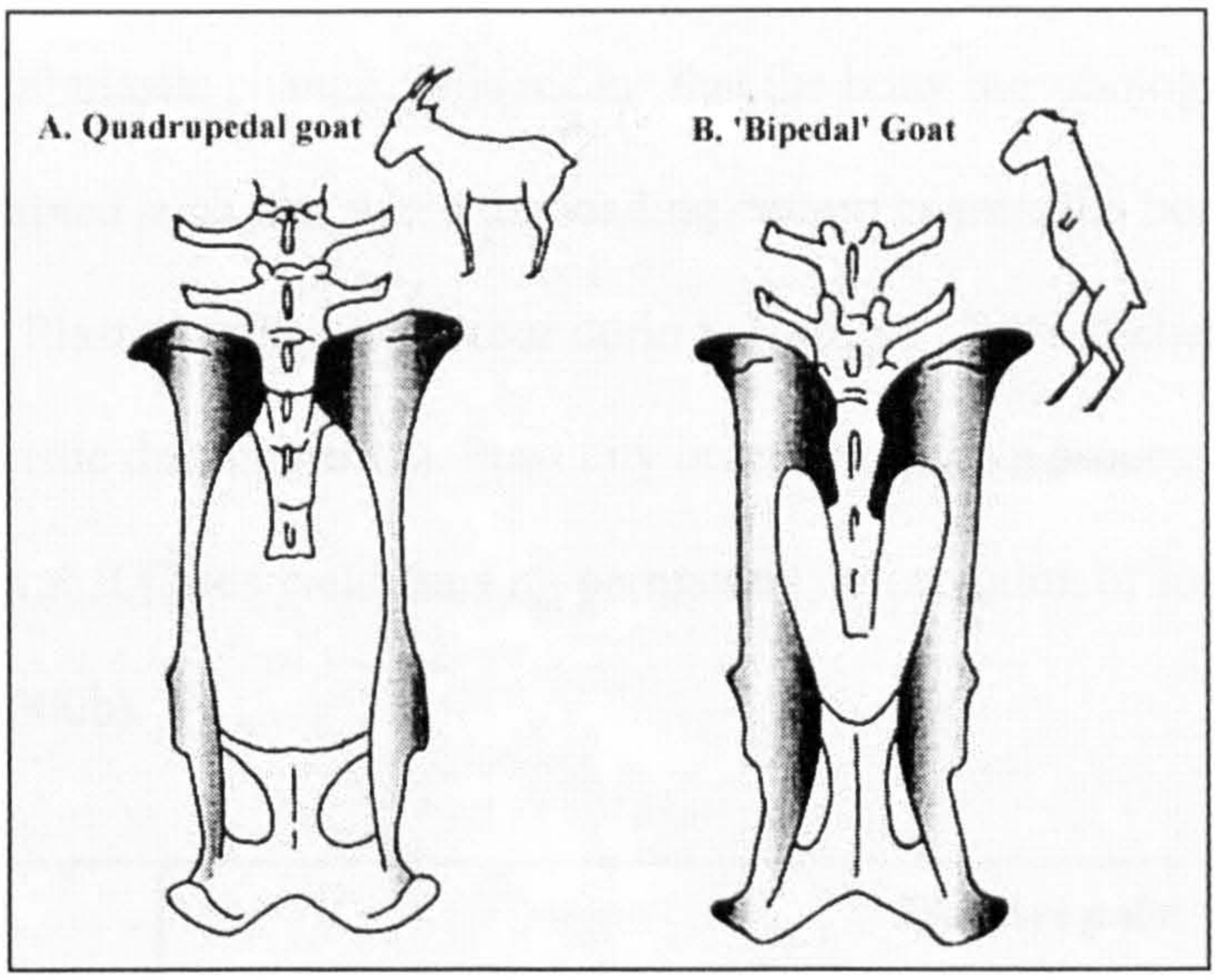

Figure 2.3: Plastic change in a 'bipedal' goat. The image on the right is that of a 'bipedal' goat. Note the changes in pelvis structure, from the elongation of the sacrum and pubis to the narrowing of the pelvic inlet when compared with the image on the left, that of a normal goat. The ilium is broadened medio-laterally as well in the 'bipedal' goat. Interestingly, there is also a change in the orientation of the transverse processes of the lumbar vertebrae from the quadrupedal form oriented in a straight medio-lateral fashion, to the bipedal form, where they are angled superior to inferiorly, to accommodate the upright posture (image modified from Roberts, 1995).

Skeletal evidence of adaptation includes short-term adaptations such as dental enamel defects like the neonatal line, a microstructural area of arrested growth observed from birth stress. This may be seen as evidence of a fleeting period of stress, while dental enamel hypoplasias, microstructural disruptions in deciduous and the first permanent molars, indicate more lasting periods of stress. More extensive adaptations to the skeletal system would be bone remodelling in relation to activity as discussed previously (Eckhardt, 2000). There are a number of empirical and experimental studies investigating the extent to which skeletal plasticity is adaptive. However, the most persuasive argument for adaptive skeletal plasticity involves the case of a bipedal goat,

born with underdeveloped forelimbs. The animal's primary mode of locomotion was hopping, a mode of locomotion that fundamentally altered the pelvic structure from that of a 'normal' goat (Roberts, 1995). These changes are demonstrated in Figure 2.3.

Changes in skeletal morphology from habitual activity patterns may be defined as developmental plastic change. This means that the bony morphology has been functionally adapted such that when the loading pattern ceases, the bone maintains the modified form. Plastic change can occur during all stages of life (Schell, 1995), although bone is most plastic during growth. Plasticity occurs through a process of microfracture, where the outermost fibres yield causing permanent deformation of form (see Figure 2.4) (Knüsel, 2000b).

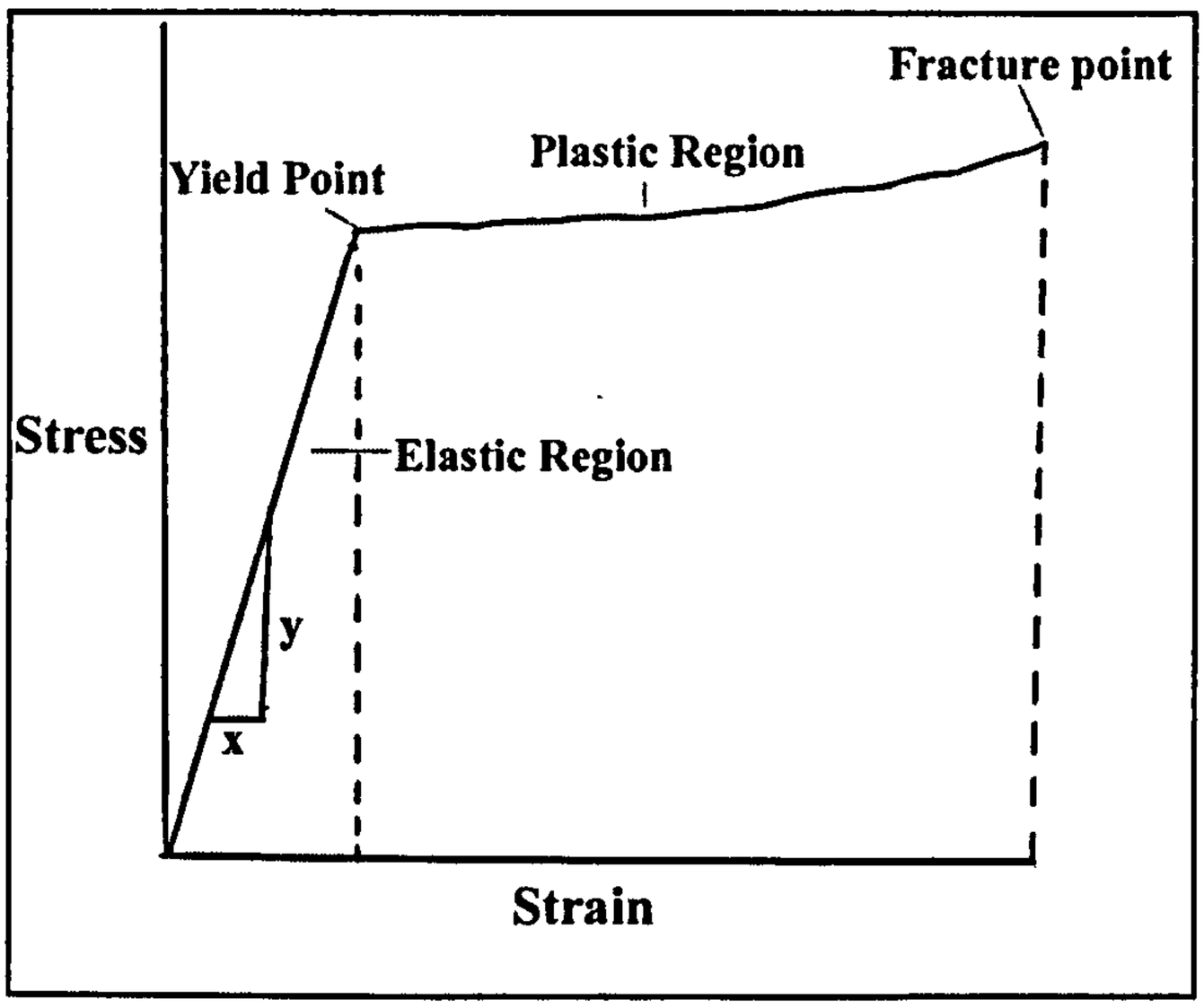

Figure 2.4: The load deformation curve for cortical bone. Stress is a product of force per unit area while strain is the changes in length per unit length. Young's modulus of elasticity, the material stiffness under normal loading, is given by the slope of the stress-strain curve (y/x). This remains constant for stresses below the bone's yield point while, beyond this, the bone is subject to plastic deformation and, with continued stress, cortical bone failure (after Lieberman, 1997).

Despite this evidence, there is still a group that believes skeletal morphology to be the result of strict genetic encoding and any differences in morphology relate to the genotype rather than to the phenotype. This view holds that variations in morphology

relate to variations in gene expression that arise from the role of *Hox* genes in limb development. *Hox* genes consist of four gene clusters, known as *Hoxa-d*, and are important components in the interpretation of positional information during limb development. Morphological changes can arise from differences in the timing of gene expression. Subtle alterations to this timing can result in severe morphological changes in the individual. Patterning defects can also arise from variations in the dosage *Hox* gene. It has been proposed that evolutionary changes in morphology may have been driven by subtle changes in the timing of *Hox* gene activation. The discovery of tissue and region-specific *Hox* enhancers suggests these morphological changes may be regionalised rather than having resulted in gross modifications of the body (Cohn and Bright, 2000).

2.5 Experimental Analyses in Mechanical Loading

The previous sections have explored the theoretical side of mechanical adaptability and the principles behind bone adaptation. The discussion now follows the practical side of bone response and discusses experimental work and practical applications in this field. Experimental work in the mechanical adaptability of the skeleton may be divided into several categories. These include analyses conducted in the fields of mechanical loading, osteoporosis studies, sports medicine and archaeology. There is also separate consideration for bone response in juveniles.

The shear volume of experimental work that is and has been conducted in the field of mechanical loading will preclude an examination of each individual piece of work. This volume of work includes studies to investigate whether the osteogenic response increases with short bursts of activity or whether it requires extensive loading. These studies showed that short periods of activity and activities which involve higher

loading rates are most effective for stimulating an osteogenic response (Robling *et al.*, 2002; Burr *et al.*, 2002). A study by Hsieh *et al.* (2001) investigated variation in strain thresholds in adult rat ulnae. This study found threshold strains varied by location on the element, being greatest in the distal shaft. At this location, the threshold for osteogenesis was 3074 microstrain while, proximally, the threshold was 1343 microstrain. This follows a theory of cellular accommodation that predicts higher strain thresholds in skeletal locations where mechanical strain stimulus is greatest. Bone formation was also found to vary according to strain magnitude. The greatest amount of new lamellar bone was formed on the medial diaphyseal surface, at the site of compressive strain and the highest strain magnitude. This was followed by bone formation on the lateral diaphyseal surface, relating to tensile strain.

Lieberman (1996) investigated cortical bone thickness in both juvenile (one-month-old) sibling pigs and genetically identical armadillo 2-month-old twins, addressing questions of the role of genetics in cortical bone adaptation. The pigs and armadillos were separated into exercised and control groups, with a twin or sibling in each group. The exercised animals displayed significant increases in cortical area and linear dimensions, as well as a greater distribution of mass around the biomechanical neutral axis (I values) when compared with the control group ($p < 0.05$). There were no significant differences in medullary area. The exercised animals also demonstrated a twenty-eight percent increase in cranial vault thickness when compared with the control group, as well as significantly increased dorsoventral and mediolateral dimensions of the cervical vertebrae and ribs ($p < 0.05$). These results indicate a systemic influence on cortical bone thickness in exercised animals. Increased activity generates cortical bone formation not just locally, at the site of mechanical loading, but systemically throughout

the skeleton. The use of siblings and genetically identical twins proves that skeletal morphology may be adapted through different activity patterns.

More basic experimental analyses include the work of Woo and colleagues (1981). They examined one-year old miniature Yucatan swine that were subjected to 12 months of exercise training. Bone samples were then subjected to four-point bending tests to failure to determine values for the maximum load before failure. The cross-sectional properties were also analysed for a section taken at a proximal location estimated by this author (from figure 1, page 781) to be approximately sixty-three percent of the maximum length. They found the mechanical properties did not change between the exercised and control groups, however the exercised group displayed a seventeen percent increase in cortical thickness and twenty-three percent increase in cortical cross-sectional area. This increase took the form of endosteal apposition rather than periosteal expansion, effectively creating a narrowing of the medullary canal.

Work by Lanyon and Rubin (1984) isolated the avian ulna to examine the type of loading, static versus dynamic, on bone remodelling. They surgically isolated the element so that the only strains were those imposed experimentally. Similar loads were used in both the static and dynamic cases, however, it was found that static loading had no effect on bone remodelling and produced endosteal resorption, while dynamic loading led to a twenty-four percent increase in cross-sectional area. Another study by these investigators found that four loading cycles per day were sufficient to maintain bone mass (Rubin and Lanyon, 1984).

Overstrain has been examined through osteotomy experiments, where a portion of the bone is removed. Skeletally mature sheep were subjected to an ulnar osteotomy to

cause an increase in peak strains on the radius. There was new bone formation, although this was more consistent with an attempt to replace the missing ulna rather than being controlled by strain magnitude (Lanyon *et al.,* 1982). This likely relates to the age of the sheep that, as adults, display a diminished response to remodelling, but as juveniles possess more malleable skeletal structures.

When considering the experimental data regarding increased mechanical loading, it is worth considering a number of points. The age of the animal when the experiment was conducted is very relevant to the outcome, as younger animals display greater responses to strain fluctuations than older ones. This will be dealt with in more depth later. Also, the changes in architecture of the bone may affect strain distribution and, consequently, bone response (Bouvier, 1985). These differences in architecture may be viewed in two ways. It is a premise of this thesis that changes in humeral architecture such as the degree of humeral torsion may affect biomechanical efficiency, so that the structure is plastically altered through repetitive activity to more efficiently distribute strain. Additionally, there are differences in architecture between the proximal and distal element of a limb with the distal limb segment tapered, allowing for energy conservation during the swing phase of locomotion. Lieberman and Pearson (2002) examined these changes in architecture to determine if there were modelling (growth) or remodelling (repair) differences between proximal and distal elements related to the presumed structural disadvantages of distal limb tapering. They found that similar loading induced higher rates of modelling in the proximal midshaft while remodelling was highest in the distal midshaft. The distal limb, as opposed to the proximal limb, also appears to be adapted to higher strains. This has interesting implications for much of the early experimental work in mechanical loading, as much of it examined the distal elements.

Other analyses include canine disuse experiments where the forelimbs of growing dogs were immobilised in a cast for 40 weeks and the subsequent bone change examined. Bone loss in the metacarpal, which was approximately fifty percent of bone mass when compared with the contralateral element, was characterised by increased periosteal resorption and decreased bone formation. Sixty-five to seventy percent of bone mass was recovered in 28 weeks, this with only 32 weeks immobilisation. The bone mass was increased through endosteal apposition and woven bone deposition on the periosteal surface (Uhtoff and Jaworski, 1978; Jaworski and Uhtoff, 1986). A later study by Jaworski *et al.* (1980) examined older dogs and found an age-related difference. The osteogenic response to immobilisation was endosteal rather than periosteal resorption, as well as increased intracortical porosity. Additionally, following immobilisation, older dogs were able to recover less bone mass.

Experimental analyses demonstrate how bone adapts in response to force. Osteogenesis responds to dynamic strains and short bursts of activity that result in periosteal expansion and endosteal inhibition. Increased activity stimulates higher rates of modelling in the proximal elements and remodelling in the distal elements. After immobilisation, juvenile bone had a greater ability for recovery of bone mass. Age-related bone loss during immobilisation differs, as juvenile bone undergoes a phase of periosteal resorption while adult bone resorbs bone from the endosteal surface. These differences in osteogenic response between adult and juvenile bone are important and warrant a closer examination.

2.5.1 Mechanical Loading and the Juvenile Bone Response

It has previously been established that the rates of modelling and remodelling are highest during the growth stages of life. Modelling is largely ineffectual on adult cortical

bone, while remodelling slows after the growth phase has ended. Therefore the effects of physical activity on the developing skeleton are key, as it is more responsive to mechanical loading (Figure 2.5). There have been a large number of analyses that have investigated the response and nature of bone development related to increased activity in immature bone when compared to mature bone.

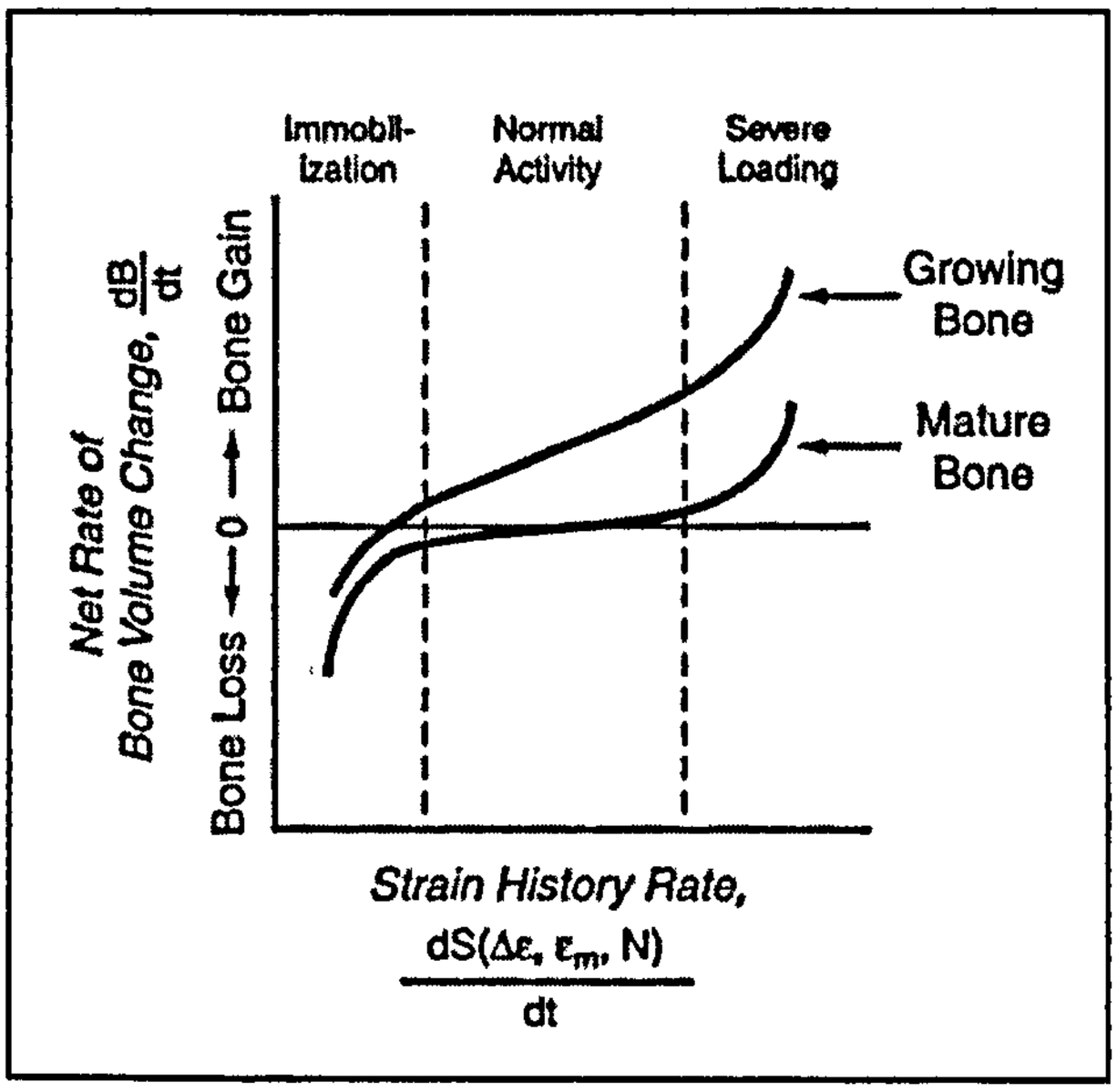

Figure 2.5: Hypothesised relationship between strain history rate and the net rate of bone volume change. This demonstrates the different rate of bone change between growing and mature bone in response to different levels of activity (after Carter and Beaupré, 2001).

Juvenile (human) bone has been found have a lower modulus of elasticity and a lower bending strength when compared with adult bone. However, it displays an increased energy absorption leading to a greater ability to undergo plastic, rather than elastic deformation (Currey and Butler, 1975). Ruff *et al.* (1994) found that prior to mid-adolescence, the periosteal envelope was most sensitive to mechanical loading while, in adults, it was the endosteal envelope that was most responsive. Therefore, increased mechanical loading in the juvenile creates thicker cortical bone while maintaining the integrity of the medullary canal, effectively increasing bone diameter. Increased mechanical loading in the adult created thicker cortical bone through intrusion into the medullary canal (Figure 2.6). These results counter those of Woo *et al.* (1981), who found increased endosteal apposition in juvenile pigs, however, as pointed out by Ruff

and colleagues (*ibid.)*, the pigs were between the ages of 1 to 2 years and that specific breed would have been sexually mature and close to full body size at that age.

One of the more recent studies examined the effects of increased activity in the femur, tibia and metatarsal of juvenile, sub-adult and adult male Dorset sheep. One group of sheep were exercised, trotting on a treadmill for 60 minutes per day for 90 days, and the other was not. Modelling, as indicated by subperiosteal expansion, was found to decline with age, but only in the femur and tibia and not the metatarsal. Yet numbers of secondary osteons, indicating remodelling, rapidly decline with age in the metatarsal, decreased negligibly in the tibia and remained static in the femur. This indicates a trade-off between modelling and remodelling in juvenile limbs, but both are reduced with age (Pearson and Lieberman, 2002). This age dampening likely relates to reductions in the number of osteoprogenitor cells that differentiate into osteoblasts, as these have been found to decrease with age (Nishida *et al.,* 1999).

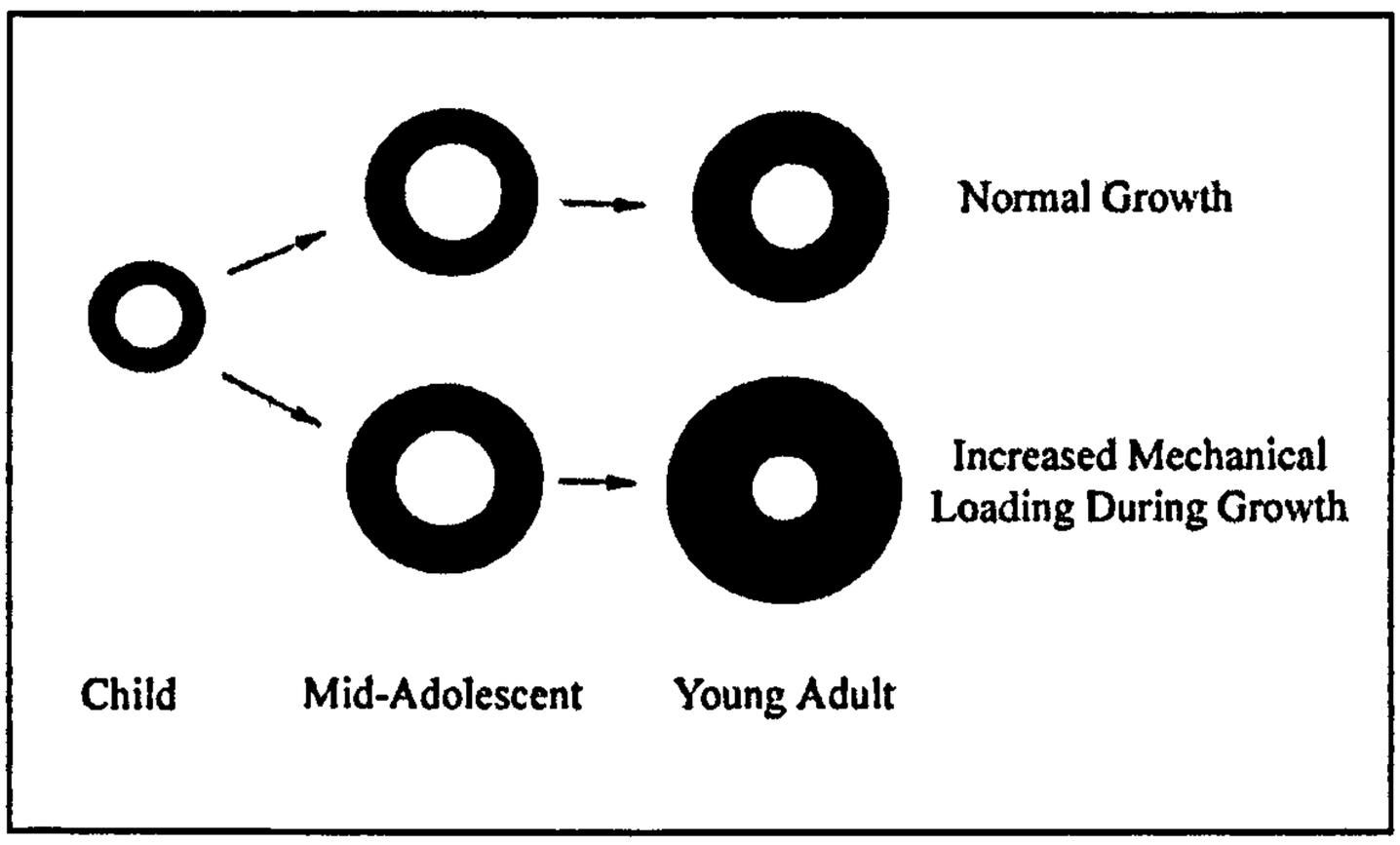

Figure 2.6: Developmental differences in cortical bone thickness between adults and juveniles under 'normal' development (top) and development with increased mechanical loading (bottom). Increased mechanical loading prior to mid-adolescence creates periosteal expansion and maintains medullary diameter. Increased mechanical in the adult reduces medullary diameter (after Ruff *et al.,* 1994).

As adults, reductions in loading inhibit periosteal expansion and increase endosteal resorption, creating cortical thinning. As juveniles, reductions in loading generate cortical thinning through increased periosteal resorption. Increased loading in

the adult creates endosteal apposition while, as juveniles, there is periosteal expansion and higher rates of bone formation. So skeletal cross-sectional geometry appears to be dependent upon the full loading history during life. However, the lack of increased bone response in the femur and tibia of adult sheep, whether related to growth or repair or not, seems to indicate that changes in the pattern of increased loading may reflect juvenile development. Adult bone appears largely affected only by decreased loading. The greatest osteogenic response is hypothesized to occur prior to puberty. The presence of the growth hormones at this time is stimulated by exercise, a process that can increase bone formation (Bass, 2000).

2.5.2 The Role of Strenuous, Habitual Loading: Sports Medicine Analyses

Intense, unilateral physical activity has been shown to create hypertrophy of the osseous elements involved. One of the early studies to recognise such changes was a radiographic study conducted by Jones and colleagues (1977). They examined a group of active professional tennis players, all of national or international ranking. Strong bilateral asymmetry was reported between the playing arm and the contralateral limb, with an average of 34.9% increase in cortical thickness in the playing arm of the male professional tennis players and a 28.4% average increase in the playing arm of the female professional tennis players. These changes took the form of a narrowing of the medullary canal, as well as increased humeral diameter. The average age of these athletes was 27 years for the men and 24 years for the women with an average time playing being 18 years for males and 14 years for females. A reanalysis of the data conducted by Ruff *et al.* (1994) found no correlation between bilateral asymmetry and either the length of playing time or the final age of the individual when examined. However, the age at which playing first began was significantly correlated with total

cross-sectional area and cortical area, but not medullary area. The expression of age-related change fit the previously identified model.

Krahl *et al.* (1994) also examined professional tennis players to determine whether or not participation in this activity resulted in any longitudinal growth differences in the ulna between the stroke and contralateral limb. Twenty nationally and internationally high-ranking tennis professionals were examined, ranging in age between 13 and 26 years. All had started playing no later than the age of 11 years. Additionally, a control group of individuals that did not participate in any type of unilateral manual labour were examined. In the tennis players, the ulna and second metacarpal of the stroke limb were both found to have a significantly greater diameter ($p < 0.01$), as well as a significantly longer length ($p < 0.01$) when compared with the contralateral limb. No lateralised differences were found in the control group. The average differences in length between stroke and contralateral limb were 3% for the ulna and 3.7% for the second metacarpal. These results are attributed to a temporary hyperaemia of the muscular system of the dominant arm, as well as a piezoelectric effect upon the growth plate, where it is stimulated by vibrations transmitted from the racket to the hand. Considering osteogenesis from activity has been found to most affect the proximal element, one must wonder what the length difference would have been identified in the humerus had it been included in the study.

Increased activity was found to increase bone mineral content in the playing arms of tennis and squash players. This effect was two times greater if the activity began prepubertal (Kannus *et al.*, 1995). Other studies investigating bone mineral content (BMC) and bone mineral density (BMD) include a 1996 study by Haapasalo *et al.*

which found intense physical loading of mature bone through playing tennis was only marginally better in increasing bone mass than everyday physical activity.

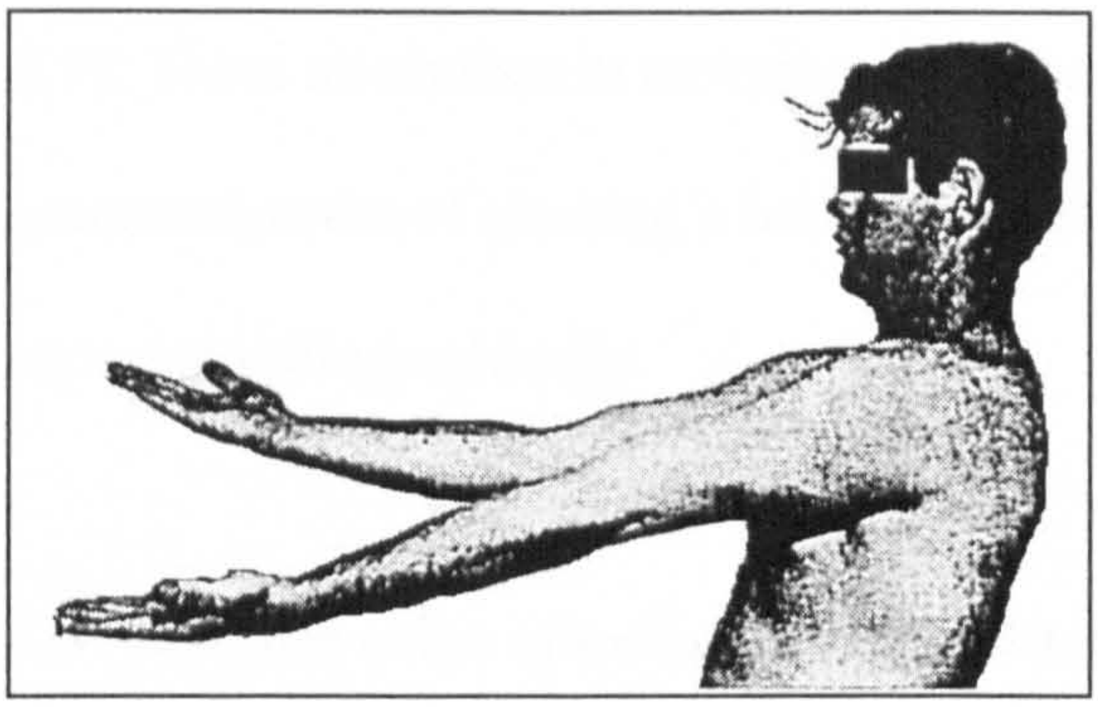

Figure 2.7: Elbow flexion contractures (left) in a professional baseball pitcher. Forearm extension is inhibited at the right elbow joint in a right-handed pitcher (modified from King *et al.,* 1969).

Figure 2.8: Valgus deformity (right) in a professional right-handed baseball pitcher. The right forearm is deviated laterally from the body when compared with the left, non-pitching arm (modified from King *et al.,* 1969).

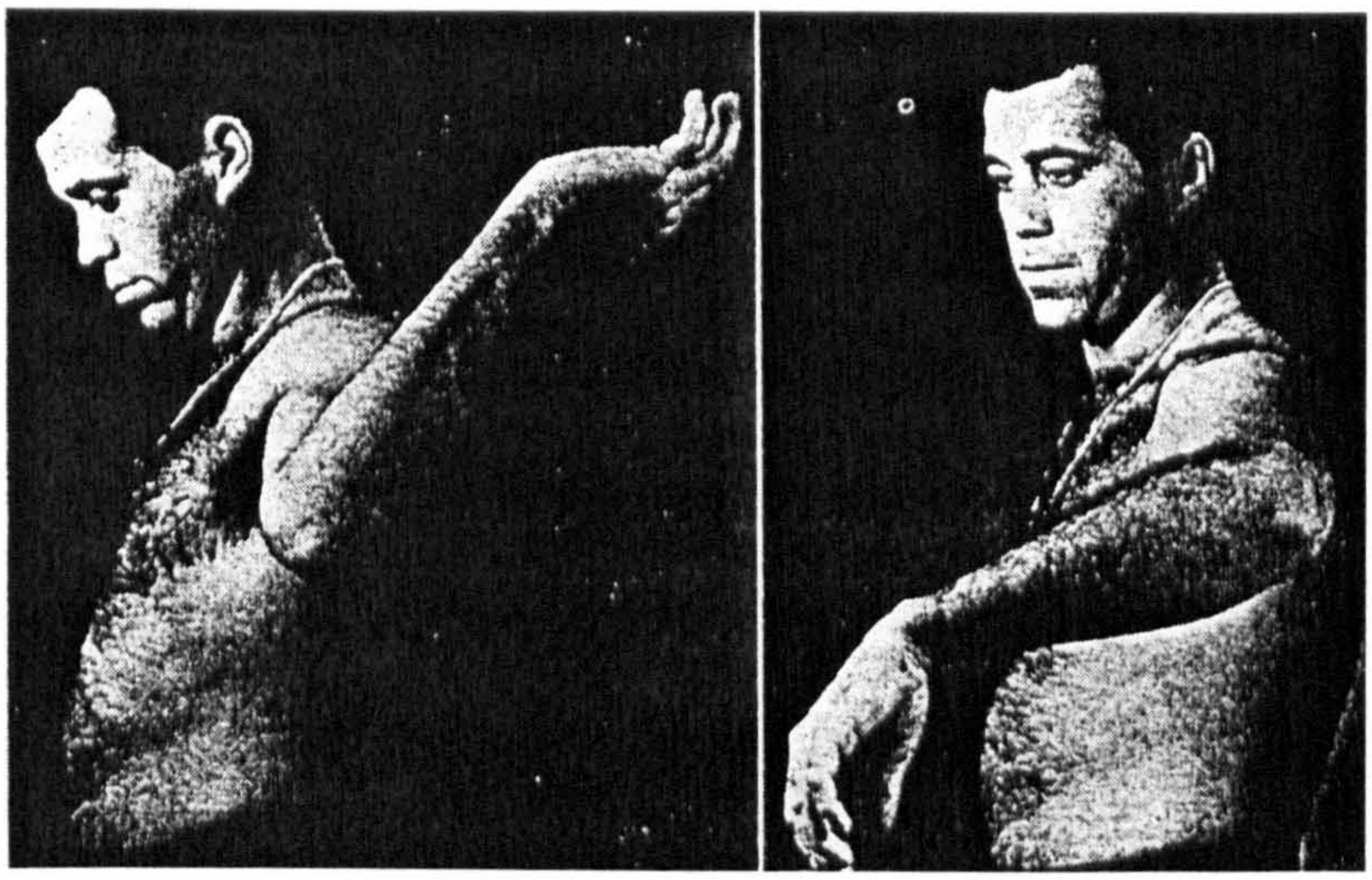

Figure 2.9: Variations in range of motion in a professional baseball pitcher. The image on the left demonstrates increased external rotation at the shoulder in the pitching arm, while the image on the right demonstrates decreased internal rotation at the should in the pitching arm (modified from King *et al.,* 1969).

Other studies have reported range of motion variations resulting from high-level sports activities. One of the earliest studies in this area was conducted by King and co-workers (1969). This study examined the elbow joint of the pitching arm in 50 professional baseball pitchers and found hypertrophy of both the soft tissue and of the humerus. Flexion contractures of the elbow were identified in over fifty percent of the

pitchers (Figure 2.7), valgus deformities (Figure 2.8) occurred in approximately thirty percent of the pitchers examined. Range of motion at the shoulder was affected, with an increase in external humeral rotation and a decrease in internal humeral rotation (Figure 2.9). These alterations in movement likely relate to an osseous adaptation to the increased stress of pitching a baseball. Increased cortical thickness and density was also reported radiographically.

Other range of motion studies include examinations of professional tennis players (Kibler *et al.,* 1996), professional baseball players (Bigliani *et al.,* 1997) and javelin throwers (Herrington 1998). All studies found increased external rotation and decreased internal rotation in the dominant, or playing arm of the overhand throwing athlete. These changes are correlated with osseous adaptations of the shoulder related to habitual activity and will be considered in more depth in the chapter discussing humeral torsion.

2.5.3 Archaeological Applications

Integration of adaptive change and skeletal anatomy in archaeological populations began with Trinkaus's 1983 study of Neandertal postcrania. The robusticity of Neandertal skeletal remains had been previously commented upon, however, this paper defines a series of functional adaptations found in Neandertal skeletons relating to robusticity or patterns of manipulation. Among these changes are increased rib thickness, a response to hypertrophy of the shoulder and back muscles attaching on to the rib. The axillary border of the scapula displays a dorsal sulcus, related to the attachment point of *M. teres minor,* one of the rotator cuff muscles responsible for lateral rotation of the humerus. Biomechanical efficiency of *M. biceps brachii* is enhanced by a medially directed radial tuberosity, which lengthens the lever arm and provides more strength during supination.

A large crest is found on the radial side of the first metacarpal, related to the increased and powerful functioning of the *M. opponens pollicis*. This muscle opposes the thumb to the rest of the hand and is used in griping actions. These and other adaptations found in the Neandertal skeleton have been interpreted to have resulted from greater postcranial strength and higher levels of activity when compared with their successors.

Trinkaus and colleagues (1991) examined several morphological features in-depth to determine the influence of robusticity and shape in Neandertal functional morphology. This involves two key principles, robusticity and shape. Variations in robusticity result from differences in biomechanical stress in similar loading patterns, while differences in shape result from differences in habitual movement patterns from biomechanical forces. A combination of robusticity and shape differences accounted for the adaptive changes in the scapulo-humeral articulation. The differences found in the pollical carpo-metacarpal articulation were attributed largely to robusticity, although this could be influenced by differences in habitual grip positions. The capitate-metacarpal articulation was found to be a function of shape, indicating different loading patterns across this articulation when compared with anatomically modern humans. Adaptational changes in the proximal femoral trabecular orientation may be a result of robusticity or may be secondary reflections of changes in shape. Cross-sectional morphology of the proximal and midshaft of the femur indicate that overall robusticity levels in Neandertals may have been only moderately greater than those found in early modern humans. However, there were significant differences in shape between the two samples. Differences in habitual levels of transverse foot stress during locomotion were identified from the diaphyseal shape of the pedal proximal phalanges.

Other archaeological applications include histomorphological studies. Stout and Lueck (1995) calculated Haversian remodelling rates for rib samples from three archaeological samples, the Early Archaic Windover site (6,900 – 8,120 Years b.p.) from east-central Florida; the Gibson sample, a Woodland site from the Lower Illinois River Valley (50 BC - AD 400), and the Ledders site (AD 1000), also of Woodland date. A modern autopsy sample was also included. The remodelling rate was calculated using a published algorithm by Frost (1987b) and the results were plotted against relative antiquity, activation frequency, net bone formation and mean annual bone formation rates. The differences found in remodelling rates, however, reflected the different ages of the adult rib *compacta* as all samples exhibited age-associated increases in net bone remodelling while decreases were found in activation rates and bone formation rates.

In a similar study, Abbot *et al.* (1996) examined dynamic bone remodelling in Late Archaic and Early Modern fossil hominids. Femoral and tibial diaphyseal fragments were compared with a pre-Columbian Native American population from Pecos Pueblo to examine osteon size, density and activation frequencies. The Pleistocene samples displayed smaller osteons and increased porosity when compared with the modern human sample. This group also displayed a lower activation frequency corresponding to lower relative bone formation rates. These findings are consistent for a skeletal structure under high mechanical loading, as higher strains will depress remodelling and stimulate modelling. However, these results could also be explained by a decrease in the threshold strain required to initiate remodelling. Reduced osteon size has also been associated with high levels of dietary and disease-related stress. So while fundamental histomorphological differences have been identified between Later Pleistocene and modern samples, it is difficult to identify the specific aetiology.

2.6 Determinants of Bone Strength: The Principles of Biomechanics

The strength of a bone may be defined by its biomechanical properties. Variations in mechanical loading affect cortical thickness, depending upon the age at which activity commenced. Other mechanical properties related to the individual's loading history may be calculated. These properties depend upon the size and shape of the structure and strength or stiffness of the material composing it. Measurement of the mechanical properties of bone is based upon the principles of beam model analysis, whereby a long bone is treated as a mechanical model. The mechanical properties measured reflect the structural properties at the measured location (Figure 2.10) (Ruff, 1992).

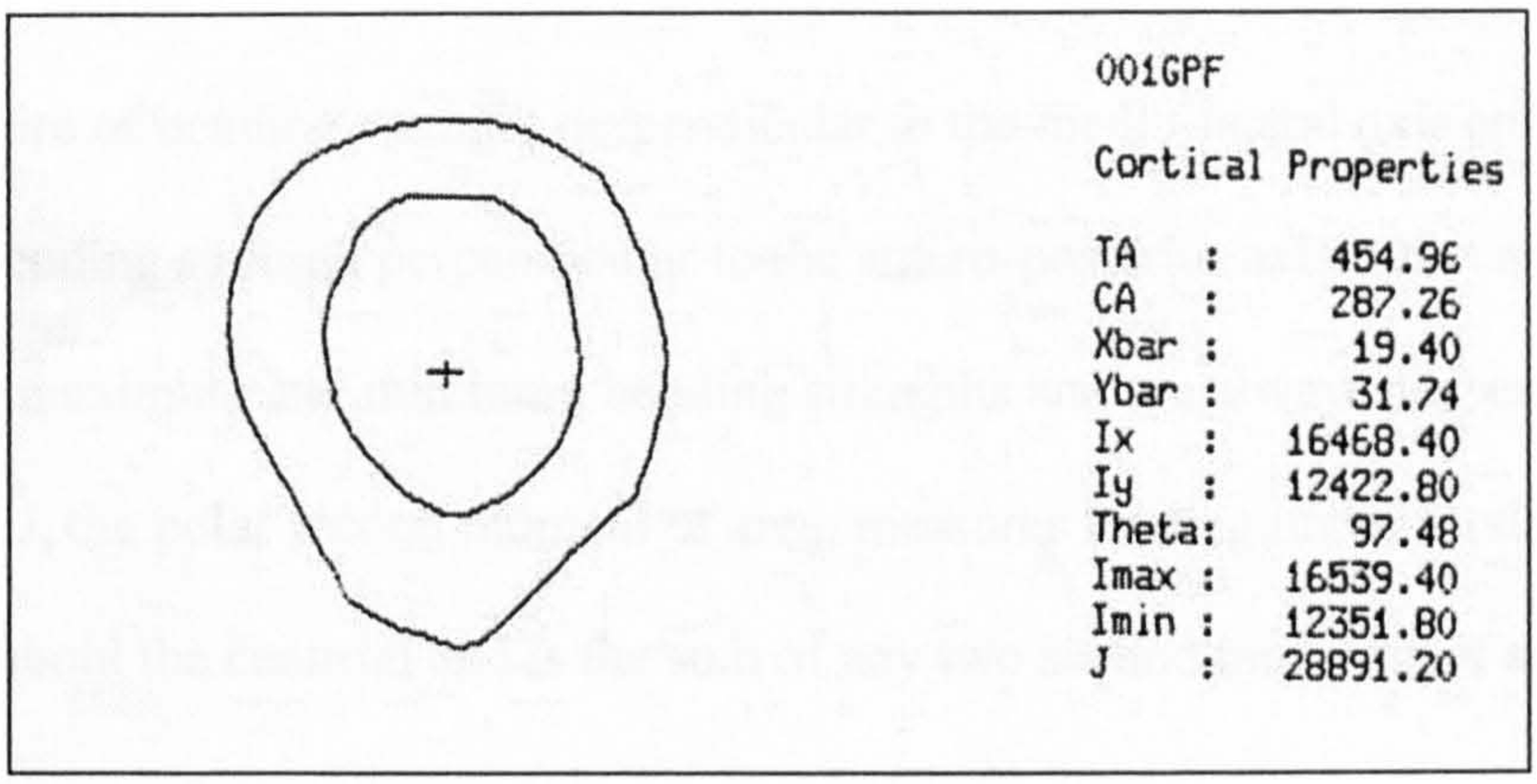

Figure 2.10: Example of a cross-sectional image and its mechanical properties. This is a computer-reconstructed cross-section of a human femur. The cross indicates the position of the centroid and the mechanical properties are listed to the side (after Ruff, 2000a).

Changes in structural properties, the cross-sectional geometry, enable inferences about behaviour through examination of how the skeletal morphology functions to counteract forces generated by movement. Differences in habitual movement patterns will be reflected in the cross-sectional geometry, as the mechanical properties relate almost exclusively to biophysical forces (Lieberman, 1997). The field of bioarchaeology has embraced biomechanical analyses and changes in cross-sectional geometry as a way of identifying changes in movement patterns between populations or at subsistence

transitions. These applications will be discussed in greater depth in the chapter on applied biomechanics.

The cross-sectional properties measured are summarised in Table 2.4. These may be considered in terms of measurements of area, such as CA, TA, MA and PCA and second moments of area, such as measures of I and J. Cortical area is a measure of a bone's strength under pure compressive or tensile loading, however, this type of pure loading pattern is uncommon. Bone is also loaded under bending and torsion, which results in adaptations in the second moments of area (SMA), these are also referred to as moments of inertia. I is an SMA that measures bending rigidity about the neutral axis. I_x is the measure of bending strength perpendicular to the medio-lateral axis and I_y measures bending strength perpendicular to the antero-posterior axis. Imax and Imin refer to the maximum and minimum bending strengths and are always perpendicular to each other. J, the polar second moment of area, measures loading under torsion. This is calculated about the centroid and is the sum of any two second moments of area calculated about a perpendicular axis, i.e. Ix + Iy (Ruff, 2000a).

As a sum of I, J may most accurately be described as an indicator of overall bending resistance. To estimate torsional rigidity, this measure should only be applied to sections that are axially symmetrical (cylindrical). Calculations of J in non-circular sections will result in overestimations of torsional rigidity and these will increase in magnitude as the sections depart from axial symmetry. Small departures from shape, up to 20%, result in negligible errors while departures up to 50% product modest errors of less than 5%. However, when the Imax/Imin ratio exceeds 1.5, the error becomes intolerable. Therefore, in sections where Imax/Imin is equal to or less than 1.5, J may be considered an accurate method for assessing torsional rigidity (Daegling, 2002).

Table 2.4: Cross-sectional properties and their mechanical significance.

Measurement	Definition	Mechanical Significance
TA	Total subperiosteal area	TA will influence the measures of shape.
CA	Cortical area	CA is a measure of strength under compressive and tensile loadings.
MA	Medullary area (TA-CA)	MA is a measure of the endosteal area.
PCA	Percent cortical area (CA/TA)*100	This is the relationship of subperiosteal to endosteal area.
J	Polar second moment of area (Ix + Iy)	The measure of torsional rigidity at the section.
I	Cross-sectional moment of area	A measure of resistance to stress in bending, as measured in the x plane (I_X) and y plane (I_y).
Imax	Maximum second moment of area	The measure of maximum bending rigidity in the plane perpendicular to the I axis.
Imin	Minimum second moment of area	The measure of minimum bending rigidity in the plane perpendicular to the I axis.
Imax/Imin	The maximum and minimum second moments of area divided by each other	A measure of asymmetry in bending strengths.
Ix/ Iy	The M/L & A/P second moments of area divided by each other	The measure and direction of asymmetry in bending strengths.

CHAPTER THREE

MATERIALS

There are several objectives directing the selection of the skeletal collections employed for this analysis. A primary goal was to create a large sample of data on humeral torsion, as there have not been large-scale investigations of this aspect of humeral architecture in archaeological samples. The core sample of this project is a group of battlefield casualties from the Battle of Towton (1461 AD) dating to the Wars of the Roses. The unusual physical morphology of these individuals relates to both robusticity and architectural changes (Knüsel, 2000a). Therefore, the sampling strategy is two-fold: to define and compare the pattern of activity-related change in the Towton population and to seek similar patterns in other archaeological populations. This requires a comparative data sample of Later Medieval period populations and a focused investigation of other battle-related or battle-injured individuals. To include a broad range of variation, two outlying samples were included, a cemetery associated with a medieval leper house and a modern, cadaver based sample. In order to position humans within the range of variation, non-human primates were also examined. This included suspensory, arboreal quadrupeds and terrestrial quadrupedal species.

As the goal is identifying activity-related change, the levels of activity vary from a suspected high activity sample such as that from a rural agricultural population to a suspected lower level activity sample such as that from a known *leprosarium*. The project seeks to identify the effects of repetitive activity linked to warfare and weapons training from an early age, an activity that is traditionally associated with males, so males rather than females were selected. However, females were included to permit assessment of potential labour distinctions in the study groups. The methods employed require complete epiphyseal fusion of the humerus, therefore this sets the minimum age

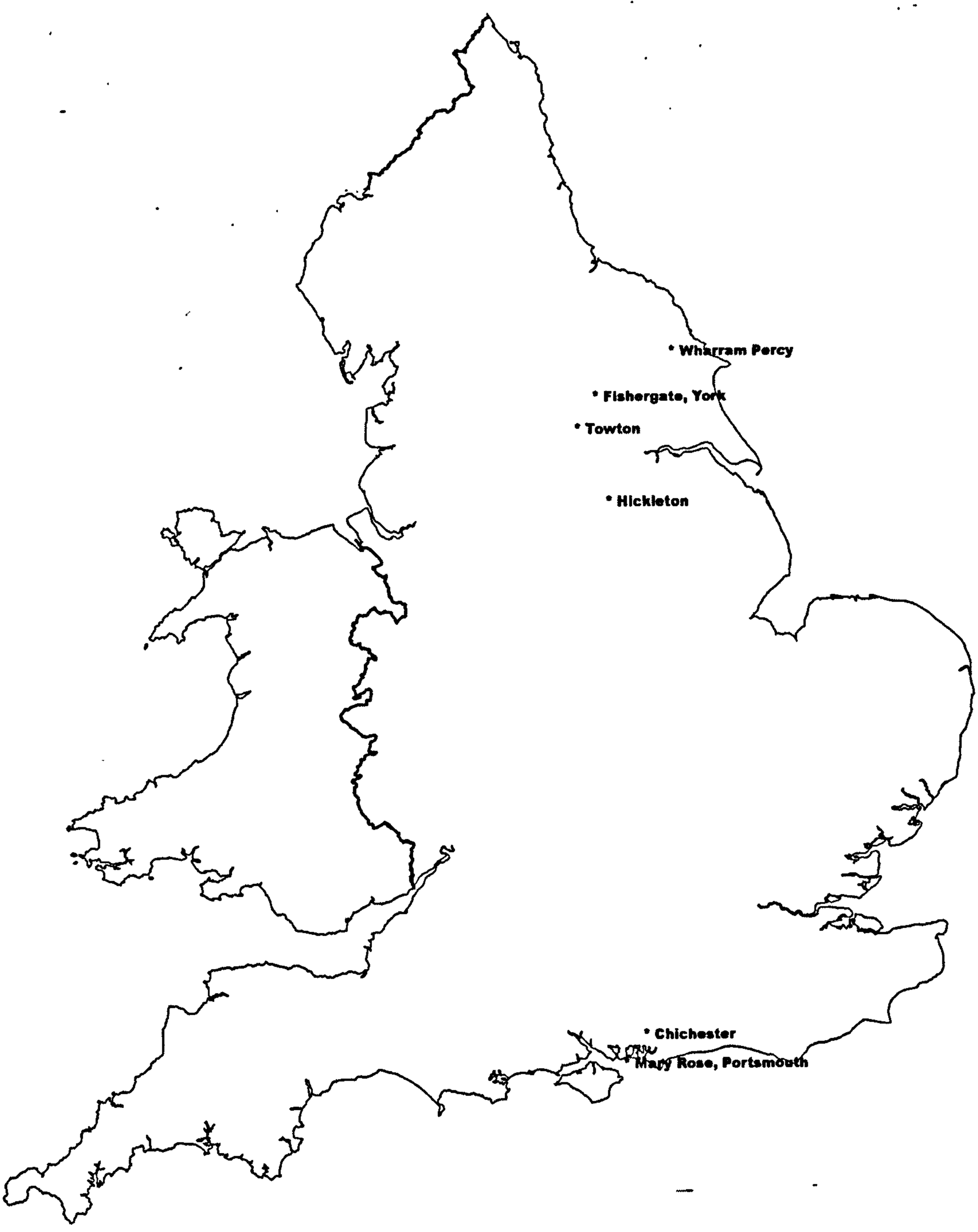

Figure 3.1: Location map of England and Wales showing the archaeological sites examined.

for inclusion at around 20 years of age at the time of death. All skeletons with at least one complete humerus were included in order to create a large enough sample for measurements of humeral torsion. All measurements were taken on the specimens by the author, although previously recorded sex and age-at-death profiles were used.

3.1 Towton

The Towton population (n = 28) consists of battlefield casualties from the historic battle of Towton (North Yorkshire, England), during the Wars of the Roses. These remains were discovered in 1996 during early construction phases of a garage block at Towton Hall, North Yorkshire. A largely voluntary staff made up of the West Yorkshire Archaeology Service and staff and postgraduate students from the Department of Archaeological Sciences, University of Bradford, conducted rescue excavation of what would prove to be a mass grave pit relating to the historic battle. There were no coffins, shrouds or identifiable grave cuts. The skeletons were articulated in the east-west directed pit with the western edge apparently the terminus of the pit while burial extended to the east into an unexcavated area (Fiorato, 2000). The skeletons were recorded using an EDM (electronic distance meter) and excavation techniques involved vertical photography of the skeletons *in situ* and EDM measurements of sixteen pre-determined anatomical markers on the skeleton. This enabled the individuation of the skeletons from their mass grave context. The skeletons were laid out in the grave both in prone and supine positions with the majority laid west to east, although others were laid east to west. One skeleton was laid in a north-south direction. Interestingly, this was the skeleton marking the western boundary of the pit. The bodies were tightly packed within the shallow grave and appeared to have been placed there contrary to the burial customs of the period (Sutherland, 2000). The Towton skeletons are now curated within the Biological Anthropology Research Centre at the University of Bradford.

The Wars of the Roses (1455 AD – 1487 AD) was a civil conflict fought between two factions each supporting their own successor to the English throne. There are probably three different groups that could be expected to have contributed to the burial, livery soldiers, mercenaries and peasants (Knüsel and Boylston, 2000). Livery soldiers were members of a noble man's retinue, raised and trained within his household to fight in his name. The mercenary soldiers were largely recruited abroad and were often highly trained specialists. They were a standard feature of European warfare from the end of the thirteenth century, although less common in England during this period (Mallet, 1999). The peasants were the least trained men on the battlefield and were often impressed into service on the way to the battlefield to make up numbers (Knüsel and Boylston, 2000). The remains represent only a small number of an estimated 28,000 casualties from the battle. The average age of those individuals selected for analysis is ca. 30 years.

3.2 Mary Rose

The Mary Rose skeletal collection also has a military origin. This collection originates from the Tudor warship the *Mary Rose*, the flagship of Henry VIII's navy that sunk during an engagement with the French in 1545 AD. The ship was found in the Solent at a 60° angle on the starboard side with anaerobic conditions preserving artefacts such as the skeletons and even items of clothing. The Mary Rose Trust was formed with Margaret Rule as Archaeological Director and excavations began in 1979 and lasted until 1982. Teams of divers brought up the commingled skeletal remains from the wreck where they were contextually labelled by deck and section. There were 12 sections across the length of the ship (40.90 metres from stem to stern) and five decks, including the castle, upper, main, and orlop desks, as well as the hold. The Anthony Roll, an administrative document relating to Henry VIII's navy, lists a total crew of 200

mariners, 185 soldiers and 30 gunners (Stirland, 2000). These remains are curated at the Mary Rose Trust, Historic Dockyards in Portsmouth, Hampshire.

This collection was re-articulated based upon morphological and metric similarity in the skeletal elements of a given context to create 92 fairly complete individuals (Stirland, 1992). However, the stratigraphical and contextual issues with the collection have led to it being treated in this analysis as largely disarticulated. Stirland (2000) identified all skeletal remains as those of males. While some humeri displayed obvious examples of a young age such as incomplete fusion of the proximal epiphysis, there is no way of reliably determining age-at-death of the older individuals directly from this element. The sample is made up of 50 'fairly complete' skeletons and 75 disarticulated contexts, often containing more than one humerus for a total of 76 right humeri, 90 left humeri, 166 total analysed.

3.3 Fishergate

The Fishergate sample is from the Church and Gilbertine Priory of St. Andrew, Fishergate in York, North Yorkshire. This collection is stored in the Archaeological Resource Centre, curated by the York Archaeological Trust (YAT). The site was excavated by YAT in 1986 revealing the main priory buildings and cemetery. The priory of St Andrew, Fishergate, belonged to the Gilbertine Order and was a house for canons (i.e. males) only. It was one of the smaller Gilbertine houses, with an initial complement of twelve canons, founded between February 1195 and 1202 AD. St. Andrew's was never a wealthy house and had received grants in 1335 AD towards the repair of buildings owing to its impoverished state. It was also exempted from the payment of the tenth on account of its poverty during the mid to late 15th century. The

Priory of St Andrew survived the Dissolution of 1535 only to be surrendered three years later, in 1538 (Kemp and Graves, 1996).

The priory of St. Andrew, Fishergate, unlike other Gilbertine foundations, was an urban establishment and remained so throughout its existence. It did maintain rural holdings, although it would appear this was for rental income rather than direct agricultural use. Novices were not admitted into the community until the age of 15 years with the majority of entrants to the Order originating from knightly or noble families. It has been recorded that benefactors of the Order joined the community later in the life of the priory. Other members would have been recruited from the ranks of administrators of baronial households and the local gentry. The lay brethren were typically recruited from the peasantry and were not sworn in until the age of 24. Their role in the community was as a ready labour force (Golding, 1995). The Gilbertine Order was poor in comparison with the other Orders (Graham, 1901). It is difficult to describe the typical daily life in the Priory of St. Andrew, as this house was unusual in several aspects. Firstly, the Gilbertine Order usually included a double house with an associated nunnery and, secondly, the priory in York was only one of two urban houses established by the Gilbertines.

The Fishergate sample in York has three distinctive burial areas relating to different economic and social status groups. These cemetery groupings date from the 13th – 16th century (phase 6) and are associated with the new Priory of St. Andrew of the Order of St. Gilbert of Sempringham. The eastern cemetery contains the burials of the members of the monastic community, indicated by the distinctive arrangement of the burials and the absence of female burials. This part of the sample is made up of thirty-five males and two females with the two female burials occurring on the northern fringe

of this group. The first row of thirteen burials is thought to represent the interments of the original twelve canons of the Priory (Kemp and Graves, 1996).

From the intramural burial locations come fifty-seven males and eighteen females. Socially identifiable contexts include two burials from the presbytery that appear to have been grouped around or beneath an altar. These burials have no markings of wealth but their location suggests importance within the community, perhaps priors or cellarers. The north transept chapel appears to have been used for high status burials and three skeletons from stone coffins were examined in this group. Three burials were included from the chapter house; one was located separately from the other two and appears to be a person of significance, a founder or prior. The other two burials include a blade-injured male and what appears to have been a fat male as suggested by the grave size. It was suspected by the excavators that these two graves were probably not members of the priory community as one had died from perimortem trauma. Burials in the cloister garth appear to be of lay men and women of enhanced socio-economic status as indicated by the presence of a number of burials in stone coffins, as well as graves lined with tiles. In the cloister garth is a grave containing three males, all blade-injured. It is suspected that these must have been secular individuals with special status within the community. Burials within the nave appear to have been of middling status, with some in stone coffins, but the majority in wooden coffins or simple graves. The crossing area also appears to have been used for interment of poorer members of the lay community (Kemp and Graves, 1993).

There is also a separate secular grouping in the southern area from which twenty-nine males and eight females were analysed. This area contains the contextually identified burial of a priest, identified by a chalice and paten found within his grave.

This cemetery appears to have been created for the resident lay workforce because it does not represent a 'normal' medieval cemetery; as there is a high ratio of males to females. It is presumed to have been used by a resident lay workforce with some parishioners interred (Kemp and Graves, 1993). There were no restrictions on lay burials, and it was open to both the wealthy and the poor (Golding, 1995).

Additionally, the Fishergate collection has two groups of blade-injured individuals in addition to those noted above. These are individuals displaying perimortem trauma from weapon injuries that occurred at or about the time of death. Hence, it may be assumed that they were combatants at the time of death. There are nine blade-injured males from the 13th – 16th century levels, four of which have been mentioned previously in the chapter house, and cloister garth. Additional intramural blade-injured burials are found, one in the crossing and two in the nave. There are also two blade-injured males buried within the southern cemetery group. However, the largest group of blade-injured individuals (20) date from the late 10th – early 11th century. It would appear from the context and the blade-injuries that these individuals may have been interred at the same time, having received their wounds in a single violent event, thought to be the Battles of Fulford or Stamford Bridge (1066 AD) or the Battles for York Castle (1067-9 AD) during William I's harrying of the North (Kemp and Graves, 1993). This early context pre-dates the founding of the Priory of St. Andrew and comes from a previously established parish church, dedicated to St. Andrew. The average age-at-death for the Fishergate males collectively is mid-30's while the blade-injured males died much younger, in their early 20's. The average age at death for the Fishergate females is early-30's. This sample has been analysed as a whole, in terms of blade-injured versus non blade-injured, as well as being divided by cemetery location.

3.4 Wharram Percy

In contrast to the battlefield and urban contexts are two rural sites. The first, Wharram Percy, dates from 950 – 1500 AD and is located on the Yorkshire Wolds. Wharram Percy was excavated as a Deserted Medieval Village Research Group project beginning in the 1950's. The site consists of a collection of medieval peasant farmsteads, two manor houses and a central church. The farms were converted to sheep pasture in the 15th century and, by 1500 AD, the village was deserted, although burials from surrounding villages continued in the church until the 19th century. These remains are housed at English Heritage, Fort Cumberland, Portsmouth, Hampshire.

There are nearly 1000 skeletons associated with this site, with approximately one-third of the graveyard excavated. The majority of the burials are simple graves of peasant farmers from the surrounding area. There are a number of higher status intramural burials dating to the seventeenth and eighteenth centuries while Anglo-Saxon stone cysts and stone slabs indicate higher status burials in the earlier phases of the site. The inclusion of a chalice and paten identify one burial as that of a priest. Phasing was established through radiocarbon dating and is divided into four periods; late Anglo-Saxon (950 - 1066 AD); early Medieval (1066 – 1348 AD); later Medieval (1348 – 1548 AD) and Post-Medieval (1540 – 1850). While the phasing of this site dates prior to the Norman conquest (1066 AD), earlier than detailed in the original project design, these early skeletons have been included for two reasons. The first is that there is no reported variation between the ninth century skeletons and the eighteenth century as this was an isolated rural parish community who would have been largely unaffected by the activities occurring outside of it (Mays pers. comm.). The second reason for the inclusion of the earlier skeletons is that the broad temporal range this site offers is excellent for determining any temporal variation in humeral torsion or robusticity. One-

hundred and fifty-one male skeletons and 95 female skeletons were examined across the four periods with an average age-at-death for the males of around 40 yrs while the female age-at-death profile is slightly younger, in the early 30's. There are indications that life was hard for the peasants of Wharram Percy as evidenced by the exceptionally high infant mortality rates and stunted growth development of the juveniles (Wrathmell, 1997). This sample has been analysed both as a homogenous unit, as well as being divided up into the different time periods to examine the temporal dimension.

3.5 Hickleton

Little is known about the second rural site, Hickleton. It consists of a small number of burials associated with St Wilfrid's Church, Hickleton, South Yorkshire. The site was excavated by the South Yorkshire County Council Archaeology Service in 1983 following a project to stabilize the church structure. Burials span the period from the establishment of the Norman church in 1050 – 1100 AD to the 1850's when an Act of Parliament stopped burials within churches. The largest number of burials occurred within the church, although there are burials associated with the churchyard (Sydes, 1984). The samples consist of eight adult males with an average age-at-death of mid-30's and eight adult females with an average age-at-death of mid to late 20's.

3.6 Chichester

The Chichester assemblage consists of the medieval leper hospital of St. James and St. Mary Magdalene and is curated at the Department of Archaeological Sciences, University of Bradford. The hospital was founded before 1118 AD as a *leprosarium* but later became an almshouse for the poor. The last recorded mention of lepers occupying the hospital was in a will dated to 1418 AD. The constitution was amended in 1540 to admit women as part of its official transformation into an almshouse. Interments date

from the 12th to 17th century with lepers, the master and occasional benefactors largely comprising the burials up to the 15th century. From the 15th to 17th centuries, burials relate to the almshouse that functioned to provide care and shelter for its inmates, individuals with various diseases, deformities or listed simply as 'idiots' (Magilton and Lee, 1989).

Excavation began in 1986 of the southeastern area of the cemetery. Three discrete areas were highlighted during the excavation, the western-most area is considered the earliest part of the cemetery. Most of the burials are male in this area, and it has the greatest concentration of leprous individuals. Many graves intersect one another as if there had been limited room for interment. The second area is more disorganised than the first, with no obvious plan for interment. This area was of mixed sex with a localised area for immature individuals. The third area is more organised, with east-west aligned graves in rows. This area is thought to relate to the almshouse phase of the site as the graves are of mixed sex and there is a wider range of pathological conditions present. The burials were interred in wooden coffins indicated by the survival of coffin nails (Magilton and Lee, 1989).

The skeletons display various pathologies from leprosy and tuberculosis to numerous traumatic lesions. One-hundred ninety-three male skeletons were examined with an average age-at-death profile in the mid 30's. Seventy-two female skeletons were examined with an average age-at-death in the late 30's. This population was analysed as a whole, as well as being divided up based on status to compare the chronically ill with the skeletally 'healthy' individuals.

3.7 Terry Collection

The Terry collection was started in the 1920's at Washington University Medical School in St. Louis, Missouri, and is now housed at the Smithsonian Institution, National Museum of Natural History in Washington, DC. The cadavers came from either unclaimed bodies or had been signed over to the state by relatives. These were then sent to the Medical School for dissection and curation of the skeletons. Consequently, these skeletons possess documentation in the form of morgue records that included known age, sex, ethnic origin, cause of death and pathological conditions. A number of the skeletons have occupations listed. The majority of the cadavers originate from the lower classes; however, from 1955-6, Missouri law required signed release documentation from the individual or their immediate family. This legal change altered the demographic profile to include more middle or upper middle class individuals (Hunt, 2000). Typical causes of death for these individuals range from cancer and heart disease to tuberculosis and syphilitic-related conditions, alcoholism and gunshot wounds. Many of the causes of death reveal the transient life many of these individuals would have lived.

The selection criteria for the Terry collection involved examining the humeri of white males only, as these are European in origin and most similar to the other samples analysed. The first priority was to examine the humeri of men of known occupations (n = 70). The next priority was to examine middle class individuals (n = 7, two of those were of known occupation). As the Terry collection has reliable age-at-death profiles for the individuals, it provides a good opportunity for an accurate temporal investigation of humeral torsion and other architectural features. Therefore, the age-at-death profile was expanded from the original age cut-off of 50 years of age to include a sample of skeletons up to the ninetieth decade of life. This has the benefit of including a number of

individuals who would have been born from 1841 onwards, a time when the American Midwest was in the process of increased settlement. Many of these older individuals would have grown up on farms rather than in a city and may be expected to display contrasting humeral morphology in their upper limbs. A total of 181 skeletons were examined from this collection: seven under the age of 20 years; 10 aged 21 – 30 years; 27 aged 31-40 years; 50 aged 41-50 years; 40 aged 51-60 years; 20 each aged 61-70 and 71-80; and 10 skeletons aged 81-90 years at death.

3.8 Non-Human Primates

In order to establish the uniqueness of the behavioural morphology of the human humerus, non-human primates were examined from the collections of the Natural History Museum, London. The collections at the Natural History Museum are largely formed of wild-shot animals; however, a small number of zoo animals are included, including one orangutan from the Jersey Zoo, Channel Islands and the female *M. aractoides* macaque. The sample consists of *Pongo pygmaeus*, commonly known as an orangutan (N = 13 male, 3 female), a species that locomotes both arboreally and with an increased frequency terrestrially, when in captivity, with their limbs displaying extreme specializations for suspensory behaviour. Females and immature orangutans are almost exclusively arboreal while older males are often found travelling across the ground. Orangutans use all four limbs whether it is by quadrumanous climbing within the trees or quadrupedally on the ground (Fleagle, 1999).

Fourteen male and nine female *Gorilla* were examined, as well as thirteen male and three female *Pan troglodytes*. Both of these species are knuckle-walking quadrupedalists with episodes of arboreality. However, chimpanzees exhibit a greater frequency of suspensory behaviour than gorillas but considerably less than that observed

in orangutans (Fleagle, 1999). The final species examined were monkeys of the genus *Macaca*. Macaques vary considerably in the extent that they are arboreal or terrestrial. All species use both settings to some extent but with different frequencies. Seven macaque species were examined, *M. sylvanus* (1 male, 1 female); one male and one female *M. nigra*; one female *M. silenus*; two female and one male *M. fascicularis*; one male *M. mulatta*; one *M. fuscata* of indeterminate sex and one male and one female *M. arctoides*. While behavioural differences related to locomotion are likely to exist between species, sample sizes regrettably require them to be considered as a whole under the genus *Macaca*.

Table 3.1: Number of humeri examined by collection and total individuals examined*.

	Right humeri	**Left humeri**	**Total individuals**
Towton	28	25	28
Mary Rose	76	90	90**
Fishergate	141	140	167
Wharram Percy	135	131	246
Hickleton	16	16	16
Chichester	149	149	271
Terry	180	180	181
Pongo	16	15	16
Pan	14	15	17
Gorilla	28	26	23
Macaca	11	12	12
Totals	**794**	**799**	**1067**

*Totals are based upon the maximum number of values returned for either humeral max. length, humeral minimum breadth or humeral torsion, whichever was greatest.
**Mary Rose totals are based upon minimum number of individuals.

CHAPTER FOUR

METHODS

A series of measurements were applied to humeri in order to characterise and define the shape difference observed in the Towton humeri. These architectural changes included variations in humeral torsion, a medio-lateral increase in the distal humeral pilaster and a diaphyseal flattening also located in the distal humeral shaft. This flattening was often found with an increased supracondylar breadth medio-laterally (Figs. 4.1 – 4.3). A lateral deviation, e.g. bowing, was often noted where the distal end of the humerus appeared in a valgus position. Humeral shaft bowing was noted both in an antero-posterior direction, as well as a medio-lateral direction. Once these changes were defined, quantification methods were developed or adapted from already existing metric variables. A series of tests were preformed in the lab over an extended period of time to determine the accuracy of the new or adapted metric techniques to ensure accurate and reliable results. Many of the measurements and indices recorded are taken from the palaeoanthropological literature, where detailed recording of morphology is essential to species designation (see, for example, Lieberman, 1997; Trinkaus, 1983).

This project may be described as an analysis of robusticity and its relationship to architectural form. As such, it is important to distinguish between factors of robusticity and shape. Changes in robusticity result from different levels of biomechanical stress while changes in shape result from different patterns of biomechanical forces (Trinkaus *et al.*, 1991). The measurement variables have been chosen to reflect robusticity and architectural differences between populations. Humeral architecture should not be correlated with body mass, as it is there is no direct relationship between humeral architecture and body size in the same way the lower limbs do vis-à-vis locomotion.

However, different body sizes exist as indicated by relative bone size. The use of robusticity and other size-standardised indices were used to accommodate this.

Figure 4.1: Architectural changes in the distal humeral pilaster region of Towton 13. The line indicates the 20% slice parameter across the pilaster. Note the increased medio-lateral supracondylar area and swelling of the pilaster on the left distal humerus. Photograph by author.

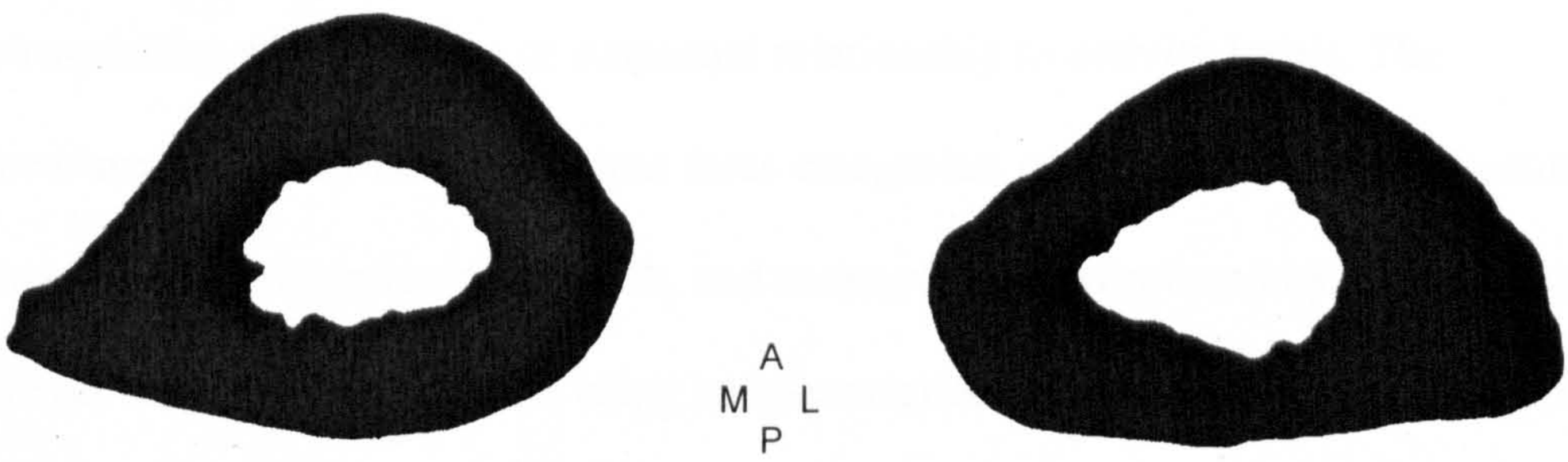

Figure 4.2: Right and left 20% slices of Towton 13. These slices correspond to the markings in figure 4.1 and demonstrate the swelling of the left pilaster compared to the right and the increase in medio-lateral dimension of the supracondylar area.

Common osteological practice to compensate for missing values through a regression equation based upon the contralateral element was not followed here as this would impose uniformity where it may not exist. As the sampling strategy was to maximize data collection, it was felt there was little to gain from this method and much to lose in the robustness of asymmetry values. Nevertheless, where maximum humeral

length could not be obtained due to fragmentation or incompleteness of one element, the maximum length of the contralateral limb was used to estimate the circumference parameter. The total variation between limbs generally falls within a few millimetres and bone topographic features can help identify the circumference location. Additionally, humeral torsion was estimated when the humerus was fractured across the humeral head but leaving enough bone such as to identify the orientation of the humeral head. Statistical analyses employed the statistics software package SPSS. The tests preformed depended upon the populations and or question asked of the data. Common tests included tests of normality, independent T-tests, both for parametric and non-parametric data, ANOVA, and bivariate correlations.

4.1 Measurement of Skeletal Variation

Skeletal variation was measured through 25 measurements of the humerus, nine indices defining robusticity and shape and three observations of pathology. These variables were chosen to record size and shape characteristics of the humerus with a specific focus on variables with a known or suspected relationship to activity levels. The measurements may be divided into three categories: measurements of architecture, measurements of articular surfaces, and measurements of robusticity. The measurements are reported here in bold face using an abbreviation of the full measurement title. A complete list of the measurements with abbreviations and operational definitions is found in Appendix I. All measurements were recorded in millimetres.

4.1.1 Measurements of Architecture

The measures of architecture were taken from established measurement criteria in addition to measurements created specifically for this analysis. Humeral shaft bowing was measured in a proximal, distal and medio-lateral location (**HPBW**, **HDBW** and

HML) (Fig. 4.3). Diaphyseal breadth (**HDT**) and supracondylar breadth (**HSB**) of the distal humerus defined changes in the pillar region at the 20% slice location. A series of angles forms the next set of architectural measurements, including the maximum humeral cubital angle (**MXCUB**).The humeral torsion angle (**TORSION**) will be dealt with in more detail later in the section. Anterior curvature (**ANTCURV**) is a measurement of the angle of humeral shaft in relation to the midtrochlear distal transverse axis (Figure 4.4). The spiral angle (**SPIRAL**) is a measurement of the bicipital groove in relationship to the axis of the humeral head. The diaphyseal flattening index (**HDT / HSB**) defines humeral morphology at the 20% slice region.

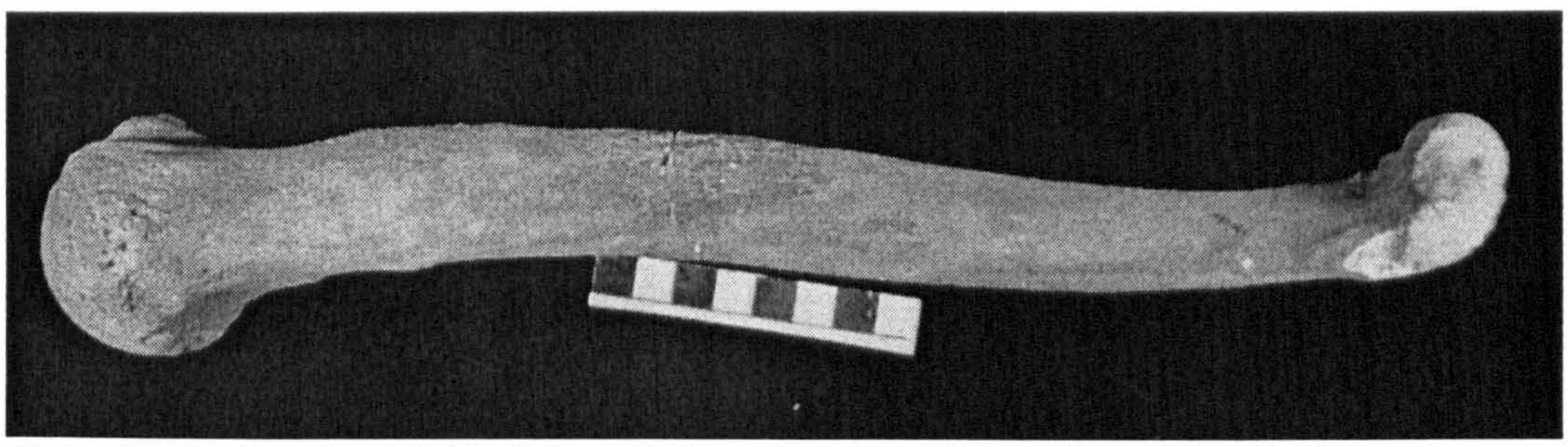

Figure 4.3: Proximal (**HPBW**) and distal bowing (**HDBW**) in the right humerus of Towton 16. The amount of proximal bowing measures the amount of posterior bowing to the proximal shaft, while the distal bowing quantifies the amount of anterior bowing to the distal shaft. Photograph by author.

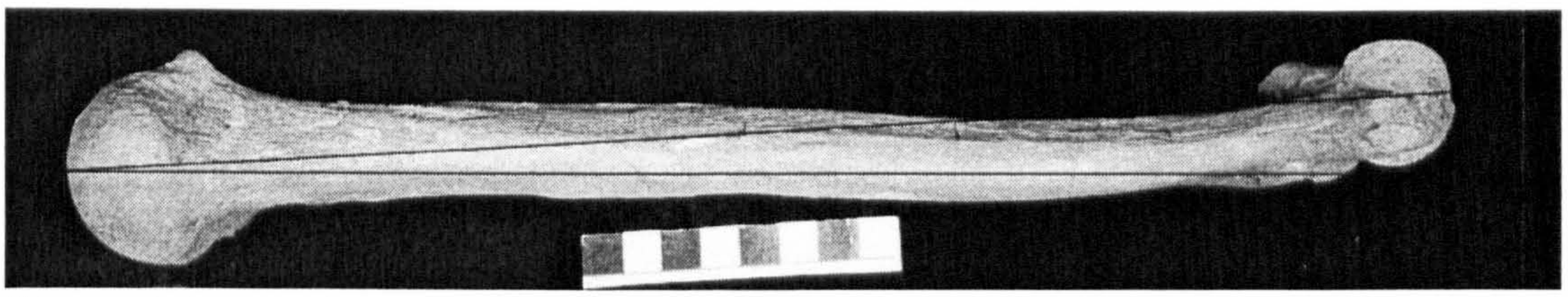

Figure 4.4: Anterior curvature of the distal humerus (**ANTCV**). The angle between a diaphyseal axis as measured from the midpoint of the humeral head, to the mid-trochlear axis, viewed medially, is measured. Note: these axes are approximate in this illustration. Photograph by author.

4.1.2 Articular Robusticity

While articular surfaces appear to be less responsive to activity levels compared to the diaphyseal shaft, they are still valuable measurements and form a large part of this analysis (Pearson, 2000; Lieberman *et al.,* 2001). Measurements of the proximal

humeral head include the transverse (**HTH**) head breadth, taken in an antero-posterior direction (or medio-lateral direction depending upon the amount of humeral torsion). This measurement forms the humeral head index, a standardisation of the transverse humeral breadth (**HTH / HL**) X 100. The distal epiphysis is characterised through measurements of the articular breadth of the trochlea (**HTB**). The capitulum is characterised by capitulum height and breadth (**HCH, HCB**). The final measurement is distal articular breadth (**HDAB**) spanning the width of the trochlea and capitulum. The indices formed by these variables include the distal articular breadth index (**HDAB / HAL**) X 100, the articular / epicondylar index (**HDAB / HEB**) X 100 and, finally, the capitular index (**HCB / HCH**) X 100.

4.1.3 Measurements of Robusticity

Robusticity measurements reflect different levels of biomechanical stress between populations and may be used to determine general activity levels. The external robusticity of a skeletal element may be described by its thickness, diaphyseal or epiphyseal, relative to length or another mechanically relevant measure of body size. Alternatively, robusticity may be determined by the degree of muscular development as inferred from muscle scars (Pearson, 2000). Therefore, a robusticity index can involve either a diaphyseal or epiphyseal variable.

Measurements of robusticity include the standard measurements of maximum humeral length (**HL**), humeral articular length (**HAL**), and the minimum diaphyseal circumference (**HC**). The humeral robusticity index is formed by minimum circumference divided by humeral length (**HC** X 100) / **HL**. The maximum breadth at midshaft (**HMXM**) and the minimum breadth at midshaft (**HMNM**) are measured to create the midshaft index (**HMXM / HMNM**). Robusticity as characterised by muscle

insertions include measurements of the greater tuberosity (**HGT**) and the greatest diaphyseal breadth at the deltoid tuberosity (**HGBD**). A more focused investigation of M. *deltoideus* measures the antero-posterior breadth of the crests forming the deltoid tuberosity (**HDB**), as well as the greatest circumference at the deltoid tuberosity (**HDC**). The deltoid index is formed from these measurements (**HDB / HDC**) X 100. Distally, the epicondylar breadth (**HEB**) was measured. This quantifies the width of the medial and lateral epicondyles which form the insertion sites for the common flexor tendons (medially) and the common extensor tendons (laterally). This is standardised to form the epicondylar index (**HEB / HL**) X 100.

4.1.4 Humeral Torsion

Anatomists, orthopaedists, sports medicine specialists and physical anthropologists have studied humeral torsion with varying conclusions. Early views saw humeral torsion as a taxonomic trait, specifically, one of the defining traits between late archaic and early modern/recent humans (see Boule, 1911-1913). These differences are now viewed as adaptive changes rather than as a taxonomic variation (Vandermeersch and Trinkaus, 1995). A definitive study of humeral torsion from fish to man concluded that humeral torsion is the result of an evolutionary, primary torsion upon which are seen the effects of ontogenetic, or secondary torsion, which is produced by muscular action (Evans and Krahl, 1945). C.P. Martin, an anatomist, summed up the implications of humeral torsion in his 1933 publication whereby he states that humeral torsion is "greater in female than in male skeletons, it is greater in weak than in strong skeletons; and, in the same individual, it is generally greater in the bone from the left side than that from the right" (1933; p. 574). This suggests that torsion is related to a relative weakness of the bone rather than muscular development. These and other theoretical aspects relating to

humeral torsion will be discussed in greater depth in a later chapter, along with the results of the analysis of humeral torsion.

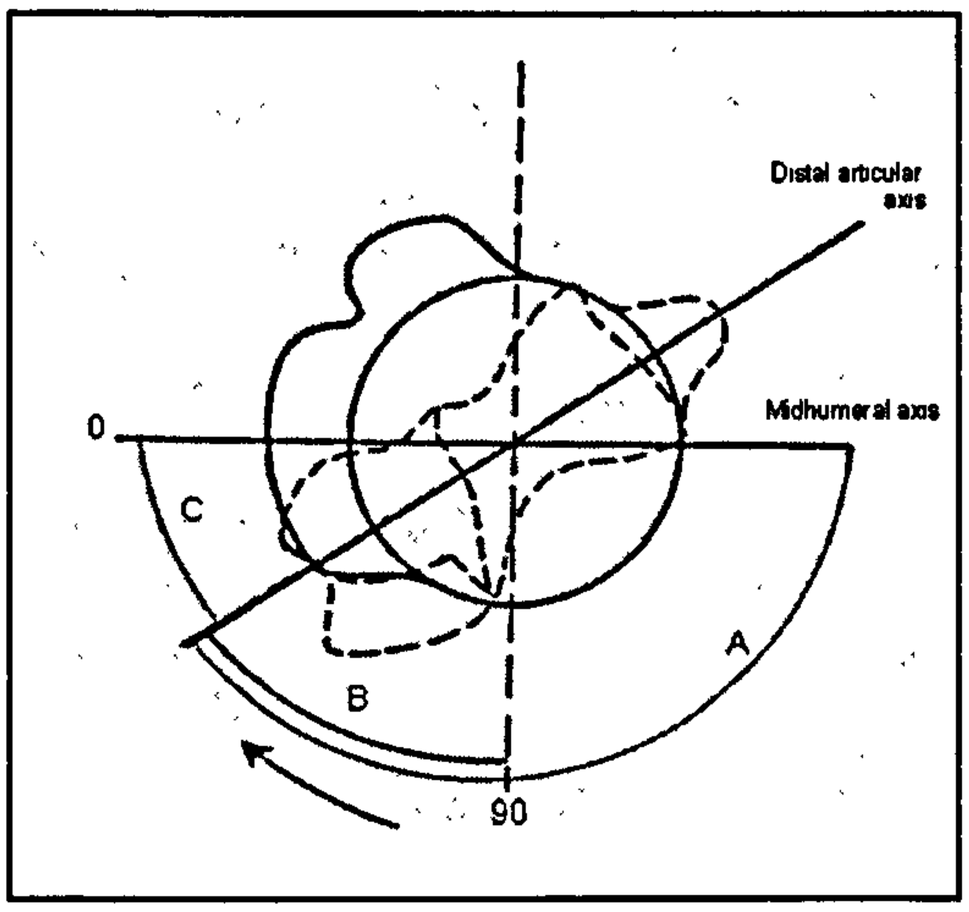

Figure 4.5: Humeral Torsion

- Anatomists and biological anthropologists quantify torsion as occurring in a medial direction (Angles A & B).
- Orthopaedic clinicians quantify torsion or 'retroversion' through the degree of posterior 'twisting' that occurs (Angle C).
- This analysis quantifies humeral torsion through measurements of Angle C.

Image modified from Krahl (1947).

While the various fields have all measured torsion in comparable ways, the method of reporting these findings vary between studies. The angle Martin was measuring, while still being that formed between the proximal and distal articular surfaces, was quantified in terms of the obtuse angle rather than the acute. Functionally, this relates to Angle A in Figure 4.5 and would give a maximum value of 180°. Studies conducted by Evans and Krahl (1945) measured torsion in terms of Angle B, as they believed a 90° rotation that occurs in embryonic development should not be included in the measurement. Therefore, using this method, the maximum value of torsion will not exceed 90°. Most clinical studies report torsion in terms of Angle C, as does this study. This method is the most straightforward as it simply reflects the angle between measured variables, with no assumed evolutionary or embryonic rotation. Therefore, the results of the study are comparable to those found in the clinical medical and sports medicine literature. Where necessary, values have been converted to relate Angle C. This involves subtracting the torsion value from either 90 or 180, depending upon the study. In practice, this would convert the value of 162°, the average for a male French

population as measured by Broca (1881), to 18° or the value of 71.8° to 18.2°, as in a population of white males as measured by Evans and Krahl (1945).

Functionally, measuring humeral torsion involves definition of the angle formed by the proximal and distal articular axes. Variations on the definition of these axes are found in the literature. Stirland (1993) used a line bisecting the muscle insertions *M. supraspinatus* and *M. infraspinatus* proximally. The distal axis was defined as a line bisecting the medial and lateral epicondyles. As these are muscle sites and, as such, subject to plastic change, when considering the orientation of the medial and lateral epicondyles, this method was not employed. Instead, the author employed the definition originally given by Krahl and Evans (1945) and followed by Larson (1996). The midhumeral axis was defined as a line drawn through the centre of the humeral head dividing it into anterior and posterior halves. This was determined by a transverse measurement across the humeral head that was then pencilled-in to form the proximal axis. In practice, this line would commonly occur between the insertion sites of *M. supraspinatus* and *M. infraspinatus*, however, this did vary enough to leave the proximal humeral axis as employed by Stirland undesirable as a rigid axis point. The distal axis was defined as a line passing through the centre of the trochlea and capitulum. This line is commonly known as both the transverse distal articular axis and the articular axis.

The measurement of humeral torsion involves a laser torsiometer, designed after the specifications found in Krahl (1976). The humerus is placed in a retort stand with the midhumeral axis aligned with 0° on the protractor and firmly clamped into place. The bone is then rotated 180° in the stand to expose the distal articular axis to the laser beam. The laser is then rotated along the protractor until reaching the distal articular axis. The measurement is then read and recorded.

4.2 Pathological Analysis

A limited study investigating pathological conditions focused on identifying any signs of repetitive stress syndrome and other injuries related or considered to be related to specific movement patterns or activities. These included avulsion injuries and lesions at the medial ulnar collateral ligament attachment point (see Appendix I).

An avulsion injury is a type of traction fracture occurring at the insertion of a tendon or ligament. This may occur in isolation or as part of a more complex fracture or dislocation. The degree of the avulsion varies. In adults only small fragments of bone may be pulled away yet in children or adolescents, an avulsion injury may result in separation of the apophysis (Resnick *et al.*, 1995). Medial epicondylar avulsion fractures have been identified in youth "little league" baseball players aged 8 to 12 years and is caused by forceful termination of wrist flexion while pitching a baseball (Gugenheim *et al.*, 1976). Avulsion injuries are recorded by location.

Figure 4.6: Fishergate 144/5266. Smooth margined lesion at the ulnar collateral ligament attachment on the inferior surface of the medial epicondyle. This may also occur on the anterior surface and may take the form of a fossa over a lesion. Photograph by author.

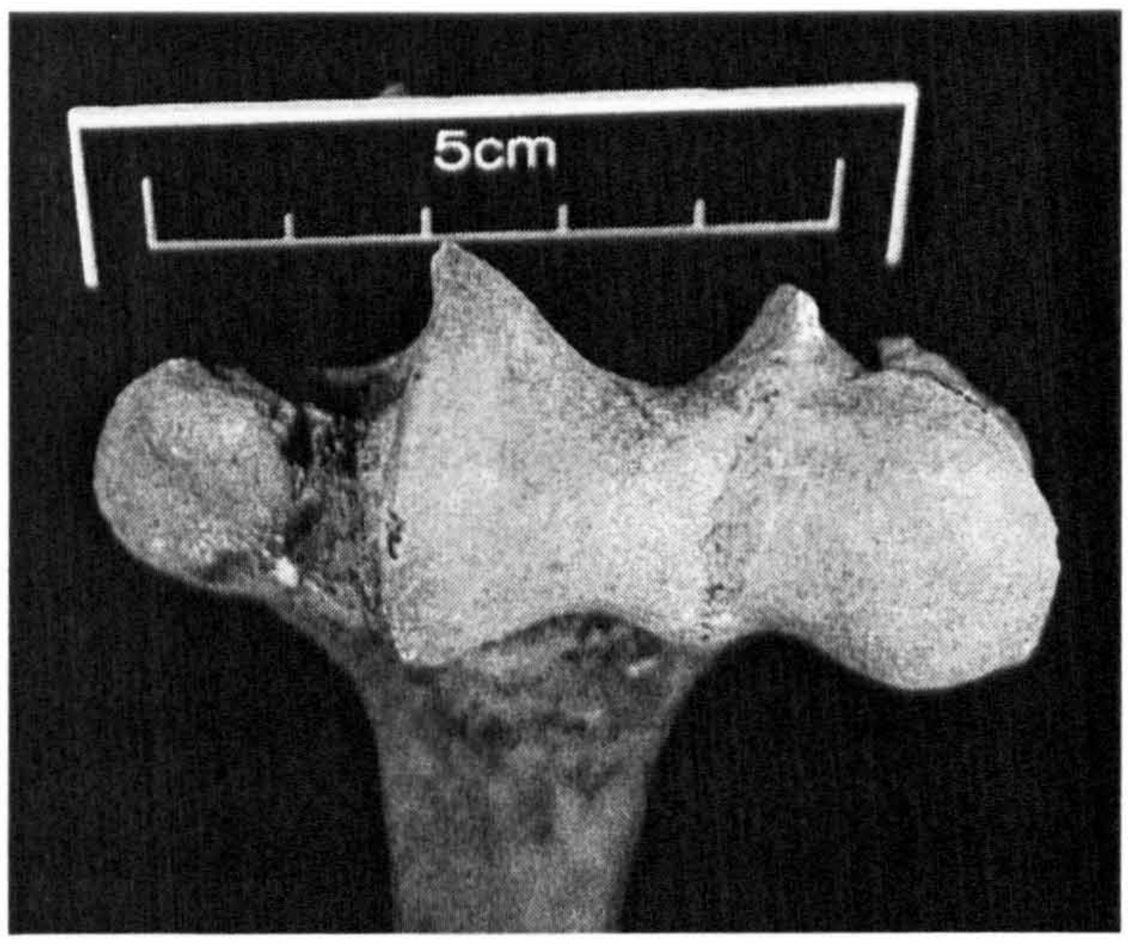

Lesions, or fossae in less extreme cases, were identified at the insertion site of the ulnar collateral ligament on the anterior or inferior surface of the medial epicondyle of the humerus (Fig. 4.6). The medial collateral ligament is responsible for elbow stabilisation against valgus stress and is associated with a medial stress syndrome associated with overhead throwing with force as found in baseball pitchers, javelin

throwers and tennis players. This type of injury may be directly related to the repetitive behaviour (Pavlov, 1995). These were recorded and analysed as present or absent whether occurring as a lytic lesion, an enthesophyte or a smooth-margined fossa.

4.3 Analyses of Asymmetry

Analyses of asymmetry are important in identifying the role of habitual behaviour in skeletal robusticity and morphology. Fluctuating asymmetry is a normal distribution of right and left side values that fall around a mean of zero. Directional asymmetry occurs in cases when the mean of one side is greater than that of the other side (Parsons, 1990). Clear directional asymmetry most likely indicates a shift in behaviour patterns (Trinkaus *et al.,* 1991). Asymmetry was calculated using several different formulae. The formula [(R - L) / (R + L / 2)] *100 (Mays *et al.,* 1999) was applied initially as this has the benefit of identifying the direction of change. A negative number relates to a left side asymmetry while a positive number equates to a right side asymmetry. The absolute difference between limbs in the humeral torsion angle was also applied. This was calculated simply as (maximum – minimum).

Another method of calculating asymmetry involves the percentage difference between sides and uses the calculation [(max / min) / min] X 100. This formula was used largely when considering biomechanical properties. Unfortunately, when applied to smaller variables, it has the effect of over-inflating the degree of change between sides as a 100% change between sides might simply be a value of 2° humeral torsion on the left and 1° of humeral torsion on the right.

4.4 Biomechanical Analysis

Cross-sectional geometric properties were calculated on a select group of paired humeri to investigate altered biomechanical patterns between individuals from the same population as well as those who had sustained peri-mortem weapon trauma. A control group of non-injured paired humeri was also examined. Cross-sectional geometry is highly influenced by mechanical loading during life and, as such, reflects loading patterns relative to behaviour (Ruff, 1992).

4.4.1 Selection Criteria

Two populations were sampled as part of the biomechanical analysis, the Towton sample and the Fishergate sample. As noted previously, the Towton group consists of a number of adult males found in a mass grave associated with the Battle of Towton, 1461 AD. All skeletons from this group exhibited peri-mortem skeletal trauma. To be included in the biomechanical study, both intact humeri were required, although there were several exceptions based upon unique morphological variation. All individuals with complete, paired humeri were selected for inclusion in the Towton population. This includes T8 who, while not paired, does display some interesting morphological variation between right and left humeri and in general from the rest of the sample. The complete right humerus displays a greatly enlarged distal articular surface, very slender shaft and a high degree of lateral bowing. The incomplete left humerus was scanned for comparison although only the two distal most slice parameters were present. A total of thirteen paired humeri were examined.

The Fishergate sample benefits from a small subsection of blade-injured individuals of 11th century date, in addition to a small number of later burials (13th – 16th century) also displaying perimortem trauma. All complete, paired humeri from blade-

injured individuals were included for analysis. Ten burials in total were selected, seven of which date from late 11th century contexts, while the remaining three date to a later period spanning 1195 AD to the 16th century. The reference sample (Fishergate control) is also from the cemeteries of St. Andrew, Fishergate in York. As the Fishergate site benefits from three discrete burial areas relating to socio-economic status, the control sample is made up of individuals from each of these cemeteries. These eight burials were selected from the other cemetery locations in order to give a broader picture of activity levels within the site as a whole, as well as functioning as a control group for the blade-injured collection. There are three burials from the southern, lay cemetery, including the burial of a man contextually identified as a priest (1195 – early 14th century AD). Four individuals originate from intramural contexts: one each from the nave, the north transept chapel, the chapter house, the latter was most likely a prior, and the cloister alley (1195 – early 14th century AD). Two ecclesiastical burials are drawn from the eastern cemetery (1195 – early 14th century AD). This control sample was selected on the basis of burial location and morphological variation to represent the diversity found within the sample as a whole. All of these groups possess similar age-at-death profiles, with both the Towton and Fishergate control groups displaying an average age-at-death of ca. 30yrs while the Fishergate blade-injured group died slightly younger, ca. 25yrs.

4.4.2 Analytical Procedures

The selected humeri were scanned using a GE Medical Systems HiSpeed NR CT-scanner at the radiography suite of St. Luke's Hospital, Bradford, West Yorkshire, United Kingdom. The settings employed were KV 120, MA 40. The humeri were marked with a thin pencil line at a point perpendicular to the long axis at 20%, 35%, 50%, 65% and 80% of maximum humeral length. This was taken as a point measured

previously from the inferior margin of the medial trochlear crest to the superior-most point on the humeral head, with 20% reflecting the most distal slice and 80% being the most proximal. The bone was placed on the gantry table and aligned with the longitudinal axis along the table's positioning beam. The slice locations were aligned manually following a visual exam. The co-ordinates were then inputted into the computer for the operation of the CT-scan. A scout radiographic image displaying the complete bone with the slice locations further confirmed the location of the slices. The scout and slice images were then printed out on standard radiography film for further analysis.

The images were scanned on an Epson Expression 1680 Pro with a resolution of 300 dpi and 8-bit colour settings. Each image was scanned with a measuring scale to ensure there was no distortion in the scanning or image manipulation process. The slice images were compared with the bone at both the maximum and minimum midshaft diameter to calculate any size distortion between the bone and the radiograph image. It was found that there was approximately a 25% increase in size from the bone to the radiographic image with all proportions maintained.

To analyse cross-sectional properties, solid coloured images were created of the slice images. This makes up for any density variation due to beam hardening or variation in cortical bone mass and allowed for the removal of any remaining trabecular bone in the medullary cavity that could distort the results. Periosteal and endosteal boundaries were defined using the Adobe Photoshop software programme. The magic wand and magnetic lasso tools were used to define the relevant boundaries. The magic wand was found to be most accurate in determining periosteal and endosteal boundaries and was used for creating the 'natural' endosteal margin. It does this by selecting out a

consistently coloured area as established by a tolerance level. This level allows one to set a pixel colour value and all pixels that fall within the set level will be isolated for manipulation. Once the relevant area was highlighted, the grey values were erased leaving the cortical bone white against a black background. This was then contrast-inverted with the resulting image ready for cross-sectional analysis.

The second method involves the magnetic lasso tool. When this is selected and moved across the relevant boundary, contrast levels between the cortical bone and the background are detected and a border is created, effectively isolating the cortical bone from the background. This is very good for separating remaining trabecular bone within the medullary canal and was used to trace in a smooth endosteal border. The detection width was seven pixels with a 20% contrast edge capable of detecting low contrasting borders. Feathering was set to 0 pixels to create a straight edge and the anchor frequency was 90 for the most precise border tracing. Once the cortical bone was isolated in the image, the magic wand tool was used to isolate and remove all shades of grey from the image, leaving a white area on a black background. This was contrast-inverted to create a black bone on a white background.

Two methods were employed in processing the CT-scan images, one using natural endosteal contours and another method smoothing the endosteal margins so that they conformed more to the techniques and images reported in the current literature, especially those involving slices created through bi-planar radiography. Endosteal boundaries, by their nature, are not smooth, rather they form a series of undulations that gradually merge with trabecular bone. By using the magic wand tool and a series of varying thresholds appropriate to each individual image the true endosteal boundary was isolated. In some cases, editing was necessary to remove spicules of trabecular bone

extending from the endosteal margin, however, the scalloped pattern of the border was retained. The smoothed boundaries were isolated using the magnetic lasso that used a lower value threshold and thus effectively removed the greatest degree of the undulations in the process, creating a slightly more 'stylised' border. This technique is comparable to that used in digitising images on various graphics tablets; it simply removes the external step of the tablet and creates the image directly on the computer. Cross-sectional analysis was performed on both sets of slice images to determine any differences that existed between biomechanical properties of the natural and smoothed borders. No significant differences were identified, therefore, those slices with the 'natural' endosteal border were used in the analysis.

Table 4.1: Momentmacro measurements of cross-sectional geometry.

Measurement	Definition	Mechanical Significance
TA	Total subperiosteal area	TA influences the second moments of area.
CA	Cortical area	CA is a measure of strength under compressive or tensile loadings.
Imax	Maximum second moment of area	The measure of maximum bending rigidity in the plane perpendicular to the I axis (Ruff, 2000).
Imin	Minimum second moment of area	The measure of minimum bending rigidity in the plane perpendicular to the I axis (Ruff, 2000).
MA	Medullary area (TA-CA)	A measure of the internal medullary cavity.
PCA	Percent cortical area (CA/TA)*100	The percentage of cortical bone relative to total area at the section.
J	Polar second moment of area (Ix + Iy)	The resistance against torsional forces at the section.
Imax/Imin	The maximum and minimum second moments of area divided by each other	A measure of asymmetry in bending strengths.
Ix/Iy	The M/L and A/P second moments of area divided by each other	The measure and direction of asymmetry in bending strengths.

The cross-sectional properties of the slices were analysed on a Macintosh OSX computer using the public domain NIH Image programme. The macro 'momentmacro' was used to calculate the cross-section properties. This macro provides the standard measurements required for biomechanical analyses such as CA, TA Ix, Iy, Imax & Imin,

however, there are additional measurements included. All of these and additional calculations are detailed in Table 4.1.

Standardisation was done with the maximum length expressed in centimetres, as millimetres produced unfeasibly large, unworkable numbers. To make the numbers more practical, Ruff *et al.* (1993) multiply these numbers by 10^8 for the measurements of area and 10^{12} for second moments of area. This produced unfeasibly large integers, therefore, the multiplication was carried out as 10^4 and 10^6, respectively.

CHAPTER FIVE

HUMERAL TORSION: REVIEW AND RESULTS

It is a well-known fact that in the higher Primates, as compared with other groups of animals, the humerus has undergone a twist so that the superior articular surfaces, which in most Mammals looks backwards, has come in them to look backwards and medially, or almost entirely medially. To this feature the name "torsion of the humerus" has been applied.

C.P. Martin (1933: 572)

Humeral torsion is a change in the relationship of the opposite ends of the humerus so that the distal and proximal articular surfaces lie in different planes.

Krahl and Evans (1945: 324)

Humeral torsion or retroversion, as it is known in the clinical literature, is a measurement of humeral architecture that describes the angle formed between the proximal and distal humeral articular surfaces. Previous chapters have highlighted how skeletal morphology may be altered in relation to mechanical loading and, specifically, how humeral torsion is quantified in this analysis. This chapter investigates humeral torsion as a measure of shape that varies relative to biomechanical forces produced by differences in habitual activity patterns. Previous studies of humeral torsion in both the clinical and anthropological literature will be reviewed, and the results of this project will be analysed. Each population will be discussed in terms of averages and outliers. Asymmetry in torsion will be examined both within and between human and non-human primate populations. A final discussion addresses inter-population variations.

Many analyses refer to torsion in relative terms, whether it is higher or lower in a population. Humeral torsion is described by Martin (1933) as a change in the orientation of the proximal articular surface. Early anatomists interpreted humeral torsion phylogenetically. The direction of the humeral head was observed to be posterior in orientation in quadrupeds and non-human primates, but in humans they saw a configuration in which increased torsion resulted in a more medially placed humeral head. Therefore, *increased* torsion refers to changes in the orientation of the humeral head such that it faces more towards the median plane rather than fully posterior. Figure 5.1 illustrates the differences between this orientation in a human with increased torsional compared to a quadruped macaque. The macaque possesses an increased angle compared to that observed in humans.

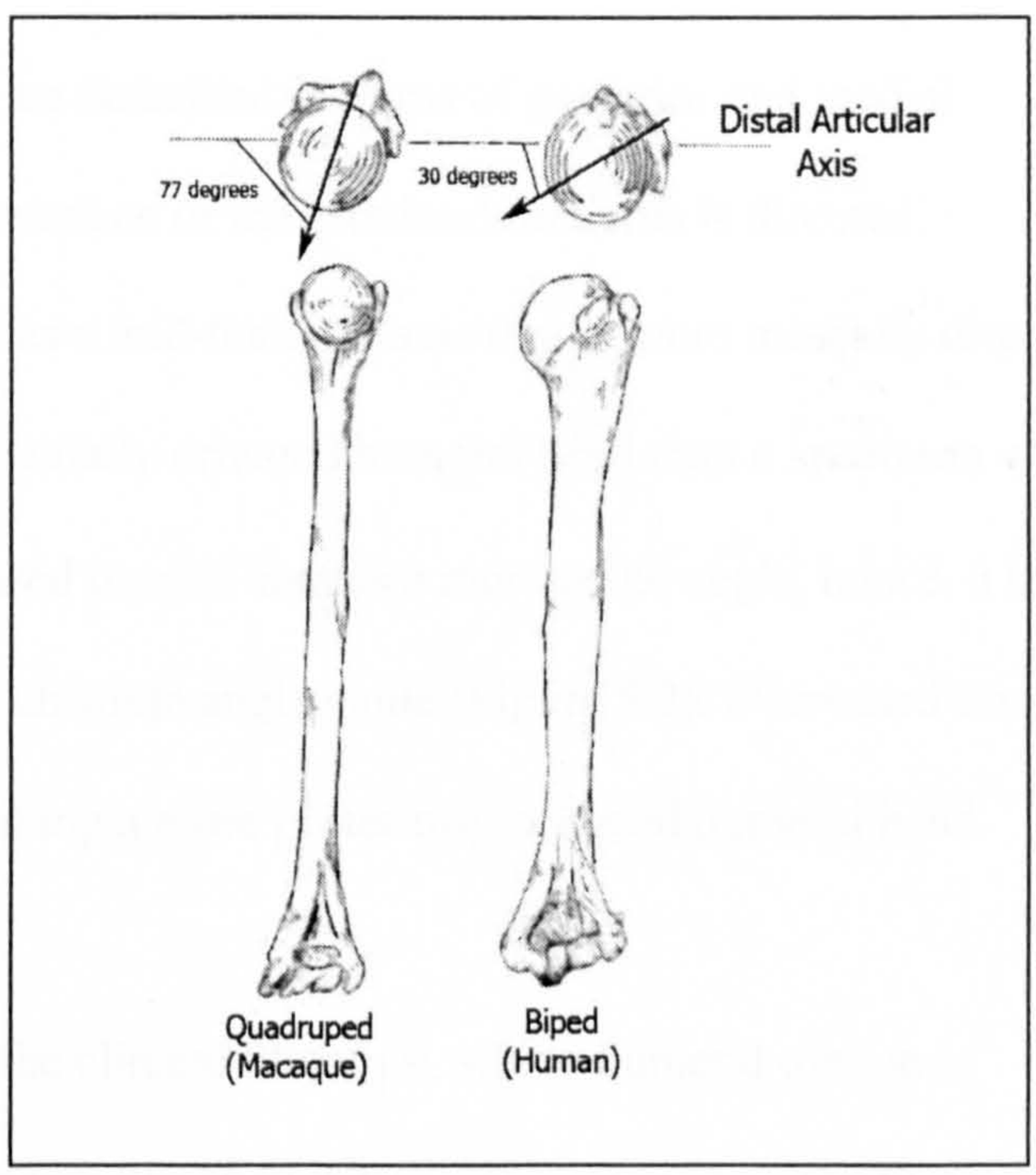

Figure 5.1: Humeral torsion in bipedal and quadrupedal species, an example of decreased torsion (increased torsional angle, 77°, and posteriorly placed caput) as found in quadrupeds (*Macaca* sp.) compared with the increased torsion (decreased torsional angle, 30°, and more medially directed caput) as found in bipeds (humans). The line with the arrow denotes the midhumeral axis (image after Ankel-Simons, 2000).

Twisting in the midhumeral axis produces a proximal articular surface that faces the median plane. In effect, increased torsion takes a more posteriorly directed humeral head and orientates it such that the midhumeral axis (or proximal articular surface) is directed more medially than posteriorly. *Decreased* humeral torsion takes a posteriorly

or postero-medially directed humeral head (the normal configuration in humans) and orientates it such that the midhumeral axis is directed even more posteriorly. This last process can also be described as retroversion, a term used to describe humeral torsion in the clinical literature.

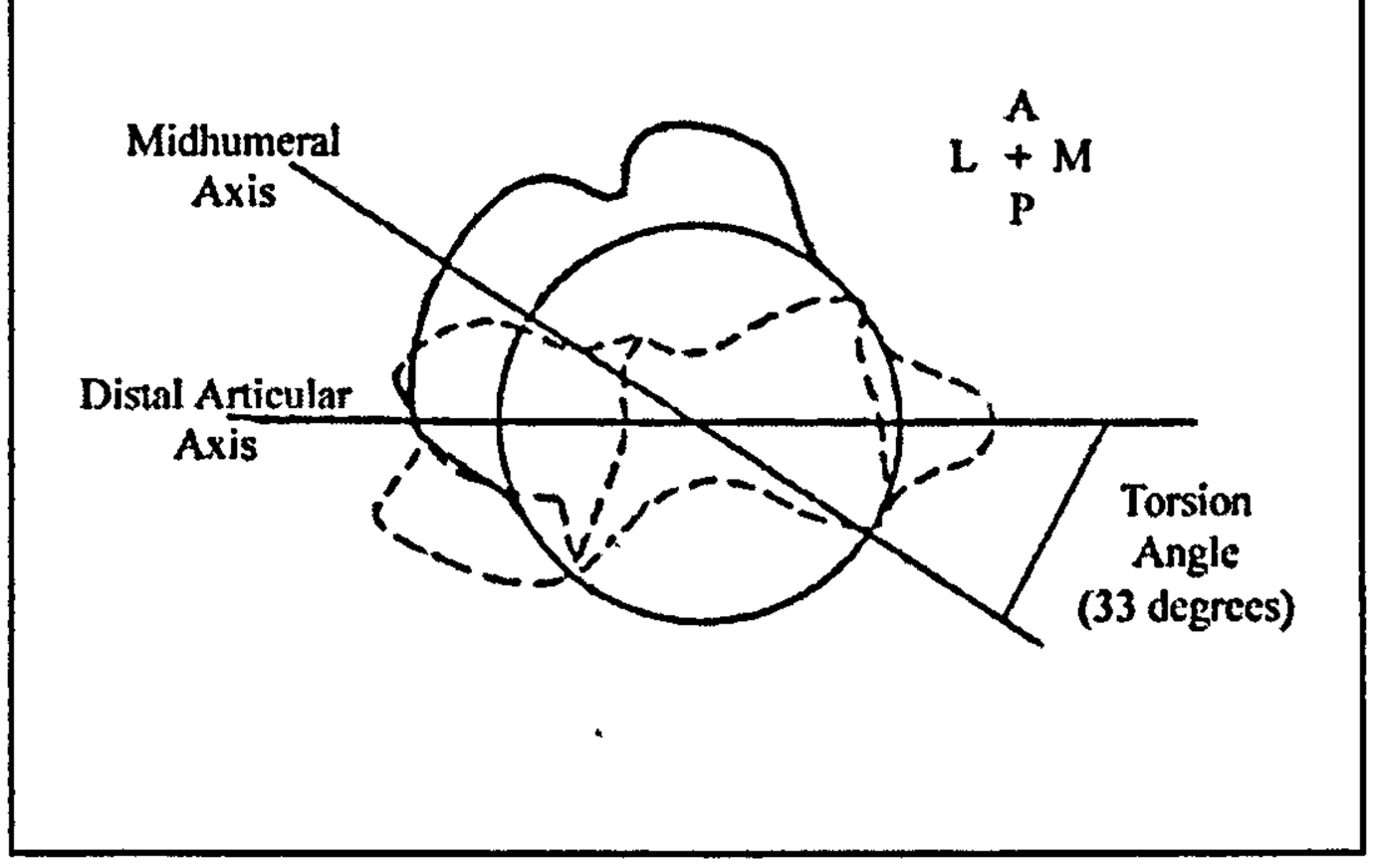

Figure 5.2: Humeral torsion in a left humerus. This image reflects the postero-medial direction of the humeral head in relation to the fixed point of the distal articular axis (image modified from Krahl, 1947).

Following this, torsion will be described in terms of posterior and medial orientations, or where the articular surface of the proximal humerus is directed. Increased torsion will be described as a mid-humeral axis that is more medially directed, i.e. 16° of torsion reflects a more medially oriented humeral head than a specimen with 40° of torsion. Functionally, increased torsion creates a more acute angle, hence, a high degree of torsion relates to a lower absolute angle value (Figure 5.2). Decreased torsion reflects a more obtuse angle, describing a more posteriorly oriented humeral head.

Confusion may arise as, in the clinical literature, where humeral torsion is referred to as retroversion. This process has been defined as "*a common condition in which an organ is tipped backwards, usually without flexion or other distortion*" (Anderson and Anderson, 1995). However, its literal translation from Latin, meaning 'to turn backwards', would be more accurate when applied to the clinical fields, as the degree of tilting to the proximal humeral articular surface is not quantified in these

studies using the term 'retroversion'. Therefore, it may be seen that the term retroversion in relation to the humeral torsion angle expressly refers to the extent of posterior direction displayed by the proximal articular surface relative to the distal articular surface. It is also based on the opposite assumption that it is the extent of *posterior* twisting (rather than medial twisting as described above) that increases humeral torsion.

Contrary to the situation in the femur, the humerus rarely displays anteversion, or a midhumeral axis that breaks into the anterior plane, effectively creating a negative measurement as quantified in this analysis. While, in this study, a very small number of humeri had humeral torsion angles of 0°, reflecting a fully medial orientation, none were found to display an anterior orientation to the midhumeral axis. Therefore, the term 'retroversion,' when applied to the humerus, is a misnomer, as its opposite, 'anteversion' rarely occurs. This is in direct contrast to descriptions of torsion in the femoral head, where both retroversion and anteversion commonly occur and there is the phenomenon of bending, as well as twisting, which affects measurement (see Dunlap *et al.*, 1953). However, in the humerus, any degree of posterior or anterior bending of the proximal shaft of the humerus should not affect the humeral torsion angle and use of the term 'retroversion' in this or any application referring to humeral torsion does not imply bending.

In a clinical publication, a humerus displaying increased 'retroversion,' rather than humeral torsion, will be one with an angle of 40°, for example. This leaves one asking the question whether the significance lies in the greater 'torsion' or in the greater absolute angle. Evolutionarily, torsion has been defined as a medial directional shift, and has been identified as increasing in the Primate order, from monkeys to great apes to

humans (Broca, 1881; Martin, 1933; Evans and Krahl, 1947). However, both increased and decreased torsion are significant, depending upon the context. For further clarification, the term 'retroversion' will not be employed, all references will be to either increased or decreased torsion or torsional angles as measured from the mid-humeral axis (see Fig. 5.2).

5.1 Studies of Humeral Torsion

5.1.1 Anatomical Considerations

There are numerous analyses of humeral torsion in the clinical literature, including anatomical, orthopaedic and sports medicine research. Torsion has been investigated as it relates to gleno-humeral stability, prosthetic design, and participation in high-level athletics. Early anatomists studied humeral torsion primarily focusing on the causes of torsion and where it occurred in the humerus, as well as species, population and ethnic variation. These studies aimed to define static traits and identify racial differences in their expression. Therefore, the result that 'primitive man' displayed less torsion (greater absolute angles), within the range of higher non-human primates, while more 'civilised races' displayed greater torsion (reduced absolute angles) is not surprising. Humeral torsion was also found to be greater in females than males, greater in a weakly developed skeleton than a more strongly developed one and varied between sides, with the left humerus displaying increased torsion (Broca, 1881; Martin, 1933). Consequently, the lower absolute torsion values (i.e. more medially orientated humeral head) correlate with what were considered the 'weaker' specimens. Martin believed that torsion was related to an inherent weakness in the bone, implying that those elements with lower humeral torsion angles had less resistance to this type of stress.

Whether intentional or not, the role of plasticity in humeral torsion was identified, as Martin (1933) believed that torsion was caused by two stresses acting upon the bone, one at the humeral head, and one at the shaft. The arch formed by the acromion and coraco-acromial ligament was thought to force lateral rotation of the humeral head during abduction of the arm and inhibit medial rotation of the humeral head during flexion. Medial rotation of the shaft is attributed to tensile diaphyseal stresses related to the activities and function of *M. pectoralis major*, *M. teres major* and *M. latissimus dorsi*. This implies that humeral torsion is a developmentally plastic trait, related to muscular strength. However, if increased torsion is related to an inherent weakness in the bone, does this mean that strong muscles shape a weak bone, increasing torsion, or do strong muscles and a strong bone work together to resist torsion? What happens in a weak bone with reduced muscular activity? Does this produce the same effect as a strong bone resisting these forces? Martin restricts torsion exclusively to within the Primate order, as he believed it to be the result of suspensory activities. However, most great apes and certainly most humans do not habitually participate in this type of activity.

Humeral torsion is not restricted to humans, or even to the Primate order. Evans and Krahl, in a 1945 publication, examined amphibians, reptiles and mammals in an attempt to determine the origin of torsion and the changes it has undergone in the evolution of humans from the crossopterygian fishes. They believed humeral torsion was the result of both phylogenetic and ontogenetic factors. Primary torsion related to the genetic potential or range of responses possible for a given species. Muscular forces interact with this to create secondary torsion.

Secondary torsion was thought to be caused by muscular forces, thus the bone was forcibly twisted by direct action (Figure 5.3). These muscles were identified as *M. subscapularis*, responsible for medial rotation above the proximal epiphyseal plate, with the medial rotators, *M. pectoralis major*, *M. teres major* and *M. latissimus dorsi,* acting below the epiphyseal plate. These muscles are referred to as the infra-epiphyseal rotators. The lateral rotators of the rotator cuff, *M. supraspinatus*, *M. infraspinatus* and *M. teres minor* were also implicated, however, a relationship was assumed between torsion and the strength of the infra-epiphyseal rotators. Krahl (*ibid.*) investigated muscle strength, as defined by cross-sectional area, and humeral torsion in 42 cadavers. Cross-sectional area was converted into muscle tension in kilograms and plotted against humeral torsion values. He found no apparent relationship between muscle strength and humeral torsion. However, when the individuals with obvious muscular atrophy, whether from disease or advanced age, were eliminated, a relationship was found between muscle strength of the infra-epiphyseal muscles as a group and humeral torsion. As muscular strength increased, so did the amount of torsion (Krahl, 1947).

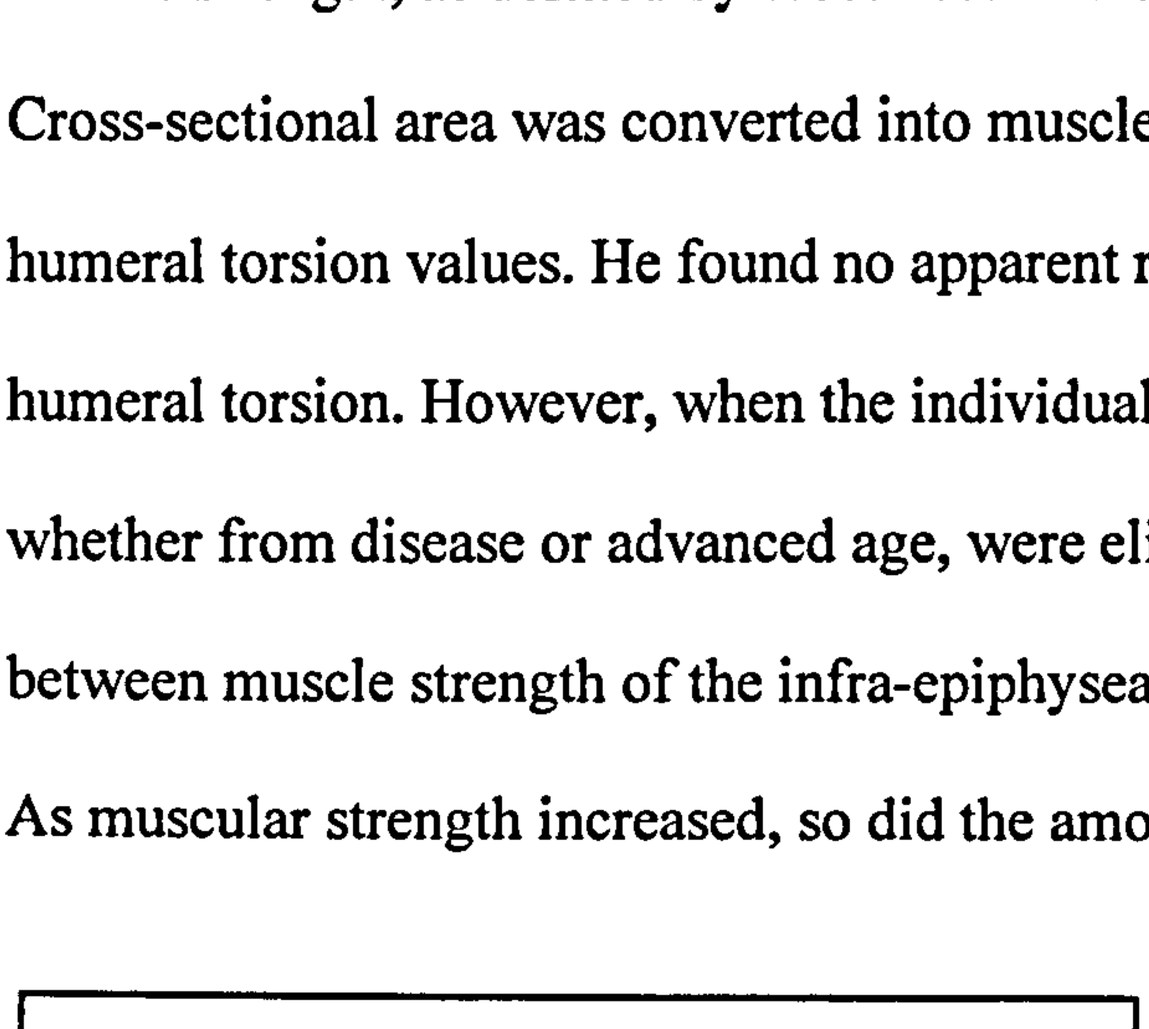

Figure 5.3: Muscular forces responsible for secondary torsion. The lateral rotators were thought to pull against the medial rotators above and below the epiphyseal plate and created, in the process, variations in humeral torsion (image modified from Krahl, 1947).

The greatest degree of secondary torsion, as developed through muscular forces, was believed to occur prior to birth. At 20 weeks, the absolute humeral torsion angle

was found to be 48° (N = 374), which represents the primary, ontogenetic torsion angle for humans. This angle decreased to 25° at birth and the final average value at adulthood is 16° (Krahl, 1947). Krahl attributed this secondary torsion to the lateral rotators pulling against resistance offered by the surroundings *in utero*, which inhibit the shaft from following the movement. So the shoulder is rotated, but the cramped uterine conditions prevent the arm from following the movement, creating torsional stresses above and below the epiphyseal plate. The change in torsion *in utero* is most likely a result of normal osseous development, although muscular influences during this stage are important (Carter *et al.*, 1987). The change in humeral torsion from birth to adulthood, though, likely occurs through modelling in response to physical demand and would be expected to reflect individual patterns rather than any pre-set condition.

The site of torsion was originally thought to be either in the diaphysis or in the proximal epiphyseal plate. The orientation of the spiral groove, a channel for the radial nerve, gives the humeral shaft the appearance of being twisted. Hence, early anatomists believed that the primary site of torsion was in the diaphysis and this action determined the site and direction of the spiral groove. However, no relationship was found between the angle of the spiral groove and the torsional angle. Torsion was also thought to develop early, before the spiral groove was fully defined, and to cease at maturity, supporting the claim that it occurred in the proximal epiphysis. The cartilaginous plate offered weak resistance to torsional forces, and the action of the medial and lateral rotators were thought to turn the shaft with respect to the proximal epiphysis (*ibid.*).

Further support for the location of torsion occurring in the proximal epiphysis was offered by an analysis of the direction of the bicipital groove. Krahl (1948) examined eighty-five humeri to determine the angle of the bicipital groove, from the

superior-most point on the humeral head to its lower limit in the group of infra-epiphyseal rotators. This measurement is known as the spiral angle, and it was found to increase in direct proportion to the torsion angle. Thus, Krahl considered that the bicipital groove indicates the direction and extent of the torsional process. However, Kate (1968) argued that torsion occurs within the diaphysis, specifically at the site of the deltoid tuberosity. Following this line of reasoning, it is the distal shaft that has shifted, as the proximal shaft is strongly anchored in position by muscles while the distal shaft is free to rotate with muscle forces.

If torsion does occur in the proximal epiphysis exclusively, then a relationship may be expected between it and the spiral angle as identified by Krahl (*ibid.*). As will be demonstrated, humeral torsion appears to be a complex phenomenon, one that is not so easily explained as the action of the lateral rotators acting above an open epiphyseal line. An open epiphysis is key, but only in that it indicates a juvenile growth phase, when modelling is most active. It is unlikely that there is a direct, physical shift in orientation of the metaphysis in relation to the diaphysis, as implied by the early anatomical literature. The relationship between torsion angles and the spiral groove, as tested in this project, will be discussed in a later chapter, as will its relationship *cubitus valgus*, a modification of the position of the medial epicondyle.

Problems with early analyses lie in the assumption that torsion was static. It was thought to begin in the foetal skeleton and continue through development. By the age of seven, torsion was thought to be more than halfway complete. One study investigated humeral torsion from the foetus to the adult (20 yrs of age) and found torsion correlated with the time of epiphyseal fusion (Krahl, 1947). A modern clinical study found humeral torsion was largely complete by the age of eight years, and in adult form by

approximately 16 years of age (Edelson, 2000). This observation is ironic, considering Krahl himself states that humeral torsion "*is a dynamic, changing process, expressing the response of a plastic and reactive structure to mechanical forces brought to bear upon it*" (Krahl, 1947: 296). However, he did not seem to recognise that this process may not stop when growth is completed and that the torsion angle may be further influenced by muscular forces throughout adulthood. The decline of modelling in adulthood does indicate that modification of humeral torsion is less likely to occur at this stage, but there were no individuals examined by Krahl who were older than 20 years of age to support this viewpoint.

Early population studies of humeral torsion focused on differences in humeral torsion between different phylogenetic groups that ostensibly revealed a presumed hierarchy among living human populations. Broca's 1881 study of humeral torsion examined the differences in humeral torsion between different European and French samples, even including the differences between Parisian neighbourhoods and other samples. Martin's 1933 study examined humans in order of their presumed primitivism. Later studies simplified these categories to examine the differences between different racial or ethnic groups. Although ontogenetic change in humeral torsion was considered by researchers, such prevailing views of phylogenetic differences within humans prevented any serious consideration of this trait.

Table 5.1 summaries the results of these studies, including a 1945 examination by Krahl and Evans, who studied the differences between sexes, limbs and 'race' in a group of Euro-American individuals and an Afro-American population. Significant differences were found between sides in the Euro-American population but not within the Afro-American population. Considering sex, no significant differences were found

between males and females in the Euro-American population, but they were significant in the Afro-American population. There were also significant differences in humeral torsion found between the Euro-American males and the Afro-American males. The identification of bilateral asymmetry in humeral torsion indicates that hand preference in unimanual activities was likely an important ontogenetic factor influencing torsion.

Table 5.1: Population studies of humeral torsion. Humeral torsion was thought to vary by race, as indicated by the diverse ethnic groups examined. While this hypothesis is likely true, the underlying cause was not identified. It is much more likely that the ethnic groups differ in humeral torsion not because of phylogeny, but due to similar ontogeny, or shared activity patterns.

Study	Population	Right	Left	Average (Bilateral)	Number of humeri
Broca (1881)	French			16°	20
	Other Europeans			18.5°	12
	Paris, Saint-Marcel			18.41°	85
	Ancient Egyptian			23.58°	12
	Paris, Saint Germain			24.06°	52
	Californians (presumed Native Americans)			28.42°	12
	Peruvians			29.74°	45
	Afro-American			36°	55
	Grand Canaries			38.81°	160
Martin (1933)	Australian natives			45.5°	N/A
	Melanesian			41°	N/A
	Negroes (presumed African)			35.8°	N/A
	Modern Swedes			16.1°	N/A
	Modern Swiss			16°	N/A
	Modern French			16°	N/A
Krahl and Evans (1945)	Euro-American males	14.1°	18.2°	15.6°	114
	Euro-American females	12.3°	16°	14.6°	64
	Afro-American males	21.8°	20.9°	21.3°	56
	Afro-American females	14.5°	14.3°	14.4°	42
Kate (1968)	Central Indian males	36.7°	39.2°	38°	50
	Central Indian females	32.8°	31.6°	32.2°	50
Edelson (1999)	Euro-American male	34.74°	28.88°		17
	Afro-American male	39.13°	34.27°		15
	Euro-American female	29.46°	26.64°		11
	Afro-American female	32.82°	26.91°		11
	Alaskan Eskimo males	54.93°	48.33°		15
	Alaskan Eskimo females	45.15°	40.61°		13
	Northern Chinese males	45.87°	41.13°		16
	Northern Chinese females	47.25°	44.83°		12
	Bedouin males	40.07°	36.21°		14
	Bedouin females	31.53°	31.00°		15
	New Mexican Indian males	42.81°	39.63°		16
	New Mexican Indian females	32.85°	30.62°		13

Kate (1968) examined torsion as a racial (i.e. ethnic) characteristic in Central India. He found significant differences between sexes, but not between sides. Edelson (1999) found significant differences in ethnic groups, with Northern Chinese, Alaskan Eskimo and New Mexican Indian populations all similar to each other, but different to Euro-American and Afro-American populations, as well as Bedouin groups. The differences identified in all of the above studies are more likely the result of shared group ontogeny, rather than any fundamental differences related to distinctions between presumed phylogenetic categories.

5.1.2 Orthopaedic Considerations

Orthopaedists are interested in humeral torsion as it relates to treatment of shoulder problems. Patients with recurrent anterior glenohumeral dislocations display increased torsion (reduced torsion angle, or a more medially directed humeral head). It is hypothesised that the increased torsion has the effect of altering the arc of shoulder rotation by decreasing the extent of external rotation possible. Thus increased torsion may be a factor predisposing to anterior glenohumeral dislocations (Dias *et al.*, 1993). Pieper (1985) examined recurrent dislocation and humeral torsion values in a group of alpine and cross-country skiers and came to similar conclusions. The average humeral torsion angle for 40 skiers suffering from recurrent anterior dislocation was 24.3° in the affected limb. The control group without dislocations ($n = 130$) had an average humeral torsion value of 40.1°. These two populations varied significantly ($p < 0.01$). A group of five individuals suffered from posterior dislocation and had an average humeral torsion angle of 55.7°.

Variation in humeral torsion must be calculated in order to undertake various surgical procedures involving the proximal humerus. A method of treating recurrent

glenohumeral dislocation is a rotational osteotomy, a surgical procedure that repositions the humeral head (Söderlund *et al.,* 1989). Torsion has also been investigated for positioning of a prosthetic articular surface. The recommended position of the humeral head for such procedures is at an angle of between 30° and 45° of torsion (Pearl and Volk, 1995; Öztuna *et al.,* 2002). The range of variation in modern populations is between 10° and 55°, with an average torsion angle of 29.8° (Nicholson and Lintner, 1997).

Kronberg and colleagues (1990) examined humeral torsion and its relationship to range of motion. They examined 100 healthy shoulders, 25 males and 25 females, with no history of pain or instability in the shoulder. The mean age was 30.5 years and 45 of the 50 subjects were right-handed. The average torsion angle between sides was significantly different ($p < 0.001$), 33° in the dominant shoulder and 29° in the non-dominant shoulder. There were no differences between sexes which is contrary to the results obtained by Kate (1968). However, Kate's work, and all other early studies only examined differences between right and left limb, rather than considering limb dominance. Greater humeral torsion angles also correlated with a larger range of external rotation at 90° of abduction. None of the shoulders fulfilled the criteria for diagnosing joint laxity, therefore, this must relate to an osseous change in the gleno-humeral joint.

5.1.3 Sports Medicine Considerations

Humeral torsion has been investigated in the sports medicine field as a variant related to strenuous activity patterns in the high-level athlete. This work follows on that of King *et al.* (1969) and Jones *et al.* (1977), as previously discussed in the chapter on skeletal tissue dynamics. Pieper (1998) investigated humeral torsion in a group of professional

handball players. This is a sport that is similar to basketball in that a 58 to 60 cm sized ball must be moved by either dribbling or passing it from one end of the court to the other. Once there, it must be thrown past a goalkeeper and into a goal from behind a 6-meter line. Therefore, this sport involves extensive overhand throwing actions.

Table 5.2: Humeral torsion in high-level athletics. Note the strong bilateral asymmetry in the sports athletes, as well as their increased humeral torsion angle when compared with those of the control groups.

Study	Sport	N.	Dominant (throwing)	Non-dominant (non-throwing)	Asymmetry*	Average age
Pieper (1998)	Professional handball players (Healthy)	38	49.08°	34.68°	14.4°	26.5
	Professional handball players with chronic shoulder pain	13	35.46°	40.62°	*-5.16°	28.15
	Control group	37	41.46°	39.70	1.76°	46.70
Osbahr *et al.* (2002)	College baseball pitchers	19	33.2°	23.1°	10.1°	N/A
Reagan *et al.* (2002)	College baseball pitchers and positional players	54	36.6°	26.0°	10.6°	19.3
Crockett *et al.* (2002)	Professional baseball pitchers	25	40°	23°	17°	18-35
	Control (non-throwing)	25	18°	19°	*-1°	18-35

*A negative value reflects the greater value occurring in the non-dominant limb.

Similar to the baseball pitchers examined by King and colleagues (*ibid.*), these players exhibited increased external rotation and decreased internal rotation in the dominant arm. The goal of the study was to identify any osseous component to these modifications in range of motion. The players examined had all started competitive handball before the age of ten and had at least five years of competitive playing experience. Significant bilateral asymmetry in humeral torsion values was identified in the group of handball players ($p < 0.01$), while the control group was non-significant ($p < 0.134$). Of the handball players, every one displayed the higher angle (decreased torsion indicated by a more posteriorly directed humeral head) in the throwing arm,

while in the control sample, twenty-one displayed the greater angle in the dominant arm and thirteen displayed the greater angle in the non-dominant limb. Interestingly, in a small sub-sample of thirteen players with chronic pain, the torsion angle was greater in the non-dominant shoulder than in the dominant one. This indicates that the variation in the torsional angle may be an adaptation that enables high-level performance without physical damage to the joint, or in other words, pain and injury-free play. Pieper's study is important, as it was the first to identify torsional adaptation in relation to strenuous, habitual activity. This and other studies are summarised in Table 5.2.

A number of studies have recently been published examining humeral torsion and its effect on range of motion in baseball pitchers. Osbahr *et al.* (2002) examined 19 college-level pitchers with an average of 7.6 years of pitching experience. The average age of the group was 19.1 years (range 18 to 21). Therefore, all of the pitchers would have been active during the key juvenile development phase. All of the subjects displayed increased external rotation at 0° and 90° of abduction, decreased internal rotation at 90° of abduction and increased humeral torsion angles in the dominant shoulder when compared with the non-dominant shoulder. All of these results were significant when comparing the dominant against the non-dominant shoulder ($p < 0.01$). Furthermore, humeral torsion was correlated with increased external rotation at 90° of abduction ($p < 0.0001$), but it was not correlated with either age or years pitched. Reagan and colleagues (2002) found similar results when examining 25 college-level pitchers and 29 college-level positional players (i.e. those who play positions other than pitcher). All subjects displayed significant differences between sides in humeral torsion and internal and external rotation at 90° abduction. The only differences between the group were that humeral torsion was correlated with external rotation at 90° abduction

in the pitchers, while both external and internal rotation at 90° abduction correlated significantly with torsion in the positional players.

Crockett *et al.* (2002) conducted a similar study on 25 professional pitchers. They examined humeral torsion and its relation to external rotation, as well as examining a control group of 25 non-throwing subjects. Significant differences were found in humeral torsion ($p < 0.001$) and external rotation and internal rotation at 90° abduction ($p < 0.001$) between dominant and non-dominant limbs in the throwing subjects. However, the non-throwing group also displayed significant differences in internal rotation between sides ($p < 0.01$). There were no significant differences between the non-dominant limb in the throwing group and either limb in the non-throwing group.

These changes of the shoulder in throwing athletes do not appear to be the result of laxity in the joint capsule, but are osseous adaptations to repetitive movements. During the 'cocking' phase of throwing, there is 67 +/- 11 N-m of torque across the gleno-humeral joint, equivalent to 90% of body mass (Zuckerman and Matsen, 1989). These forces acting across a developing proximal humeral physis - where ninety percent of humeral growth is occurring after the age of 11 years - will affect humeral architecture (Osbahr *et al.*, 2002). Crockett and colleagues (2002) postulate that such osseous adaptations of the humerus are necessary for high-level performance. Those pitchers competing during key growth phases will have the best chance of undergoing these skeletal adaptations and becoming an elite baseball pitcher. The development, they believe, adapts the dominant upper limb for increased performance and decreases the chances for injury.

Physically, an increase in the torsional angle enables the athlete to extend the cocking phase of their throw and thus further accelerate the object thrown. Additionally, these osseous changes of the shoulder joint may serve as an adaptive mechanism to protect against injury. During the late 'cocking' phases of throwing, the arm is in a position of 90° abduction and maximum external rotation is achieved (Figure 5.4). In this position, the inner fibres of the rotator cuff musculature and the posterosuperior glenoid labrum would be impinged had the osseous adaptation not occurred (Reagan *et al.*, 2002). In the study of handball players, there is a 13.62° difference in torsion of the dominant limb between those players without chronic pain and those with it (Pieper, 1998). Therefore, it would appear that increased humeral torsion angles (i.e. a more posteriorly oriented humeral head) are an osseous adaptation enabling high-level performance without pain.

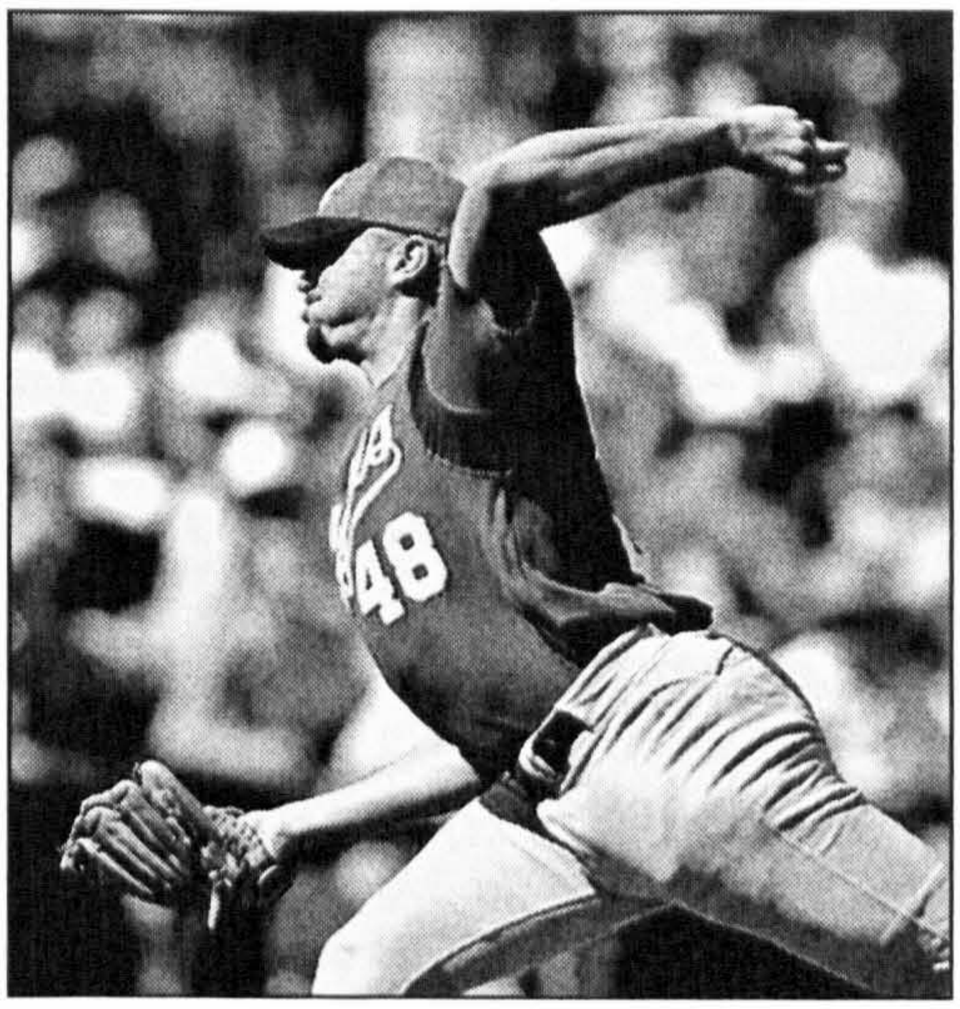

Figure 5.4: A professional baseball pitcher engaged in the late cocking phase of throwing. The pitching, or dominant arm (left) is in a position of 90° of abduction with maximum external rotation. The external rotation allows the forearm and hand to be positioned behind the athlete's head. This effectively increases force and acceleration of the ball when released (Image from www.kcroyals.com).

5.1.4 Humeral Torsion in the Anthropological Literature

Humeral torsion has been considered in a number of anthropological fields, including palaeoanthropology and primatology. Historically, the degree of humeral torsion was viewed as a taxonomic trait, specifically, one of the defining traits distinguishing late archaic and early modern humans (Boule 1911-1913). These differences are now viewed

as an adaptive change rather than taxonomic variation (Vandermeersch and Trinkaus, 1995).

Churchill (1996) investigated humeral torsion within the context of diaphyseal shape in samples of Eurasian late archaic and early anatomically modern humans. These populations were combined with four samples of recent human populations to test two different models relating to postcranial evolution. A number of postcranial variables, the humeral torsion angle included, were investigated as part of a correlation model that also included aspects of body form: body size, chest shape and robusticity. Humeral torsion was found to be negatively correlated with chest shape and to have no relationship with skeletal robusticity. This indicates that larger-chested individuals tend to have a more posteriorly directed humeral head (decreased torsion) and led to the conclusion that humeral torsion was more a function of scapular position on the thorax than to do with activity.

Carretero and colleagues (1997) investigated humeral torsion as one of a number of traits in the upper limb of postcranial remains from the Sima de los Huesos (SH) hominid site in Sierra de Atapuerca, Spain. The low humeral torsion (high angle values) reported for Neandertals and found in the SH hominids led the authors to conclude that the torsion angle is directly related to the shape of the deltoid tuberosity, whether it is 'open' (broad) or 'closed' (narrow). The lower the humeral torsion (i.e., the higher the torsion angle), the narrower the deltoid tuberosity was hypothesised to be. When torsion is increased, the lateral crest of the deltoid tuberosity 'opens' to the posterior diaphyseal shaft. Churchill and Smith (2000) investigated the relationship between humeral torsion and the deltoid tuberosity but found no correlation between torsion and deltoid width in a sample of 304 mixed sex recent and fossil humans, including Neandertal samples.

The humeral torsion angle was investigated in hominoid species with the conclusion that torsion varied with limb function and the demands for positioning of the elbow. Increased torsion (decreased angle) is only necessary if function demands that the elbow and forearm movements follow a roughly parasagittal plane (Larson, 1988). The high degree of torsion in the African apes, as opposed to other hominoid species, appears to be a reflection of quadrupedal locomotion, as this requires a parasagittal orientation of the elbow and forearm. The high degree of torsion observed in humans may either have evolved as an accommodation to tool-making, an activity requiring the changes in habitual manipulation, or it may be a shared derived feature in hominoids that provides evidence for a knuckle-walking stage in human evolution. However, the fossil evidence does not appear to support the latter proposal at this stage. It would appear more likely that the high extent of humeral torsion reflects an independent evolutionary stage facilitating the demands of habitual manipulation and tool-making (Larson, 1996; Aiello and Dean, 1990). Table 5.3 illustrates humeral torsion in relation to locomotion.

Table 5.3: Humeral torsion in hominoid species. A general trend of increased torsion may be observed from species that practice suspensory forms of locomotion to quadrupedal knuckle-walkers and bipeds. The translated value is for direct comparison with the results of this study which does not include the 90° ontogenetic twist accommodated for in the anthropological research. It is calculated as 180° – published value = translated value.

Study	Population	Published value	Translated value	Locomotion
Larson (1988)	*Macaca sp.*	112° – 128°	51° - 68°	Mixed
	Hylobates sp.	128° - 145°	35° - 52°	Suspensory
	Pongo pygmaeus	120° - 162°	18° - 60°	Mixed
	Pan troglodytes	139° – 159°	21° - 41°	Quadrupedal
	Gorilla gorilla	154° – 173°	7° - 26°	Quadrupedal
Vandermeersch and .Trinkaus (1995)	*H. sapiens neanderthalensis*	125° – 149°	31° - 55°	Bipedal
	H. sapiens sapiens	134.5 °- 164°	16° – 45.5°	Bipedal

5.2 The Discrepancy between Clinical and Archaeological Values

Throughout the course of this project, a discrepancy has been identified between humeral torsion values as reported in the clinical literature and those obtained during this analysis. If the clinical average is 29° and surgical procedures to reposition the humeral head place it at an angle of between 30° and 45°, why is there such disparity between modern and archaeological sample values?

The humeral torsion angles as reported by Krahl in various analyses (1947, 1976) are similar to those obtained in this study and contrast with the modern clinical values. This project uses the same piece of equipment as Krahl employed, a torsiometer which has been designed following his specifications (Krahl, 1976). The clinical method involves CT or radiographic images and mathematical algorithms to calculate what is the same angle. This indicates that there must be a form of distortion in the clinical method. Öztuna *et al.* (2002) tested this, measuring humeral torsion in twenty skeletal humeri, first, using a specially developed frame and, secondly, using radiographs and a conversion algorithm. They found the correlation between the two techniques to be reliable, with an average difference between techniques of 0.9°. Interestingly, their population average was 23°, similar to that found in the Terry population in the present study. Although the origin of the skeletal elements is not specified, they are presumed to have been modern cadaver samples. The humeri examined by Krahl are from the Huntington Collection of the U.S. National History Museum and from the University of Maryland School of Medicine (Krahl and Evans, 1945). This collection is similar to the Terry collection, employed as part of the present research, being derived from documented cadavers acquired by a medical school.

Unfortunately, this still does not fully answer the question of the disparity. If the radiographically obtained angle correlates with the skeletally obtained angle, then there must be another factor influencing the discrepancy. The Huntington Collection was curated around the turn of the last century, while the samples from the Terry collection were curated largely from the 1920s and 1930s, although specimens were still being added in the 1960s. It is possible that there is a strong temporal aspect to humeral torsion in 'modern populations', such that individuals alive today will display reduced torsion (increased angles) relative to people from fifty and one hundred years ago. This will be tested using the Terry collection data. However, if an increased angle is a form of accommodation to activity, then why would it increase temporally as the majority of people are thought to be becoming increasingly less active, as food is obtained primarily from a store, transport is via motor vehicles and there is less manual labour involved in day-to-day activities? There are an increasing number of high-level athletes, but they form a distinct minority in populations. This may reflect an overall general increase in body size, both stature and body mass that is found in modern populations.

5.3 Humeral Torsion: Primary Hypothesis and Secondary Issues

A primary aim of this project is to examine the nature of humeral torsion and its relationship as a trait susceptible to variations in mechanical loading. Thus inter and intra-population variations may be interpreted as reflective of different habitual activities. However, there are still a number of fundamental questions that remain, including what is the normal or average expected angle of humeral torsion? Increased and decreased torsion is relative to a set value. However, how may this point be defined? The clinical average, as previously stated, is 29.8°. However, humeral torsion is highly variable across populations, and as will be seen, the values in the archaeological populations are unique when compared to the clinical average. Because

of this, a modern-cadaver based sample was added to the project to test whether this difference occurs as a result of the quantification method, or if these differences between archaeological and modern populations are supported.

The primary hypothesis is that the humeral torsion angle is modified through strenuous activity patterns. Increased, high-level physical activity, such as performed by the professional throwing athlete, has been found to increase the humeral torsion angle. Therefore, this project seeks to identify similar patterns – increased humeral torsion angles correlated with other indicators of increased activity patterns - in the archaeological record. However, there are a number of secondary issues related to humeral torsion that need clarification.

5.3.1 Humeral Torsion and Robusticity

Martin (1933) believed that humeral torsion and humeral robusticity were linked, as the torsion observed was related to an inherent weakness in the bone structure. The gracile humerus, then, displays a reduced angle (a more medially directed caput) while a more robust humerus displays an increased angle (a more posteriorly directed caput). Results from the clinical literature do indicate that the dominant limb demonstrates a higher humeral torsion angle when compared with the non-dominant limb. However, this appears linked with strenuous activity in the dominant limb rather than an innate weakness in the non-dominant limb.

If increased activity levels produce more cortical bone, the limb should reflect higher robusticity values and less 'twisting' as there is now the strength via increased thickness to resist these forces. However, if bone is deposited following mechanical requirements, then 'resistance is futile' as the bone will be deposited in such a way as to

mimic continental drift, moving the caput in a direction in-line with those forces. If increased torsion is related to a more gracile skeletal element, it would be expected that the non- dominant limb will have a reduced angle when compared with that of the dominant, have less robust measurements and decreased cortical thickness.

Problems with this hypothesis, however, include how to identify the dominant versus the non-dominant limb in archaeological specimens – individuals who, unlike those clinically examined, cannot state hand preference. As shall be examined in the biomechanical analysis, there may be problems identifying limb dominance from external measurements when compared with internal cross-sectional properties. This will be further addressed in later chapters on robusticity and biomechanics.

5.3.2 Mechanical Forces Affecting Humeral Torsion

The viewpoint espoused by the early anatomists saw humeral torsion as an ontogenetic process, increasing developmentally from a high angle *in utero* to a reduced angle at birth and an even smaller angle at the final stage, adulthood. However, the in the clinical viewpoint, changes in the humeral torsion angles are assumed to result directly from mechanical forces and not a set developmental pattern. In what may be interpreted as an adaptation to functional demands, suspensory primates display higher absolute humeral torsion angles. This form of locomotion places great stress across the shoulder joint, and the posterior placement of the humeral head is likely an osseous adaptation to the movement and forces generated.

From both the primatology and sports medicine fields, it may be seen that a posteriorly placed humeral head is related to a powerful overhand activity. In

suspensory non-human primates, this activity effectively throws their bodies through space, as opposed to pitchers who throw an object. In pitching, a conservative estimate of the joint reaction forces shows 90% of the body weight being transmitted through that area (Zuckerman and Matsen, 1989). Therefore, increased torsion angles may relate to powerful overhand movements, such as that seen in suspensory primates and the throwing athlete.

5.3.3 Is Torsion Exclusive?

An increased humeral torsion angle results in a more posteriorly placed humeral head. However, the direction of the humeral caput is relative to the distal articular surface. If torsion is not exclusive to the proximal shaft, then it is possible that the variation in this angle relates to modifications occurring in both proximal and distal epiphyses. A valgus deformity might create a secondary rotation in the distal articular axis. *Cubitus valgus* has been identified by King and colleagues (1969) in professional baseball pitchers. This is a lateral deviation of the distal epiphysis which increases the carrying angle and causes the forearm to be laterally deviated. This deviation effectively increases the humeral torsion angle, as the distal articular surface, rather then being aligned in a medio-lateral plane under normal conditions, is oriented more posteriorly. Accurate measurements of the valgus deformity should identify any role it plays in the torsion angle.

5.4 Humeral Torsion: Population Results

The first question this research addresses concerns what constitutes normal in humeral torsion. What is the average expected torsional angle? If torsion is strongly related to behaviour, one may expect it to vary between populations. However, to address this, it

Figure 5.5: Boxplot graph demonstrating the average and range of humeral torsion angles (right and left limbs combined) among all populations examined. The key may be found in Table 5.4. The transverse line represents the median value, the box is the interquartile range, the whiskers represent the spread and circles represent outliers.

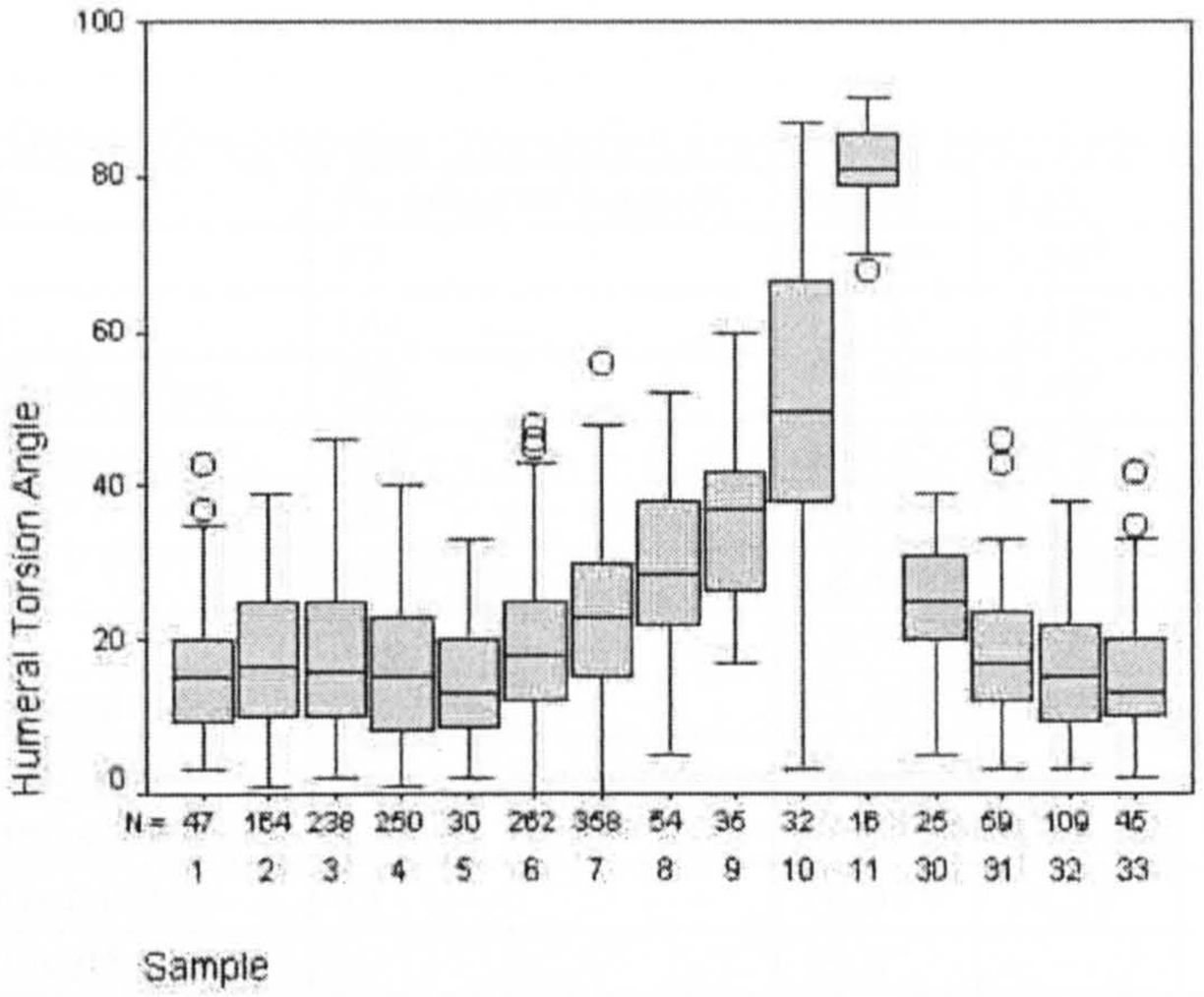

Table 5.4: Key to population codes. Note: the populations are ordered relative to expected robusticity based on archaeological contextual information (see Chapter 3). The Fishergate site has been split additionally into the three separate cemetery areas and a blade-injured group.

Population code	**Population**	**Population code**	**Population**
1	Towton (T)	9	*Pan sp.*
2	Mary Rose (MR)	10	*Pongo sp.*
3	Fishergate (FG)	11	*Macaca sp.*
4	Wharram Percy (WP)	30	FG – blade-injured
5	Hickleton (HK)	31	FG eastern cemetery
6	Chichester (CH)	32	FG intramural cemetery
7	Terry (TR)	33	FG southern cemetery
8	*Gorilla sp.*		

must first be determined what a normal population average is. As noted in Figure 5.5 and Table 5.5, the average degree of humeral torsion in either the archaeological or modern collections does not approach the values reported in the modern clinical literature. The archaeological samples vary from 14.58° to 25.44°, indicating a more medially placed humeral head, on average, when compared with modern clinical values. The modern, cadaver-based sample does display a higher average humeral torsion angle (22.70°), although this, too, does not approach that reported in the clinical literature. These changes would perhaps indicate a diachronic aspect to humeral torsion, with the

angle increasing (producing a more medially oriented humeral head) in individuals from the medieval period to modern times. The highest average torsion angles are found among the non-human primate species.

Table 5.5: Descriptive Statistics: Population averages for both limbs (pooled sex).

Population	Number of humeri	Mean	S.D.	Minimum	Maximum
Towton	47	15.76°	9.08°	3°	43°
Mary Rose	164	17.18°	9.45°	1°	39°
Fishergate (collective)	238	17.74°	9.49°	2°	46°
Wharram Percy	250	16.44°	9.72°	1°	40°
Hickleton	30	14.58°	8.77°	2°	33°
Chichester	262	18.64°	9.12°	0°	48°
Terry	358	22.70°	9.85°	0°	56°
FG blade-injured	25	25.44°	8.40°	5°	39°
FG eastern cemetery	59	18.44°	9.26°	3°	46°
FG intramural cemetery	109	16.28°	8.64°	3°	38°
FG southern cemetery	45	16.07°	10.37°	2°	42°
Modern clinical*	--	29.8°	--	10°	55°
Gorilla sp.	54	28.68°	10.50°	5°	52°
Pan sp.	35	35.97°	11.18°	17°	60°
Pongo sp.	32	51.43°	20.6°	3°	87°
Macaca sp.	16	81.31°	6.43°	38°	90°

*Nicholson and Lintner (1997)

The populations chosen represent a broad range of potential activity levels from the very active to the infirm (See Chapter 3, Materials). An active, combat-related context is suggested by the blade-injured samples from the Towton and Fishergate samples, as well as the men from the *Mary Rose*, King Henry VIII's flagship which sank in 1545 AD. As the Fishergate site benefits from strong contextual information and discrete burial areas, this collection has been divided into a blade-injured sample; the eastern, ecclesiastic cemetery sample; the intramural burials; and the southern, lay cemetery. Wharram Percy and Hickleton are rural farming populations, while the Chichester sample is from a leper hospital and later almshouse. The Terry collection was selected to investigate any temporal aspect of humeral torsion, as well as to determine if the variation in humeral torsion between reported clinical values and the archaeological samples was a function of methods employed or differences in activity patterns. Non-

human primates were also investigated. It is expected that humeral torsion varies as a function of differences in habitual activity patterns. Therefore, fundamental differences should exist between human and non-human primate samples in both the absolute angle of torsion and the levels of asymmetry between limbs.

The range of variation between archaeological samples is small, within 3°. However, a large standard deviation and broad range of values indicates that this trait is not ontogenetically constrained. Interestingly, when the Fishergate population is divided according to its discrete contexts, the blade-injured sample stands out with the highest average bilateral torsion angle (25.44°), highlighting an actual difference of 11° between samples. Because of this difference, this sample will be separated into the four different contextual and social groups, the blade-injured sample, the eastern cemetery, the intramural cemetery and the southern cemetery area for future analysis. While a broad range of values and a high standard deviation may be expected within the human populations, it is perhaps surprising to find the greatest standard deviation to occur in three of the four non-human primate species. It would be expected that these populations would demonstrate more constrained values of humeral torsion, reflecting less variation in activity patterns. This could be due to a number of causes, including the origins of the samples. The majority of specimens were 'wild shot', however, there are a number of specimens that originated from zoos, including an orangutan from the Jersey Zoo, in the Channel Islands, who displayed considerably lower humeral torsion angles (3° and 17°) when compared with the other *Pongo* specimens. Additionally, this variation may relate to differences in activity patterns between sexes or sexual dimorphism, the latter to be tested in a later section.

On the population level, the average torsion angle values vary significantly between the archaeological populations, the non-human primate species and the modern sample (Terry collection). Examination of the data shows that not all samples display a normal distribution in humeral torsion angles. Despite this, one-way ANOVA was still calculated, as samples sizes are large enough to compensate for any variation in data. As biometric data, there is no reason to assume the data is not a random sampling, and that any skew to the data is reflective of anything more significant than random biological variation. As the sample sizes vary, Hochberg's GT2 was chosen for the post-hoc analysis as it is designed to cope with situations in which sample sizes are very different (Field 2000).

Table 5.6: Humeral torsion within human populations, sides averaged. ANOVA, Post-hoc Hochberg's GT2: Human populations, sexes pooled. MR = Mary Rose, WP = Wharram Percy, HK = Hickleton, CH = Chichester, FG BI = Fishergate blade-injured, FG east = Fishergate eastern cemetery, FG intra. = Fishergate intramural cemetery, FG south = Fishergate southern cemetery.

	Towton	MR	WP	HK	CH	Terry	FG BI	FG East	FG Intra.
Towton	-								
MR	1.000	-							
WP	1.000	1.000	-						
HK	1.000	1.000	1.000	-					
CH	.999	1.000	.684	.965	-				
Terry	.001**	.000**	.000**	.001**	.000**	-			
FG BI	.007**	.010**	.001**	.005**	.096	1.000	-		
FG east	1.000	1.000	1.000	1.000	1.000	.189	.258	-	
FG intra.	1.000	1.000	1.000	1.000	.975	.000**	.003**	1.000	-
FG south	1.000	1.000	1.000	1.000	1.000	.002**	.014*	1.000	1.000

*p < 0.05; ** p < 0.01

Significant differences in humeral torsion were identified between archaeological, modern and non-human primate samples (Tables 5.6, 5.7). The modern Terry collection differs significantly from all populations, except for the Fishergate eastern cemetery and blade-injured group. This last sample varies significantly from all samples except that from Chichester, the Terry collection and the eastern Fishergate

cemetery. The degree of humeral torsion in the non-human primate samples varies significantly between all non-human primate species examined, as well as between all human samples, with the exception of the *Gorilla* and Fishergate BI samples ($p < 1.000$). Humeral torsion varies significantly between archaeological, modern and non-human primate samples, including the two blade-injured populations. It has even been found to vary between samples from a single archaeological population, between the Fishergate blade-injured individuals and the intramural high status burials and those from the southern, lay cemetery. There is no significant variation between the blade-injured individuals and the eastern, ecclesiastical cemetery.

Table 5.7: ANOVA, Post-hoc Hochberg's GT2: Non-human primate species compared with human populations, sexes pooled, sides averaged.

Population	***Gorilla***	***Pan***	***Pongo***	***Macaca***
Towton	.000**	.000**	.000**	.000**
Mary Rose	.000**	.000**	.000**	.000**
Wharram Percy	.000**	.000**	.000**	.000**
Hickleton	.000**	.000**	.000**	.000**
Chichester	.000**	.000**	.000**	.000**
Terry	.003**	.000**	.000**	.000**
FG blade-injured	1.000	.005**	.000**	.000**
FG eastern cemetery	.000**	.000**	.000**	.000**
FG intramural cemetery	.000**	.000**	.000**	.000**
FG southern cemetery	.000**	.000**	.000**	.000**

**Sig. ($p < 0.01$)

The Fishergate blade-injured group possess an increased torsional angle compared to the other groups. Looking back to previous discussion, this implies that the relevant distinction to humeral torsion is an increased angle, or decreased torsion creating a more posteriorly placed humeral head. The average torsional angle of the Fishergate blade-injured sample is increased such that it is comparable to that of the Gorilla. This similarity – a greater torsional angle - was also found within the sports medicine literature, which also identified an increased angle as an adaptation to strenuous unimanual activity.

The samples were divided into groups based upon combatant status. All individuals with blade-injuries formed one group, the Mary Rose collection, with its inferred combatant status formed a second group, and these two samples were compared with all males without blade injuries. Population differences between samples based upon blade-injured status were tested using one-way ANOVA and were found to be significant ($p < .003$). Post-hoc analysis identified significant differences in humeral torsion angle between the Mary Rose sample and those without blade injuries ($p < .014$), as well as those with blade injuries ($p < .004$).

Table 5.8 summarises the average humeral torsion angles for each group, although it should be considered that the high average humeral torsion angles of the Terry collection and the Fishergate BI sample will be influencing both the non blade-injured and the blade-injured groups. When the modern Terry collection is excluded, leaving only archaeological collections analysed, there is still a significant difference between populations ($p < .002$), however, it is now the blade-injured sample that is unique from the non blade-injured sample ($p < .002$) and the Mary Rose sample ($p < .003$).

Table 5.8: Humeral torsion angle by combatant status, sides averaged. Population differences are significant ($p < .003$, ANOVA).

Sample	No. of humeri	Mean	S.D.
Non blade-injured males*	1020	19.51°	9.86°
Non blade-injured males (archaeological)**	662	17.79°	9.43°
Blade-injured males	110	21.08°	9.96°
Mary Rose	164	17.18°	9.45°

*This sample includes the Terry collection; **Archaeological samples only

In summary, an 11° difference in average humeral torsion values (right and left limb combined, both sex groupings) has been identified between archaeological samples, as well as in the modern Terry collection. The sample with the lowest average humeral torsion angle (most medially oriented humeral head) is the rural site of

Hickleton. This is followed by the Towton sample, the southern Fishergate cemetery, the intramural cemetery from Fishergate, the rural site of Wharram Percy and the men of the Mary Rose. Those samples falling within the higher range of average humeral torsion values are the Fishergate blade-injured sample, with the highest average angle, followed by the Terry collection, the Chichester sample and the Fishergate eastern cemetery sample. There are significant differences between groups based upon combatant status. There is no patterning to the humeral torsion value relative to the archaeological context such as blade-injured or rural sites grouped together. The humeral torsion values for the non-human primate samples increase as the mode of locomotion changes from terrestrial quadruped (*Gorilla*) to arboreal quadruped (*Macaca fascicularis*) (Fleagle, 1999).

Despite the relatively constrained grouping of humeral torsion values, with the majority of archaeological samples falling with 3° of variation, the large standard deviation in average humeral torsion angle indicates that this trait is not ontogenetically constrained. Significant differences in humeral torsion angles were identified both between and within the human collections. The angle of humeral torsion displayed by all non-human primate species is unique to each species, with the exception of the Fishergate blade-injured and the *Gorilla* samples. This leads to the conclusion that the 0mode of adaptation in humeral torsion is that of an increased humeral torsion angle (more posteriorly placed humeral head). There does not appear to be a 'normal' humeral torsion angle, but rather a range of variation that has a central tendency within human populations.

5.4.1 Sex Differences in Humeral Torsion

The second question to be addressed is how does humeral torsion vary between males and females within population samples? If differences in humeral torsion angles reflect behaviourally adaptive responses, then significant differences would be expected between the sex groups given culturally mediated differences in male and female labour (Murdoch and Provost, 1973). This hypothesis is tested by application of Kruskal-Wallis's nonparametric test statistic for independent samples. This method was chosen over the Mann-Whitney test statistic for independent samples because Kruskal-Wallis allows for more than two conditions. Ordinarily, Mann-Whitney would be applicable, as sex groups are either male or female. However, a large number of the non-human primate specimens, as well as a limited number of individuals from the Chichester sample were indeterminate in terms of sex; therefore, an additional condition had to be included. The addition of a third condition in the human samples did not affect the results, as a Mann-Whitney analysis, ran concurrently, identified exactly the same results in these samples.

Table 5.9: Differences between sexes for all populations (Kruskal-Wallis non-parametric test statistic for independent samples). Those populations not listed were composed of all males.

Population	Chi-square	df	Significance
Wharram Percy	5.625	1	.018*
Hickleton	1.355	1	.244
Chichester	1.179	2	.278
Gorilla sp.	4.232	2	.040*
Pan sp.	.812	2	.368
Pongo sp.	15.605	2	.000**
Fishergate eastern cemetery	4.016	1	.045*
Fishergate intramural cemetery	2.244	1	.134
Fishergate southern cemetery	3.973	1	.046*

*p < 0.05; ** p < 0.01

Differences in humeral torsion between males and females were identified in several samples (Table 5.9), including that from Wharram Percy, the eastern and southern cemeteries at Fishergate and both *Gorilla* and *Pongo* species. However, it

should be noted that females form a minority of the samples, and any significance, or lack thereof, may be a factor of sample size (Table 5.10). This is most likely the case with the Fishergate eastern sample, as females make up only three of the 57 skeletons sampled in this area. The Fishergate southern cemetery sample has ten females out of a total of forty-two individuals. The sample sizes are, however, robust enough in the Wharram Percy sample to confidently identify patterned differences as reflected by changes in humeral torsion between males and females.

Table 5.10: Population frequencies: Humeral torsion by sex.

Population	No. of humeri	Mean	S.D.	Minimum	Maximum
Towton	47	15.76°	9.08°	3°	43°
Mary Rose	164	17.18°	9.45°	1°	39°
Wharram Percy (males)	153	17.61°	9.81°	1°	40°
Wharram Percy (females)	97	14.58°	9.32°	1°	35°
Hickleton (males)	15	16.66°	9.86°	2°	33°
Hickleton (females)	15	12.50°	7.26°	2°	27°
Chichester (males)	191	19.14°	9.39°	0°	48°
Chichester (females)	68	17.30°	8.40°	1°	37°
Chichester (indeterminate)	3	17.67°	6.43°	13°	25°
Terry	358	22.70°	9.85°	0°	56°
FG BI	25	25.44°	8.40°	5°	39°
FG eastern (males)	54	19.44°	8.96°	3°	46°
FG eastern (females)	3	8.66°	5.13°	3°	13°
FG intramural (males)	83	15.76°	8.49°	4°	38°
FG intramural (females)	22	18.40°	9.07°	4°	34°
FG southern (males)	32	17.70°	11.11°	2°	42°
FG southern (females)	10	11.00°	4.87°	2°	19°
Modern clinical*	--	29.80°	--	10°	55°
Gorilla sp. (males)	22	25.77°	10.04°	8°	40°
Gorilla sp. (females)	16	32.43°	11.91°	5°	52°
Gorilla sp. (indeterminate)	16	28.93°	8.91°	12°	42°
Pan sp. (males)	11	34.90°	12.26°	20°	57°
Pan sp. (females)	18	38.88°	10.13°	25°	60°
*Pan sp. (*indeterminate)	6	29.16°	10.57°	17°	42°
Pongo sp. (males)	23	42.91°	14.99°	3°	68°
Pongo sp. (females)	7	80.00°	4.89°	75°	87°
Pongo sp. (indeterminate)	2	49.50°	2.12°	48°	51°
Macaca sp. (males)	12	82.25°	6.22°	70°	90°
Macaca sp. (indeterminate)	4	78.50°	7.14°	68°	84°

Differences between males and females were identified in two of the non-human primate species, *Gorilla* and *Pongo*. However, the male zoo orangutan with the

extremely low humeral torsion angles could be skewing the results in this instance. It is plausible that the broad range of humeral torsion values displayed in the non-human primate species, certainly within the Gorilla sample, is a function of sexual differences in body mass or sexual differences in activity.

The results seem to support the hypothesised link between increased torsion being found in females rather than males. Where male and female samples exist in one sample, females do display increased torsion, or lower absolute angles, in all samples with the exception of the Fishergate intramural sample, when compared with the male samples. These differences are largely non-significant as demonstrated above, although there is a large disparity in sample sizes that is likely influencing the results. In the non-human primate samples, the females display decreased torsion when compared with the males, as the average angle in these samples is greater in all species.

Table 5.11: Population differences in humeral torsion, side averaged (ANOVA, Post-Hoc Hochberg's GT2). Males only. MR = Mary Rose, WP = Wharram Percy, HK = Hickleton, CH = Chichester, TR = Terry, FG BI = Fishergate blade-injured, FG east = Fishergate eastern, FG intra. = Fishergate intramural, FG south = Fishergate southern.

	T	MR	WP	HK	CH	Terry	FG BI	FG east	FG intra.
Towton	--								
MR	1.000	-							
WP	1.000	1.000	-						
HK	1.000	1.000	1.000	-					
CH	.967	.998	1.000	1.000	-				
TR	.000**	.000**	.000**	.849	.004**	-			
FG BI	.006**	.008**	.020*	.445	.212	1.000	-		
FG east	1.000	1.000	1.000	1.000	1.000	.530	.439	-	
FG intra.	1.000	1.000	1.000	1.000	.439	.000**	.001**	.992	
FG south	1.000	1.000	1.000	1.000	1.000	.595	.356	1.000	1.000

*p < 0.05; ** p < 0.01

Population differences in humeral torsion are significant when considering average differences by sex (p <0.00) (ANOVA). Closer examination shows results similar to the analysis of pooled sex data. Considering the males, the Terry collection differs significantly when compared to all groups, except those from Hickleton,

Fishergate BI, Fishergate eastern and southern cemeteries. The Fishergate blade-injured males differ significantly from all populations, except those from Hickleton, Chichester, Terry, and the Fishergate eastern and southern cemeteries (Table 5.11). There are no significant differences in humeral torsion values between the female samples in the human collections, although there are significant differences between the female non-human primate groups. These differences extend to comparison between non-human primates and the female archaeological samples (Table 5.12, 5.13). When comparing the human and the non-human male collections, the torsion angle is significantly increased in the Hickleton, Chichester, and Fishergate blade-injured, eastern and southern cemetery samples so as to not differ significantly from that found in the *Gorilla* species. Humeral torsion in the Fishergate blade-injured sample is decreased such that it does not vary significantly from the chimpanzee sample.

Table 5.12: Population differences in humeral torsion, side averaged (ANOVA, Post-hoc Hochberg's GT2). Females only.

Population	**Wharram Percy**	**Hickleton**	**Chichester**	**Fishergate eastern**	**Fishergate intramural**
Wharram Percy	-				
Hickleton	1.000	-			
Chichester	.908	.927	-		
FG eastern	1.000	1.000	.989	-	
FG intramural	.877	.801	1.000	.950	-
FG southern	.999	1.00	.513	1.00	.383

Table 5.13: ANOVA, Post-hoc Hochberg's GT2, males only, human and non-human primate collections. The difference in humeral torsion angles is significant between all female samples.

Population	***Gorilla***	***Pan***	***Pongo***	***Macaca***
Towton	.007**	.000**	.000**	.000**
Mary Rose	.010**	.000**	.000**	.000**
Wharram Percy	.024*	.000**	.000**	.000**
Hickleton	.411	.000**	.000**	.000**
Chichester	.223	.000**	.000**	.000**
Terry	1.000	.004**	.000**	.000**
FG BI	1.000	.518	.000**	.000**
FG eastern	.425	.000**	.000**	.000**
FG intramural	.001**	.000**	.000**	.000**
FG southern	.339	.000**	.000**	.000**

*p < 0.05; ** p < 0.01

5.4.2 Side Differences in Humeral Torsion

While differences in the humeral torsion angle between sexes may be hypothesised, so too may there be differences between limbs. This was tested using the Mann-Whitney non-parametric statistic for independent samples. These values are summarised in Table 5.14. Differences between right and left limbs in humeral torsion were not significant in any human sample, except the male sample from the eastern cemetery at Fishergate ($p < 0.021$) (Table 5.15). Significant differences were identified between limbs in the indeterminate sex group of the *Gorilla* sample. This group is composed of a number of isolated humeri rather than paired humeri from single individuals, and it is more likely that the nature of the sample has artificially influenced this statistic than indicating any substantially significant differences between limbs in the sample.

Table 5.14: Humeral torsion in males and females, right and left side differences. FG = Fishergate.

	Males				Females			
Population	**No.**	**Right**	**No.**	**Left**	**No.**	**Right**	**No.**	**Left**
Towton	26	14.96°	21	16.76°	-	-	-	-
Mary Rose	77	16.11°	87	18.12°	-	-	-	-
Wharram Percy	74	17.25°	79	17.94°	49	14.06°	48	15.12°
Hickleton	8	17.37°	7	15.85°	8	13.06°	7	11.85°
Chichester	99	19.63°	92	18.60°	32	17.03°	36	17.55°
Terry	179	23.68°	179	21.73°	-	-	-	-
FG blade-injured	13	26.84°	12	23.91°	-	-	-	-
FG eastern	22	22.31°	34	16.79°	1	10.00°	2	8.00°
FG intramural	47	16.41°	39	14.71°	12	18.41°	11	19.00°
FG southern	19	17.81°	14	18.42°	7	11.42°	5	9.40°
Gorilla sp.	11	26.72°	11	24.81°	8	32.87°	8	32.00°
Pan sp.	6	32.50°	5	37.80°	9	39.33°	9	38.44°
Pongo sp.	11	42.18°	12	43.58°	3	78.33°	4	81.25°
Macaca sp.	6	82.00°	6	82.50°	2	82.50°*	2	74.50°*

*sex indeterminate

The results do not support the hypothesised link that increased torsion is found in the right limb when compared with the left. The results for right versus left limbs are mixed as there is no strong directional trend when considering torsion by limb (i.e. increased angles in the right when compared with the left). Analysis of dominant versus

non-dominant limb rather than right versus left limb might elucidate more complex patterns to humeral torsion angles; however, assessment of limb dominance is complicated in archaeological material, as will be discussed in greater detail later.

Table 5.15: Differences between sides for all populations. Mann-Whitney non-parametric test for independent samples. M = males, F = females, Ind. = indeterminate.

Population	Z (M)	Z (F)	Z (Ind.)	Sig. (M) (2-tailed)	Sig. (F) (2-tailed)	Sig. (Ind.) (2-tailed)
Towton	-1.073	-	-	.283	-	-
Mary Rose	-1.367	-	-	.172	-	-
Wharram Percy	-.353	-.845	-	.724	.398	-
Hickleton	-.463	-.638	-	.643	.523	-
Chichester	-.813	-.566	-.1225	.416	.571	.221
Terry	-1.717	-	-	.086	-	-
Gorilla sp.	-.493	-.211	-2.390	.622	.833	.017*
Pan sp.	-.549	-.221	-.443	.583	.825	.658
Pongo sp.	-.062	-.540	-1.000	.951	.589	.317
Macaca sp.	-.081	-	-1.225	.932	-	.221
Fishergate blade-injured	-.736	-	-	.462	-	-
Fishergate eastern	-2.310	-.000	-	.021*	1.000	-
Fishergate intramural	-.699	-.092	-	.484	.926	-
Fishergate southern	-.091	-.409	-	.927	.683	-

*p < 0.05

5.4.3 Bilateral Asymmetry

Significant differences in humeral torsion values were identified between right and left limbs in only two of the samples analysed. However, this test result was based only on the population average for right versus left limb torsion angles. Analysis of bilateral asymmetry is more accurate for identifying variations in humeral torsion angle between limbs because it examines such differences in each individual separately. Bilateral asymmetry was calculated using two different methods. Standardised bilateral asymmetry was evaluated using the formula [(R-L)/((R+L)/2)]*100, while absolute asymmetry, calculated for comparison with the sports medicine literature, was evaluated using the formula (maximum - minimum).

The greatest standardised bilateral asymmetry among the males in humeral torsion angles is found in the Fishergate southern cemetery sample, followed by the

rural Wharram Percy sample, the Mary Rose sample and the eastern cemetery at Fishergate (Table 5.16). Of the remaining combatant populations, Towton and the Fishergate BI samples, the Towton sample falls within the higher range of asymmetry values, while the Fishergate blade-injured population falls within the lowest average asymmetry values, second only to the Hickleton population when considering the human samples.

Table 5.16: Average asymmetry of humeral torsion (males only). Asymmetry is calculated by (maximum - minimum) for comparison with the clinical literature, so the values represent the absolute difference in torsion angle between limbs. Bilateral asymmetry using the standardised formula (R-L)/((R+L)/2)*100 is also calculated. Note, in samples with high levels of bilateral asymmetry, such as a humeral torsion angle of 5°(left) and 28° (right) will result in an asymmetry score of 139.39. FG = Fishergate.

Population	N	Mean Asymmetry (standardised)	Maximum Asymmetry (standardised)	S.D.	Mean Asymmetry (absolute)	Max. Asymmetry (absolute)	S.D.
Towton	**16**	45.84°	137.50°	38.15°	6.06°	22°	5.50°
Mary Rose	**26**	47.61°	175.00°	39.02°	7.46°	28°	5.99°
FG (BI)	**12**	32.76°	139.39°	37.77°	6.95°	23°	6.98°
FG (east)	**20**	46.71°	114.29°	36.38°	7.85°	26°	6.45°
FG (intramural)	**33**	44.82°	120.00°	30.66°	5.92°	17°	4.20°
FG (south)	**12**	51.97°	111.11°	29.24°	7.20°	17°	4.23°
Wharram Percy	**67**	51.19°	163.64°	43.42°	7.40°	23°	5.77°
Hickleton	**7**	30.55°	42.42°	12.52°	4.29°	9°	2.98°
Chichester	**76**	39.28°	200.00°	35.49°	6.63°	25°	5.67°
Terry	**177**	39.34°	200.00°	39.29°	6.96°	24°	5.43°
Gorilla	**12**	19.49°	40.00°	15.20°	4.69°	11°	3.06°
Pan	**8**	14.08°	46.15°	15.50°	5.40°	12	4.27°
Pongo	**10**	28.32°	140.00°	40.65°	8.90°	19	6.33°
Macaca	**7**	4.05°	8.38°	3.27°	3.71°	7	2.81°
Professional handball players*	**51**	--	--	--	14.39°	29°	5.95°
College baseball pitchers**	**19**	--	--	--	10.1°	--	4.7°
College baseball players***	**54**	--	--	--	10.6°	--	--

*Pieper (1998); ** Osbahr *et al.* (2002) ***Reagan *et al.* (2002)

The non-human primates demonstrate the smallest degree of standardised bilateral asymmetry of any sample analysed, although not the smallest amount of

absolute asymmetry in the torsion angle. This difference between methods is further demonstrated in the archaeological and modern samples. The greatest mean absolute asymmetry among males is now found in the *Pongo* sample, followed by the ecclesiastic, Fishergate eastern cemetery, although the Mary Rose sample still falls third. The Hickleton falls within the mean asymmetry levels found in remaining non-human primate samples. Each population sample, however, displays individuals with a difference between sides exceeding that found in the handball and baseball players (see values in Table 5.16).

The average degree of bilateral asymmetry (standardised) in the female samples is higher than that of the corresponding male samples, with the exception of the Fishergate intramural population, where the males exhibit a higher degree of asymmetry (Table 5.17). The differences in standardised humeral torsion asymmetry between males and females were non-significant for all populations, with the exception of the Hickleton sample ($p < .004$).

Table 5.17: Average asymmetry of humeral torsion between archaeological and non-human primate populations (females only). Note, in samples with high levels of bilateral asymmetry, such as a humeral torsion angle of 5°(left) and 28° (right), will result in an asymmetry score of 139.39. FG = Fishergate, Asy = asymmetry.

Population	N	Mean Asy. (standardised)	Max. Asy (standardised)	S.D.	Mean Asy. (absolute)	Max. Asy. (absolute)	S.D.
FG (east)	1	26.09°	-	-	3.00°	3°	3°
FG (intra)	7	38.43°	66.67°	23.84°	7.00°	12°	3.09°
FG (south)	4	76.95°	133.33°	50.51°	6.00°	12°	2.94°
Wharram Percy	42	59.93°	163.64°	39.77°	6.97°	17°	4.29°
Hickleton	7	77.00°	127.27°	34.46°	8.35°	13°	3.70°
Chichester	25	46.26°	166.67°	39.12°	6.76°	16°	4.38°
Gorilla	6	17.58°	40.00°	15.32°	7.16°	15°	5.03°
Pan	4	14.59°	28.57°	12.47°	5.75°	12°	5.05°
Pongo	2	6.45°	12.90°	9.12°	3.00°	6°	4.24°
Macaca	3	8.28°	8.75°	17.45°	6.33°	13°	6.50°

Population differences in the level of bilateral asymmetry (standardised) were initially tested using ANOVA for males and females separately, as any lack of statistical weight to the sex differences may largely be a function of sample size disparity. Population differences for males ($p < .023$) and females ($p < .006$) were significant yet the limited sample sizes for the females prevented post-hoc analysis. Despite the significant result of the ANOVA analysis, the post-hoc test revealed that no two individual populations, either human or non-human primates, varied significantly from each other. There were no significant differences in bilateral asymmetry when examining the samples by blade-injured status (Table 5.18).

Table 5.18: ANOVA (males only). Bilateral asymmetry in blade-injured versus non blade-injured population samples. The Mary Rose collection forms a separate grouping as they have an inferred battle context rather than one directly identifiable through weapon trauma. Population frequencies for each group, in their respective column form the last line of the table. Note, in samples with high levels of bilateral asymmetry, such as a humeral torsion angle of 5°(left) and 28° (right) will result in an asymmetry score of 139.39.

Population	**Blade-injured (N = 31)**			**Mary Rose (N = 26)**			**Non blade-injured (N = 381)**		
Blade-injured	--						--		
Mary Rose	.837			--			--		
Non blade-injured	.999			.751			--		
	Mean	**S.D.**	**Max.**	**Mean**	**S.D.**	**Max.**	**Mean**	**S.D.**	**Max.**
Population frequencies	40.24°	37.83°	139.39°	47.61°	39.01°	175.00°	41.05°	35.76°	163.64°

The results for population differences between male samples ($p < .491$) and female samples ($p < .922$) in absolute asymmetry are not significant. However, closer examination of the absolute difference between limbs is warranted for comparison with the clinical literature. An average difference of 14.39° was identified by Pieper (1998) in professional handball players, while college-level baseball players displayed slightly reduced asymmetry of 10.6° and 10.1° (Reagan *et al.*, 2002; Osbahr *et al.*, 2002). The mean asymmetry values for each population all fall below 10°, however, there are a number of individuals with outlying asymmetry values in relation to their respective

population mean (Figures 5.6, 5.7). These will be discussed in greater detail in the individual population sections.

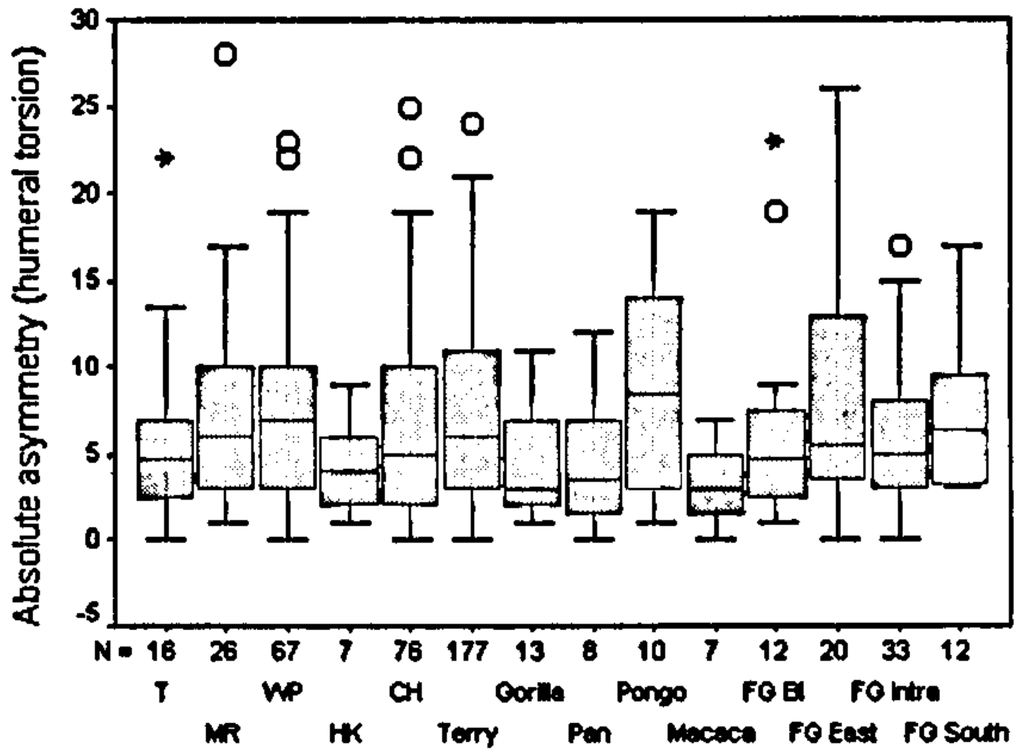

Figure 5.6: Humeral torsion asymmetry (absolute) in males only. This is calculated as the individual difference between the maximum torsion angle – the minimum torsion angle regardless of side.

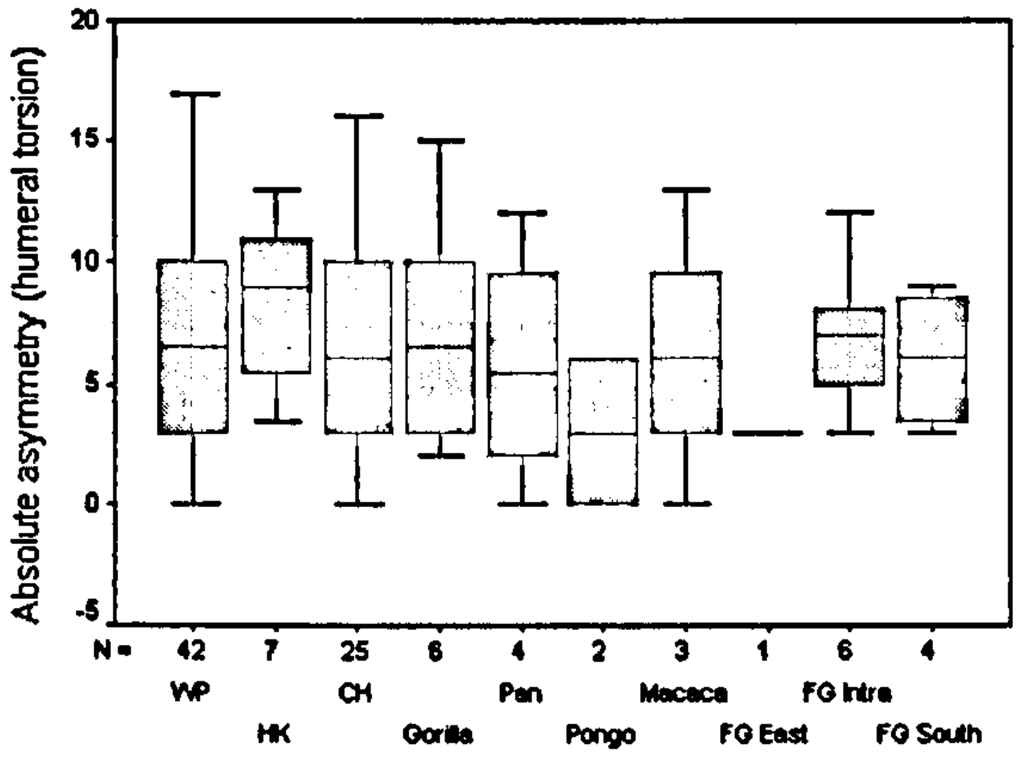

Figure 5.7: Humeral torsion asymmetry (absolute) in females only. This is calculated as the individual difference between the maximum torsion angle – the minimum torsion angle regardless of side.

5.5 Towton

The Towton sample displays directional asymmetry in humeral torsion angles, with the greatest degree of asymmetry found in individuals with increased torsion angles in the left limb (Figure 5.7). Nine of the sixteen individuals with paired humeri have increased torsion angles in the left limb, while only six displayed increased right-sided torsion angles. One individual, T10, displays no asymmetry between limbs. Functionally, this indicates an activity pattern creating moderate left-sided asymmetry. Three individuals, T22, T41 and T16, display healed weapon trauma received in earlier conflicts. This antemortem trauma distinguishes those individuals with previous and possibly regular involvement in combat from individuals who may have been experiencing combat for the first time or were otherwise untrained. T16 and T40 display the greatest degree of asymmetry in the collection, although in the first case, it is right-sided and in the latter,

it is left-sided. T25 and T41, also with healed blade trauma, however, fall within the lower range of bilateral asymmetry. There are no significant differences in humeral torsion angles between those individuals displaying antemortem blade trauma and those who do not.

Figure 5.8: Degree of asymmetry in humeral torsion: Towton. A negative value reflects increased torsion angles in the left limb when compared with the right. The white bars indicate previous healed weapon trauma. Negative values indicate left-sidedness.

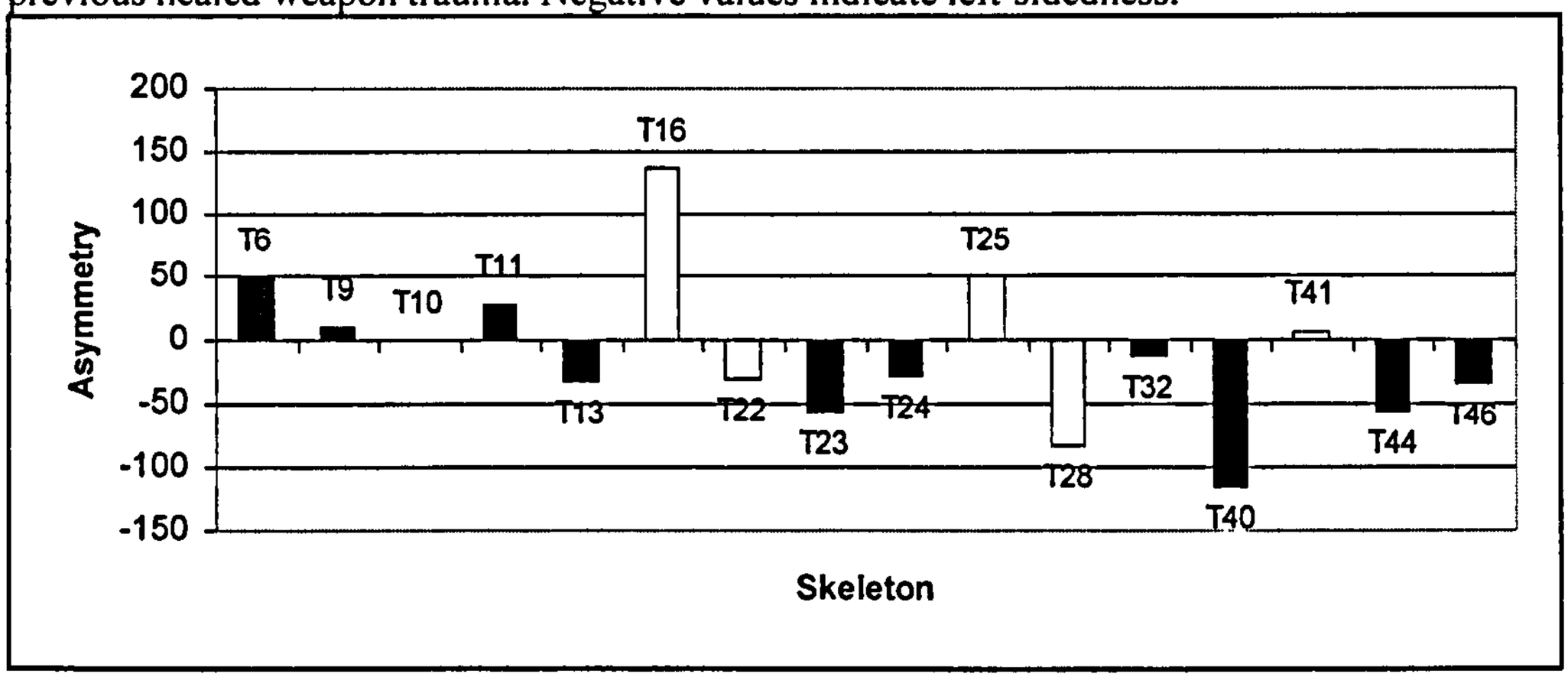

The level of bilateral asymmetry is an indicator of differential use patterns between limbs. However, there are different interpretations possible. Those individuals with high asymmetry values most likely began activity at a young age that modified the humeral torsion angle in one limb to an extent greater than that of the other. Yet, it is equally plausible that symmetry between limbs reflects a similar activity pattern across both limbs, or that the activity or movement pattern was begun post-pubertal and thus did not have as great of an influence on humeral morphology. Given the antemortem trauma to T16 and T41, the level of high asymmetry is likely a result of participation in warfare or weapons training from an early age. Those individuals with lower asymmetry values likely began training only at a later age, or may reflect an activity pattern imposing similar loading across both limbs. This will be examined in greater detail later through biomechanical analysis.

There are two statistical 'outliers' in the Towton population, as indicated in Figure 5.3. These individuals are T8R and T36/37R, who display increased torsion angles when compared with the rest of the collection. There are no left-side torsion angles for either T8 or T36/37. T8, however, stands out by virtue of its variant architecture. It has distinct medio-lateral bowing to the humeral shaft, as well as an unusual morphology of the humeral head that has been identified as a suspected case of slipped proximal epiphysis (pers. obs.). If this diagnosis is accurate, it may explain the increased angle. T8 is one of the oldest and tallest individuals found in the assemblage, and is quite gracile. T36/37 is a young adult male with multiple perimortem injuries to the cranium (Novak, 2000).

There is one statistical outlier in absolute asymmetry as identified in Figure 5.5, T16. The absolute difference between limbs is 22°, in excess of asymmetry of professional and experienced athletes as seen in Table 6.2. T16 is an older male aged between 46 and 50 years. As discussed previously, he is distinguished by antemortem (healed) weapon trauma to the mandible. The healed nature of this wound indicates medical treatment and that that this man was likely a veteran of previous campaigns. Further to the healed trauma, he displays an additional ten peri-mortem cranial injuries (Novak, 2000). T16 appears to fall into the category of the 'professional' combatant, as might others in a similar context with absolute asymmetry values that exceed those of the athletes.

5.6 Mary Rose

The Mary Rose sample is a largely disarticulated sample with a selected number of 'reconstructed' individuals based upon similar morphology. Asymmetry in humeral torsion has been calculated on those individuals with paired humeri, although it must be

considered that these are largely artificial relationships based on morphological similarity between right and left humeri. Similar to the Towton sample, torsion angles are predominantly left-sided, (sixteen out of twenty-six specimens). However, the degree of asymmetry is not as great, as the majority of the values are 50° or less (Figure 5.9). Two individuals stand out, MR44 and MR49, with strong right-sided asymmetry. MR49 is a statistical outlier in the absolute angle difference between limbs, with a difference of 28° between right and left limbs. Similar to T16, these results indicate that this man may have been a 'professional' combatant.

Figure 5.9: Bilateral asymmetry in humeral torsion: Mary Rose. Negative values indicate left-sidedness.

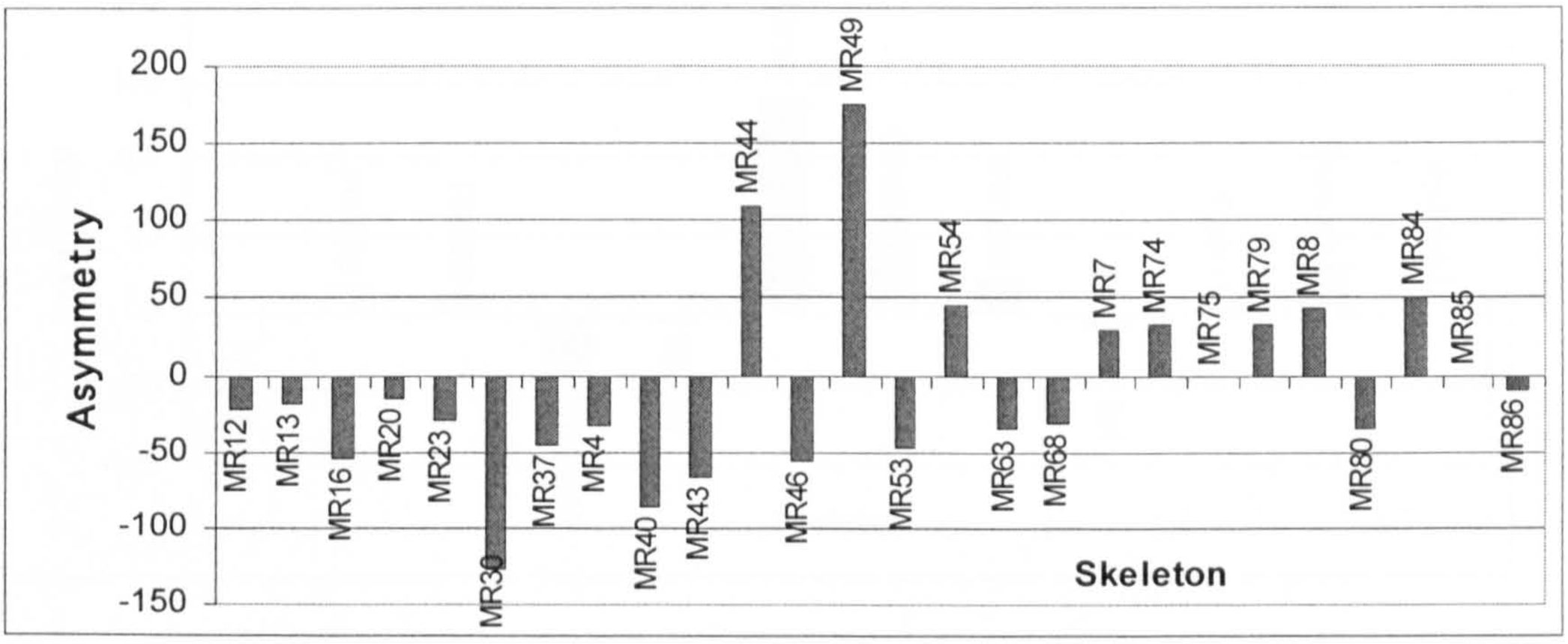

5.7 Fishergate

The Fishergate blade-injured individuals show strong right-sided asymmetry (Figure 5.10). Eight individuals display right-sided directional asymmetry while four individuals display left-sided asymmetry. The majority of these individuals date to the 10th / 11th century, although there are three individuals from later periods, FG5356, FG2270 and FG7052. These three males are from intramural burial contexts and date to between the 14th and 16th centuries. Functionally, the Fishergate BI individuals appear to have been participating in an activity from an early age creating strong directional bilateral asymmetry. This activity involved strenuous use of the right limb. There are two

individuals displaying outlying values for absolute asymmetry. FG6191, with a difference between limbs of 23°, falls as an extreme outlier, while FG1589 has a difference between limbs of 19°. FG6191 is a young male (20 – 30 years of age), from Period 4, relating to the late 10th – early 11th century levels. FG1589 is a male aged 30 – 40 years and is also from the late 10th – early 11th century levels (Stroud and Kemp, 1993). The asymmetry values in excess of that found in experienced athletes indicates that these men were likely 'professionals'.

Figure 5.10: Bilateral asymmetry in humeral torsion: Fishergate (blade-injured). Dark grey bars are period 4 (10th / 11th century), white bars are from the 14th – 16th centuries. Negative values indicate left-sidedness.

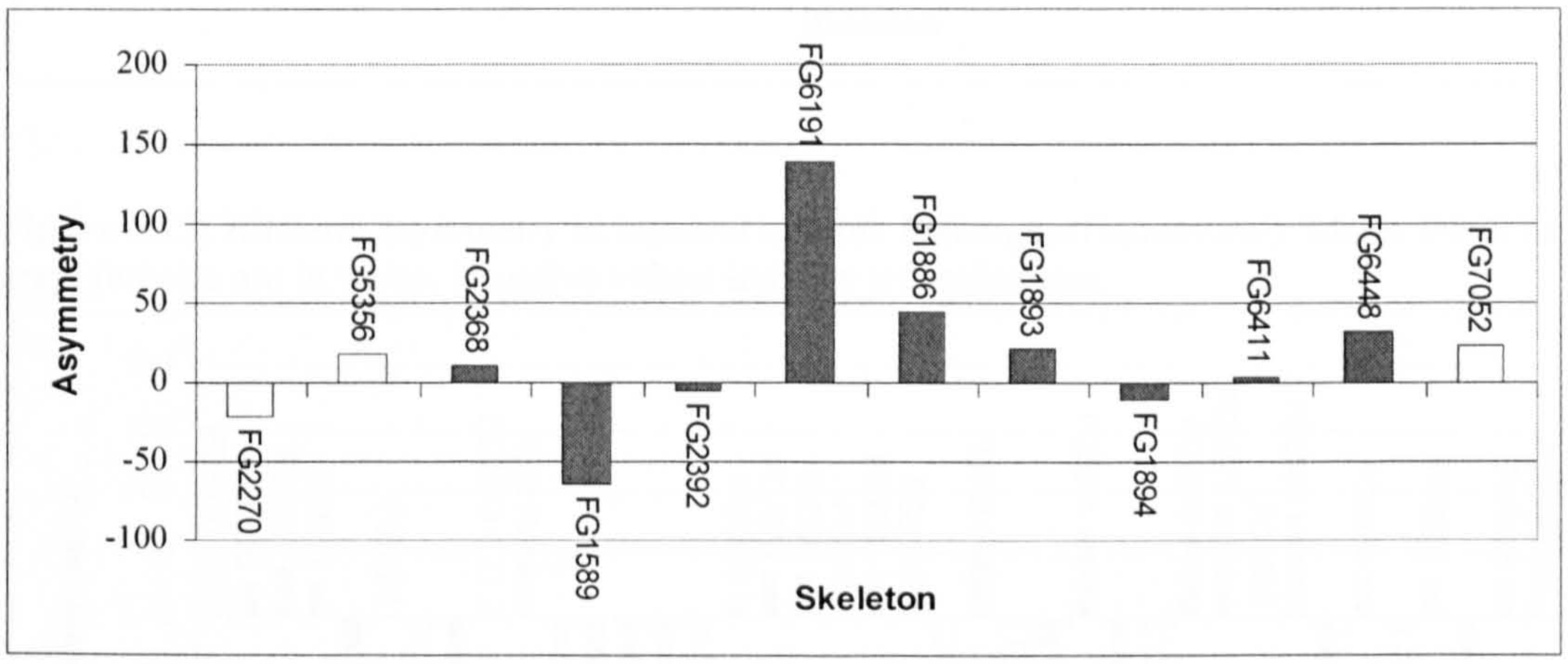

Bilateral asymmetry in the eastern cemetery, Period 6, 12 to 16th centuries, is moderate, although directional. Fourteen of the 20 individuals display right-sided asymmetry in humeral torsion (Figure 5.11). One female skeleton, FG10268, is found in this group. There are two outliers in this population sample, both displaying increased torsion angles; these are FG5062 (left humerus) and FG5724 (right humerus). The level of asymmetry in FG5062 is low while the actual torsion angles, however, are high (R: 33°, L: 46°). FG5724, in comparison, has a higher degree of bilateral asymmetry, with the right humeral torsion angle of 43° compared to the left (17°). Functionally, this group appear to have been engaged in an activity preferentially involving the right

shoulder, similar to the Fishergate blade-injured sample, but creating moderate to strong bilateral asymmetry when compared to the other samples.

Figure 5.11: Bilateral asymmetry in humeral torsion: Fishergate (eastern). Dark grey bars represent males, the white bar represents the female. Negative values indicate left-sidedness.

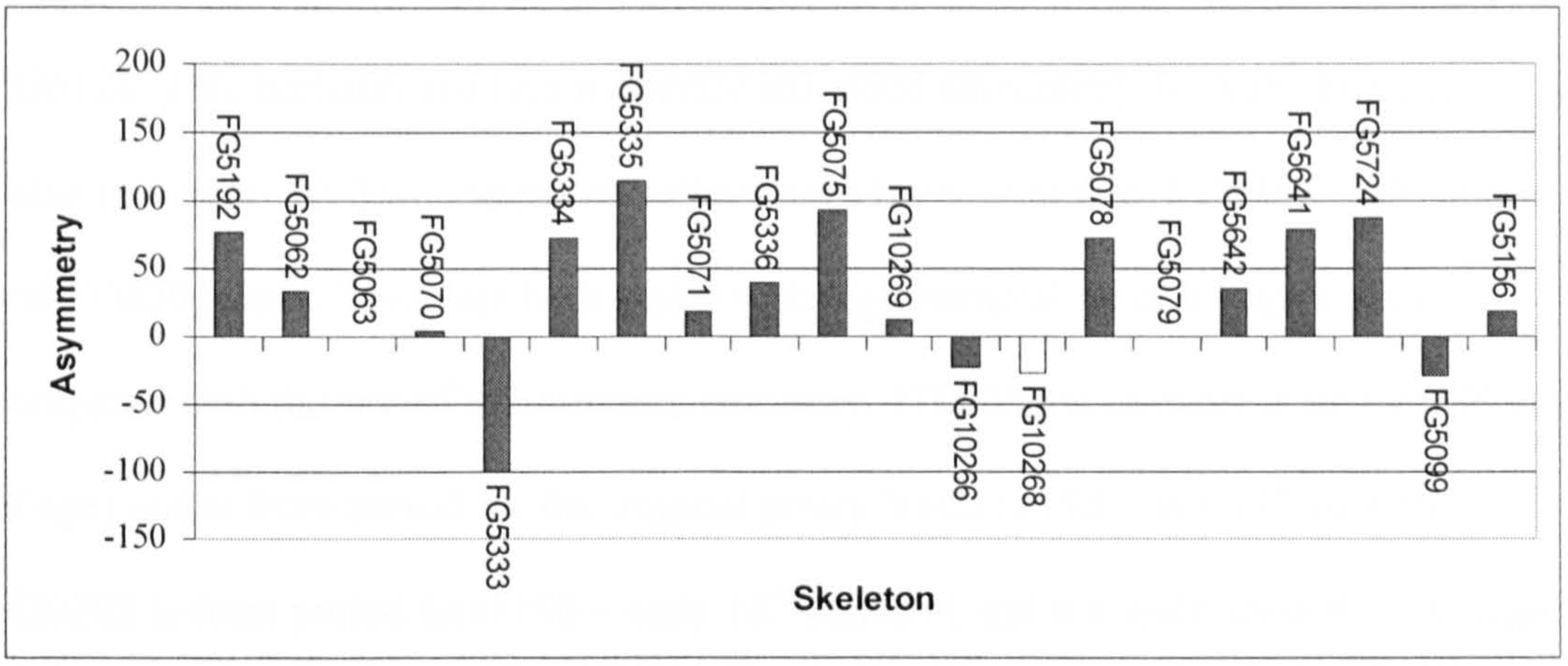

Figure 5.12: Bilateral asymmetry in humeral torsion: Fishergate (intramural). Males are in dark grey, females are in white. Negative values indicate left-sidedness.

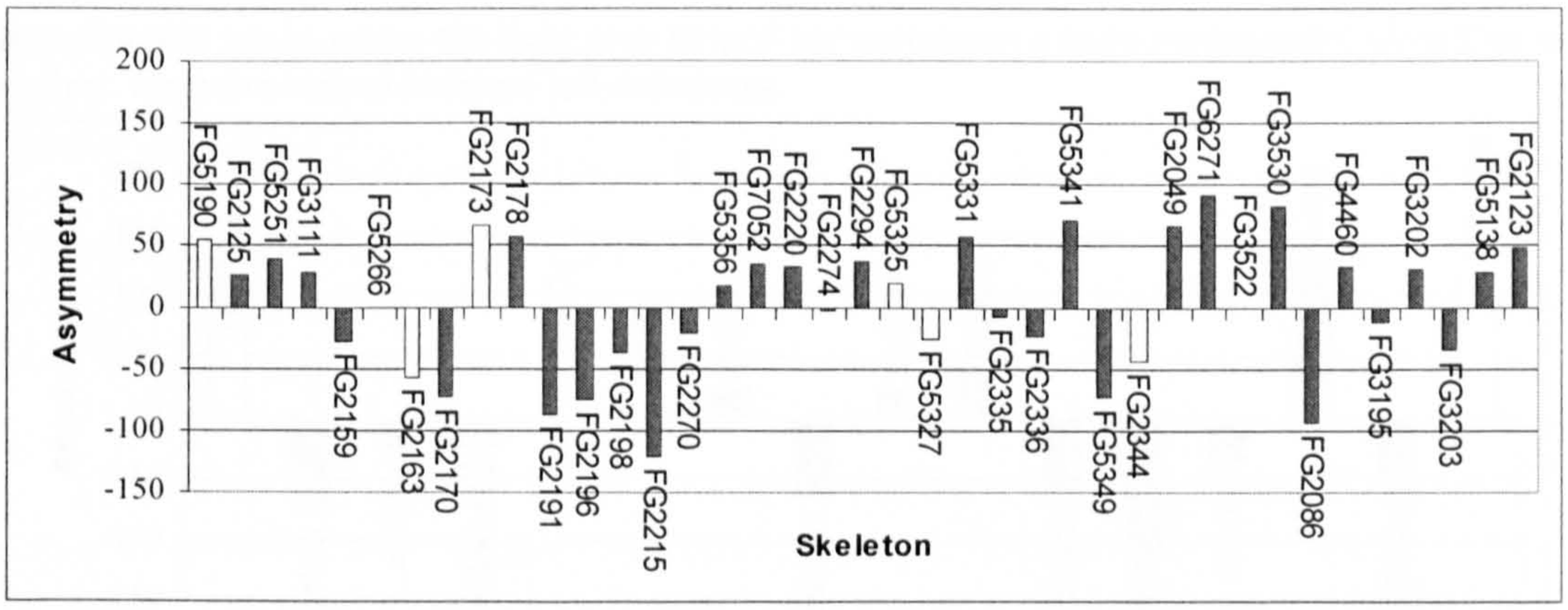

The intramural individuals at Fishergate also display more moderate bilateral asymmetry when compared with the blade-injured sample (Figure 5.12). Seventeen of the 39 individuals show left-sided asymmetry while two show no asymmetry at all. The females display both right and left-sided asymmetry in a range similar to the male values. FG5331 is an outlier in this sample, with an absolute asymmetry of 17° between limbs in the humeral torsion angle (Figure 5.6). The burial of this older male (40 – 50 years) dates to the earlier levels, 1195 – 13th century, and is located in the crossing area.

The Fishergate southern cemetery displays moderate, right-sided, directional asymmetry (Figure 5.13). Similar to the intramural sample, the females in this grouping tend to have equally strong asymmetry when compared with the males. This is similarly mixed between right and left humeri. One burial has been identified as that of a priest, FG6128. This skeleton displays moderate left-sided asymmetry between humeri, with a value just over -50. Two statistical outliers have been identified, FG6303, right and left, and FG6202 right. These are both males with high humeral torsion angles when compared with the rest of the southern cemetery. FG 6303 is an older male (40 -50 years of age) and is from period 6a, the original priory levels (1195 – late 13th century). FG6202 is from period 6z (1195 – early 16th century) and is a male aged 30 – 40 years (Stroud and Kemp, 1993).

Figure 5.13: Bilateral asymmetry in humeral torsion: Fishergate (southern). Males are in dark grey, females are in white, the light grey striped bar represents a male contextually identified as a priest. Negative values indicate left-sidedness.

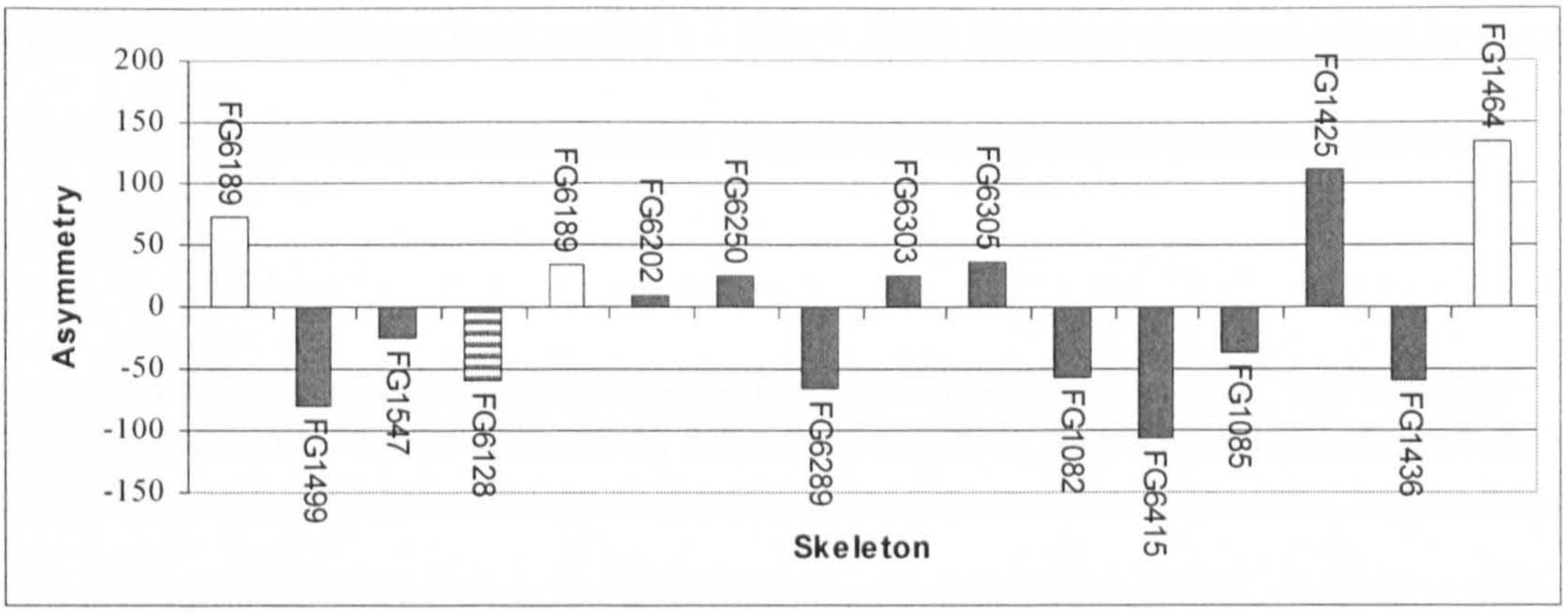

5.8 Wharram Percy

The rural Yorkshire population of Wharram Percy is spread over a broad temporal expanse, from the late Anglo-Saxon period (950 – 1066 AD) to the post-Medieval periods (1540 – 1850 AD), with two phases relating to the Early Medieval (1066 – 1348 AD) and Later Medieval (1348 – 1548 AD) periods. There is a lack of strong temporal boundaries to individual phases, as many skeletons are dated to a more general time

frame, i.e. period 1 – 2 (950 – 1348 AD) (Table 5.21). Despite this, humeral torsion was investigated via one-way ANOVA in an attempt to identify any temporal differences across the site.

Table 5.19: Humeral torsion by period (males only) in the Wharram Percy sample.

Period	**No.**	**Mean**	**S.D.**
Undated	28	12.85°	9.28°
Period 1 (950 – 1066 AD)	5	14.40°	14.36°
Period 1 – 2 (950 – 1348 AD)	60	20.66°	9.70°
Period 2 (1066 - 1348 AD)	22	18.27°	9.59°
Period 2 – 3 (1066 – 1548 AD)	4	17.25°	4.42°
Period 3 – 4 (1348 – 1850 AD)	2	21.00°	12.72°
Period 4 (1540 – 1850 AD)	30	15.53°	8.74°

Population differences in the humeral torsion angle were identified both between males ($p < .021$) and females ($p < .017$) when considering the time period, however, the small sample sizes for the females preclude any further post-hoc analysis. The only result with statistical significance was between the average humeral torsion values of the undated males and those from period 1 - 2 ($p < .010$). No clear temporal patterning, i.e. a general increase or decrease in humeral torsion values across the periods, was thus identified.

Figure 5.14: Bilateral asymmetry in humeral torsion: Wharram Percy males. The white bar (EE13) represents the burial contextually identified as a priest. Negative values indicate left-sidedness.

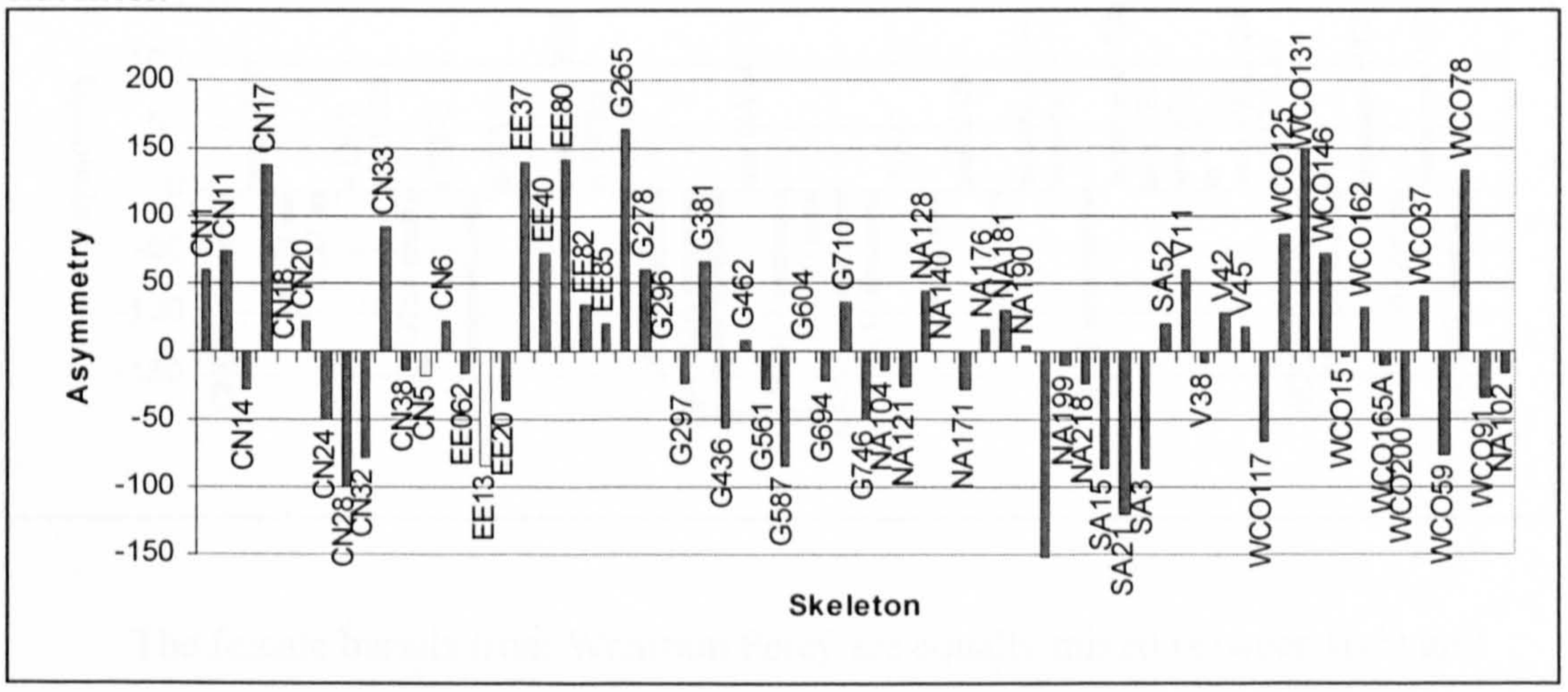

The males display a broad range of bilateral asymmetry in humeral torsion angles (Figure 5.14). Thirty-two males have left-sided asymmetry compared to thirty males with right-sided asymmetry. Four burials display no asymmetry at all. The strongest asymmetry occurs on the right-side, indicating an activity pattern that alters architecture strongest in, predominately, the right limb. There are a number of unique individuals, including a priest, EE13; two blade-injured skeletons, EE03, SA34; two individuals with blunt force trauma, G379 and G715; as well as two burials in stone-lined graves (V38 and V51). Only the priest has torsion values for both right and left humeri. This individual demonstrates increased left-sided asymmetry. Compared to the priest from the Fishergate southern cemetery, this value is not as great but also favours the let side. There are no outliers in humeral torsion, but there are two statistical outliers in absolute asymmetry, EE37 and CN17. EE37, displaying an absolute difference of 22° between limbs, EE37 is a male aged between 40 – 50 years, and is from period 1 – 2. CN17 is a male aged between 30 – 40 years and is from period 4 and displays an absolute difference between limbs in humeral torsion angle of 23°.

Figure 5.15: Bilateral asymmetry in humeral torsion: Wharram Percy females. Negative values indicate left-sidedness.

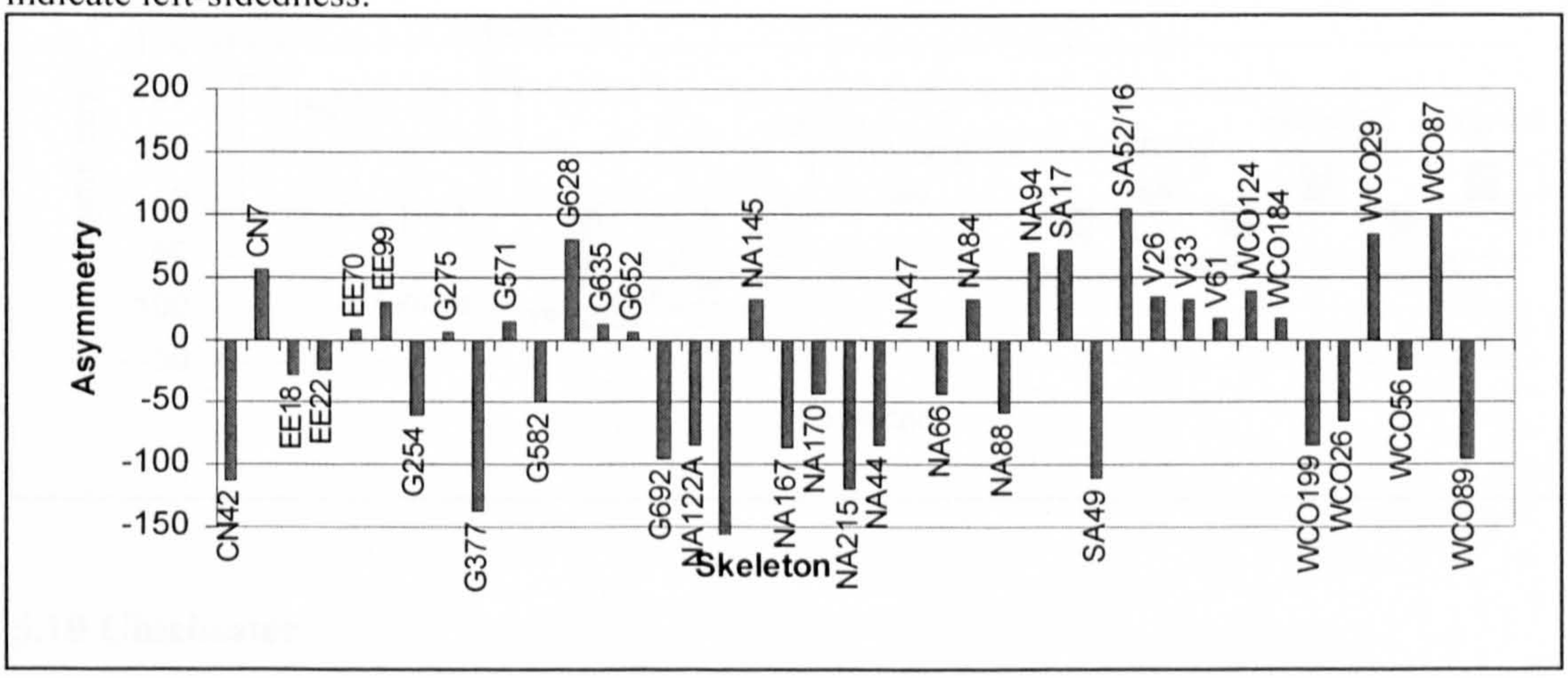

The female burials from Wharram Percy are equally mixed between right and left side asymmetry; 20 left, 20 right, 1 symmetrical, however, the greatest degree of

asymmetry is found in the left-sided individuals (Figure 5.15). This is in contrast to the males from this site, who display relatively equal levels of asymmetry whether right or left sided. The female sample from this site displays a higher average degree of bilateral asymmetry when compared with the males (59.93° for the females, 51.19° for the males). There are no statistical outliers in this population sample (Figure 5.7).

5.9 Hickleton

The Hickleton sample is also a rural Yorkshire population. Asymmetry is low in the Hickleton males when compared with the Wharram Percy group. Again, the highest levels of asymmetry are found in the female skeletons (77° compared with 30.55°). In the Wharram Percy female sample, though, this tends to be left-sided while, in the Hickleton sample, females display stronger bilateral asymmetry to the right but with mixed directional asymmetry between sides (Figure 5.16). There are no special contexts or statistical outliers for this sample (Figures 5.6, 5.7).

Figure 5.16: Bilateral asymmetry in humeral torsion: Hickleton. Males are dark grey, females are white. Negative values indicate left-sidedness.

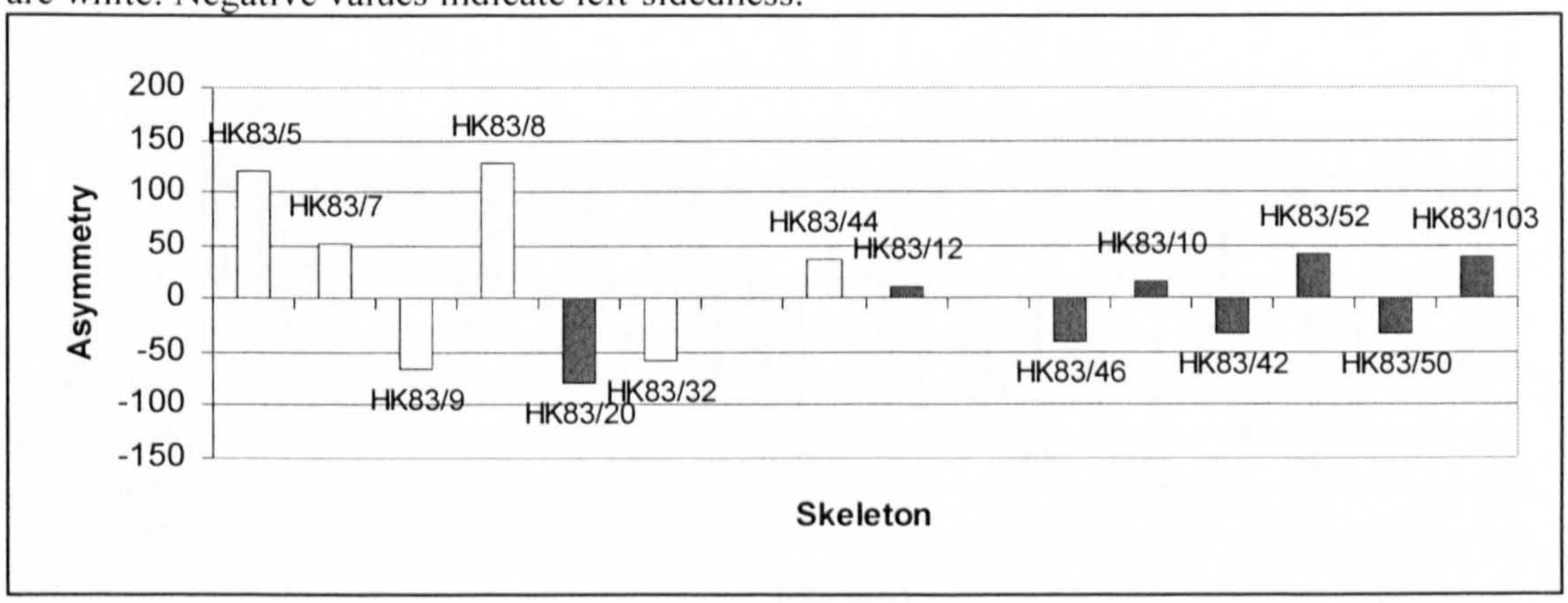

5.10 Chichester

The Chichester male sample displays strong right-sided directional asymmetry in humeral torsion (Figure 5.17). Thirty-six individuals display right-sided asymmetry, while 33 display left-sided asymmetry and five burials display no asymmetry.

Individuals are divided by health status, with light grey striped bars representing individuals with leprosy and white bars representing possible or borderline cases of leprosy (Fay, 2002). There is no strong separation between those individuals bearing lesions of infectious disease and those without, as cases of strong asymmetry are identified in both affected an unaffected groups. The degree of bilateral asymmetry would be expected to be influenced by the age at which the disease was acquired and would only be expected to affect architecture and movement patterns if the individual had fallen ill during key juvenile development periods. Application of one-way ANOVA demonstrates no statistical significance in humeral torsion angles between the different health status groups in this sample, whether the pooled sex ($p < .281$) or by males ($p < .132$) and females ($p < .065$). The different health status groups are as follows: indeterminate; no sign of disease; probable (lepromatous) leprosy; borderline (lepromatous) leprosy; lepromatous leprosy; and tuberculosis.

Figure 5.17: Bilateral asymmetry in humeral torsion: Chichester males. Light grey striped bars are individuals diagnosed with leprosy, White bars are borderline or possible leprosy cases. The remaining individuals show no discernible infectious pathology or do not have sufficient preservation for pathological analysis. Negative values indicate left-sidedness.

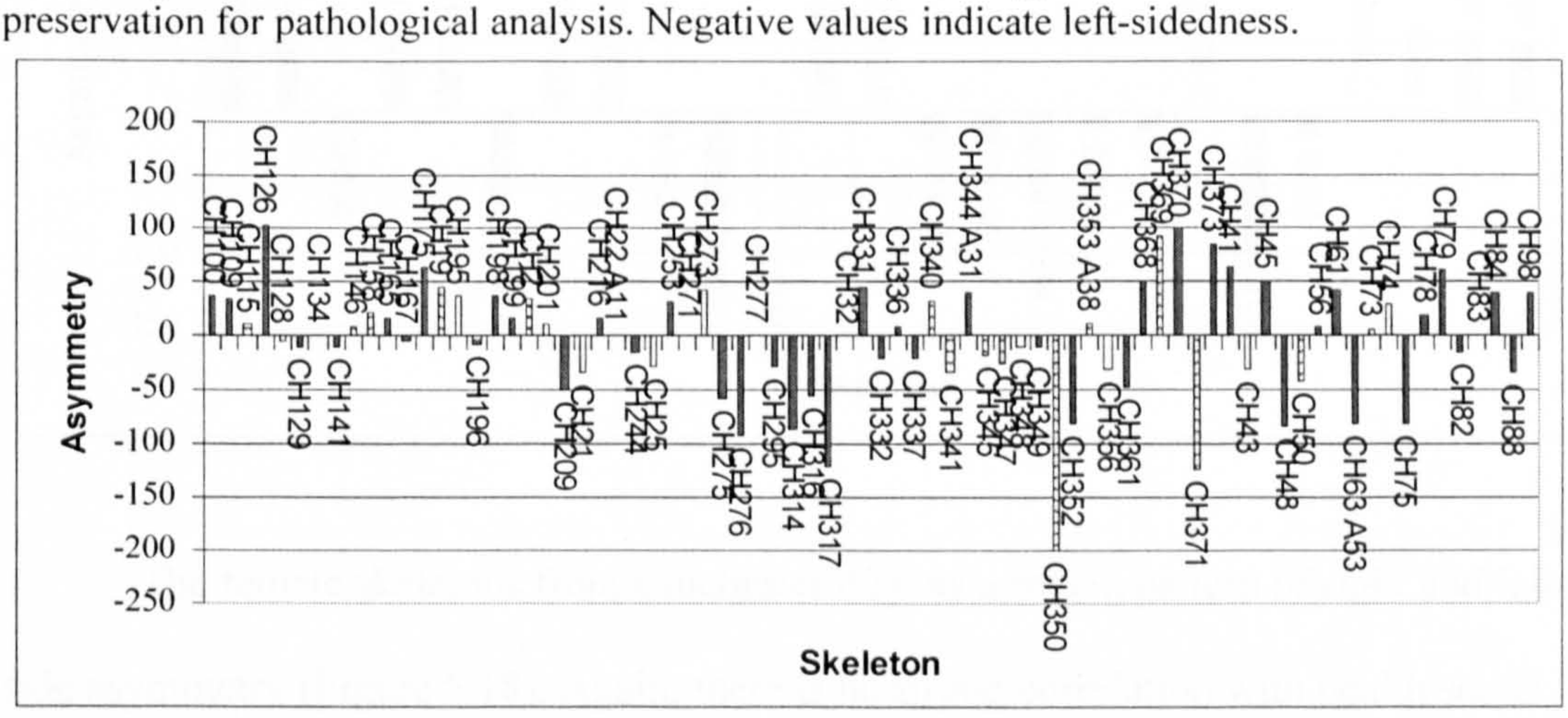

There are three statistical outliers in this sample, CH 115 (right side), CH82 (left side) and CH44 (left side). CH115, a leprous male, has high torsion angles for both right and left limbs, 43° and 48°, respectively. This individual had sustained fractures of both

forearms and of the right femur with right-side shoulder compression, so these values could reflect crutch use (Knüsel and Göggel, 1993). CH82, a male without sufficient preservation to diagnosis leprosy, displays a left-side angle of 46° with the right side also being high at 39°. CH44, a male with borderline leprous symptoms, has only a left side angle of 45° due to lack of preservation of the right humerus. There are two outliers in the absolute asymmetry values, CH126 and CH276. CH126, with an absolute difference between limbs in humeral torsion angle of 25°, is a male, 45+ years of age at death and with insufficient skeletal preservation for pathological analysis. CH276, a male aged 30 – 40 years, has an absolute difference of 22° between limbs and possesses no signs of infectious disease.

Figure 5.18: Bilateral asymmetry in humeral torsion: Chichester females. Light grey striped bars are individuals diagnosed with leprosy, white are borderline or possible leprosy cases and black signifies tuberculosis. The remaining individuals show no discernable pathology or do not have sufficient preservation for pathological analysis. Negative values indicate left-sidedness.

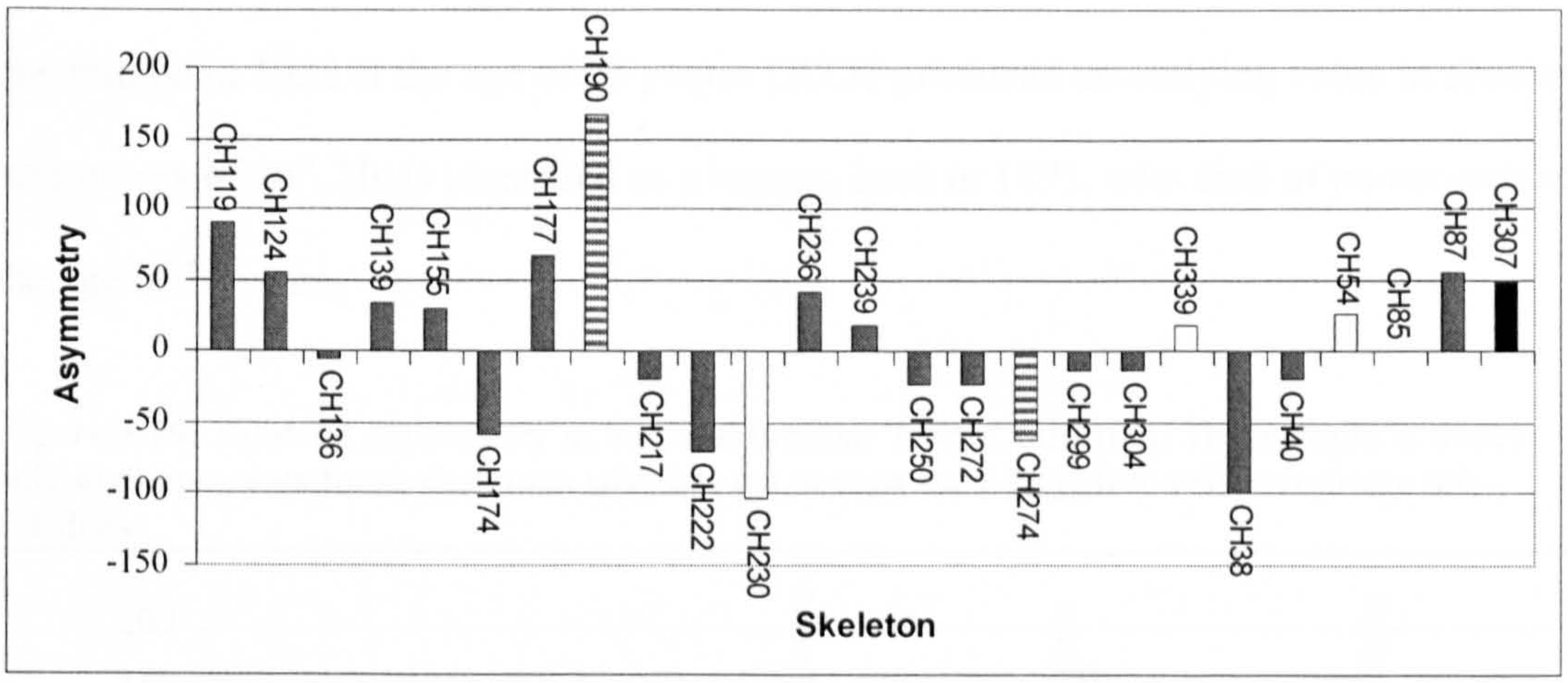

The female skeletons from Chichester display a mixed pattern of right and left-side asymmetry (Figure 5.18). Again, there is no strong correlation with health status and either level or direction of bilateral asymmetry. The level of bilateral asymmetry is higher in the female sample (46.26°) when compared with the males from this sample (39.28°).

5.11 Terry Collection

The Terry sample was included as a modern comparative sample. For ease in exploring the data, the sample was divided into two groups, one of known occupation and all others. The occupations listed for these individuals tend to be general, such as labourers and salesmen. However, specific occupations are listed, such as a watchmaker (TR946) and a cigar maker (TR234). The individuals with listed occupations display the strongest degree of asymmetry on the right side, in a pattern similar to the Fishergate blade-injured individuals (Figure 5.19). This side also comprises the majority in terms of directional asymmetry (36 right-sided, 24 left-sided and three with no asymmetry). There is one statistical outlier in this sample, the right humerus of TR1089 (Fig. 5.5). This individual displays a right-side torsion angle of 56° compared with the left of 45°. Despite the absolute angle difference, he has a moderately low standardised asymmetry (21.78) indicating parity between limbs. TR1089 is listed as a labourer who died from pneumonia in 1932 at the age of 43 years. TR755 produced an outlying value in absolute asymmetry of 24°. He is identified as a beggar, born in 1893, who died of pneumonia at the age of 36 years.

Figure 5.19: Bilateral asymmetry in humeral torsion: Terry Collection. This sample is males only and represents those skeletons with known occupations. Negative values indicate left-sidedness.

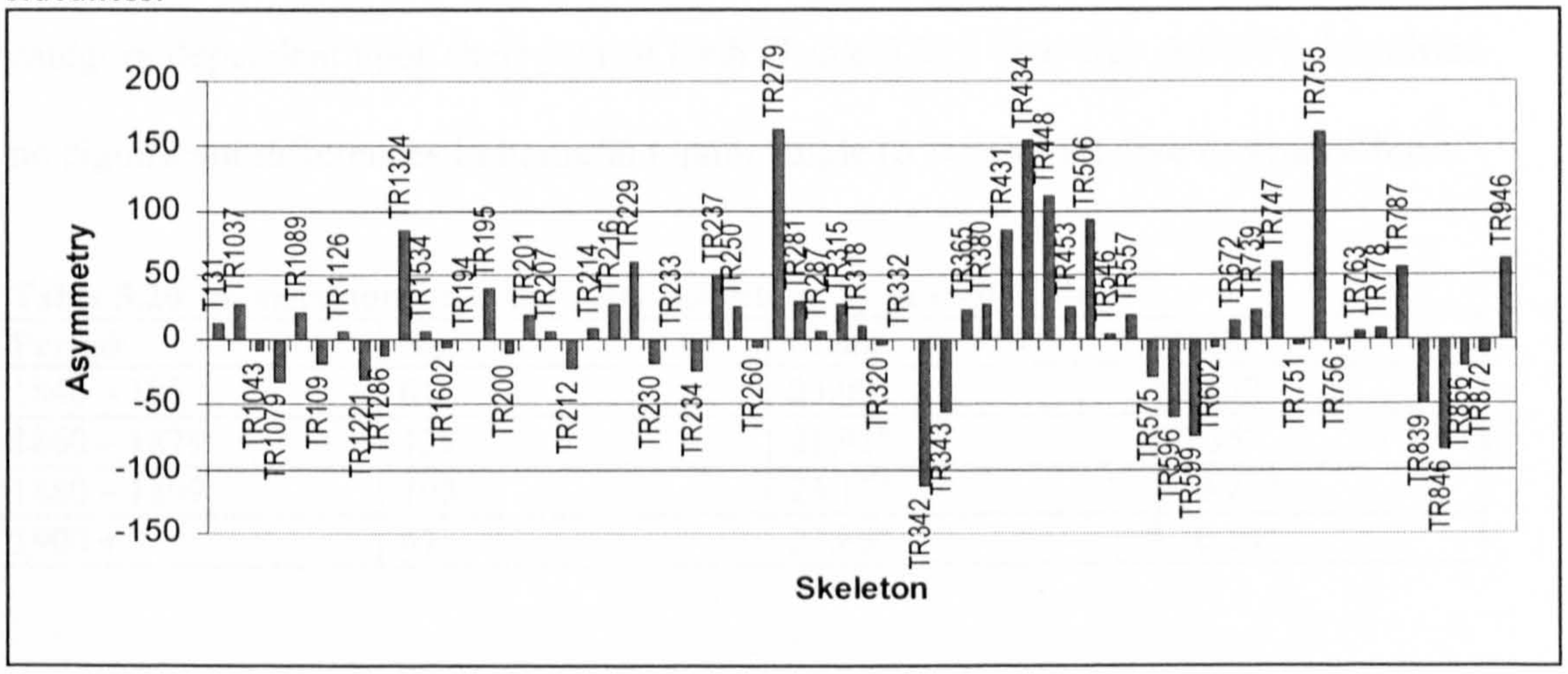

Figure 5.20: Bilateral asymmetry in humeral torsion: Terry collection. This sample is males only and comprises all individuals with no recorded occupation. Negative values indicate left-sidedness.

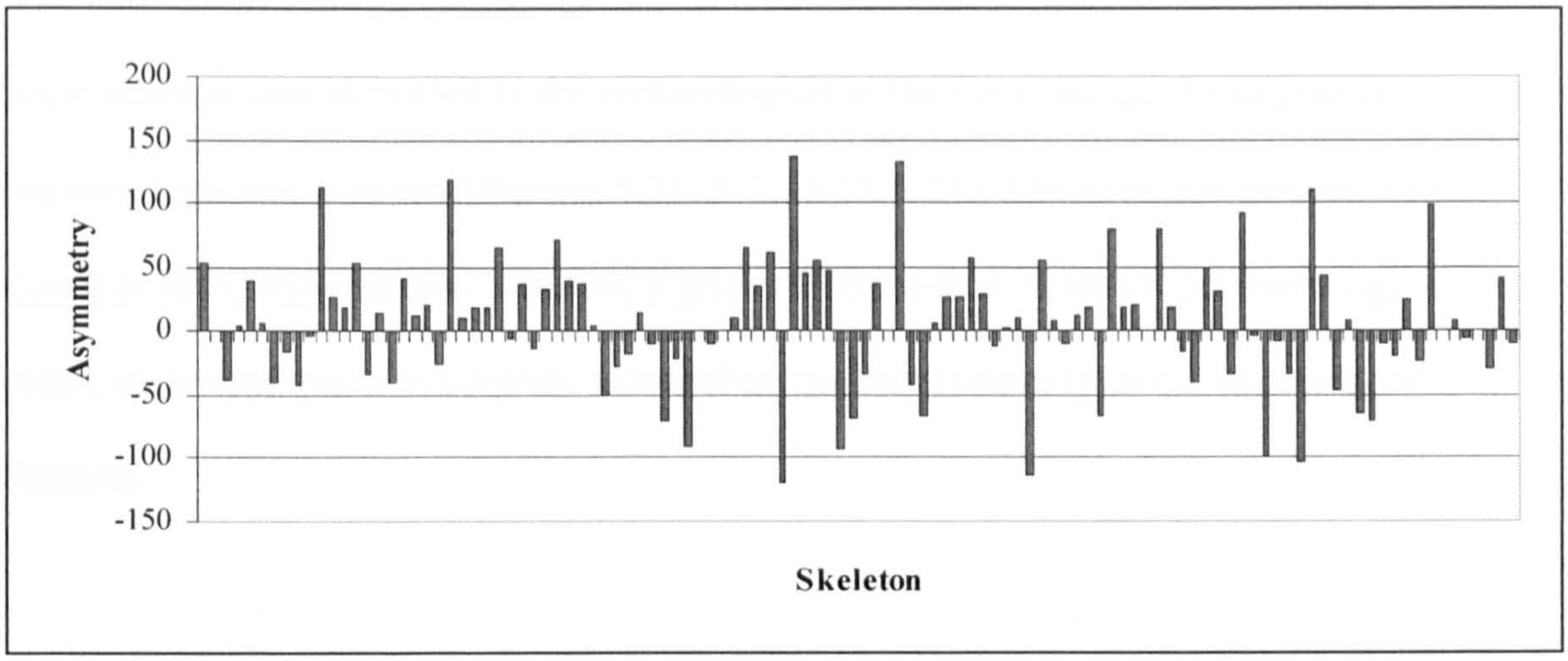

The remaining individuals from the Terry collection, those with no known occupation, are detailed in Figure 5.20. Again, these are largely right-sided in terms of asymmetry, 60 right-sided, 44 left-sided and seven with no asymmetry. Directional asymmetry is strongest on the right side, however, there are a number of individuals displaying strong directional asymmetry on the left side. There are no statistical outliers in this group in humeral torsion angles.

To test for differences in humeral torsion angle relative to time period, the sample, in its entirety, was divided into 20-year blocks. Each individual was assigned a category dependent upon their year of birth (Table 5.22). One-way ANOVA identified no significant differences in humeral torsion angle ($p < .600$) relative to year of birth.

Table 5.20: Humeral torsion in the Terry collection, by year-of-birth.

Period	**No.**	**Mean**	**S.D.**
1840 – 1859	61	23.09°	10.32°
1860 – 1879	139	21.91°	9.35°
1880 – 1899	103	23.15°	10.21°
1900 +	47	23.89°	10.10°

5.12 Non-Human Primates

The non-human primate specimens display a similar random pattern in directional asymmetry as that identified in the archaeological collections, though the degree of asymmetry is not as strong (Figures 5.21, 5.22, 5.23, 5.24). The strongest asymmetry is found in the *Gorilla* sample, where it is primarily right-sided (eleven specimens right-sided, eight specimens left-sided). Bilateral asymmetry is equally mixed in males and females.

The chimpanzee specimens are similarly mixed between right and left-sided asymmetry with no strong variation between sexes. They display reduced levels of asymmetry when compared with the gorilla specimens, although this asymmetry is still greater than that found in the orangutan and macaque groups. This is possibly related to differences in manipulative behaviours in these groups. The level of bilateral asymmetry is equally mixed between limbs in the *Pongo* sample and generally reduced when compared with the gorilla and chimpanzee specimens. There is one exception that skews the *Pongo* data. Specimen 1973.2 has a very high degree of bilateral asymmetry, although not statistically an outlier in this sample, and originates from a zoo. The low humeral torsion angles exhibited in this specimen (3° and 17°) in comparison to the remaining *Pongo* sample have previously been discussed. Unfortunately, both the age at which the animal entered the zoo and the artificial habitat in which the animal was maintained are unknown. If the specimen was born in the zoo, it would explain the variant torsion angles, as its activity patterns would be expected to be fundamentally altered from an orangutan raised in the wild, as orangutans are known to 'fist-walk' when on substrates. This type of locomotion may be the norm for animals in a zoo. Further information about its zoo habitat – which could not be obtained at this time -

would indicate whether decreased suspensory locomotion or increased terrestrial locomotion is responsible for the adaptive change in humeral torsion angle.

Figure 5.21: Bilateral asymmetry in humeral torsion: *Gorilla* sp. Dark grey bars are male, white bars are female. Negative values indicate left-sidedness.

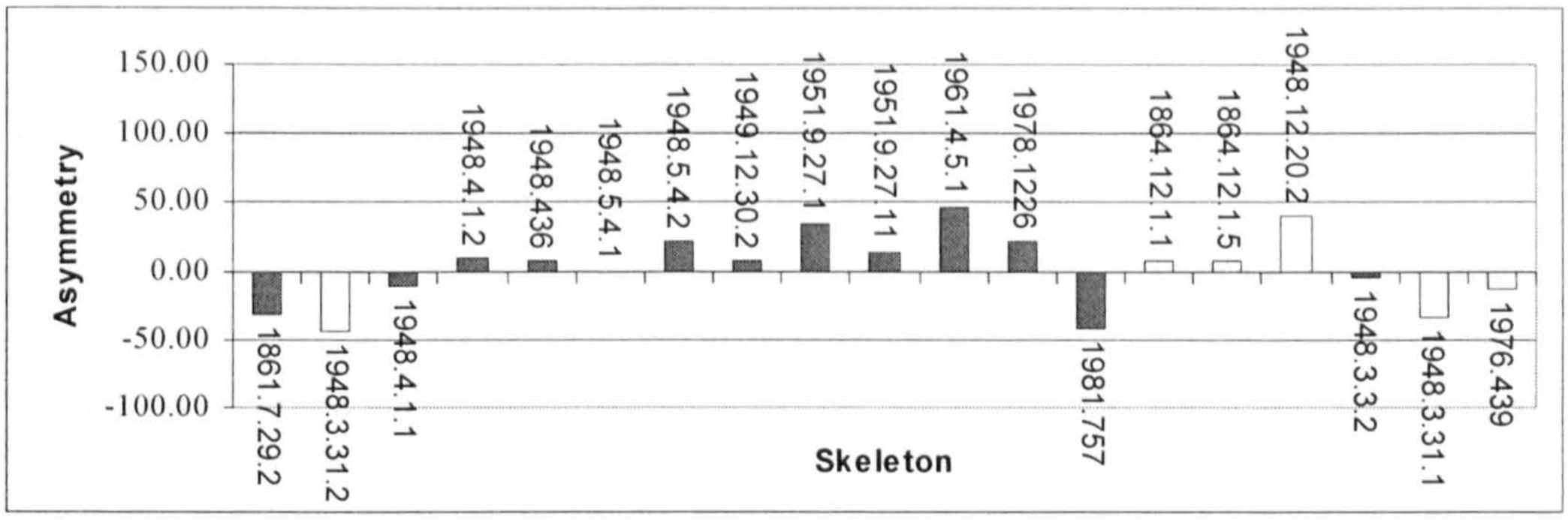

The macaque specimens display the lowest degree of bilateral asymmetry, as expected for group of mixed terrestrial and arboreal quadrupeds (Fleagle, 1999). Despite this, only three of the ten animals display symmetry in humeral torsion. There is one statistical outlier identified in the *Macaca* population, 1855.12 (left humerus). At 68° on the left side and 81° on the right side, this female monkey shows relatively high bilateral asymmetry for the macaque specimens, due in large part to the low left limb torsion angle. 1976.2 (female) was also a zoo specimen, however, this animal does not show any difference from the presumed 'wild shot' animals.

Figure 5.22: Bilateral asymmetry in humeral torsion: *Pan* sp. Dark grey bars are males, white bars are females. Negative values indicate left-sidedness.

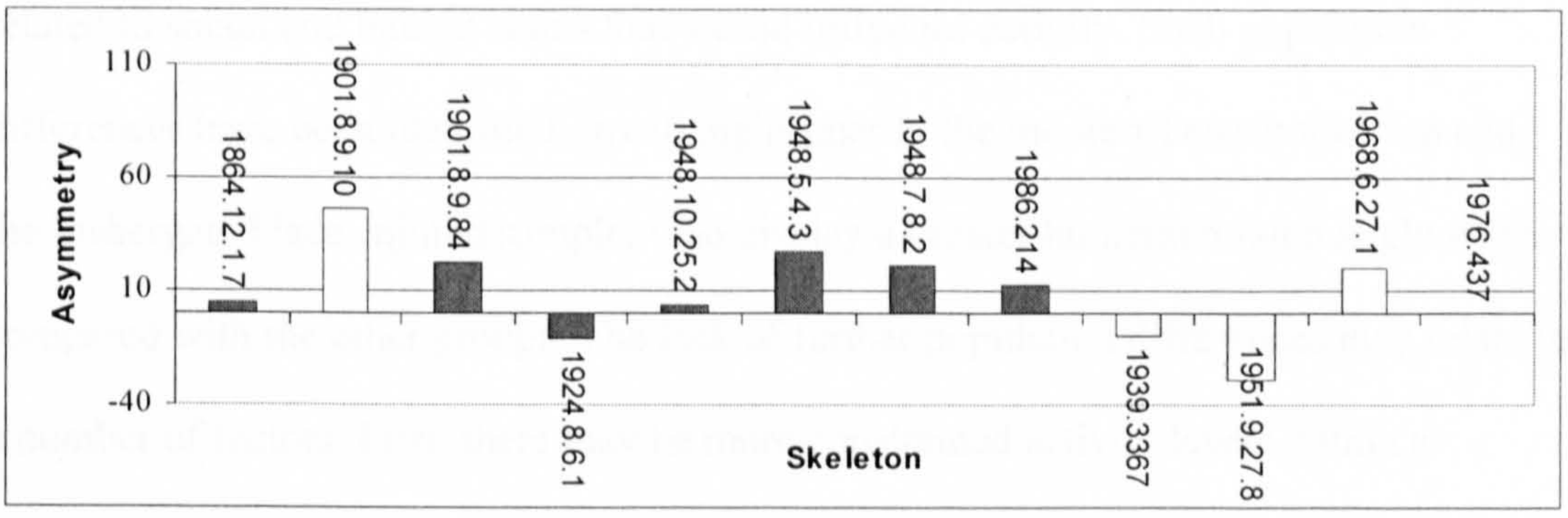

Figure 5.23: Bilateral asymmetry in *Pongo* species. Dark grey bars are males, white bars are females. Negative values indicate left-sidedness.

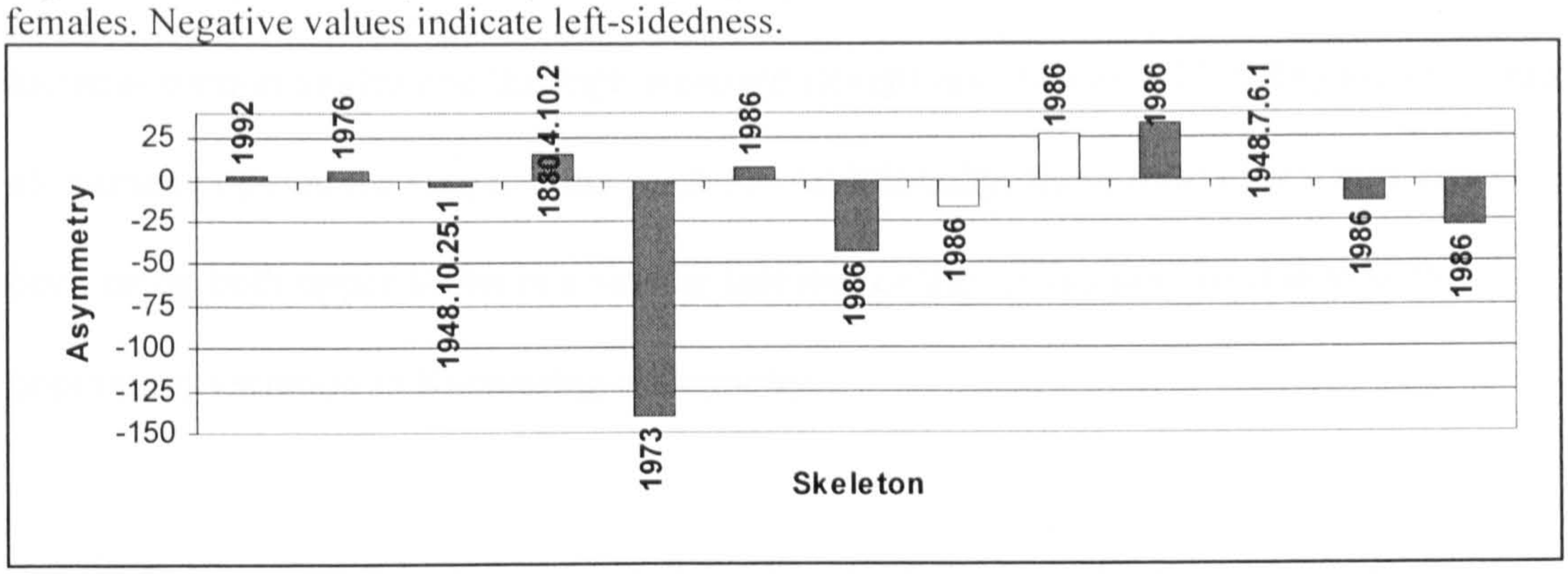

Figure 5.24: Bilateral asymmetry in *Macaca* species. Dark grey bars are males, white bars are females. Negative values indicate left-sidedness.

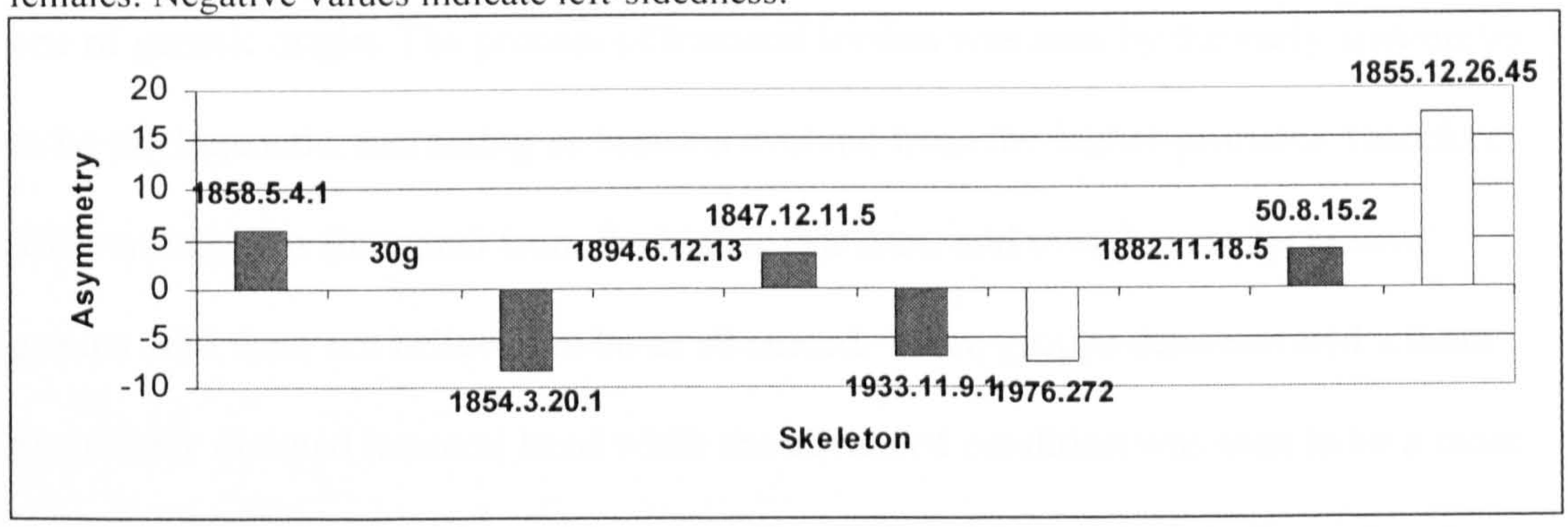

5.13 Discussion

This project endeavours to identify what is normal within the range of humeral torsion angles. It is hypothesised that if the humeral torsion angle is strongly related to behaviour or movement patterns, or locomotor differences in non-human primates, then significant differences will be identified. This requires strong contextual information related to social and habitat status that would influence activity. Such population differences have been identified, involving primarily the modern Terry collection and the Fishergate blade-injured sample, who display a greater humeral torsion angle when compared with the other groups. The lack of further population differences may relate to a number of factors. First, there may be more constrained activity levels within a population, or simply, a lower number of individuals participating in a behaviour pattern frequent enough or from an early enough age to modify the humeral torsion angle, as

has been proposed to be the case in modern groups studied. Certainly, the broad range of humeral torsion angles and the high standard deviations (Tables 5.17, 5.18) found within all human populations support this premise. Additionally, these individuals may have been using both upper limbs in a similar fashion, or the results may be due to within-population variation in fluctuating asymmetry.

This project has also attempted to identify the nature of adaptation in the humeral torsion angle, whether an increased or decreased angle is an acquired trait or one of genetic origin. The process of humeral torsion was seen by the early anatomists to be phylogenetic, increasing as humans evolved from the higher primates, therefore differentiating us (humans) from the higher primates, and even human 'primitive' groups who were not believed to be as advanced. These groups demonstrated a more posteriorly directed humeral head while the advanced condition was seen to be a more medially placed humeral head. However, the results of this analysis indicate that the humeral torsion angle is not ontogenetically constrained, but is adapted through biomechanical forces. One movement pattern that has been correlated with an increased humeral torsion angle is overhand throwing with force among high-level athletes. This creates a movement pattern in which the arm is abducted to an angle of at least 90° with the forearm and hand flexed and then rapidly extended.

If an increased humeral torsion angle is an adaptation to strenuous movement, then the results from the Terry collection appear counter-intuitive. This modern, cadaver based-population should be the least strenuously active of those analysed. The decreased physical demands of life in an industrial society are responsible for some of the greatest differences in bone mass when compared with pre-industrial (early agricultural) societies. This difference is greater than that identified between hunter-gatherers and

sedentary populations (Pearson, 2000). Yet the Terry collection demonstrates the greatest average humeral torsion angle among all human populations analysed. While this collection is largely made up of the lower classes of society, transient and indigent individuals, it is unlikely that life in industrial St. Louis, Missouri, would have been as physically demanding as that of a medieval farmer, although, the level of overall activity is not expected to alter humeral torsion, but the type of activity or movement pattern. It could be, though, that the Terry individuals were, in youth, much more active than indicated by their last profession or lack thereof before death.

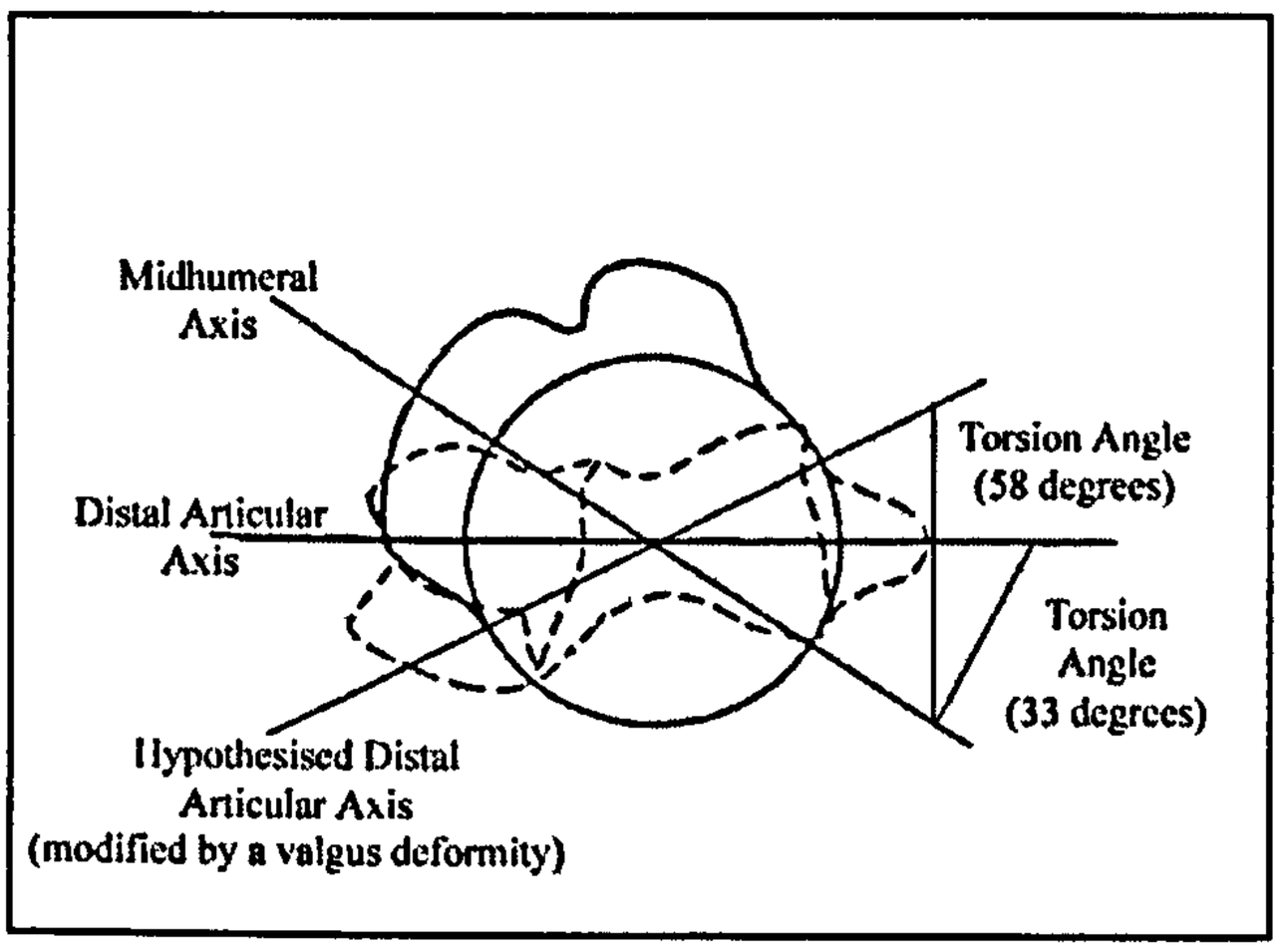

Fig. 5.25: Increased humeral torsion angle under the influence of a valgus deformity of the distal humeral shaft (image modified from Krahl, 1947).

Given the broad range of values found in the archaeological populations, one must ask whether there is an activity or movement pattern associated with a decreased humeral torsion angle. A valgus deformity of the distal elbow (*cubitus valgus*) has been identified among professional baseball pitchers and has also been related to overhand throwing with force. Specifically, it is one aspect of a (distal) medial stress syndrome (King *et al.*, 1969). *Cubitus valgus* relates to a lateral twisting of the distal-most humeral shaft, however, this modification would increase the humeral torsion angle rather than decrease it (Fig. 5.25). It is theoretically possible that the significant differences in humeral torsion angles exist in the high-level throwing athlete as a result of a valgus

deformity that alters the orientation of the distal articular axis, rather than a change in orientation of the proximal articular axis.

This modification to the distal humeral shaft indicates that the site of humeral torsion is not limited to the proximal shaft, supporting the hypothesis that torsion is not exclusive to the proximal humerus. The results of this analysis, Terry collection excepted, indicate that the form of accommodation in the humeral torsion angle is an increased angle, or decreased torsion of the humeral head with respect to the shaft. Whether this is due to the exclusive action of a valgus deformity on the distal articular surface, with no alteration to the proximal humeral shape, or if the proximal articular surface is moving more posteriorly is unclear. Both these phenomena result in an increased humeral torsion angle. There are no clinical or sports-related activities identified that decrease the humeral torsion angle.

If differences in humeral torsion angles are related to behaviour patterns, then significant differences should be identified between human and non-human primate species in both the humeral torsion angle and the level of asymmetry. Such differences have been identified, as the angle of humeral torsion is significantly different between all non-human primate species and all human populations, with the exception of the *Gorilla* and Fishergate BI samples. While the level of standardised asymmetry in humeral torsion angles was primarily non-significant between human and non-human primate samples, the level, maximum value and standard deviation of bilateral asymmetry is lower in all non-human primate species when compared with the human samples. This indicates more homogeneous activity patterns, with little variation between limbs in the non-human primate samples due to locomotor constraints and

restricted manipulative capacities when compared with those of humans. The remaining human samples indicate greater heterogeneity in activity patterns.

Significant inter-population differences have been identified when considering males only; however, there are no significant differences in the humeral torsion angle when considering females only. If humeral torsion angles are strongly linked to behaviour and movement patterns, the females then appear to demonstrate similar activity patterns across all samples, whereas, the males appear to be engaged in a broader range of activities. However, the disproportionately small number of females in the samples must be considered a limiting factor in assessing this apparent sex-linked difference.

When considering bilateral asymmetry, the samples with martial connections are expected to display the highest degree of bilateral asymmetry, as evidence of unimanual activities related to warfare, as well as increased activity levels required to train with and wield weapons. It also hypothesised that the lowest levels of bilateral asymmetry will be found in the non-human primate species, as well as the modern comparative sample (Terry) and the medieval *leprosarium* and almshouse (Chichester). However, the highest average levels of bilateral asymmetry were found in the Fishergate southern cemetery sample, followed by the rural site of Wharram Percy and the Mary Rose sample. Of the samples with martial connections, both the Towton and Mary Rose samples have high levels of bilateral asymmetry, 45.84° and 47.61°, respectively. However, the Fishergate blade-injured sample, with an average asymmetry of 32.76°, falls among the lower range of values. These differences between martial samples may indicate different patterns of weapon use – unimanual versus bimanual or may indicate shield use in the Fishergate blade-injured sample. Only the rural site of Hickleton displayed a lower

average asymmetry (30.55°) when considering the human samples, however, this site has a broad timespan, unlike the other sites used in this study. The individuals from Chichester and the Terry collection indeed display relatively low levels of average bilateral asymmetry (39.28° and 39.34°, respectively) while the non-human primate samples display the lowest average asymmetry of all samples (G*orilla* sp. 19.49°; P*an* sp. 14.08°; *Pongo* sp. 28.32°; *Macaca* sp. 4.05°). These values are for the males only. In those archaeological collections with a substantial number of females, the level of bilateral asymmetry was greater than that of their male counterparts. This indicates that the daily routines of the females in these samples, from the rural sites of Wharram Percy and Hickleton, as well as the *leprosarium* and almshouse of Chichester, consisted of either unimanual activities or movement patterns that were biased towards one limb.

The sports medicine literature includes studies of bilateral asymmetry in the high-level athlete. Differences in torsion angles between sides of 10° or more were statistically significant. It is possible that meaningful differences would be identified in this analysis were dominant versus non-dominant limbs identifiable archaeologically. As will be demonstrated in a later chapter, it is difficult to identify limb dominance in archaeological samples, as humeral robusticity, humeral length, or cross-sectional geometric properties can all be used to assess it, but these variables may contradict one another. Using a basic analysis of maximum – minimum humeral torsion angle, there were no population samples that approached the average difference between the limbs of the high-level athlete. However, a number of individuals that display an absolute angle difference between limbs equal to or in excess of that of the high-level athlete were identified in all samples. In the Towton sample, T16 is an older male with extensive healed blade-trauma to the face and mandible indicating his status as a combat veteran. He has an absolute difference between limbs of 22°, far in excess of the average

difference found in professional throwing athletes. The greatest absolute asymmetry between limbs, 28°, is found in a man from the Tudor warship, the *Mary Rose*, MR49. An older man, FG5724, buried in the ecclesiastical cemetery (eastern, 1195 AD – early 14th century) at Fishergate has an absolute difference in humeral torsion angles between limbs of 26°. TR755, a man from the Terry collection, attributed as a beggar, has an absolute angle difference between limbs of 24°. This man died of pneumonia in 1929 aged 36. This was during the American economic depression, a time when many men were left penniless and on the streets. It is impossible to tell what his profession might have been prior to this time. These extreme values contribute to an increased range identified by archaeological groups studied here and further support the hypothesis that an acquired response is indicated in the humeral torsion angle.

There is no clear diachronic change in humeral torsion angles in the individuals included in this study. The Wharram Percy sample (950 AD – 1850 AD) and the Terry collection (1840 AD – 1941 AD) were both analysed according to time period with no significant differences in the humeral torsion angle identified. Unless the diachronic change in humeral torsion angles has occurred within the last 50 years, an unlikely prospect, it appears most likely that, despite the results of Öztuna *et al.* (2002), there is a discrepancy between values as measured by clinical radiographs when compared with those measured skeletally, as in this analysis.

5.14 Conclusions

The humeral torsion angle, a measurement of architecture and diaphyseal shape, has been demonstrated to vary among populations; significant differences in the humeral torsion angle have been identified both between and within population samples. The humeral torsion angle in non-human primates varies significantly with all species

examined (*Gorilla, Pan, Pongo* and *Macaca*), as well as between the archaeological and modern human samples, with the exception of the male Gorilla specimens and the males from the Fishergate blade-injured sample. The humeral torsion angle did not vary significantly between archaeological samples, but did vary significantly from the non-human primate samples.

The modern cadaver-based Terry collection was found to display a significantly increased humeral torsion angle when compared with the martial-related samples from Towton and the *Mary Rose*, the rural site of Wharram Percy, the medieval *leprosarium* and almshouse of Chichester, as well as the high status individuals from the intramural cemetery at Fishergate, but not with the ecclesiastics from the eastern cemetery or the lay brethren from the southern cemetery of Fishergate. If the Terry collection represents a heterogeneous mix of activity variants, as seems to be the case from listed occupations, then these two cemetery samples may be similarly heterogeneous with respect to activity.

The Fishergate blade-injured sample also displayed a significantly increased humeral torsion angle when compared with the other combatant samples from Towton and the *Mary Rose*, the males from the rural sites of Wharram Percy and Hickleton and the high status individuals from the Fishergate intramural cemetery, but not with the ecclesiastics from the eastern cemetery or the lay brethren from the southern cemetery.

The humeral torsion angle in the female samples (from the eastern, intramural and southern cemeteries of Fishergate, as well as the rural sites of Wharram Percy and Hickleton and the *leprosarium* and almshouse of Chichester) was not found to vary significantly from each other in any of the archaeological samples analysed, although it

is significantly different between the females from the archaeological samples when compared with the non-human primate species.

While the results of the ANOVA determined significant differences in bilateral asymmetry between both males and females of all populations, human and non-human, no two collections were found to vary significantly from each other. The level of bilateral asymmetry does not follow any strong social or contextual patterning. It is lowest in the non-human primate samples, while among the humans, the highest levels are found in the rural site of Wharram Percy, although the other rural site of Hickleton, conversely, displays the lowest level of bilateral asymmetry among males. The high status group at Fishergate, the intramural cemetery, the naval sample from the *Mary Rose*, the ecclesiastic sample from the eastern cemetery at Fishergate and the Towton sample display the next highest levels of bilateral asymmetry among males. The Terry collection, the Chichester male sample and the Fishergate blade-injured males are among the lowest in terms of asymmetry. This highlights a fundamental difference in activity or movement patterns between the combatant samples, as the Towton and Mary Rose groups fall within the higher range of asymmetry, indicating perhaps a preference towards unimanual activity when compared with the Fishergate blade-injured sample. Although, as will be demonstrated in later chapters, this result is contradicted by cross-sectional and external measurements of bilateral asymmetry.

The Towton and Mary Rose populations both display left-sided directional asymmetry while the blade-injured sample and the eastern cemetery from Fishergate display strong right-sided directional asymmetry. The remaining samples from urban and rural sites, a collection of individuals displaying lesions from infectious diseases and the remaining Fishergate groups display mixed asymmetry between limbs. The

modern Terry sample is also mixed between limbs, although with tendencies to right-sided asymmetry. The non-human primate samples also display mixed asymmetry, although the degree is reduced when compared with the human populations. Many individuals from each sample have an absolute difference between limbs in excess of that average identified in professional and experienced athletes.

The question of greater importance – an increased torsion angle that produces a medially rotated humeral head - has been addressed with the conclusion that an increased humeral torsion angle, or reduced torsion of the humeral shaft is the mode of accommodation to strenuous activity. This is certainly accurate when considering torsion as an architectural adaptation to overhand throwing in the high-level athlete, with regard to handball and baseball players. However, if increased humeral torsion angles are an adaptation to a specific movement pattern or activity, it does not explain the results from the Terry collection or recent human populations which both possess increased humeral angles in an industrialised, apparently low-activity society. This increase in torsion angle in modern populations, though, could be due to increased chest width in comparatively well-fed populations, as indicated by Churchill (1996). Results indicate that humeral torsion is not an isolated phenomenon, but influenced by other factors of humeral morphology or body proportions.

Increased humeral torsion was generalised by Martin (1933) to correlate with 'weak' or 'gracile' skeletons, as represented by females and the left humerus. The results of this analysis are generally consistent with the generalisation that females display increased torsion (reduced angles) when compare with the males, however, there is no strong link between increased or decreased torsion and side. The question of

correlation with a 'weak' skeleton requires further consideration of humeral robusticity which is the subject of a later chapter.

Humeral torsion has thus been shown to be highly variable within and between populations. This is consistent with the hypothesis that humeral torsion is an adaptive shape response, modelling the humerus during growth to individual requirements. High levels of (absolute) asymmetry between limbs, in excess of those identified in the professional athlete, have been identified in a number of individuals from each sample. This indicates that some individuals in each population, such as T16 or MR49, seem to have been engaged in forceful strenuous movements of the shoulder, while the great majority do not seem to have been so engaged. Functionally, an increased angle seems to relate to an osseous response that increases external rotation and decreases internal rotation at 90° of abduction. Overhand throwing is one generalised activity that has been shown to be associated with an increased humeral torsion angle. In this context, researchers have considered that this morphological change occurs as an adaptation to facilitate the overhand throwing motion.

CHAPTER SIX

BIOMECHANICAL ANALYSIS

This chapter investigates biomechanical properties of the humerus in a select group of blade-injured individuals from the Towton and Fishergate collections, as well as a comparative sample of individuals without any signs of antemortem or perimortem weapon trauma from the three discrete burial areas of the Fishergate site. Further, this chapter will examine the relationship between these properties and humeral architecture in an effort to better understand the interaction between form and function within groups possessing weapon-related injuries. The purpose of this analysis is to test the hypothesis that variations in diaphyseal shape, bilateral asymmetry and robusticity, as defined by the humeral torsion angle and cross-sectional geometric properties, exist between blade-injured and non blade-injured samples that relate to differences in movement patterns repeatedly performed during training for and involvement in armed conflict.

The Towton population, casualties of the Wars of the Roses battle of Towton (Burgess, 2000), display distinctive modifications in humeral architecture in conjunction with high external measures of humeral robusticity (Knüsel, 2000a; Rhodes, 2002). The architectural adaptations, as discussed in a previous chapter, include variations in humeral torsion within the population and, bilaterally, within individuals. The distal humerus often displays a flattening of the pillar, extension of the medial supracondylar ridge and a lateral deviation of the shaft forming a valgus deformity. The closest parallel to these modifications in humeral form have been noted in professional baseball pitchers who display humeral hypertrophy, valgus deformities and increased external humeral rotation with decreased internal humeral rotation (King *et al.*, 1969). It is the aim of this chapter to examine bilateral differences in cross-sectional geometry in two blade-injured samples and a comparative sample chosen to represent the normal range of variation

found in the Medieval period, as well as identify what role architectural adaptations play in mechanical competence.

6.1 Applications of Biomechanical Analyses in the Archaeological Literature

Architectural development within limb bones involves two key principles, shape and robusticity. Differences in habitual patterns of biomechanical forces lead to changes in shape, whereas, differences in the level of biomechanical stress affect robusticity (Trinkaus *et al.*, 1991). Skeletal tissue is a dynamic entity capable of sensing and reacting to mechanical loading. It responds to activity patterns differentially depending on loading regimes. Biomechanical analysis is a technique widely applied to identify strenuous behaviour in population samples from Australopithecines (Ohman *et al.*, 1997) to modern-day athletes (Jones *et al.*, 1977; Qu, 1992; Ruff *et al.*, 1994; Trinkaus *et al.*, 1994). Temporal trends in postcranial robusticity within *Homo* have been investigated through biomechanical analyses and a trend of decreasing diaphyseal robusticity from the early Pleistocene to more recent periods has been identified (Ruff *et al.*, 1993; Trinkaus, 1997). Trinkaus and colleagues (1994) found the effects of differential loading on recent human humeri to be reflected in the amount and distribution of cortical bone. Other palaeoanthropological applications of cross-sectional geometry include the study by Ben-Itzhak *et al.* (1988), who examined the differences in humeral properties between Neandertals and early and recent *H. sapiens*, and Trinkaus and Churchill's (1999) study which investigated diaphyseal cross-sectional geometry in Near Eastern Middle Palaeolithic late archaic and early modern humans. The humeri of the two groups were found to display similar cross-sectional diaphyseal shape; however, the late archaic humans display significantly increased robusticity when cortical area and polar moments of area were scaled to humeral length, indicating strong differences in the levels of habitual activity between the two populations.

Ruff and Larsen (1990, 2001) assessed prehistoric and contact period populations to examine changes in subsistence strategy and the effects of Spanish colonization on behavioural patterns, as well as skeletal robusticity of males and females on the Georgia Coast of the United States. The application of cross-sectional geometry to femora and humeri of males and females of these periods identified behavioural changes related to the advent of agricultural technology. A reduction in femoral and humeral robusticity, as well as sexually dimorphic changes, were identified between the prehistoric, agricultural and contact period populations. In an analysis of the original pre-contact pre-agricultural, pre-contact agricultural and contact period populations, differences in bilateral asymmetry were identified that demonstrated that the transition to agriculture brought about more profound changes in female upper limb patterns as opposed to those of males (Fresia *et al.*, 1990).

Bridges (1989) investigated the changes in robusticity across the agricultural transition in population samples of the southeastern United States to determine if Mississippian period agricultural activities were more physically demanding than Archaic period hunting and gathering ones and to identify any changes in the sexual division of labour. Specifically, in the Archaic period, hunting relied on an atlatl while during the Mississippian period a bow and arrow was adopted. While the Mississippian men displayed stronger femora than their archaic counterparts, there were no significant differences in humeral strength among men of the two groups. Agricultural period females displayed significant increases in both femoral and humeral strength, indicating more diverse activity patterns. Levels of bilateral asymmetry decreased in both males and females in the Mississippian period, although the reduction in asymmetry in males was not as great as that seen in the females. This change is associated with processing corn among the females and bow use among the males. Most recently, Stock and

Pfeiffer (2001) investigated mobility patterns in foraging groups, terrestrially-based southern African Later Stone Age (LSA) individuals and marine-based Andaman Islanders. The application of cross-sectional geometry identified differences in mobility patterns as the terrestrial-based foragers demonstrated stronger femora, tibiae and first metatarsals compared to the Andaman Islanders, while the latter group demonstrated significantly stronger claviculae and humeri when compared to the LSA group. These results are important as they suggest that there is a localized osteogenic response related to habitual behaviours. The study also suggests that the proximal limb bones are more responsive to mechanical loading than distal ones. This is also consistent with the research results of Lieberman *et al.* (2002). These analyses of changes in diaphyseal cross-sectional morphology demonstrate the value of biomechanical analyses in identifying differences in activity patterns.

6.2 Populations Analysed

Humeral cross-sectional morphology is analysed in two different groups of blade-injured males, those from the Towton mass grave (Fiorato *et al.*, 2000) and those buried in the cemeteries of St. Andrew, Fishergate, York (Fishergate) (Stroud and Kemp, 1993). It also examines a comparative group of non blade-injured males from the Fishergate site. The Towton population comprises all paired humeri from the sample, totalling 13 blade-injured individuals. These individuals date to 1461 AD. The Fishergate blade-injured (BI) sample is comprised of the paired humeri from 10 individuals, seven of whom date from late 11th century contexts (period 4), while the remaining three date to a later period spanning 1195 AD to the 16th century. The reference sample (Fishergate comparative) is also from the cemeteries of St. Andrew, Fishergate, in York. It should be noted that, although these individuals do not display peri-mortem blade injuries, it cannot be firmly established that they did not train with

weapons. These individuals were selected to represent the range of values found in a population cross-section of the cemeteries.

The Towton population consists of battlefield casualties from the historic battle of Towton (North Yorkshire, England), during the Wars of the Roses. The Wars of the Roses (1455 AD – 1487 AD) was a civil conflict fought between two factions each supporting their own successor to the English throne. The remains represent only a small number of an estimated 28,000 casualties from the battle. These remains were discovered in 1996 during early construction phases of a garage block at Towton Hall, North Yorkshire. There were no coffins, shrouds or identifiable grave cuts. The bodies were tightly packed within the shallow grave and interred contrary to the burial customs of the period (Sutherland, 2000).

The Fishergate sample in York has three distinct burial areas relating to different socio-economic groups, and thus may be expected to reveal different activity levels. The three discrete burial areas include an ecclesiastical cemetery to the east of the priory church, intramural burials within the priory buildings, and a secular and lay burial area to the south. The majority (seven out of ten) of the Fishergate blade-injured individuals originate from an early context pre-dating the foundation of the new Priory of St. Andrew, Order of St. Gilbert of Sempringham in the 12th century. They are found in what later became the southern secular and lay cemetery area and the nave (Stroud and Kemp, 1993). The remaining three blade-injured men originate from later periods of the site, and all were found in intramural burial contexts, the dates and locations of which are as follows: one burial from the area of the crossing dating to 1195 – late 13th century AD, one burial in the nave dating to the mid 14th century AD and one burial from the cloister garth dating to the 13th – 16th century AD.

Table 6.1: Skeletons analysed. Special contexts are noted in the Towton sample, the Fishergate specimens are listed by context, where relevant, either Period 4 (late 11th century) or by cemetery location (1195 AD – 16th century). T = Towton, FG = Fishergate.

Towton	Context	Fishergate blade-injured	Context	Fishergate comparative	Context
T6	--	FG1589	Period 4	FG1425	Southern
T11	--	FG1886	Period 4	FG1436	Southern
T13	--	FG1893	Period 4	FG2178	Nave*
T16	Antemortem weapon trauma	FG2270	Nave*	FG3195	Chapter House*
T22	Antemortem weapon trauma	FG2392	Period 4	FG3202	Cloister alley*
T23	--	FG5356	Crossing*	FG5071	Eastern
T24	--	FG6191	Period 4	FG5138	N. transept chapel*
T32	--	FG6411	Period 4	FG5336	Eastern
T40	--	FG6448	Period 4	FG6128	Southern
T41	Antemortem weapon trauma	FG7052	Cloister garth*	--	
T44	--	--		--	
T46	--	--		--	

*Intramural location

The comparative sample is made up of individuals from each of these burial areas. There are three burials from the southern, lay cemetery, including the burial of a man contextually identified as a priest through his interment with a mortuary chalice and paten (1195 – early 14th century AD). Four individuals originate from intramural contexts: one each from the nave, the north transept chapel, the chapter house (most likely a prior), and the cloister alley (1195 – early 14th century AD). Two ecclesiastical burials are drawn from the eastern cemetery (1195 – early 14th century AD). All of these groups possess similar age-at-death profiles, with both the Towton and Fishergate comparative groups displaying an average age-at-death of ca. 30 years, while the Fishergate blade-injured group died at a slightly younger age of 25 years. Table 6.1 details the skeletons analysed, by age and context. A more detailed selection criteria for this analysis may be found in full in Chapter 5: Methods.

Diaphyseal asymmetry is compared with published data. These populations include a modern, Euroamerican sample from the Maxwell Museum, University of New

Mexico. This sample represents a variety of activity patterns found in modern humans. An Amerindian Georgia Coast sample originates from a Spanish mission horticulturalist population. The prehistoric "Late Horizon" California Amerindian group is a largely sedentary hunter-gatherer population, as is the prehistoric Jomon sample. A group of international professional tennis players and a sample of European Neandertals are included to represent the extremes of asymmetry.

Architectural changes are characterized by measurement of the humeral torsion angle. This was measured after Krahl and Evans (1945), and forms the angle between the mid-humeral axis, proximally, and the distal articular axis. However, in reporting the figures, there was no accommodation made for the 90° ontogenetic twist by adding 90° to the raw values as detailed by Krahl and Evans because, without this modification, the values are directly comparable to clinical measures of humeral 'retroversion'. In practice, the measurements of torsion are then 90° less than those reported in much of the palaeoanthropological literature, i.e. 22° instead of 112°. Asymmetry was measured as a percentage of the total value using the formula [(max-min)/min]*100. This formula has numerous benefits, among them, the removal of any presumed right-side dominance that prevails in many asymmetry calculations. When expressed as a percentage, left-sided dominance does not result in a negative numeral, which, when averaged across the population, negates the strength of the right-side values. Additionally, expression of asymmetry as the percentage of variation from the total value enables comparison across studies.

The selected humeri were scanned using a GE Medical Systems HiSpeed NR CT-scanner. The settings used were KV 120, MA 40. Prior to scanning, the humeri were marked at a point perpendicular to the long axis at 20%, 35%, 50%, 65% & 80% of

maximum humeral length. This was taken as a point measured previously from the inferior margin of the medial trochlear crest to the superior-most point on the humeral head, with 20% reflecting the most distal slice and 80% being the most proximal. The humeri were oriented on the gantry table in a standardized antero-posterior position, parallel to the longitudinal axis of the positioning beam. This beam was oriented such that it bisected the humerus into equal medial and lateral halves as determined by the proximal and distal articular surfaces. The full analytical procedures and slice preparation protocols are found in more detail in Chapter 5: Methods.

The cross-sectional properties analysed may be divided into two broad categories, measures of diaphyseal robusticity and measures of diaphyseal shape. The measures of diaphyseal robusticity include total subperiosteal area (TA), cortical area (CA), the percent of cortical area (PCA) and the polar second moment of area (J). The minimum and maximum second moments of area, Imax and Imin, are also measured. The cross-sectional measure of shape, Ix/Iy, is a measure of circularity, defining asymmetry and direction in bending strengths. These properties were analysed on a Macintosh OS X computer using the public domain NIH Image program (developed at the U.S. National Institutes of Health and available at http://rsb.info.nih.gov/nih-image/). The macro 'momentmacro' was used to calculate the cross-sectional properties. These values were size standardized following Ruff *et al.* (1993), using humeral length^{3} for cross-sectional properties and humeral length$^{5.33}$ for second moments of area. These values were multiplied by 10^{4} and 10^{6}, respectively, to produce the final reported values. As a point of procedure, in estimations of torsional rigidity, J should only be applied to sections that are axially symmetrical (cylindrical). Calculations of J in non-circular sections will result in overestimations of torsional rigidity and these will increase in magnitude as the sections depart from axial symmetry. However, in sections where Ix/Iy

is equal to or less than 1.5, J may be considered an accurate method for assessing torsional rigidity (Daegling, 2002). All data analysed conform to this rule. Using the statistical software package SPSS, the data were then analysed using ANOVA to test for population differences in cross-sectional geometry and levels of bilateral asymmetry by slice location. Hochberg's GT2 was used for post-hoc analysis. Non-parametric analyses were preformed to determine side differences and correlations between variables.

6.3 Results

6.3.1 Diaphyseal Loading and Robusticity

Cortical area is an indicator of general level or magnitude of mechanical loading, while total area and the percent of cortical area may reflect differences in age-at-onset of activity patterns. There are no significant differences between populations in CA or TA at any of the slice locations (Table 6.2). Cortical thickness is greatest in the Fishergate blade-injured (FG BI) population at all slice locations, except for that recorded at the 20% slice (where the Towton sample is marginally thicker), followed by those of the Towton sample (Figure 6.1). However, the Towton sample displays the greatest total area at all slice locations, followed by those of the Fishergate BI group (Figure 6.2). This population, while displaying the greatest CA at 80%, has the least TA at this slice parameter. The Fishergate comparative group displays the lowest levels of humeral cortical thickness at all slice parameters, as well as the lowest total area at the 20% - 65% levels.

Figure 6.1: The average cortical area (CA) of both sides, by slice and population. FG BI = Fishergate blade-injured, FG Comp = Fishergate comparative.

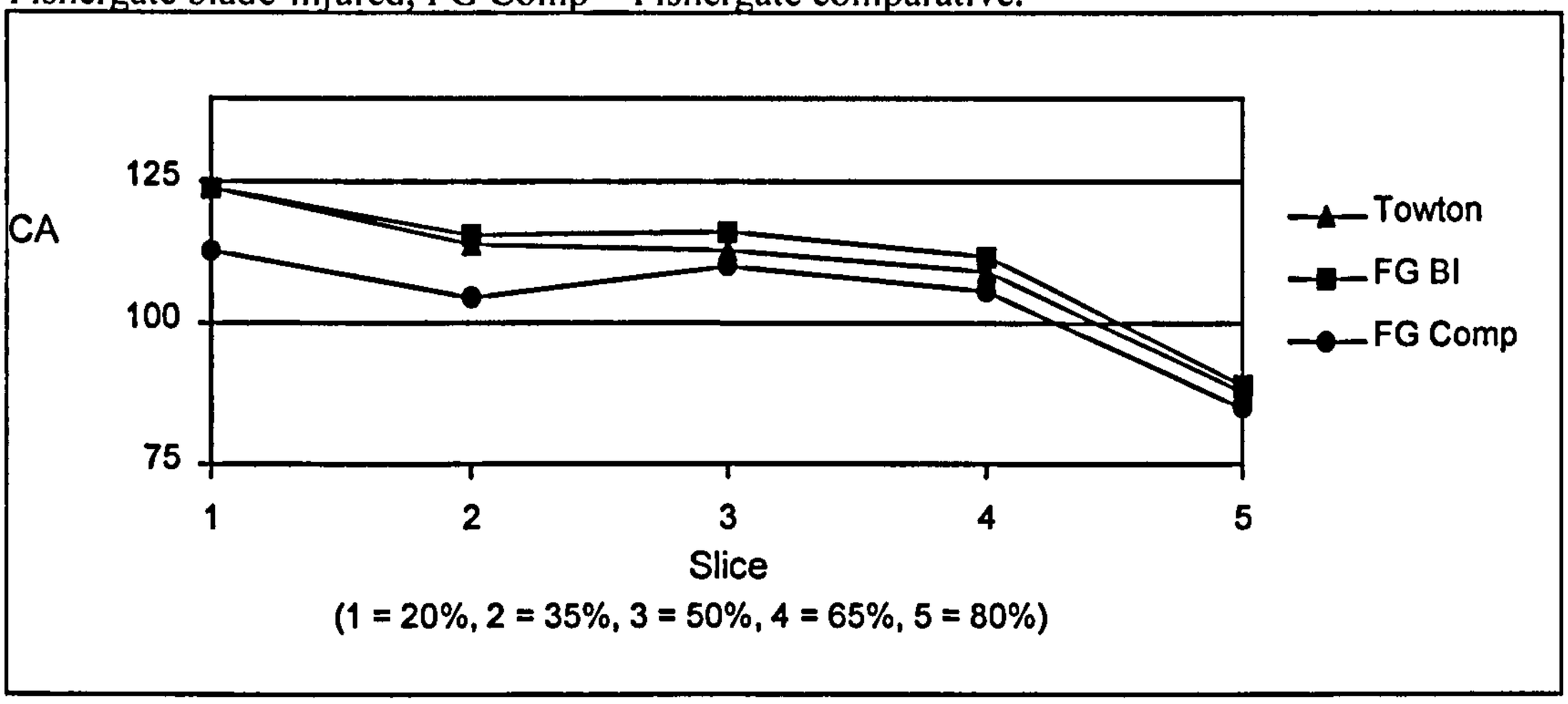

Figure 6.2: The average total area (TA) for both sides, by slice and population. FG BI = Fishergate blade-injured, FG Comp = Fishergate comparative.

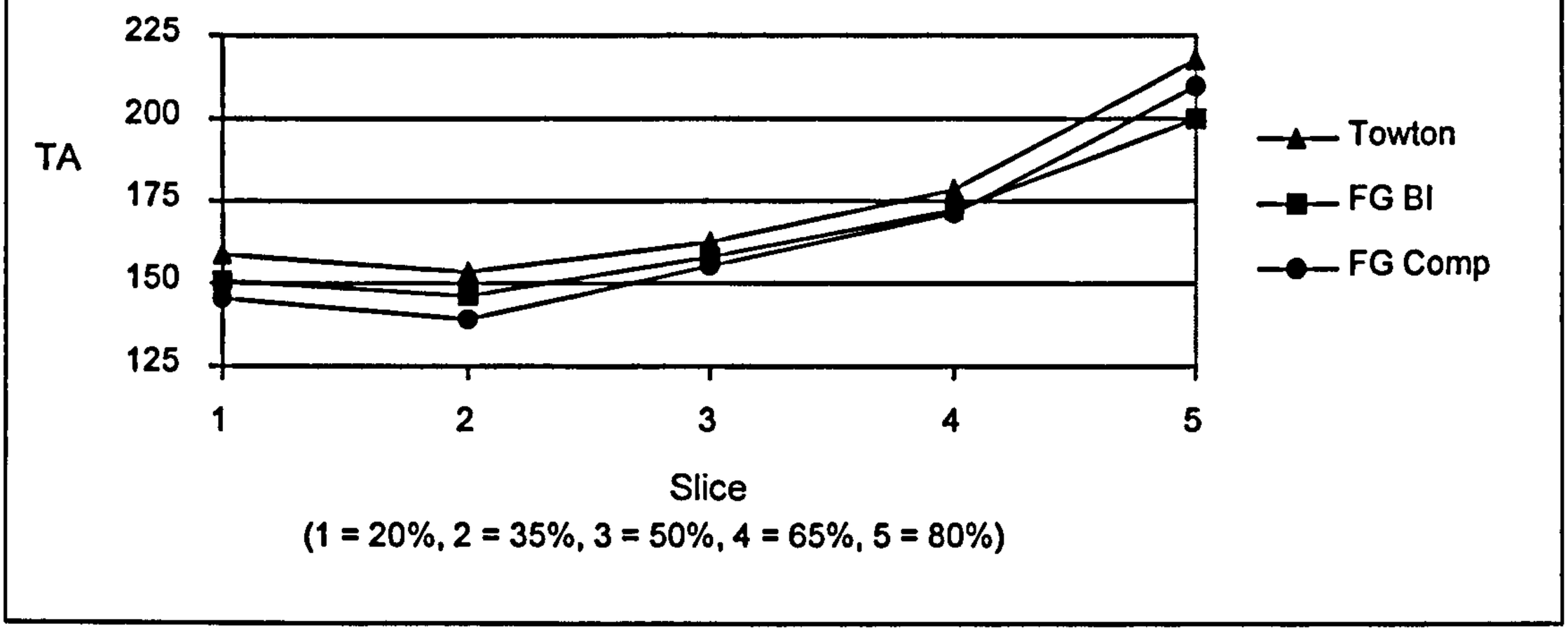

Figure 6.3: The average percent cortical area (PCA) for both sides, by slice and population. FG BI = Fishergate blade-injured, FG Comp = Fishergate comparative.

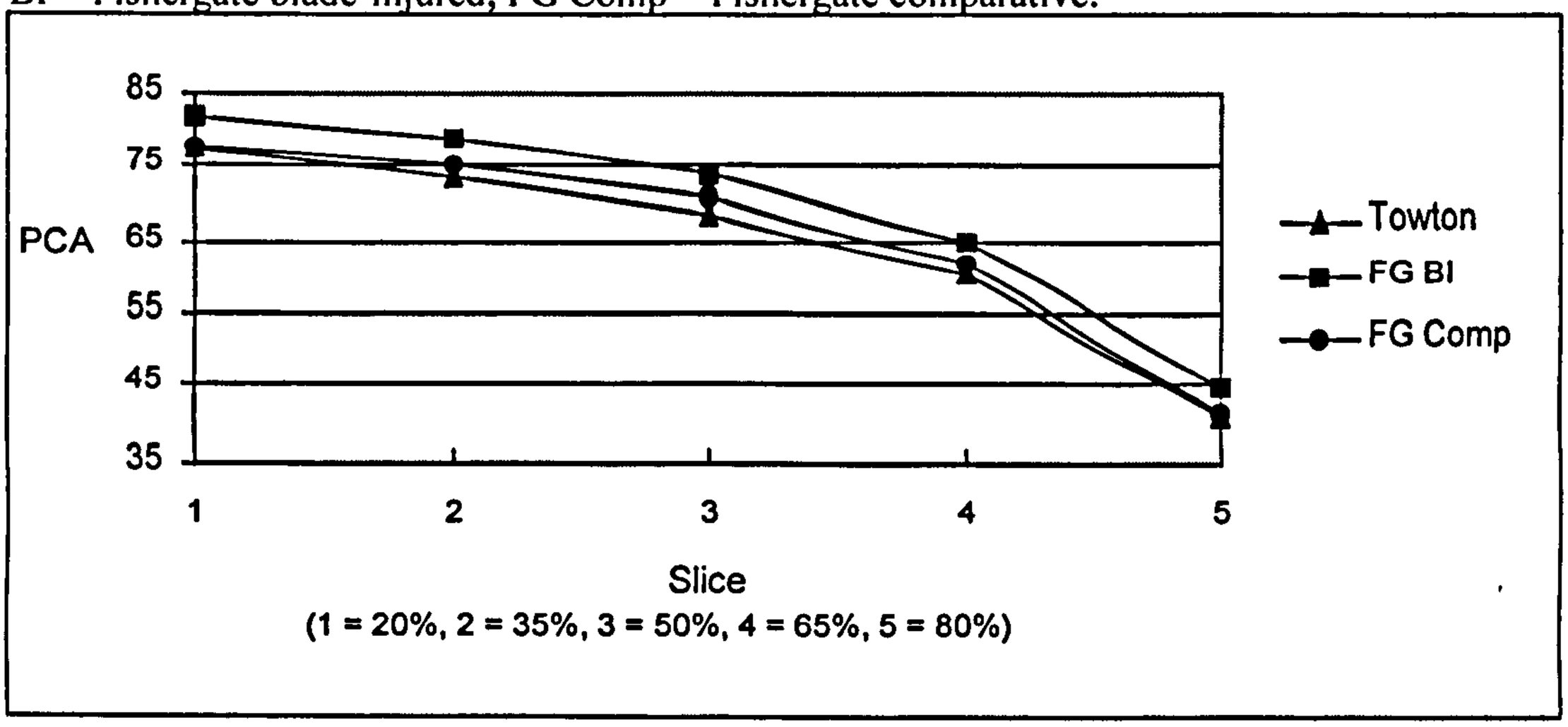

Table 6.2: Cross-sectional geometric properties, by slice parameter, and mean humeral torsion angles for all populations. The last column is the measure of statistically significant difference between the populations in a one-way ANOVA. Post hoc analysis shows the significance in PCA occurring between the Towton and the Fishergate BI samples at all slice parameters ($p < .026, .030, .017, .037, .026$). The differences in J/length$^{5.33}$ occur between the Towton and the Fishergate comparative samples at 20% ($p < .021$) and 35% ($p < .040$). The difference in Imax occurs between the Towton and the Fishergate comparative sample ($p < .017$). Statistically significant variation in Ix/Iy occurs between the Towton and Fishergate BI samples at 50% ($p < .033$) and 65%. ($p < .001$). The humeral torsion angle is significant between the Fishergate BI sample and both the Towton ($p < .016$) and the Fishergate comparative groups ($p < .002$).

	Towton			FG Blade-injured			FG Comparative			Sig.
20%	N	Mean	SD	N	Mean	SD	N	Mean	SD	
TA/length^3	25	158.93	31.08	20	150.59	16.31	18	145.37	19.54	.183
CA/length^3	25	123.99	24.64	20	123.71	15.43	18	112.63	17.72	.145
PCA	26	77.36	5.61	20	82.19	6.43	18	77.51	6.02	.017*
J/length$^{5.33}$	25	502.50	200.35	20	436.51	97.01	18	376.80	89.63	.025*
Imax	25	326.26	165.64	20	303.98	83.01	18	248.20	59.47	.109
Imin	25	147.12	41.96	20	132.52	26.68	18	128.58	33.67	.193
Ix/Iy	26	.576	.151	20	.548	.130	18	.610	.138	.400
35%										
TA/length^3	24	153.56	24.73	20	146.17	15.88	18	139.38	22.35	.114
CA/length^3	24	114.15	20.95	20	115.37	15.97	18	104.20	18.73	.143
PCA	25	73.38	6.39	20	78.94	7.41	18	74.93	7.22	.032*
J/length$^{5.33}$	24	389.05	114.86	20	353.67	70.82	18	312.74	92.56	.046*
Imax	24	221.69	71.98	20	195.43	41.26	18	170.28	51.06	.021*
Imin	24	166.45	47.55	20	158.23	32.09	18	142.45	42.50	.187
Ix/Iy	25	1.10	.207	20	1.16	.139	18	1.07	.197	.294
50%										
TA/length^3	25	162.85	26.14	20	158.07	19.49	18	154.94	23.26	.539
CA/length^3	25	112.88	19.90	20	115.99	16.36	18	109.88	19.85	.610
PCA	26	68.57	6.17	20	73.62	8.27	18	70.85	4.97	.044*
J/length$^{5.33}$	25	434.88	121.97	20	405.15	88.14	18	377.65	110.55	.240
Imax	25	257.35	81.57	20	243.47	53.34	18	225.47	69.29	.346
Imin	25	167.72	46.17	20	161.67	36.90	18	152.18	43.11	.501
Ix/Iy	26	.949	.144	20	1.05	.126	18	.987	.080	.039*
65%										
TA/length^3	25	178.72	29.87	20	172.41	28.19	18	171.25	27.23	.645
CA/length^3	25	108.93	19.42	20	111.79	18.51	18	105.37	17.61	.573
PCA	26	60.32	5.52	20	65.21	7.56	18	61.67	4.86	.029*
J/length$^{5.33}$	25	475.74	138.95	20	454.92	134.42	18	425.09	125.74	.477
Imax	25	265.03	86.52	20	254.65	74.43	18	235.60	68.87	.478
Imin	25	208.01	55.23	20	200.26	62.03	18	189.48	58.97	.595
Ix/Iy	26	1.01	.151	20	1.19	.145	18	1.08	.167	.001**
80%										
TA/length^3	25	217.53	38.20	20	200.21	31.73	18	209.38	44.14	.325
CA/length^3	25	87.99	16.64	20	88.96	16.10	18	85.18	16.33	.764
PCA	25	40.76	5.56	20	44.72	6.81	18	41.10	5.02	.061
J/length$^{5.33}$	25	538.66	150.56	20	478.82	139.58	18	484.19	194.00	.388
Imax	25	290.43	83.48	20	260.99	71.7	18	257.90	99.73	.373
Imin	25	237.95	64.96	20	217.80	70.69	18	226.28	95.31	.676
Ix/Iy	25	.900	.130	20	.938	.131	18	.909	.124	.619
H. torsion angle	25	16.08	9.06	20	24.58	9.95	18	14.11	8.02	.002**

*Sig. p = 0.05; ** Sig. p = 0.01

The percentage of cortical bone to total subperiosteal area reflects remodelling by subperiosteal deposition and endosteal resorption. The Fishergate BI sample displays the greatest percent cortical area (PCA), indicating thicker cortical bone and a reduced medullary canal diameter, while the Towton sample shows the lowest PCA, indicating subperiosteal expansion with endosteal resorption that results in an overall thinner cortex (Figure 6.3). These differences between the two blade-injured populations are significant at all slice parameters (20%: $p < .026$; 35%: $p < .030$; 50%: $p < .017$; 65%: $p < .037$; 80%: $.p < .026$). The control sample falls between the two blade-injured samples, although it is most similar to the Towton group.

Figure 6.4: J, population average of both sides, by slice location.

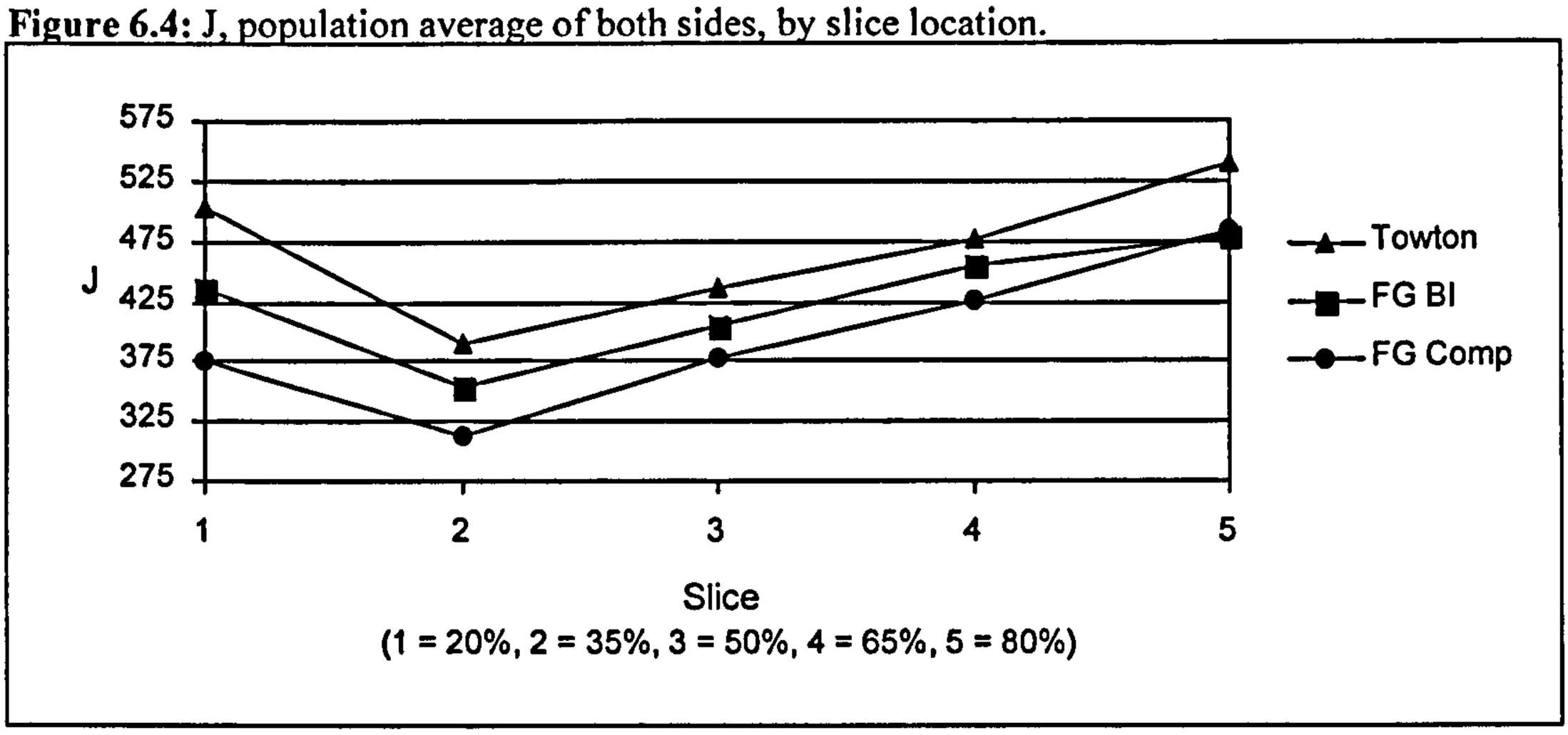

The polar second moment of area, J, may most accurately be described as an indicator of overall bending resistance or robusticity and is also a measure of the magnitude of mechanical loading. Diaphyseal robusticity, as demonstrated by J, is greatest not in the population with the thickest cortical bone, but in the population with the greatest total area, Towton. At the 20% and 35% slices, there is significant variation in bending resistance between the Towton sample and the Fishergate comparative group ($p < .021$ & $.040$). As J is a measure of resistance to torsional forces, a relationship might then be expected between it and humeral torsion. The population with the lowest average humeral torsion angle does display the lowest resistance against torsional

forces. This is the Fishergate comparative group, with an average humeral torsion angle of 14.11°. However, while the Towton and Fishergate BI samples vary significantly in humeral torsion (Table 6.1), $p < 0.01$ (16.08° and 24.58°, respectively) they show no statistical difference in J values. Contrary to the expectation based on the humeral torsion values, the Towton group displays the greatest resistance to torsional forces across all slice parameters while Fishergate BI group, the group with the highest average humeral torsion, falls intermediately.

Figure 6.5: Imax, average of both sides, by slice and population.

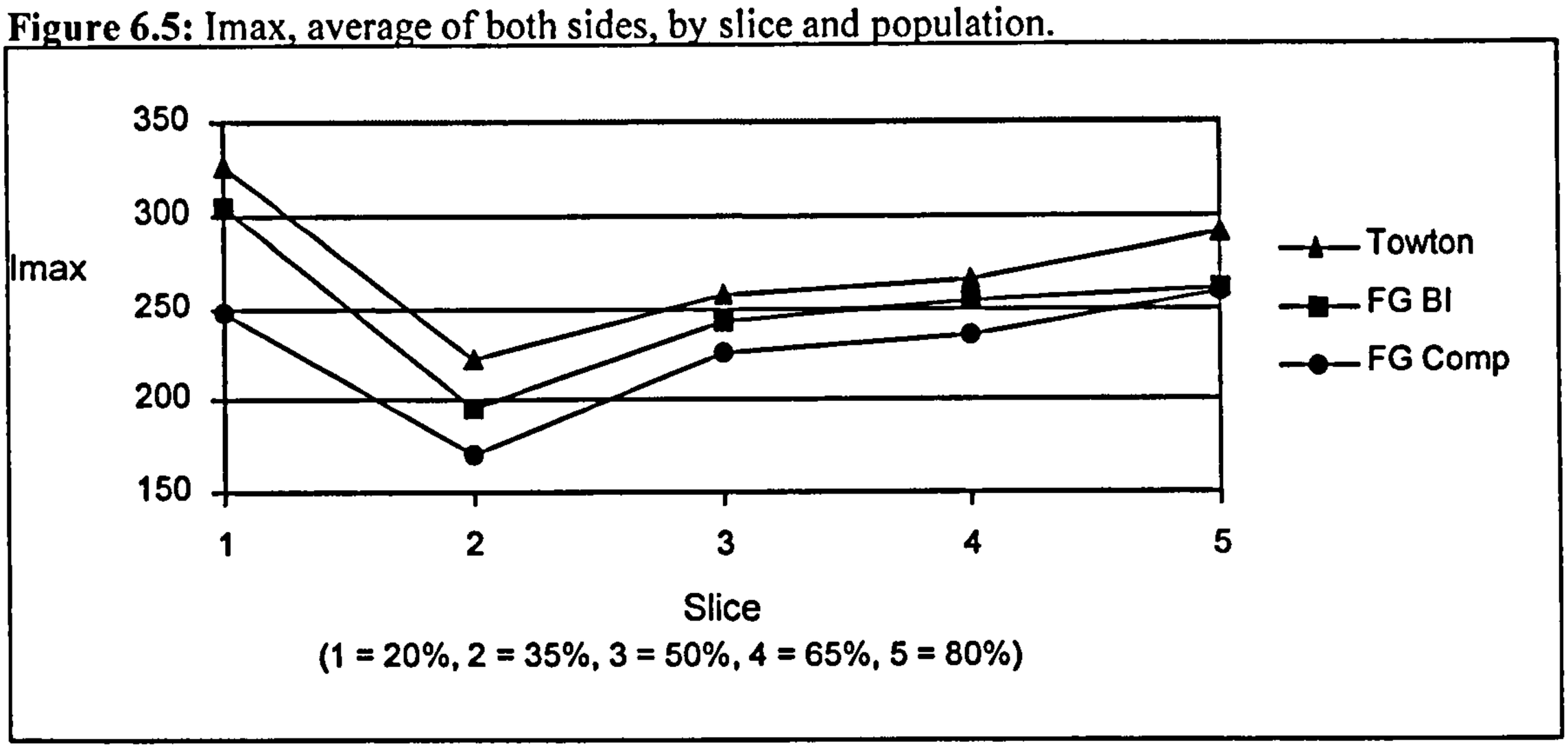

Figure 6.6: Imin, average of both sides, by slice and population.

Imax and Imin quantify the maximum and minimum second moments of area, measuring the bending rigidity perpendicular to the neutral axis (Ruff, 2000a). The

greatest maximum resistance to bending stresses is found in the Towton sample, similar to the measures of diaphyseal robusticity (J). This is followed by the Fishergate blade-injured and comparative samples. At the 35% slice, there are significant differences in Imax between the Towton and the Fishergate comparative samples ($p < .021$), with the Towton sample displaying a significantly increased rigidity at this location, indicating an increased bone failure point under loading. This may relate to architectural features noted in this region, diaphyseal flattening, where the typically triangular pillar region is visually 'flattened' (losing the apex of the triangle), but in fact is reinforced with extra bone along medial and lateral margins of the anterior surface. An increased supracondylar breadth is also characteristic of this area (see Figure. 4.1). Towton again displays the greatest minimum bending rigidity (Imin), followed by the Fishergate BI and comparative samples. There are no significant differences between samples in this parameter.

6.3.2 Diaphyseal Shape

Diaphyseal shape is characterized by Ix/Iy. This parameter has the benefit of revealing both the strength and direction of bending resistance. The Fishergate blade-injured group displays greatest resistance to bending strength in the medio-lateral (M/L) plane at 20% combined while, at all other slice parameters, the greatest bending resistance occurs in the antero-posterior (A/P) plane. The Towton and Fishergate comparative groups display the most generally rounded sections, although the Towton sample falls lowest in value from the mid to proximal humeral shaft. Significant differences exist between blade-injured populations in the direction of bending strengths across the midshaft (50%) and mid-proximal humerus (65%), with the Towton samples displaying increased M/L breadth at 50% (<1.0) and greater circularity at 65% (closest to 1.0), while the FG BI sample is more circular at 50% and has a greater A/P breadth at 65%.

Figure 6.7: Ix/Iy, average of both sides, by slice and population. FG BI = Fishergate blade-injured, FG Comp = Fishergate comparative.

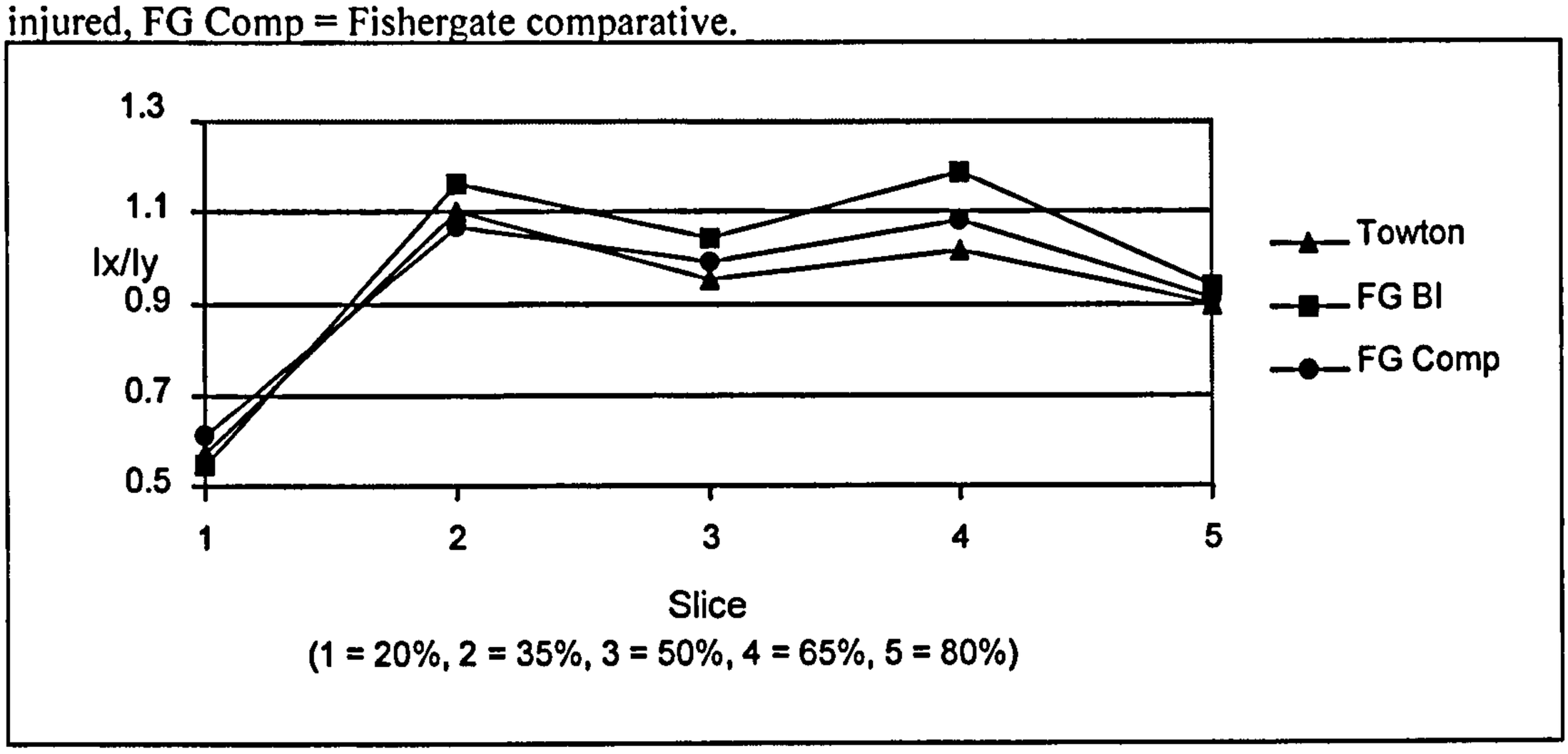

6.3.3 Diaphyseal Asymmetry

Pronounced diaphyseal asymmetries have been found in analyses of professional tennis players that highlight the degree of plasticity possible within humans. In this study, there are no significant differences found in diaphyseal robusticity as measured by TA, CA, PCA, Imax, Imin or J between sides in any of the populations examined (Table 6.3). However, there are significant differences in diaphyseal shape (Ix/Iy) between sides in the Towton collection at 35%, 50% and 65%. The percentage of bilateral asymmetry varies between populations (Table 6.4). Asymmetry in TA, CA and PCA are low overall, with the greatest range found at the 80% slice in the Fishergate comparative sample and in the 20% slice in the Towton sample. Asymmetry in Imax and Imin exceeds that demonstrated in TA and CA, although asymmetry in J is greatest of the diaphyseal robusticity values. This reflects marked bilateral differences in resistance to bending strains.

The measure of diaphyseal shape (Ix/Iy) is most bilaterally asymmetric. There is considerable variation between limbs at 20%, 35%, 50% and 65% in the Towton sample, while the Fishergate BI sample shows more conformity in these measurements

Table 6.3: Differences between sides in humeral cross-sectional properties and measures of architecture, by slice parameter.

Mann-Whitney Analysis	TA	CA	PCA	J	Imax	Imin	Ix/Iy	Humeral Torsion
Towton								.728
20%	.376	.538	.801	.186	.225	.689	.125	--
35%	.331	.424	.574	.361	.331	.691	.002**	--
50%	.894	.894	.880	.894	.936	.503	.014*	--
65%	.744	.957	.479	.894	.979	.579	.014*	--
80%	.728	.100	.650	.979	.936	.769	.123	--
FG BI								.227
20%	.939	.353	.579	.436	.579	.247	.631	--
35%	.353	.393	.393	.315	.280	.190	.739	--
50%	.393	.436	.971	.353	.393	.280	.143	--
65%	.436	.739	.393	.529	.529	.353	.436	--
80%	.436	.793	.739	.481	.481	.481	.684	--
FG Comp								.530
20%	.297	.222	.931	.666	.297	.605	1.000	--
35%	.796	.436	.258	.666	.796	.387	.605	--
50%	.546	.605	.863	.297	.297	.605	.546	--
65%	.489	.863	.387	.546	.605	.489	.931	--
80%	.605	.340	.863	.605	.666	.546	.136	--

*Sig. p = 0.05; **Sig. p = 0.01

between limbs, as demonstrated by lower asymmetry values. There is significant variation found in the percentage of bilateral asymmetry identified between populations. The high level of asymmetry in Ix/Iy as demonstrated by the Towton sample is unique at 35% (Ix/Iy). Significant differences in the level of bilateral asymmetry found at the 65% mid-proximal slice (Ix/Iy) and 80% proximal slice (CA) are also identified, although post-hoc analyses were non-significant for any two population groups. At the 80% slice, there is also significant variation identified between the Towton sample and the Fishergate comparative sample in asymmetry of J values ($p < .030$). Conversely, it is the Fishergate comparative sample that displays the highest level of bilateral asymmetry at this location.

Table 6.4: Bilateral asymmetry in cross-sectional properties, by slice parameter, for all populations. The values are expressed as a percentage of the total value. The last column is the measure of significance for a one-way ANOVA. At 35%, the Towton sample is unique, varying from both other samples ($p < .041$ & .037 respectively). At 65% (Ix/Iy) and 80% (CA), the post-hoc results are non-significant for any two population groups, while at 80% (J), there is significant difference between the Towton and the Fishergate comparative samples ($p < .030$).

	Towton			**Fishergate BI**			**Fishergate Comparative**			**Sig.**
	Median	**Min**	**Max**	**Median**	**Min**	**Max**	**Median**	**Min**	**Max**	
20%										
$TA/Length^3$	7.48	.51	13.48	5.59	1.00	14.95	4.23	2.03	18.15	.852
$CA/Length^3$	6.28	.38	13.76	7.60	.07	19.75	3.25	.34	18.66	.843
PCA	2.29	.81	8.51	2.40	.06	7.20	.950	.43	2.64	.074
$J/length^{5.33}$	14.24	.39	37.85	12.15	3.58	32.92	19.46	3.82	42.82	.827
Imax	9.71	3.22	56.01	11.58	1.94	41.55	17.06	1.27	48.05	.913
Imin	9.59	.67	41.00	12.14	.62	52.60	18.19	1.66	32.97	.527
Ix/Iy	22.68	1.10	66.43	4.18	.66	72.54	13.74	1.79	23.94	.104
35%										
$TA/Length^3$	6.46	.96	21.25	5.39	.68	14.06	4.69	.07	16.2	.467
$CA/Length^3$	6.87	.21	21.87	8.05	.50	19.99	7.85	.26	44.01	.732
PCA	1.56	.22	6.51	4.45	.80	8.33	4.41	.19	11.97	.157
$J/length^{5.33}$	16.68	.30	44.64	12.44	1.22	36.93	17.61	.84	36.48	.843
Imax	13.32	.14	65.81	10.26	.05	42.03	12.96	1.65	37.25	.533
Imin	18.82	1.58	41.04	12.96	1.65	37.25	11.76	4.43	45.06	.943
Ix/Iy	28.07	.62	89.24	8.29	1.42	17.50	6.25	.57	19.52	.017*
50%										
$TA/Length^3$	2.40	.26	20.91	3.96	.48	15.31	3.75	.43	15.49	.960
$CA/Length^3$	3.69	1.55	22.84	6.25	.69	19.05	6.58	.70	16.81	.986
PCA	1.14	.01	7.74	3.52	.15	8.51	2.69	.45	7.56	.377
$J/length^{5.33}$	5.09	.27	45.39	10.40	.91	32.65	5.78	2.49	35.06	.852
Imax	7.23	1.58	42.45	7.00	1.30	29.37	13.17	.51	40.82	.457
Imin	5.38	.20	48.96	7.55	.84	38.21	9.16	1.95	26.94	.986
Ix/Iy	19.48	1.47	53.67	7.23	.99	28.38	9.20	.91	40.58	.065
65%										
$TA/Length^3$	4.41	.93	19.10	6.25	1.06	16.49	5.47	.46	27.77	.801
$CA/Length^3$	6.41	1.59	17.01	4.62	.07	13.46	6.24	.44	33.52	.417
PCA	5.63	.24	15.43	4.38	1.54	13.29	2.17	.14	10.93	.396
$J/length^{5.33}$	6.60	.35	36.24	11.24	.16	32.23	12.56	1.17	68.20	.534
Imax	8.03	1.64	42.47	10.52	.46	30.42	10.99	4.27	72.40	.531
Imin	6.46	.43	30.65	12.05	3.15	37.48	7.93	.09	63.04	.521
Ix/Iy	14.58	.23	40.58	7.91	3.63	14.69	10.56	.22	18.79	.031*
80%										
$TA/Length^3$	3.72	.03	15.72	4.45	.76	20.56	8.14	1.98	16.00	.394
$CA/Length^3$	7.29	.08	12.27	5.45	1.73	14.03	12.50	2.02	46.07	.044*
PCA	6.93	1.22	12.60	4.66	.16	16.01	5.54	.23	25.93	.913
$J/length^{5.33}$	7.05	1.07	20.98	6.68	.86	31.99	16.73	4.73	60.85	.026*
Imax	8.26	.95	24.12	10.97	2.12	34.29	13.97	2.78	71.15	.240
Imin	6.75	1.27	34.96	5.62	.53	29.07	16.42	4.33	49.34	.103
Ix/Iy	6.93	.05	36.64	6.58	.13	11	9.32	.81	21.38	.455

*Sig. p = 0.05; ** Sig. p = 0.01

Table 6.5: Bilateral asymmetry in cross-sectional properties: Population comparisons at the 35% and 50% slice locations. For comparison among populations, the differences between sides are expressed as a percentage of the total value.

		35% CA	35% J	50% CA	50% J
Towton	Median	6.87%	16.68%	3.69%	5.09%
	Range	0.2-21.8	0.3-44.6	1.5-22.8	0.2-45.3
	N	11	11	12	12
Fishergate BI	Median	8.05%	12.44%	6.25%	10.40%
	Range	0.5-19.9	1.2-36.9	0.6-19.0	0.9-32.6
	N	10	10	10	10
Fishergate Comparative	Median	7.85%	17.61%	6.58%	5.78%
	Range	0.2-24.6	0.8-36.4	0.7-16.8	2.4-35.0
	N	9	9	9	9
Euroamerican*	Median	7.6%	9.6%	7.4%	13.6%
	Quartile range	3.2-11.7	3.3-19.7	3.1-13.9	5.1-19.1
	Range	0.7-32.8	0.3-41.6	1.1-50.4	0.1-34.3
	N	38	38	38	38
Jomon (Japanese)*	Median	5.4%	8.9%	7.9%	5.6%
	Quartile range	3.7-7.6	3.2-11.7	3.8-11.0	3.8-10.6
	Range	0.4-27.3	0.3-22.5	0.3-26.0	0.9-25.9
	N	24	24	25	25
Amerindian Georgia Coast*	Median	4.9%	8.7%		
	Quartile range	2.1-9.0	3.4-12.0		
	Range	0.0-16.3	0.8-24.6		
	N	37	37		
Amerindian California*	Median	6.2%	11.2%		
	Quartile range	2.7-9.8	4.8-21.2		
	Range	0.5-47.6	0.1-42.5		
	N	71	71		
Tennis players*	Median	33.9%	56.6%		
	Quartile range	25.1-53.0	37.5-85.9		
	Range	17.2-68.4	13.6-118.2		
	N	45	45		
European Neandertals**	Median	19.1%	56.6%		
	Quartile range	11.5-48.8	49.6-95.2		
	N	3	5		

*(Trinkaus et al., 1994)
** (Trinkaus and Churchill, 1999)

To determine how levels of diaphyseal asymmetry differ between the medieval populations, comparisons were made with other previously studied archaeological populations (Table 6.5). The data is taken from Trinkaus *et al.* (1994) and Trinkaus and Churchill (1999). It should be noted that the comparative samples are combined sexes while the Towton and Fishergate samples are males only. The two Fishergate samples display higher levels of asymmetry in cortical area than the comparative samples at the 35% location. Asymmetry in CA is highest at 35% in the Fishergate blade-injured

sample, followed by the Fishergate comparative sample, the Euroamerican sample and, finally, the Towton sample. When the focus shifts to the 50% location, the three later medieval samples fall within the lower range of variation, as the highest percentage of asymmetry is found in the Japanese Jomon sample. The level of asymmetry demonstrated by all three medieval populations at 35% in J values is higher than the modern and archaeological comparative populations. However, at 50%, the greatest asymmetry is found in the modern Euroamerican sample, followed by the Fishergate BI group. None of the later medieval samples falls within the range of the two extreme populations composed of the professional tennis players and European Neandertals. This demonstrates how unusual the professional athletes are – more unusual then even the late Pleistocene Neandertal populations.

6.4 The Pattern of Mechanical Loading

6.4.1 Population Mean Right vs. Left Limb

The general pattern of cortical bone distribution throughout the humerus is similar in the two blade-injured populations but with one key difference. The Towton sample, as a group, is left-side dominant in both cortical bone deposition and robusticity. All populations show a pattern of greatest cortical bone deposition at 20%, followed by a reduction at 35%, an increased or levelling of CA at 50% relative to the 35% slice, and then a general reduction in levels to 80% (Fig. 6.8). This occurs absolutely across all samples with one exception. The Towton sample does not follow this pattern in the left limb; instead, it shows decreased cortical bone deposition at the 50% slice. Although diaphyseal robusticity is similar between the right and left mid and proximal humeral shaft, the left distal humerus of the Towton individuals appears to be subjected to higher levels of strain, as indicated by the elevated J values in this area (Fig. 6.9). This sample also displays increased robusticity at 80% when compared with the Fishergate BI group.

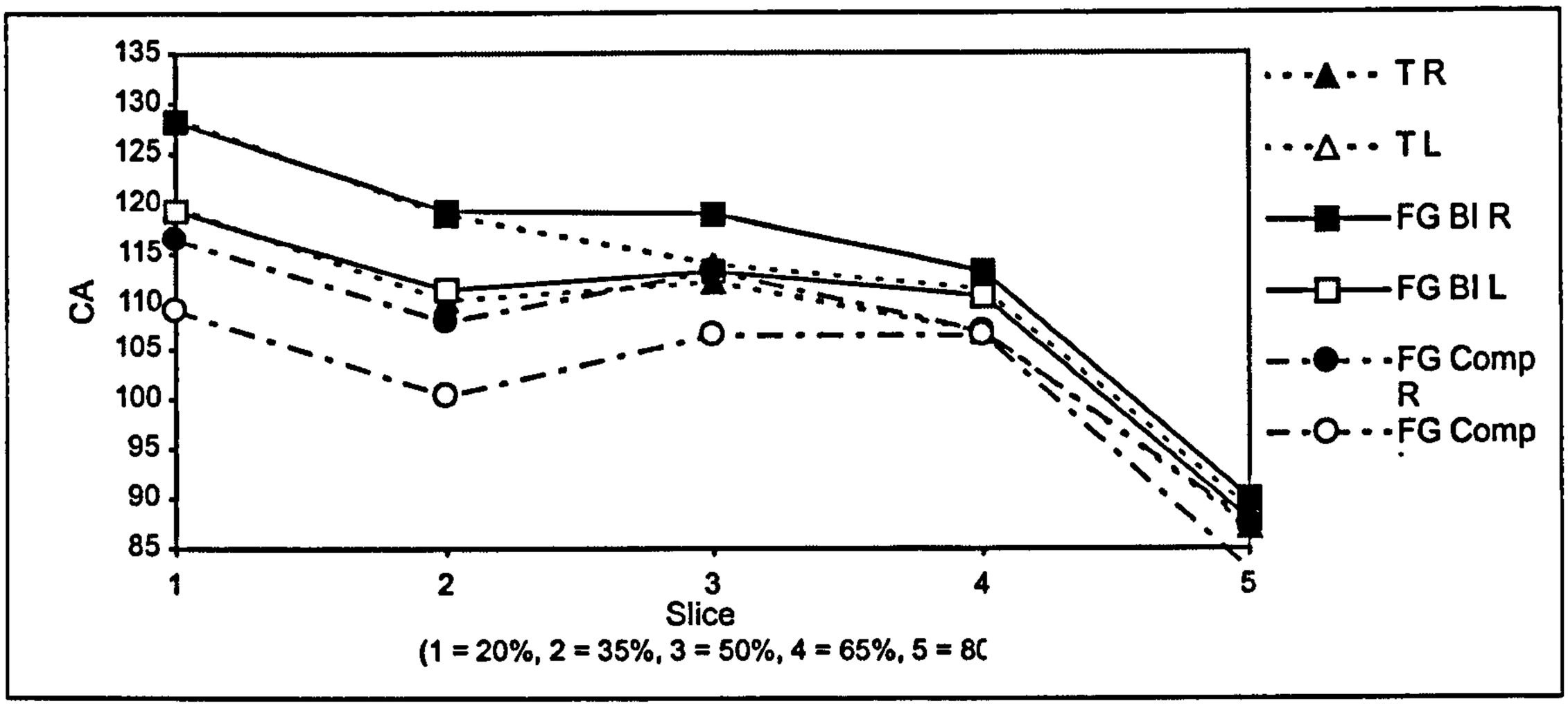

Figure 6.9: The pattern of biomechanical robusticity (J) between the right and left humerus, all samples. Note the strong distal left-sided dominance in the Towton sample when compared with the other two samples. Interestingly, they display decreased robusticity at 80% in relation to 65% while the other two samples display increased robusticity at 80% relative to 65%. This figure is based upon the population mean for each slice parameter. T = Towton, FG BI = Fishergate blade-injured, FG Comp = Fishergate comparative; R = right, L = left.

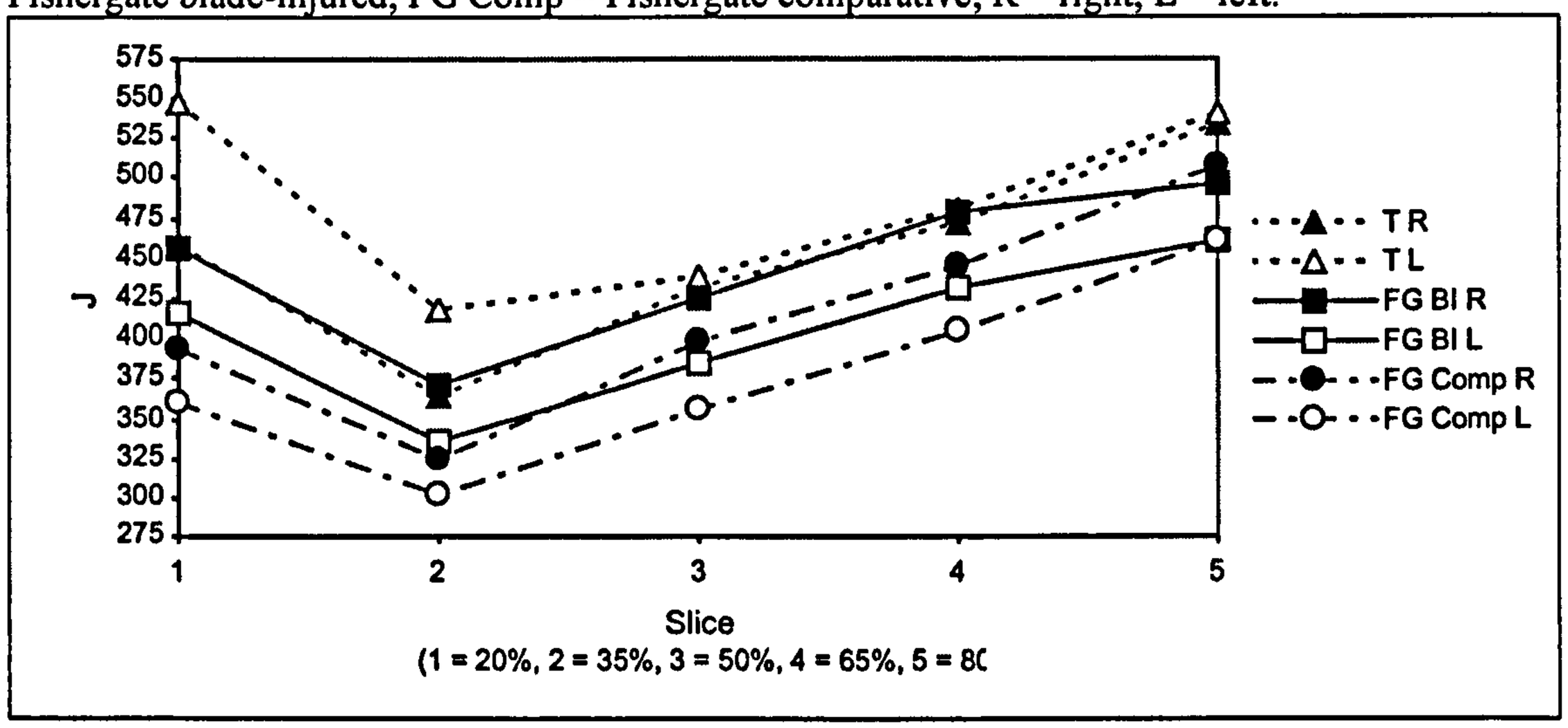

Fig. 6.10: The pattern of total area (TA) between the right and left humerus, all samples. Again, there is left-sided dominance in the Towton sample when compared with the other collections. This figure is based upon the population mean for each slice parameter. T = Towton, FG BI = Fishergate blade-injured, FG Comp = Fishergate comparative; R = right, L = left.

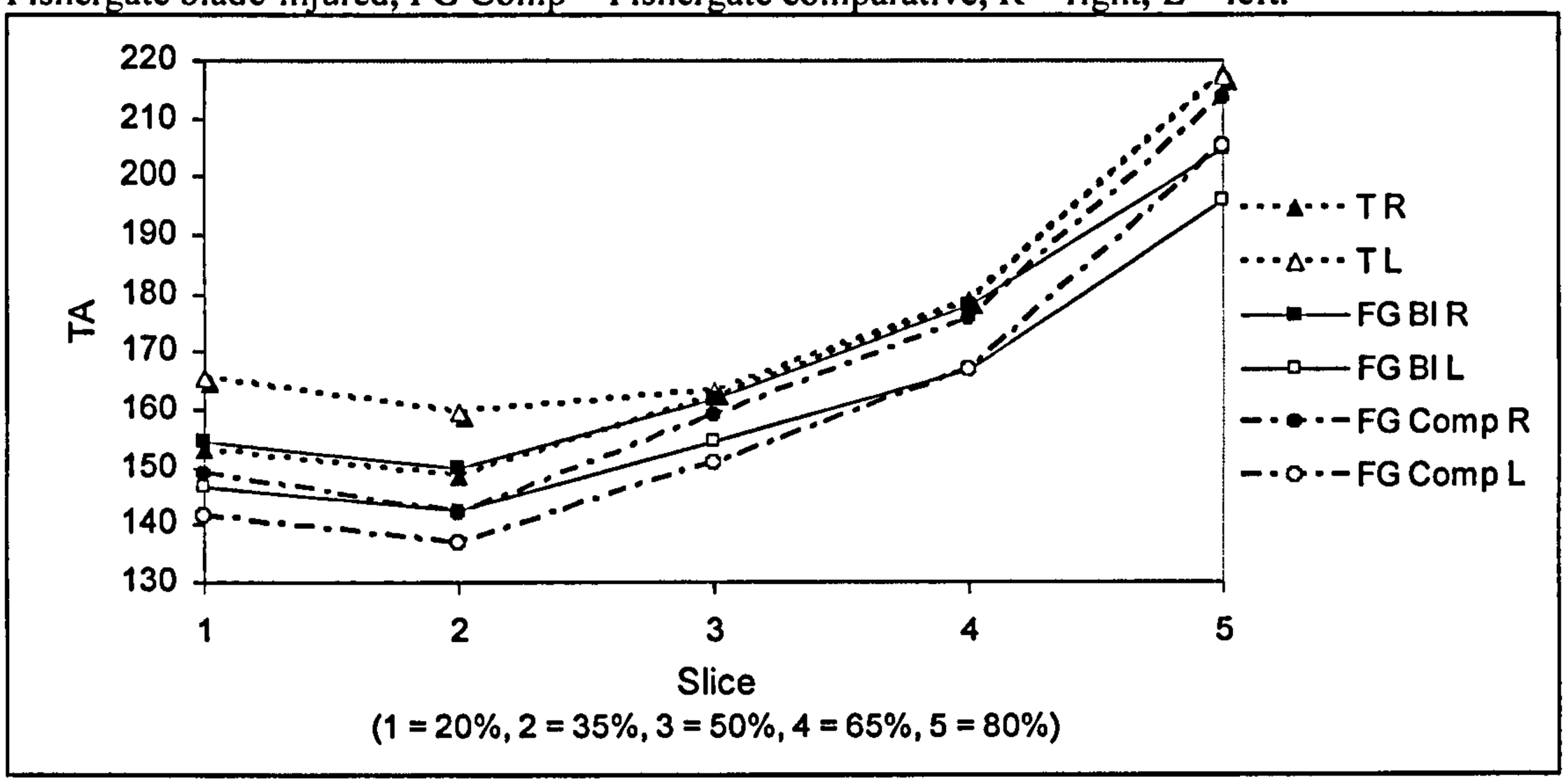

Figure 6.11: The pattern of PCA between right and left humerus, all samples. The greatest percent of cortical bone is found in the Fishergate blade-injured sample while the least amount of cortical bone to total area is found in the Towton sample. T = Towton, FG BI = Fishergate BI, FG Comp = Fishergate comparative; R = right, L = left.

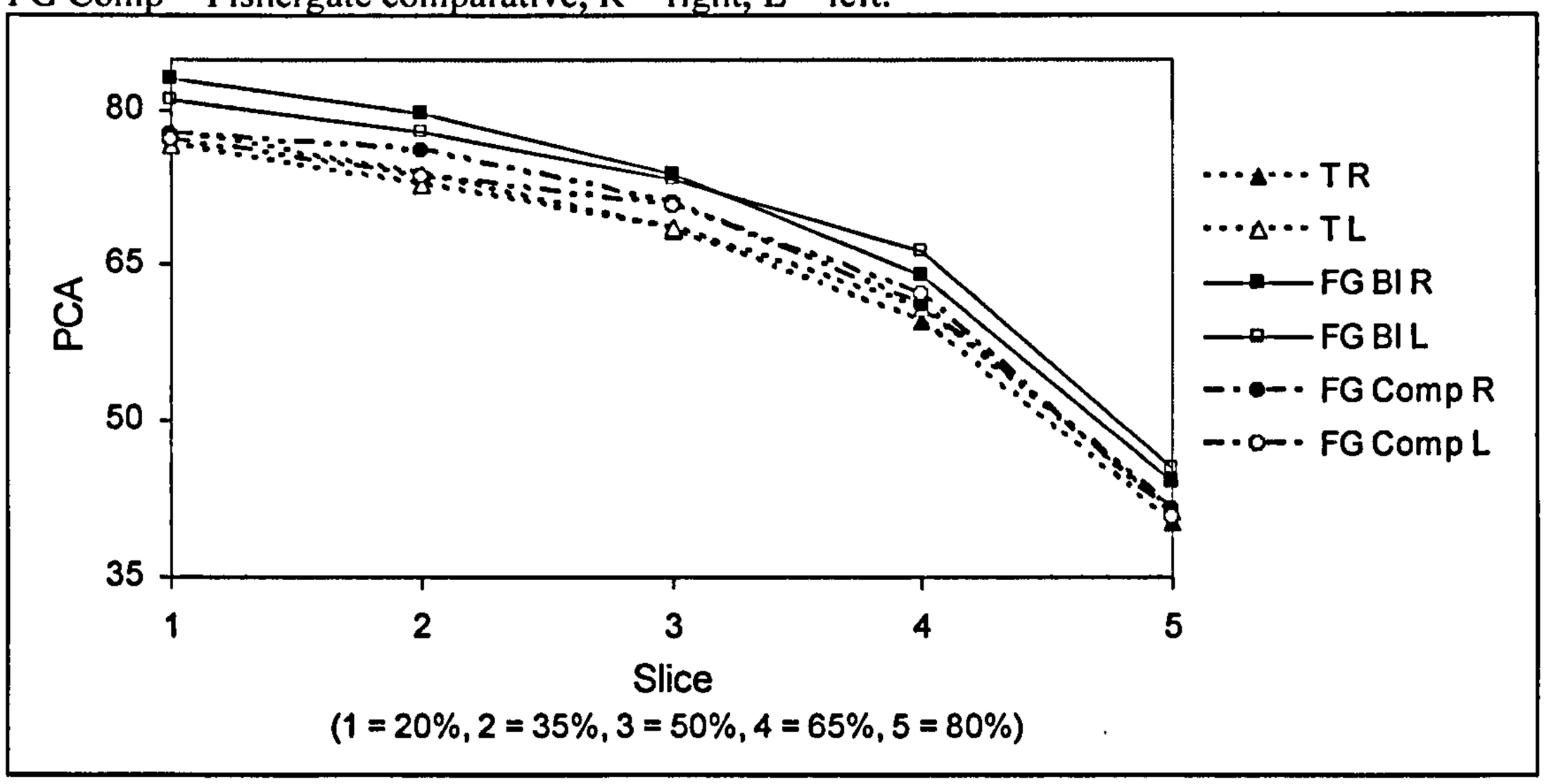

The difference between sides in PCA is minimal (Figure 6.11). The greatest PCA is found in the Fishergate BI sample, although this crosses over from the right distal humeral shaft, which displays the highest PCA, to the left proximal humeral shaft. The Towton sample also follows this pattern, shifting from the highest percent cortical area in the right distal shaft to the left proximal shaft. The Fishergate comparative sample,

though, displays the opposite pattern, with the greatest PCA in the left distal shaft and crossing over to the right proximal shaft.

Figure 6.12: The pattern of Imax between right and left humerus, all samples. The maximum resistance to bending strains are found in the left humerus, Towton sample, while the least amount of cortical bone to total area is found in the Fishergate comparative sample, left limb. T = Towton, FG BI = Fishergate blade-injured, FG Comp = Fishergate comparative; R = right, L = left.

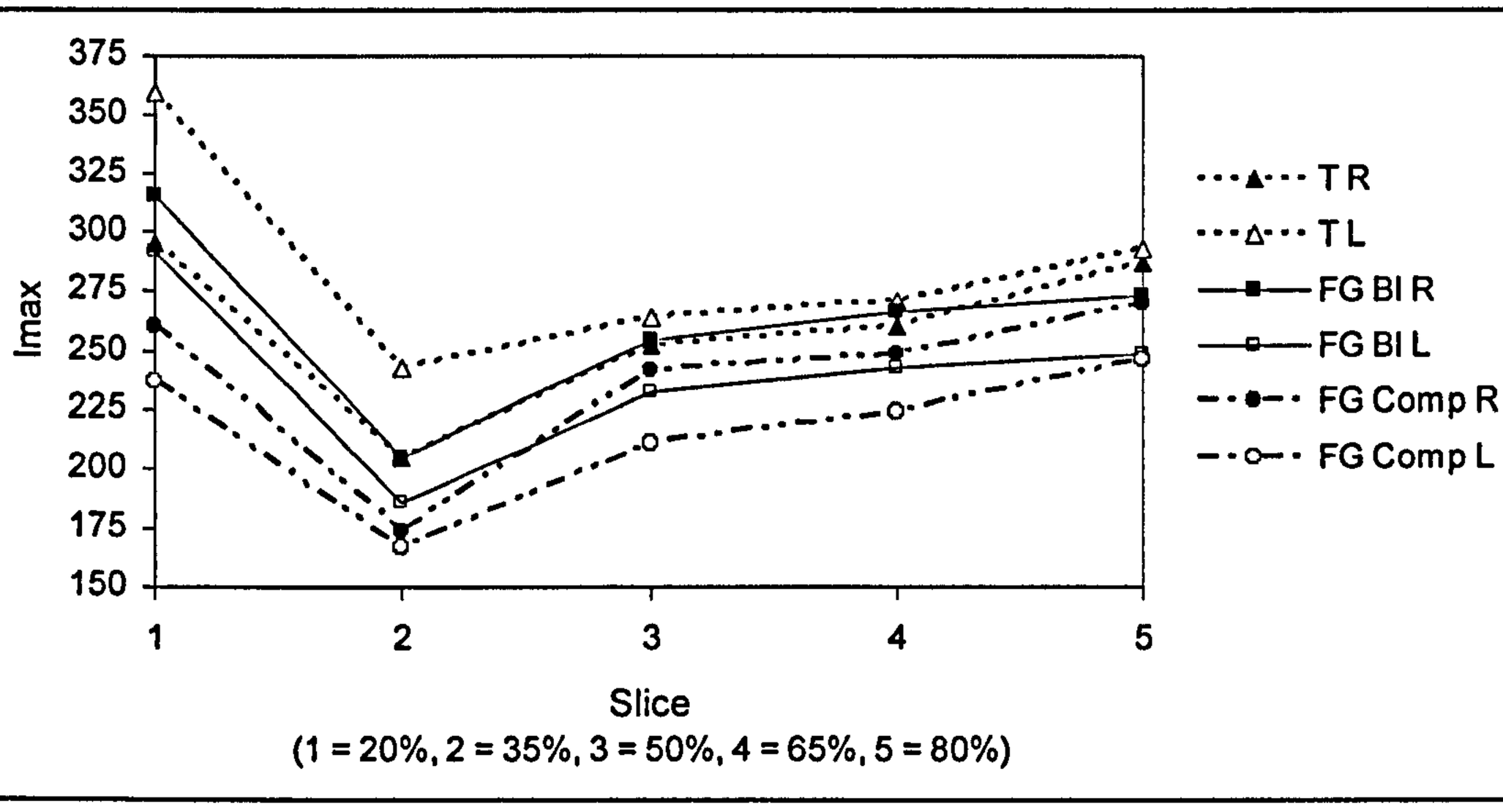

The bilateral patterning of Imax follows that of J (Figure 6.12). The left distal diaphysis of the Towton sample again displays elevated values in comparison to the other groups, indicating greater bending rigidity at these locations. Both Fishergate samples display right-side dominance, rather than the left-side dominance found in the Towton sample. The sample and side with the least bending rigidity is the left diaphysis of the Fishergate comparative group. The slice with the greatest bending rigidity and, consequently, robusticity is the distal, 20% parameter in this population. This is in contrast to Imin, which displays the greatest minimum bending rigidity instead at the proximal, 80% slice (Figure 6.13). Again the left diaphysis of the Towton sample displays the greatest values in this cross-sectional property, while the right diaphysis of the Fishergate comparative sample displays the lowest values. At the 35% slice, the left humerus of the Towton sample displays a marked increase in the minimum bending rigidity when compared with the other samples and sides.

Figure 6.13: The pattern of Imin between right and left humerus, all samples. The greatest minimum resistance to bending strains are found in the Towton sample, left humerus, while the least amount of cortical bone to total area is found in the left limb, Fishergate comparative sample. T = Towton, FG BI = Fishergate blade-injured, FG Comp = Fishergate comparative; R = right, L = left.

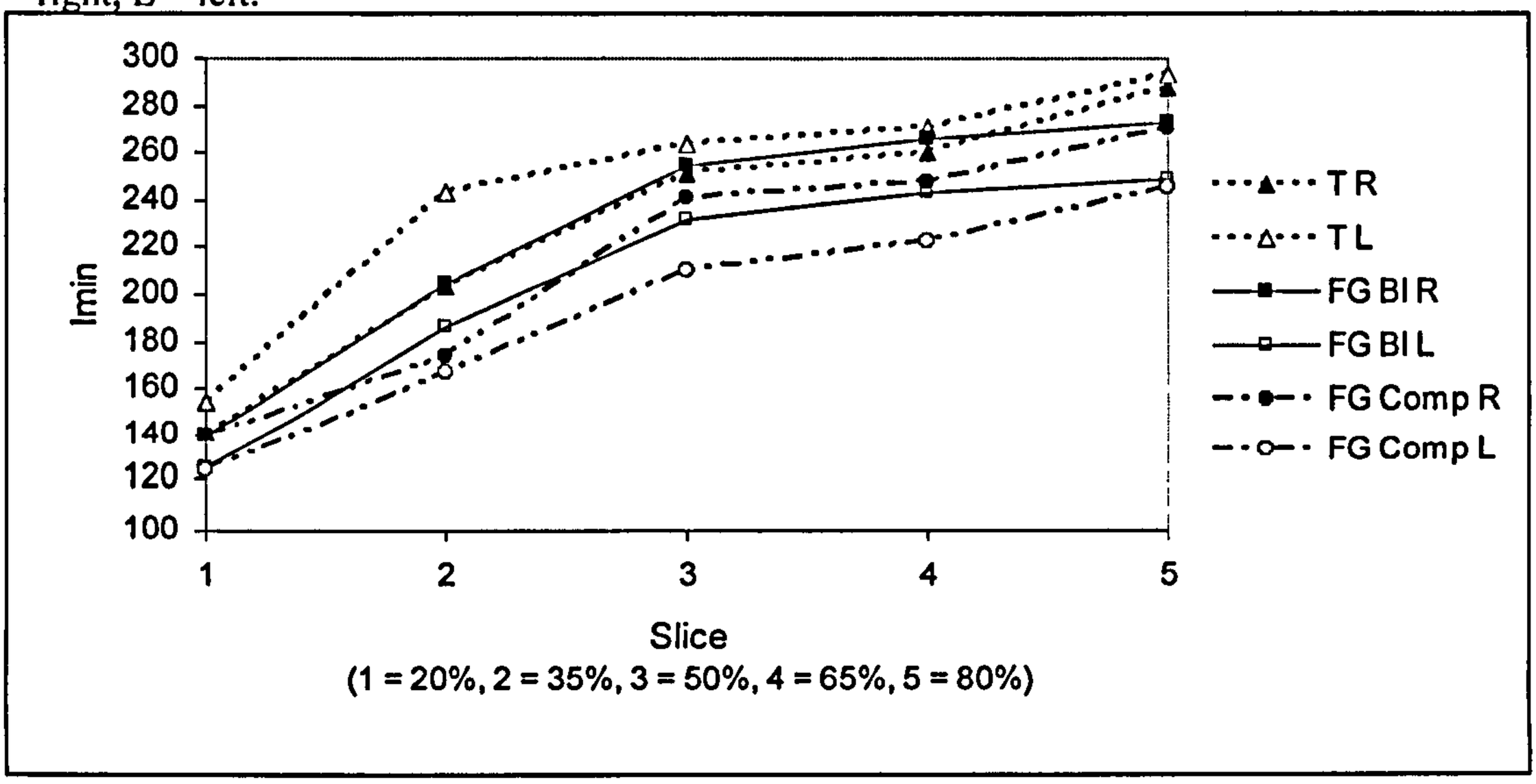

Fig. 6.14: The pattern of diaphyseal shape (Ix/Iy) between right and left humerus, all samples. The left limb of the Towton sample displays the greatest medio-lateral breadth, while the left limb of the Fishergate BI sample displays the greatest antero-posterior breadth. This figure is based upon the population mean for each slice parameter. T = Towton, FG BI = Fishergate blade-injured, FG Comp = Fishergate comparative; R = right, L = left.

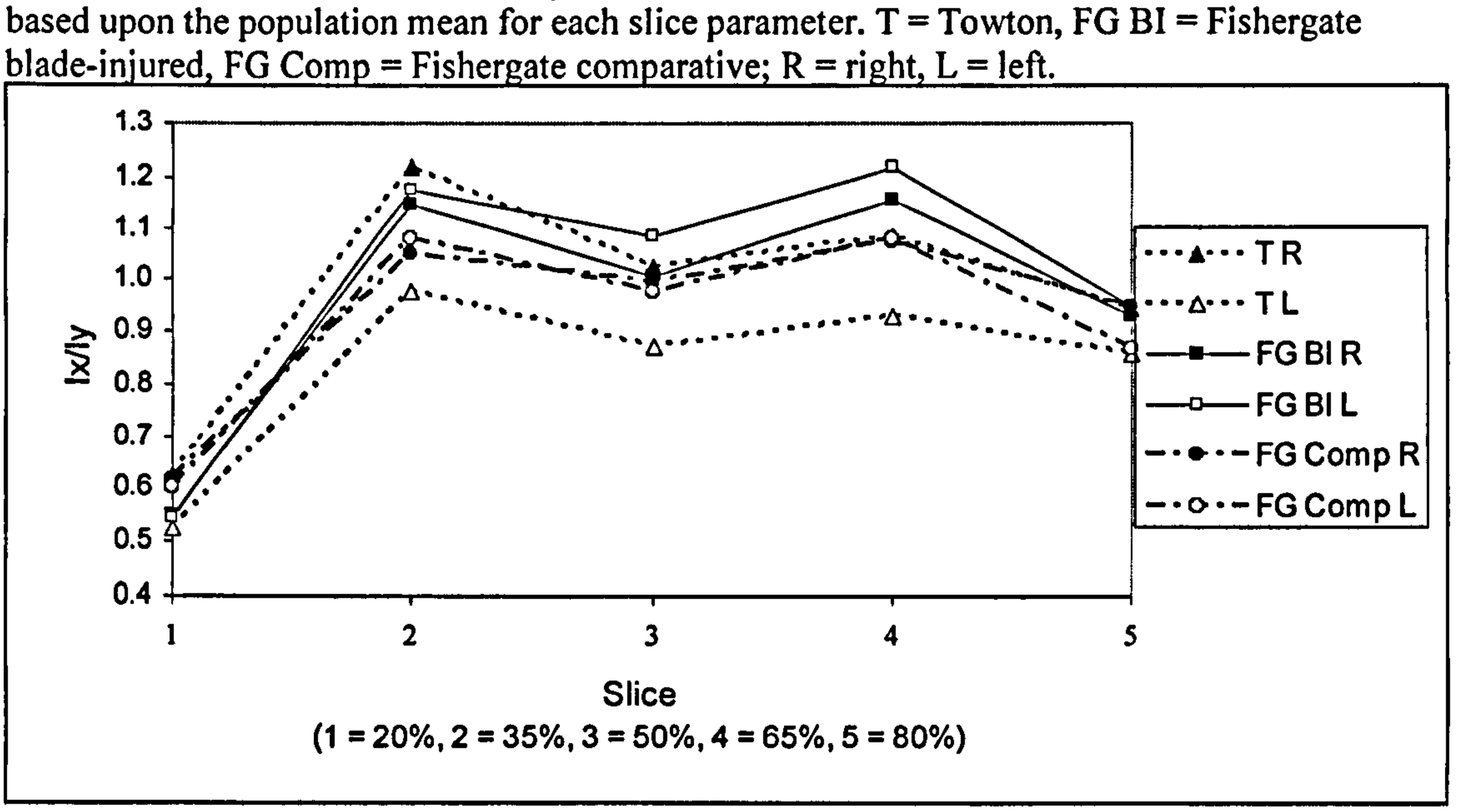

The strong bilateral asymmetry in diaphyseal shape demonstrated by the Towton sample is visible in Figure 6.14. The average value for the Towton left humerus at all slice parameters falls below the line of circularity (1.0), indicating greater medio-lateral bending resistance than found in the other samples, although the right humerus of the

Towton sample displays the greatest antero-posterior bending strength at 35%. The two Fishergate samples display the greatest A/P bending not in the right humerus, as in the Towton sample, but in the left. These differences indicate a pattern to diaphyseal shape and limb dominance whereby one limb displays either circularity or increased M/L bending while the contralateral limb follows a trend towards greater circularity and increased A/P bending resistance.

6.4.2 Individual Patterns of Mechanical Loading

Many individuals deviate strongly from their population average loading pattern when examined in isolation. Fluctuating asymmetry has previously been identified with the humeri of the Towton population. This pattern was originally isolated in Towton 16 & Towton 41 (Knüsel 2000a), however, it is found in both Fishergate populations as well. What does vary is the direction it takes. The Fishergate groups display the most individuals with a side in which all slices demonstrate predominance of the right or left within a single limb (cortical area). The Fishergate BI sample displays three with right-sided dominance (FG2392, FG6448 and FG7052) (Table 6.7). The Fishergate comparative sample numbers three with right-sided dominance (FG3202, FG5138 and FG5336) and three with left-sided dominance (FG1425, FG2178 and FG6128, the priest from the Southern cemetery). Towton, the largest of the groups, also has six individuals with all slices of a single limb being dominant, three right-sided, T16, T22 (both displaying antemortem weapon trauma) and T44. The three left-sided individuals are T24, T31 and T41, the latter also displays antemortem weapon trauma. Figure 6.15 demonstrates this pattern.

Table 6.6: Individual patterns of mechanical loading. CA and J patterning reflect the shift in dominance from the distal-most slice parameter to the proximal-most slice parameter. Therefore, a pattern of LLLRL reflects a pattern of greatest cortical area in the left side 20%, 35% and 50% slices, then a pattern shift to greatest cortical area in the right 65% slice, followed by another pattern shift to the greatest cortical area again in the left 80% slice.

	Context	Age (years)	CA pattern	J Pattern
T6	Blade-injured	16 – 20	LLLRL	L
T11	Blade-injured	36 – 45	LLLRR	L
T13	Blade-injured	36 – 45	LLLLR	LLLLR
T16*	Blade-injured, antemortem weapon trauma	46 – 50	R	L-RRR
T22	Blade-injured, antemortem weapon trauma	26 – 35	R	R
T23	Blade-injured	26 – 35	RLRLR	LLLRR
T24	Blade-injured	36 – 45	L	LLLRR
T32	Blade-injured	16 – 25	L	LLLLR
T40	Blade-injured	36 – 45	LLLRR	LLLRR
T41	Blade-injured, antemortem weapons trauma	26 – 35	L	L
T44	Blade-injured	26 – 35	R	R
T46	Blade-injured	26 – 35	LLRRL	LLRRL
FG1589	Blade-injured (10^{th} / 11^{th} ct.)	17 – 25	RRRRL	R
FG1886	Blade-injured (10^{th} / 11^{th} ct.)	20 - 30	RLLRR	R
FG1893	Blade-injured (10^{th} / 11^{th} ct.)	40 – 50	RRLLR	R
FG2270	Blade-injured, Nave, (early to mid 14^{th} ct.)	30 – 40	RLRLR	LLRRR
FG2392	Blade-injured (10^{th} / 11^{th} ct.)	30 – 40	R	R
FG5356	Blade-injured, Crossing (1195 – late 13^{th} ct.)	30 – 40	LRLRL	LRRRR
FG6191	Blade-injured (10^{th} / 11^{th} ct.)	20 – 30	RRRRL	LRRRL
FG6411	Blade-injured (10^{th} / 11^{th} ct.)	20 – 30	RRRRL	RRRRL
FG6448	Blade-injured (10^{th} – 11^{th} ct.)	20 – 30	R	LRRRR
FG7052	Blade-injured, Cloister garth (13^{th} – 16^{th} ct.)	20 – 30	R	RRLRR
FG1425	Southern cemetery (late 13^{th} – early 14^{th} ct.)	20 – 30	R	R
FG1436	Southern cemetery (late 13^{th} – early 14^{th} ct.)	20 – 30	LRRLL	LLRLR
FG2178	Nave (early – mid 14^{th} ct.)	40 – 50	L	LLRLL
FG3195	Prior, Chapter house (1195 – early 14^{th} ct.)	40 – 50	RLRLL	RLRLR
FG3202	Cloister garth (1195 – early 14^{th} ct.)	20 – 30	R	R
FG5071	East cemetery (1195 – early 14^{th} ct.)	30 – 40	RRRLR	R
FG5138	N. transept chapel (1195 – early 14^{th} ct.)	20 – 30	R	R
FG5336	East cemetery (1195 – early 14^{th} ct.)	20 – 30	R	R
FG6128	Priest, Southern cemetery (1195 – late 13^{th} ct.)	40 – 50	L	L

*There is no left side data for T16, slice 2 (35%).

Many individuals display contralateral shifts in cortical area. However, this, too, varies between populations. Both Fishergate samples display a typical pattern of greatest cortical area in the right distal diaphysis. This shifts to the left proximal diaphysis in three individuals in the Fishergate blade-injured sample (FG 1589, FG6191 and FG6448). There are no individuals from the Fishergate comparative sample with a single contralateral shift in cortical area. In the Towton sample, though, three

individuals display a single contralateral shift in CA (T11, T13 and T40). However, rather than following a pattern of greatest CA in the right distal shaft that shifts to the left proximal shaft as seen in the Fishergate sample, these individuals demonstrate the opposite pattern. The left distal diaphysis has the greatest cortical area and the shift is then to the right proximal shaft in these men. Figure 6.16 illustrates this pattern.

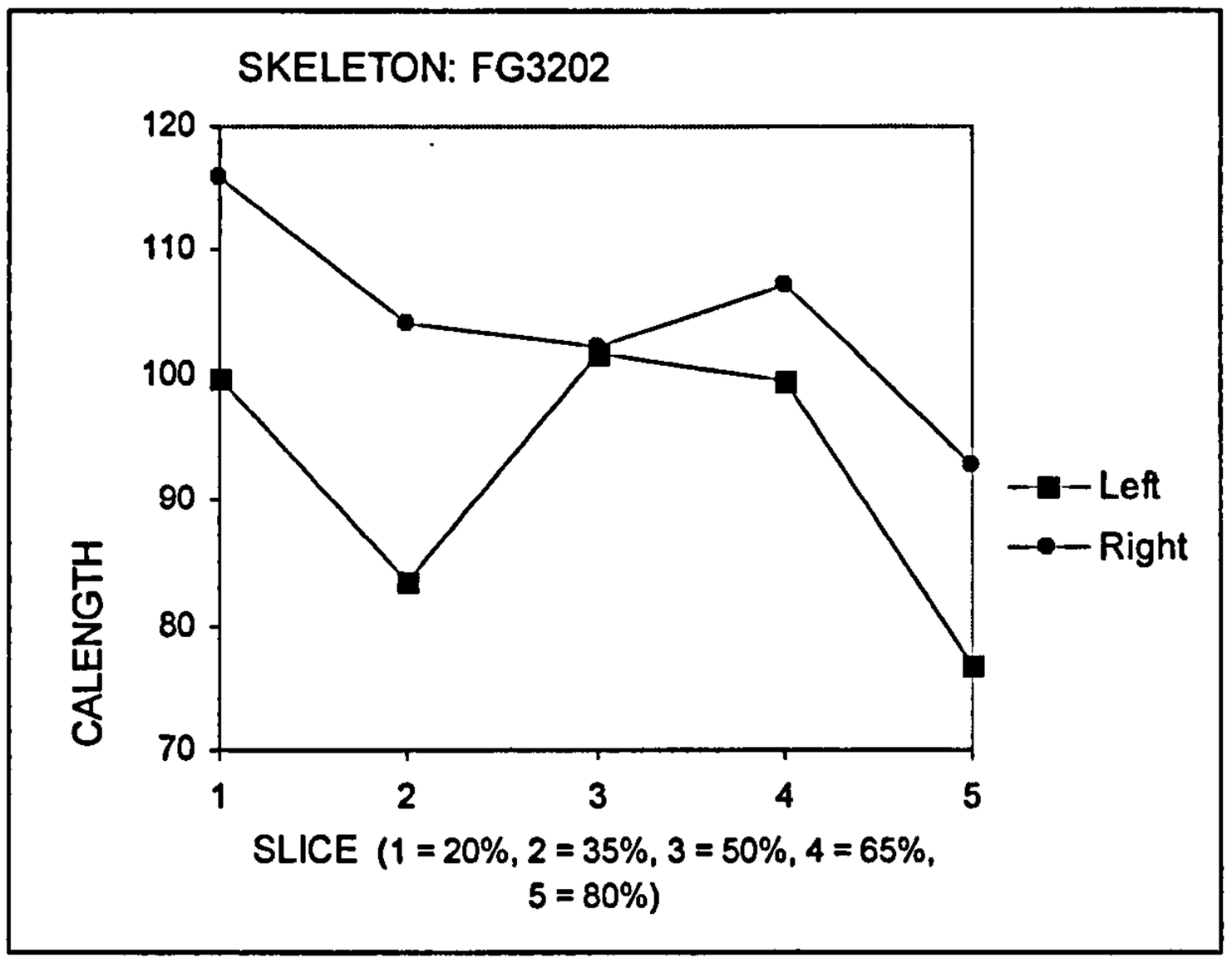

Figure 6.15: Individual patterns of mechanical loading (CA). An example of dominance in cortical area found throughout a single limb. This example is FG3202, from the cloister garth, part of the Fishergate intramural cemetery. It displays right-side dominance in cortical area. Note the increased extent of differences between sides in the distal and proximal humeral diaphyses, while the midshaft slice parameter is nearly equal between sides.

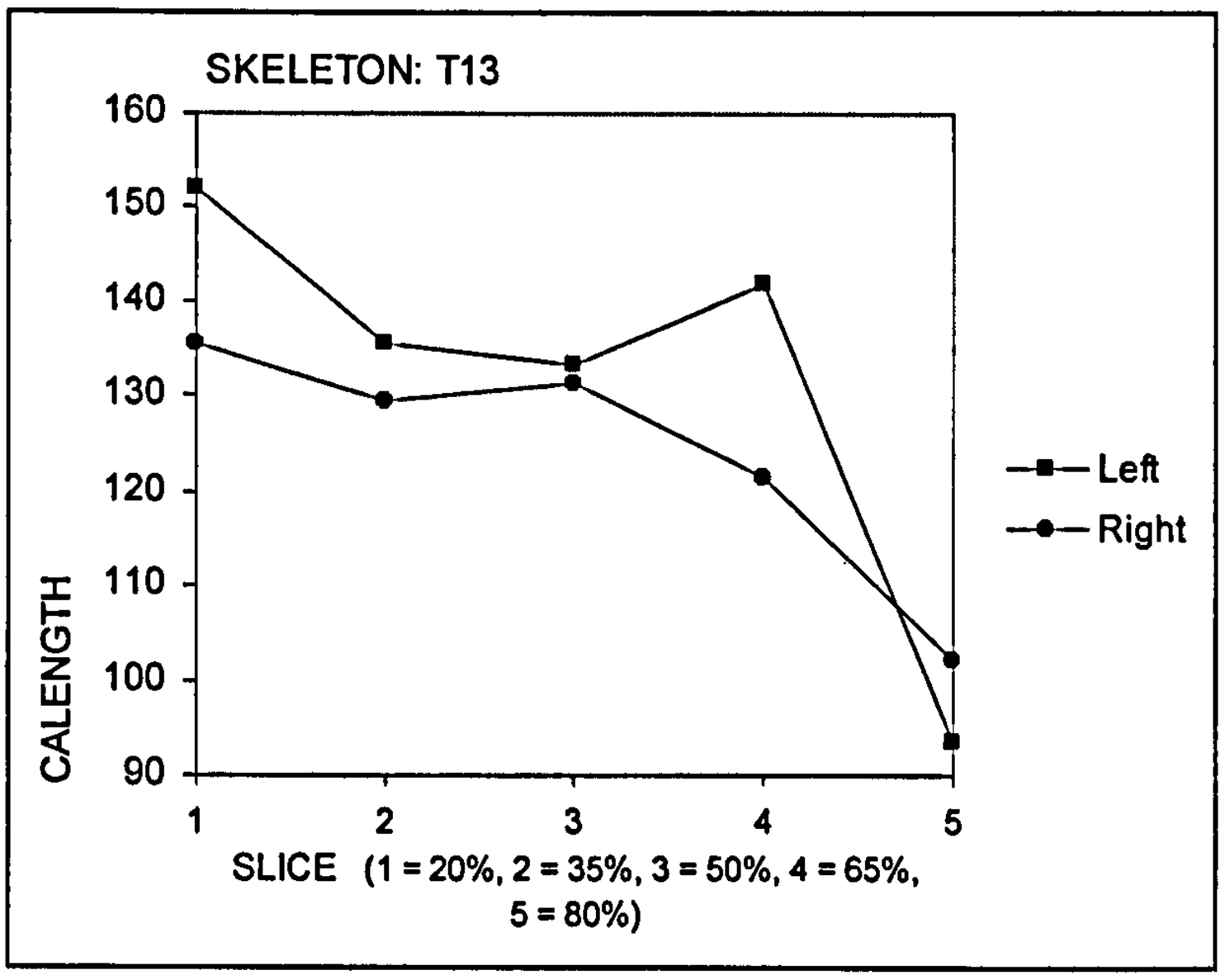

Figure 6.16: Individual patterns of mechanical loading (CA). An example of a contralateral shift in cortical area. T13, from the Towton population, represents the typical pattern of this sample, left-side dominance in the 20%, 35%, 50% and 65% slices followed by a contralateral shift to the greatest cortical area in the right 80% slice.

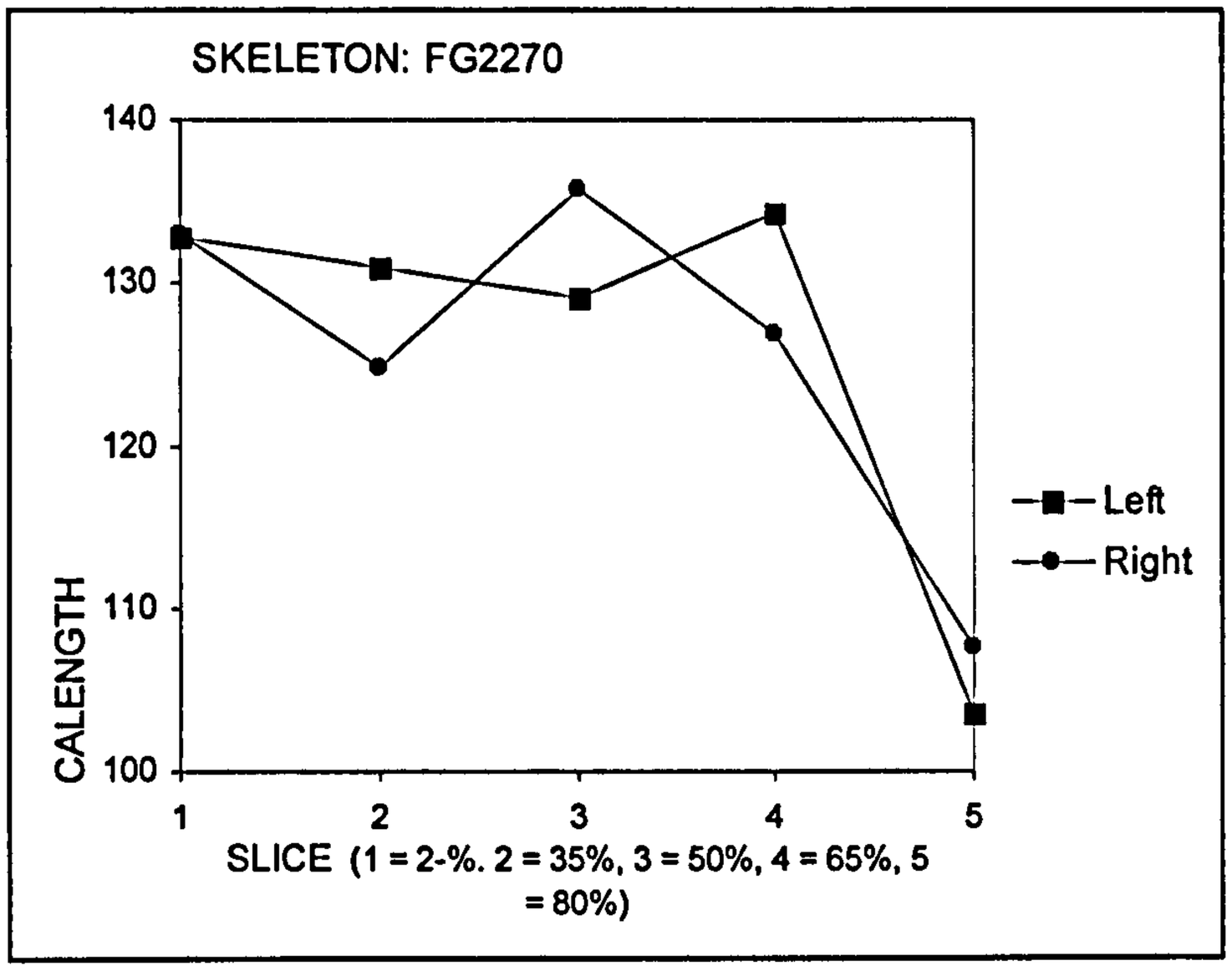

Figure 6.17: Individual patterns of mechanical loading, an example of a multiple cross over pattern in cortical area. FG2270, a blade-injured individual, originates from the nave, part of the Fishergate intramural cemetery. This specimen demonstrates a multiple contralateral shift, with the greatest cortical area shifting from left to right at each slice parameter.

In two individuals from the Fishergate blade-injured sample, the greatest cortical area crosses to right-side dominance in the proximal diaphysis (FG1886 and FG1893), while two individuals display a fluctuating pattern in cortical area at each slice parameter (FG2270 and FG5356). In the Fishergate comparative sample, a multiple crossover pattern occurs in three individuals, FG1436, FG5071 and FG3195, the prior from the chapter house. This individual displays a shift in greatest cortical area at each slice parameter. The Towton sample also displays three individuals with a multiple crossover pattern in cortical area. T6 and T46 begin with left-side dominance in the distal shaft which crosses over to a right-side dominance at the midshaft and shifts back to left-side dominance at 80%. One individual, T23, displays contralateral shifts in cortical area between each slice parameter. This individual, though, is the shortest of the groups, and possesses disproportionately short tibiae and no asymmetry as measured from external measures. Figure 6.17 demonstrates a multiple cross-over pattern.

Diaphyseal robusticity (J) has also been found to display fluctuating asymmetry within individuals. The Fishergate blade-injured sample consists of four individuals with a straight right-sided dominance in diaphyseal robusticity (FG1589, FG1886, FG1893

and FG2392), three individuals with a left distal to right proximal cross-over (FG2270, FG5356 and FG6448) and one individual, FG6411, with a right distal to left proximal cross-over pattern. FG6191 displays a multiple cross-over pattern, from the left distal diaphysis to the right midshaft that crosses over to the left proximal diaphysis, while FG7052 displays the reverse pattern, a cross-over from the right distal to the left midshaft and back to dominance in the right proximal diaphysis. The comparative sample from Fishergate is comprised of five individuals with right-sided dominance in diaphyseal robusticity (FG1425, FG3202, FG5071, FG5138 and FG5336), one individual with left-sided dominance in diaphyseal robusticity (FG6128), and three individuals with multiple cross-over patterns. FG2178 displays a left-distal, right midshaft, left proximal pattern while FG1436 and FG3195 display a more complex multiple cross-over pattern. The Towton sample displays three individuals with left-sided dominance (T6, T11 and T41), two with right-sided dominance (T22 and T44), six with a cross-over pattern from the left distal diaphysis to right proximal diaphysis (T13, T16, T23, T24, T32 and T40) and finally, one individual with a multiple left-sided cross-over pattern (T46).

6.5 Discussion

There are two possible explanations for the differences in the percentage of cortical bone between blade-injured groups. The first relates to age-at-onset of activity. Increases in physical loading of tennis players during childhood showed marked periosteal expansion with inhibited endosteal resorption that resulted in overall thicker cortical bone in the dominant limb. This is most similar to the Fishergate BI sample, which has a greater amount of cortical bone relative to total area in all slice locations. Increased loading at later stages of life resulted in stimulated endosteal expansion / deposition and inhibited periosteal expansion, increasing cortical area internally rather than externally (Ruff *et*

al., 1994). Conversely, the Towton sample displays stimulated periosteal growth but with subsequent endosteal resorption, effectively creating greater humeral diameters with less bone material that resulted in the lowest percentage of cortical bone to total area. This does not fit either age-related pattern, which leads to the second possibility – that of biomechanical efficiency in the Towton sample. It is plausible that architectural changes developed in childhood and adolescence have the potential to create a system of accommodation to mechanical forces to produce greater efficiency though a reduction in cortical bone deposition. Equally, it may be said that the higher humeral torsion values seen in the Fishergate blade-injured group represent a higher level or direction of strain than that seen in the other two populations and that this increased strain has stimulated greater cortical bone growth. This may be through more strenuous use of the upper limb. In either case, this data indicates significant differences between blade-injured groups in habitual behaviour at the elbow and shoulder.

Those individuals displaying fluctuating asymmetry in cortical area do not necessarily display a similar degree of asymmetry in diaphyseal robusticity as defined by J (see Table 6.5). In the Towton sample, of 12 individuals, two display complex CA patterning but single side dominance in J values, while three display fluctuating shifts in diaphyseal robusticity (J) but have a single side dominance in CA. In the Fishergate BI sample, of 10 individuals, three display fluctuating asymmetry in CA but single side dominance in J while two display the reverse – fluctuating asymmetry in J but single side dominance in CA. Of nine in the comparative sample, one individual displays single side dominance in CA and fluctuating asymmetry in J while another individual displays the opposite pattern. Interestingly, of the three individuals with antemortem weapon trauma indicating previous combat experience and, subsequently, inferred long-term weapon use, two display simple side dominance in both CA and J (T22, right-side;

T41, left-side). T16 displays a single contralateral shift in diaphyseal robusticity (dominance in the left distal diaphysis shifting to the right from the 35% slice) and simple right-side dominance in CA. This further indicates the complexity of the relationship between the amount of cortical bone in the humeral shaft in relation to diaphyseal robusticity.

The population with the greatest diaphyseal robusticity as measured by J (torsional rigidity) across the humerus is not that with the greatest amount of cortical bone. Therefore, in the Towton population, it appears that resistance to increased strain magnitude is met by means other than increased cortical bone. This implies a two-stage process to humeral plasticity, one in which humeral shape is modified to accommodate powerful motions initially, presumably during the juvenile period when bone is most responsive, and then increases in cortical thickness as these movements continue. However, if the shape is adapted such that it adequately compensates for increased force, there is no need for greatly increased cortical thickness. It would appear that the greater total area is a more efficient form of resistance to bending strain. Therefore, increased cortical thickness and decreased medullary width, while equated with increased activity levels, do not equate to greater efficiency in distributing torsional forces across the humerus.

The humeral torsion angle, as a measure of architecture, is correlated with all measures of diaphyseal loading and robusticity (Table 6.7). However, the nature of this correlation varies between populations. In the blade-injured samples, the correlation is negative. As the humeral torsion angle increases, as in athletes, to a more posteriorly oriented humeral head, the amount of cortical bone, total area and diaphyseal robusticity

Table 6.7: Correlation between measurements of diaphyseal shape and cross-sectional geometry. While the relationship between humeral torsion and TA, CA, Imax and J is significant for all populations, its nature varies. The blade-injured samples display a significant negative correlation, while the comparative sample is positively correlated. Only the Towton sample displays a significant correlation between Ix/Iy and CA and J values, although the Fishergate BI sample displays a significant positive correlation between Imax and Ix/Iy. All values are standardised by humeral length.

		TA/Length^3	CA/Length^3	Imax	J/length$^{5.33}$	Ix/Iy
Humeral torsion angle Towton	Pearson Correlation	-.249**	-.291**	-.177*	-.202*	.054
	Sig. (2-tailed)	.005	.001	.049	.024	.554
	N	124	124	124	124	124
Humeral torsion angle FG BI	Pearson Correlation	-.318**	-.316**	-.351**	-.391**	-.038
	Sig. (2-tailed)	.001	.001	.000	.000	.704
	N	100	100	100	100	100
Humeral torsion angle FG Comparative	Pearson Correlation	.370**	.425**	.496**	.499**	-.084
	Sig. (2-tailed)	.000	.000	.000	.000	.431
	N	90	90	90	90	90
Ix/Iy Towton	Pearson Correlation	-.113	-.307**	-.460**	-.340**	--
	Sig. (2-tailed)	.210	.001	.000	.000	
	N	124	124	124	124	
Ix/Iy FG BI	Pearson Correlation	.104	-.123	-.346**	-.084	--
	Sig. (2-tailed)	.305	.222	.000	.407	
	N	100	100	100	100	
Ix/Iy FG Comparative	Pearson Correlation	-.084	-.068	-.124	.022	--
	Sig. (2-tailed)	.431	.522	.243	.835	
	N	90	90	90	90	

*Sig. p = 0. 05; **Sig. p = 0.01

(J) decreases. However, in the non-blade injured sample, the opposite is true. As the humeral torsion angle increases to a more posterior orientation, so too does the resistance to strain and the amount of cortical bone. Therefore, an increased humeral torsion angle in the blade-injured sample is not related to hypertrophy of the limb. However, increased humeral torsion angles are related to limb hypertrophy, as identified in the professional athletes and in the comparative sample of non blade-injured individuals. It is possible that the increased humeral torsion angle in the blade-injured samples represents an adaptation to an increased strain environment, in which the shape is altered to more efficiently distribute strains. Equally, the use of weapons may alter the

architecture as a result of a movement pattern different from the professional throwing athlete, which results in decreased humeral torsion.

Diaphyseal shape (Ix/Iy) is negatively correlated ($p < .000$, both samples) with the maximum bending rigidity (Imax) in both blade-injured populations although, in the Towton population, this relationship between diaphyseal shape extends to CA and J. So, as the diaphysis becomes less circular, the bending rigidity increases. Increased M/L bending, or alternatively, decreased A/P bending is then significantly correlated with increased bending rigidity (Imax) in both blade-injured populations only, as well as increased robusticity (J) and cortical bone deposition (CA) in the Towton sample.

Changes in humeral torsion have been demonstrated to relate to specific behaviour patterns and may be seen as a form of adaptation to strenuous activity, although it is one that differs in relation to the population sample. A number of studies have recently been published examining bilateral differences in humeral torsion (Gjerdrum *et al.*, 2003) and, functionally, its effect on range of motion in baseball pitchers. In college and professional-level athletes, significant differences in the humeral torsion angle were identified between limbs, with the dominant limb displaying an increased angle (more posteriorly oriented humeral head) when compared with the non-dominant limb and control groups of non-throwing individuals. This correlated with changes in range of motion, functionally increasing external rotation and decreasing internal rotation at 90 of abduction (Osbahr *et al.*, 2002; Reagan *et al.*, 2002; Crockett *et al.*, 2002).

These changes to the shoulder in throwing athletes do not appear to be the result of laxity in the joint capsule, but are osseous adaptations to repetitive movements.

During the 'cocking' phase of throwing, there is 67 +/- 11 N-m of torque across the gleno-humeral joint, the equivalent of 90% of body mass. These forces acting across a developing proximal humeral physis, where ninety percent of humeral growth is occurring after the age of 11 years, will affect humeral architecture (Osbahr *et al.*, 2002). It may be argued that these osseous adaptations to the humerus are necessary for high-level performance. Those pitchers competing during key growth phases will have the best chance of undergoing these skeletal adaptations and becoming an elite baseball pitcher. The development pre-positions the dominant limb in a protective adaptation that allows for increased performance and decreases the chances for injury (Crockett *et al.*, 2002). Physically, an increase in the torsional angle, a more posteriorly placed humeral head, enables the athlete to extend the cocking phase and thus further accelerate the throw. Following this, it is reasonable to assume that such architectural adaptations may also lead to greater biomechanical efficiency, similar to that hypothesized to have existed in the Towton group. These changes, though, are likely to be operating at a reduced level in the non-professional athlete, as the levels of bilateral asymmetry that indicate the degree of plasticity are not as extreme as those found in the professional athlete.

Significant differences in diaphyseal shape (Ix/Iy) have been identified between both blade-injured populations (50% and 65%) and between sides in the Towton sample (35%, 50% and 65%), indicating fundamental differences in loading and movement patterns. At the mid-distal 35% slice, the differences in movement patterns largely relate to flexion and extension at the elbow. Increased A/P bending is largely directed by *M. brachialis* anteriorly and the medial head of *M. triceps brachii*, which extends the arm and forearm, posteriorly. *M. brachialis* will have the greatest influence on diaphyseal shape as it is the primary flexor of the elbow joint. The M/L bending increases originate,

however, largely from the development of a lateral supracondylar ridge, the insertion point of *M. brachioradialis*. This muscle is responsible for both flexion of the forearm and pronation of a supine forearm and supination of a prone forearm.

At the midshaft 50% slice, M/L breadth will be directed laterally by *M. deltoideus* and medially by *M. coracobrachialis.* The anterior fibres of *M. deltoideus* flex and medially rotate the humerus, while the middle fibres abduct and the posterior fibres extend and laterally rotate the arm. *M. coracobrachialis* primarily acts upon the shoulder joint as a weak flexor and stabilizer. It is also responsible for adduction of the arm and may be seen as an antagonist to *M. deltoideus.* Antero-posterior breadth will be largely influenced by *M. brachialis & M. triceps brachii.* At the mid-proximal 65% slice, the A/P broadening will largely be a result of *M. pectoralis major*, an adductor, medial rotator and flexor of the arm, as well as the anterior & posterior fibres of *M. deltoideus*. The medial head of *M. triceps brachii* has been found to insert into the medial margin of the proximal shaft, where it influences bone morphology, while the lateral head of *M. triceps brachii* will influence A/P breadth.

Functionally, these differences between populations and between limbs relate to increased flexion, pronation and supination at the left 35% level of the humeral shaft, where they create greater M/L bending when compared with the opposing limb. Extension-related movement patterns act to increase A/P bending, as observed in the right humerus of the Towton sample (Fig. 6.18) (Schmitt *et al.*, 2003). At 50%, the differences between blade-injured populations are slight, but significant, as the Towton sample displays an average Ix/Iy of .95 compared with the 1.05 Ix/Iy value in the Fishergate BI sample. Therefore, the increased M/L breadth in the Towton sample relates to movement patterns involving abduction, adduction and rotation as opposed to

simple flexion and extension that acts to increase A/P breadth. The differences between sides, with increased M/L bending in the left humerus compared to the right, are demonstrated in Figure 6.19. At 65%, population differences relate to increased circularity in the Towton sample (Ix/Iy: 1.0), while the Fishergate BI sample displays increased A/P breadth (Ix/Iy: 1.2). This increased breadth relates to movement patterns involving flexion and extension, as well as medial rotation and adduction. The left humerus displays a more circular Ix/Iy ratio when compared with the right humerus, which demonstrates increased A/P breadth (Fig. 6.20).

Figure 6.18: Diaphyseal shape differences at 35% in Towton 40. Left Ix/Iy: .652, right Ix/Iy: 1.234. The last image is a mirror image of right superimposed upon left to demonstrate differences in M/L and A/P breadth (anterior is towards the top of the page and lateral to the right).

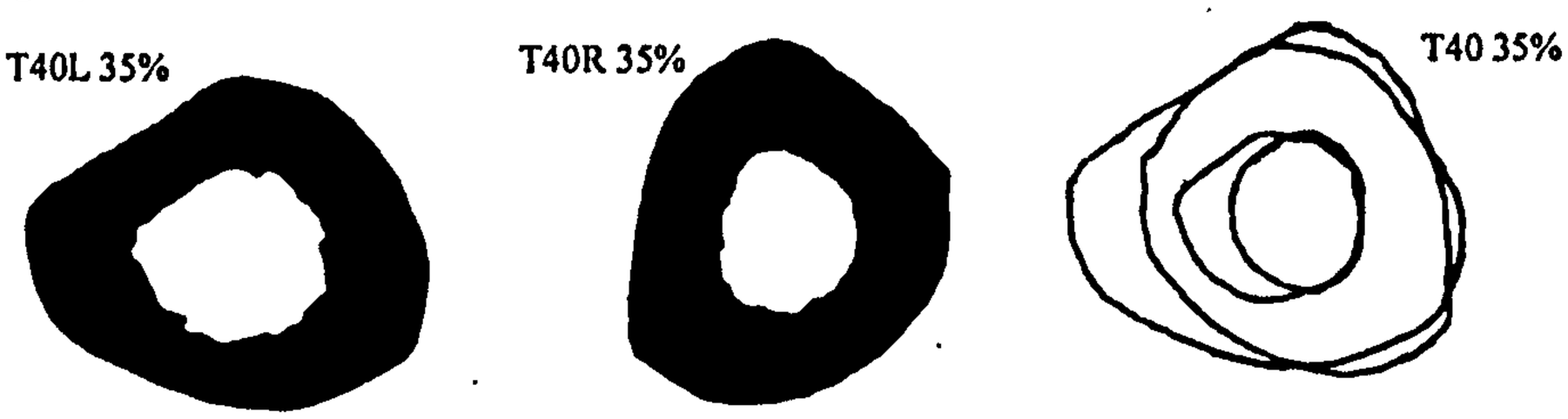

Figure 6.19: Diaphyseal shape differences at 50% in Towton 13. Left Ix/Iy: .638, right Ix/Iy: .980. The last image is a mirror image of right superimposed upon left to demonstrate differences in M/L and A/P breadth (anterior is towards the top of the page and lateral to the right).

Figure 6.20: Diaphyseal shape differences at 65% in Towton 16. Left Ix/Iy: .984, right Ix/Iy: 1.291. The last image is a mirror image of right superimposed upon left to demonstrate differences in M/L and A/P breadth (anterior is towards the top of the page and lateral to the right).

The identification of differences in diaphyseal shape between the two blade-injured populations indicates differences in movement patterns most likely related to their status as combatants. Historically, the aristocracy and landed gentry made up a high proportion of royal armies, despite the formal obligation of knight service lapsing in the 13th and 14th centuries (Dyer, 1989). War was the profession of the aristocracy, who also retained men, livery soldiers, who supported and fought on behalf of their lord, as is suspected to have been the case for some of the men buried at Towton. Whether the youth grew up to be a knight or, as a younger son, was sent to join a monastery, such as the Priory at Fishergate, York, both would have learned to hunt and would have trained in armed and unarmed combat techniques. Relationships were cemented between aristocratic families through the practice of sending sons to train in other households. This arrangement effectively gave the lord his own army with which he could maintain his dominance and provide security for his followers. It also provided the King with a ready platform for the recruitment of armies into war (Waugh, 1991). Tournaments appear in the historical sources from the 12th century AD. Aside from forming a popular form of entertainment that lasted through the 15th century and beyond, this venue provided a valuable training ground to develop skill with the lance and sword, weapons of the upper class (Ayton, 1999). Perhaps more significant is a 14th-century law that required every male from the age of 7 to 17 years to have a longbow and practice with it. Training in the longbow had to start early in order to develop the technique required for proficiency, as this weapon was dependant upon strength and lengthy training. Archery practice was considered so vital that various kings made repeated proclamations on the importance of continual practice, even to the point of outlawing other forms of sport such as football (Waller, 2000a). Therefore, if these blade-injured individuals were trained combatants, they should and do display both intra-population and inter-population differences in cross-sectional properties.

While many of these individuals examined would have trained with weapons from an early age, it is interesting that the Towton group displays such an unusual biomechanical patterning when compared with the Fishergate groups. This most likely relates to the type of weapon employed. From the analyses above, it seems the Fishergate blade-injured individuals trained with unimanual weapons held in the right hand, while the Towton individuals appear to have trained in a weapon requiring both hands, but with increased exerted strain on the left distal limb. This may relate to the change in tactics and weaponry associated with the rise of the longbow, as well as differences in social standing. The advent and dominance of the longbow from the early 14th century changed medieval English combat. It placed this weapon in the hands of the commoner while the aristocracy and landed gentry favoured the sword and shield (Hardy, 1992). Certainly the presence of these men in a mass grave near the battlefield indicates a lower status, as the bodies of the gentry would have been carried away from the battlefield for special interment (Knüsel and Boylston, 2000). The increased robusticity on the left limb in the Towton sample is not likely related to a type of defensive equipment, as heavy shields had gone out of use by the Late Medieval period. The armour of the ordinary soldier may have included a buckler, a small, circular shield made of wood and covered by leather, or a pavise, a large rectangular shield, inserted into the ground for a bowman to shelter behind. However, the majority of the combatants had no defensive equipment, as listed in the Bridgeport Muster Roll, a document listing arms and armour of the English infantryman in the 15th century (Richardson, 2000). The use of a buckler or pavise would not be expected to alter humeral architecture.

There is still debate as to whether alterations in cross-sectional geometry reflect the magnitude of strain or the number of loading cycles, implying that a one-time event

rather than habitual activity may be responsible for changes in cross-sectional geometry. Most recent analyses demonstrate that short periods of activity and activities that involve higher loading rates are most effective for stimulating an osteogenic response (Robling *et al.*, 2002; Burr *et al.*, 2002). This form of intermittent dynamic strain would be consistent with high-level weapon training. Further experimental analysis would clarify the relationship between specific movement patterns identified and the possible weapons responsible for the change. However, English medieval society was one that adhered to conformity, and it is believed that the contextual information is strong enough to support the previous statements regarding weapon use in the blade-injured individuals.

6.6 Conclusions

Is there a unique physical signature to warrior activity? From 1181 AD, in the first Assize of Arms for England, men were required to own certain weapons relative to their social status and to be prepared to use them in the service of the King (Contamine, 1984). Many of these individuals may have participated to some degree in weapon-related training during the key juvenile development period, when bone is most responsive to phenotypic plasticity, yet there does not appear to be a single signature to indicate such training. This may relate to changes in training or technology through time or simply individual preference in weapons. Despite this, it has been shown here that differences in the patterns and levels of mechanical loading, as well as humeral architecture, exist both between and within blade-injured populations, as well as a representative sample of medieval society.

The men of the Towton population appear to have been engaged in a habitual activity that preferentially loaded the left humerus when compared with the right. This

disparity is strongest in the distal humeral shaft. The loading pattern varies such that it creates significant differences between limbs in diaphyseal shape from the mid-distal to the mid-proximal shaft. These changes may relate to a type of weapon requiring both hands, possibly a longbow. Additionally, architecture (humeral torsion angle) and cross-sectional properties interact differently in this sample when considered against the comparative group, as does the significance of the relationship between diaphyseal shape and diaphyseal robusticity when compared against both Fishergate samples.

The Fishergate blade-injured men appear to have been engaged in a habitual movement pattern that creates right-side dominance in cross-sectional geometric properties. This is carried through all slice parameters and may relate to weapon use, most likely a right-handed, unimanual weapon. This blade-injured sample also displays variations in architecture and cross-sectional properties when considered against the comparative sample. The Fishergate comparative sample, as a group without weapon injuries, follows a similar pattern of mechanical loading to the Fishergate BI group, being right-side dominant with little difference in loading patterns between the right and left limbs. Robusticity in this sample is significantly decreased when compared with the Towton sample.

The results indicate that humeral torsion is correlated with strenuous activity as identified through limb hypertrophy, however, this relationship changes depending upon the sample. In the blade-injured populations, it is decreased humeral torsion angles that correlate with limb hypertrophy, however, the comparative sample follow the model identified in professional throwing athletes, with increased humeral torsion angles correlated with limb hypertrophy.

The results of this study, then, suggest that long-term training with weapons from youth contributes not only to alterations in limb use but may be used to complement and extend historical treatments of changes in technology and social standing.

CHAPTER SEVEN

ANALYSIS OF SKELETAL VARIATION: RESULTS

This chapter investigates humeral measurements among all population samples to identify differences between groups in humeral morphology – architecture, articular size and robusticity. Bilateral asymmetry is investigated among the human and non-human primate species to identify variation in activity patterns between limbs. A further goal is to infer limb dominance from bilateral differences in humeral length. The relationship between humeral measurements and the humeral torsion angle is investigated through correlation analysis. Finally, this chapter compares external measurements of robusticity with the results of the cross-sectional analysis from Chapter Six.

The core sample of this analysis is the Towton population. These individuals demonstrate unusual humeral architecture, thought to relate to strenuous activity patterns (Knüsel, 2000a; Knüsel and Boylston, 2000; Rhodes 2002) (Figs. 7.1, 7.2). These alterations in humeral morphology include increased diaphyseal bowing and alterations to the pilaster, increasing supracondylar (M/L) breadth with diaphyseal flattening in the distal shaft. There is also a lateral deviation of the distal shaft giving the appearance of a cubitus valgus deformity. The measurements chosen for analysis both characterise the unusual morphology found in the Towton sample and focus on variables with a known or suspected relationship to activity patterns. The purpose of this analysis is two-fold. First, it seeks to identify patterns similar to those found in the Towton sample in other medieval populations and to identify any difference in humeral morphology related to behaviour patterns. Secondly, it seeks to identify any differences between blade-injured individuals and the remaining populations that might determine whether these men were pre-selected for war, or if they were caught up in its wake.

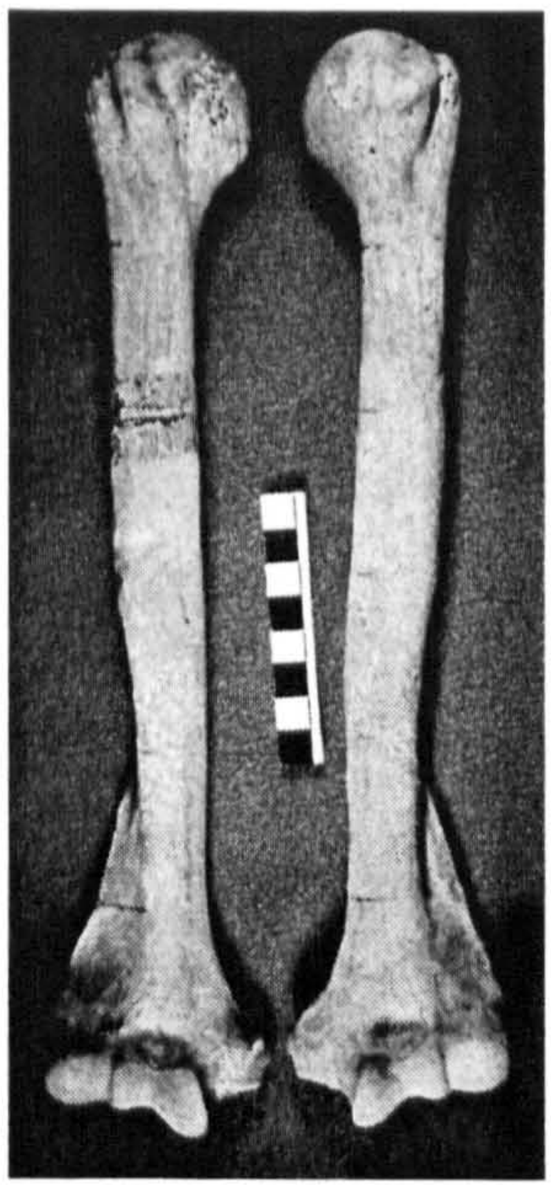

Figure 7.1 (left): T32, paired humeri, anterior view. This picture demonstrates the unusual morphology found in the Towton sample. Note the medio-lateral breadth increase in the supracondylar region. Photograph by author.

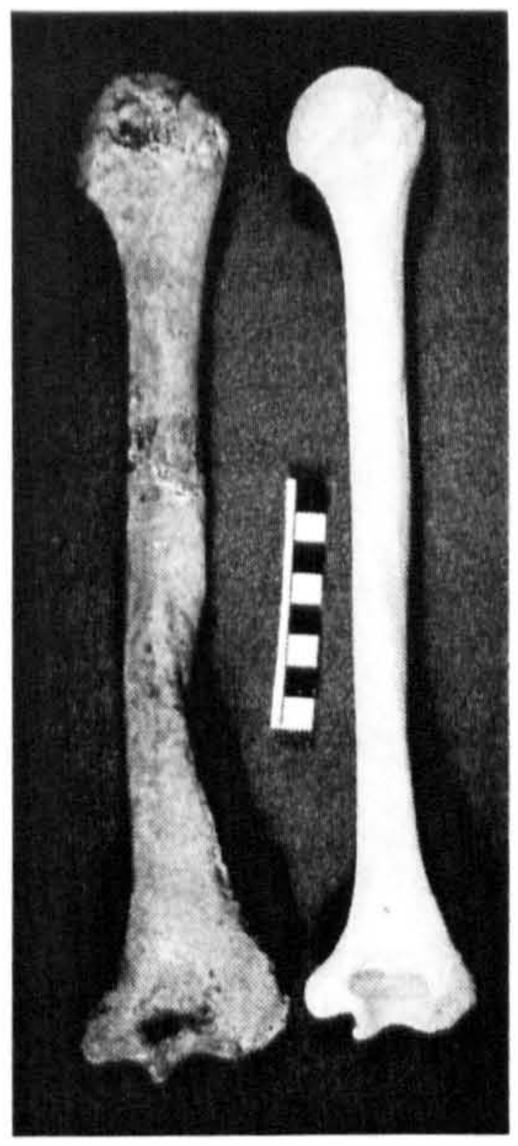

Figure 7.2 (right): T32, right humerus and lab specimen, posterior view. This image demonstrates the unusual morphology found in the Towton sample. Note the increased breadth of the supracondylar region and accentuated deltoid tuberosity compared with the lab specimen. Photograph by author.

The data consists of both raw measurements and skeletal indices determined from these measurements. The data is organised according to the variable type, whether it is a measurement of architecture, articular size or robusticity. Preliminary analyses (Mann-Whitney non-parametric test for independent samples) indicate significant differences between males and females in the majority of the variables. Therefore, male and female groups will be analysed and discussed separately in each section.

The data is analysed using the SPSS statistical software package. Population differences are tested using ANOVA, with Hochberg's GT2 post-hoc test. Differences between sexes are tested using the non-parametric Mann-Whitney's U analysis because variables are not normally distributed. Correlations are calculated using the non-parametric Spearman's Rho rather than Kendall's Tau because the data set is large and does not have a large number of tied ranks (Field, 2000). For ease in data analyses, the sex determination of each skeleton has been assigned either 1, for male, or 2, for female. There are two individuals from Chichester classified as indeterminate for sex assessment, however, these specimens have been removed from the data set as neither one is complete and the statistics on such a small data set are unreliable. There are only

two females, neither one complete, recovered from the Fishergate eastern cemetery. These have also been removed from the analysis following the aforementioned statistical problems. Those skeletons identified as probable male are included with the males while those skeletons listed as probable female are included with the females. This should not affect the data as those skeletons assigned to the 'probable' categories form a distinct minority in the few population samples where they occur (Wharram Percy, Chichester, the intramural cemetery of Fishergate and the southern cemetery of Fishergate). The Mary Rose sample is assumed to be composed of males, although the disarticulated nature of the remains precludes any definite statements of sex determination.

The full data set comprises 20 measurements, four angles, including the humeral torsion angle, and nine indices characterising the humerus. Because this comprises a large data set, the basic statistics – mean, standard deviation, minimum and maximum for each variable - will be included within tables at the end of this chapter. The populations analysed were chosen to represent a broad range of potential activity levels - from the very active to the infirm (See Chapter 3, Materials). An active, combat-related group is represented by the blade-injured individuals from the Towton (T) and Fishergate (FG) samples, as well as the men from the *Mary Rose* (MR), King Henry VIII's flagship which sank in 1545 AD. The urban priory population of St. Andrew, Fishergate, is divided into the discrete burial areas: a blade-injured sample (BI); the eastern, ecclesiastic cemetery sample; the high status intramural burials, including the burials of five blade-injured men; and the southern, lay cemetery, including the burials of two blade-injured men. These blade-injured men are included within their cemetery samples, except in the analyses comparing the blade-injured men with the remaining populations. A rural, farming lifestyle is represented by the Wharram Percy (WP) and

Hickleton (HK) samples, while the Chichester (CH) sample is from a leper hospital and later almshouse. The Terry (TR) collection is included to represent a modern, post-industrial population sample and non-human primates, *Gorilla* sp., *Pan* sp., *Pongo* sp. and *Macaca* sp. are included for comparison of species-specific bilateral asymmetry.

7.1 Measurements of Architecture

7.1.1 Measurements of Architecture – Males

Measurements of architecture reflect differences in humeral shape. These vary in relation to the types of mechanical loads a bone undergoes. Humeral torsion is not included in this analysis; it forms a separate chapter. The measures of architecture investigated include proximal (**HPBW**), distal (**HDBW**) and medio-lateral humeral diaphyseal bowing (**HML**). The humeri from the Towton sample are characterised by increased diaphyseal bowing. This bowing may be a form of accommodation, altering diaphyseal shape to compensate for high strain levels, essentially creating a pre-buckled strut. The maximum cubital angle (**MXCB**) is investigated to draw out any change possibly relating to a valgus deformity. *Cubitus valgus* is identified by an increased carrying angle of the forearm. The degree of anterior curvature (**ANTCV**) of the distal diaphysis will identify any changes in the angle between the diaphysis and the mid-trochlear surface when viewed medially. The diaphyseal flattening index (**DIAPFLAT**) was also investigated to characterise humeral morphology at the 20% slice region. A number of humeri from the Towton population demonstrate an antero-posterior flattening of the diaphysis in the distal 20% slice region. This flattening most commonly occurs in conjunction with medio-lateral expansion that appears to surround the pilaster with additional bone and makes the feature unrecognisable. This index was created to characterise this humeral form (see Measurements, Chapter 5 for more details). A full description of all measurements may be found in Appendix I.

Table 7.1: Population differences in the measurements of architecture (males only).

ANOVA	HPBW	HDBW	HML	MXCB	ANTCV	DIAPFLAT
Sig.	.005**	.000**	.000**	.000**	.000**	.033*

*Sig. p = 0.05; **Sig. p = 0.01

All measures of humeral architecture vary among populations (males only) (Table 7.1). The population with the highest mean level of proximal bowing (**HPBW**) of the humeral shaft is not the Towton sample, but the Mary Rose collection (10.54 mm) (Table 7.2, found at the end of this chapter). This is followed by the Wharram Percy sample (10.28 mm), the blade-injured sample from Fishergate (10.21 mm) and the eastern cemetery at Fishergate (10.19 mm). Proximal bowing is the posterior curvature of the proximal humeral shaft (See Chapter Four, Methods). The sample with the lowest mean level of proximal bowing is the Chichester population (9.76 mm), followed by the southern cemetery at Fishergate (9.85 mm) and the Terry collection (9.94 mm). The greatest individual level of proximal bowing, however, is found in the Towton sample. The right humerus of Towton 46 measures 18.59 mm. This sample also contains the individual, T24, right humerus, with the lowest amount of proximal bowing (4.42 mm). The amount of proximal diaphyseal humeral bowing is significantly different only between the Mary Rose sample and both the Chichester ($p < .002$) and Terry collections ($p < .007$) (Table 7.3).

The population with the greatest mean distal humeral bowing (**HDBW**) is the blade-injured sample from Fishergate (18.85 mm), followed by the Terry collection (18.54 mm), and the Mary Rose sample (16.56 mm). Distal bowing describes the anterior bowing of the distal humeral shaft (see Chapter Four, Methods). The Towton population demonstrates the lowest average amount of distal bowing of the humeral shaft, with a mean of 9.25 mm. The amount of distal bowing is highly variable between populations, differing significantly between combatant-related groups and even within

cemetery areas in the Fishergate sample. Table 7.3 lists all significant differences between individual population samples.

Table 7.3: ANOVA: Post-Hoc, Hochberg's GT2. All significant relationships among external measurements of architecture (males only). Each column contains the measurement variable or variables that demonstrate a significant difference between the relevant population groups. For example, in column 1, distal bowing of the humeral shaft and anterior curvature of the distal humeral shaft differ significantly between the Towton and Mary Rose samples.

ANOVA Post-Hoc	Towton	Mary Rose	WP	HK	CH	Terry	FG BI	FG East	FG Intra
Towton	-								
Mary Rose	HDBW .000** ANTCV .000**	-							
Wharram Percy	HDBW .000** ANTCV .001**		-						
HK				-					
CH	HDBW .000** ANTCV .007**	HPBW .002** HML .000** ANTCV .045*			-				
Terry	HDBW .000** ANTCV .005**	HPBW .007** HDBW .005** HML .000**	HDBW .000**		HDBW .000**	-			
FG BI	HDBW .000** MXCB .006**	HML .030* MXCB .003**	MXCB .002**		MXCB .003**	MXCB .025*	-		
FG Eastern	HDBW .000**					HDBW .004**	MXCB .000**	-	
FG Intra	HDBW .001**	HDBW .002**			HML .005**	HDBW .000** HML .000** MXCB .008**	HDBW .001** HML .042* MXCB .000**		-
FG South	HDBW .014*					HDBW .000**	HDBW .000**		

*Sig. p = 0.05; **Sig. p = 0.01

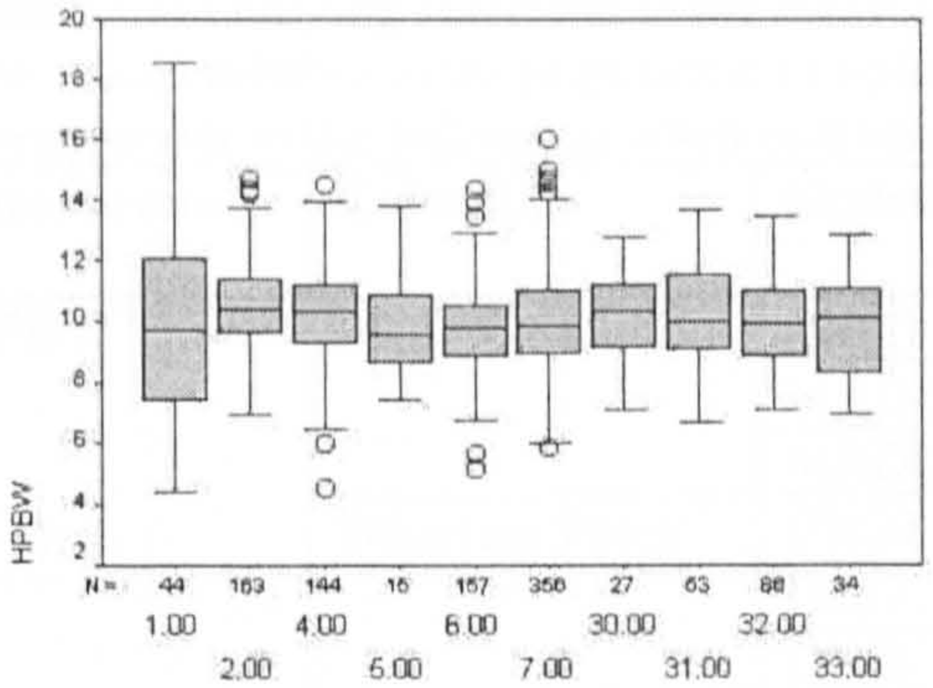

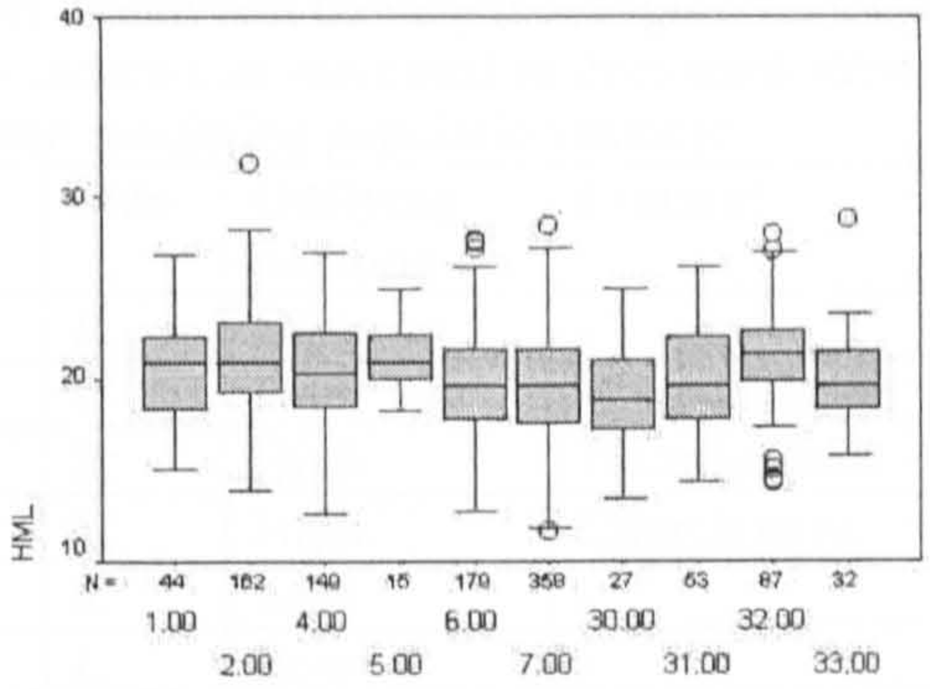

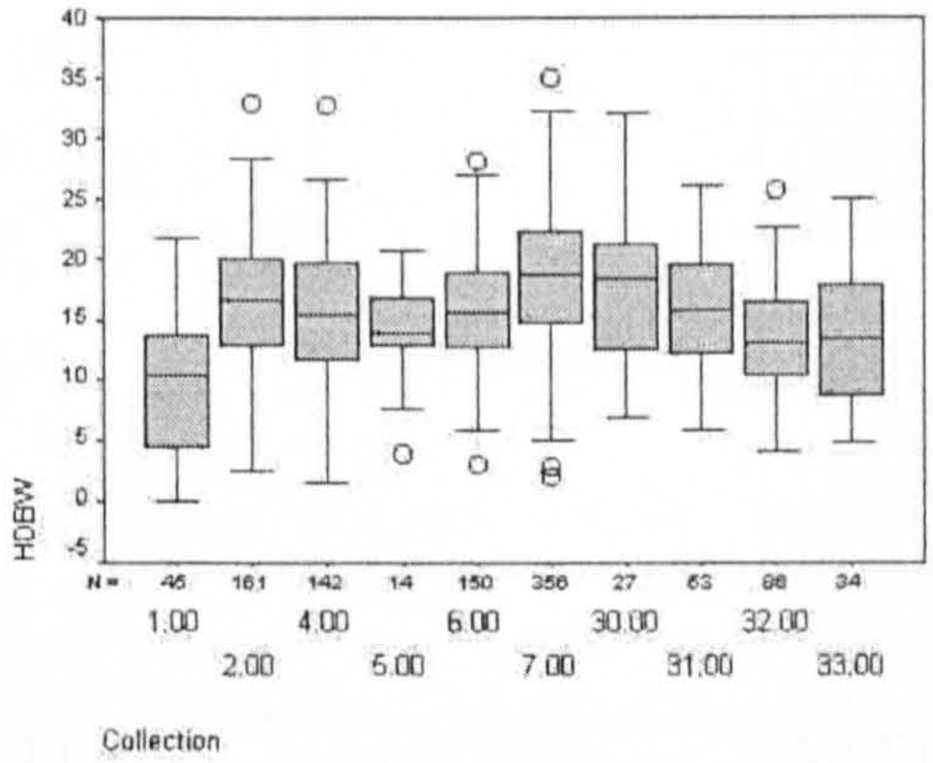

Figure 7.3: Boxplot graphs of the measurements of diaphyseal bowing: proximal (HPBW), medio-lateral (HML) and distal bowing (HDBW) – males only. The circles represent outliers. Note: the centre line represents the population median rather than the mean as reported in the main body. 1 = Towton, 2 = Mary Rose, 4 = Wharram Percy, 5 = Hickleton, 6 = Chichester, 7 = Terry collection, 30 = FG BI, 31 = FG eastern, 32 = FG intramural, 33 = FG southern cemetery. Individual outliers are detailed in Table 7.4.

The Fishergate intramural sample has the greatest mean amount of medio-lateral bowing (**HML**) of the humeral diaphysis (21.28 mm). This is the curvature of the humeral shaft in a medio-lateral plane. The Hickleton and Mary Rose samples follow closely, both with a mean of 21.22 mm. The lowest amount of M/L bowing to the humeral diaphysis is found in the blade-injured individuals from Fishergate (19.11 mm), followed by the Terry collection (19.60 mm) and the Chichester sample (19.81 mm). Significant differences in the amount of medio-lateral bowing exist between populations, both between combatant-related contexts and other populations. Table 7.3 details this further.

The maximum cubital angle (**MXCB**), an angle formed by placing the distal articular surface flat against the edge of an osteometric board and measuring the angle between this and the diaphyseal axis, is greatest in the intramural cemetery at Fishergate

Table 7.4: Outlying skeletons in the measurements diaphyseal bowing (see Figure 7.3). High or low values relative to the population samples may indicate an increased or decreased strain environment in the individual when compared to the remaining population sample.

Measurement	Collection	Skeleton	Side	Outlying position	Context
HPBW	Mary Rose	MR17	R	High	-
		MRDIS60	L	High	Disarticulated
		MRDIS20	R	High	Disarticulated
	Wharram Percy	CN20	L	High	Church nave
		G587	R	Low	-
		G710	L	Low	-
	Chichester	CH141	L	High	Skeletally healthy*
		CH337	R	High	Skeletally healthy*
		CH355	R	High	Skeletally healthy*
		CH57	L	Low	-
		CH341	R	Low	Lepromatous leprosy*
	Terry collection	TR1089	L	High	Labourer
		TR311R	R	High	-
		TR645	R	High	-
		TR216	L	High	Farm hand
		TR111	L	High	-
		TR750	R	High	-
HDBW	Mary Rose	MRDIS68	R, L	High	Disarticulated
	Wharram Percy	G482	L	High	-
	Hickleton	HK42	R	Low	-
	Chichester	CH23	R	High	Possible leprosy*
		CH352	R	Low	Skeletally healthy*
	Terry collection	TR1089	R	High	Labourer
		TR588	L	Low	-
		TR506	L	Low	Cook
	FG intramural	FG311	R	High	Chapter house
HML	Mary Rose	MRDIS48	R	High	Disarticulated
	Chichester	CH25	R, L	High	Possible leprosy
		CH37	R	High	-
	Terry collection	TR343	L	High	labourer
		TR411	L	High	Paper cutter
	FG intramural	FG2196	R	High	Nave
		FG2191	R	High	Nave
		FG2335	R. L	Low	Nave
		FG2270	L	Low	Blade-injured, Nave
	FG Southern	FG6283	L	High	-

*(Fay, 2002)

(103.66°), followed by the eastern cemetery at Fishergate (103.23°). The population with the lowest average cubital angle is the Fishergate blade-injured sample (99.68°), followed by the southern cemetery at Fishergate (101.59°) and the Terry collection (102.11°). The blade-injured sample from Fishergate is unique in its mean maximum cubital angle, differing significantly from all samples, with the exception of Hickleton

and the southern cemetery at Fishergate (see Table 7.3). Other populations that differ significantly in the mean cubital angle are the Terry collection and the Fishergate intramural cemetery sample ($p < .008$).

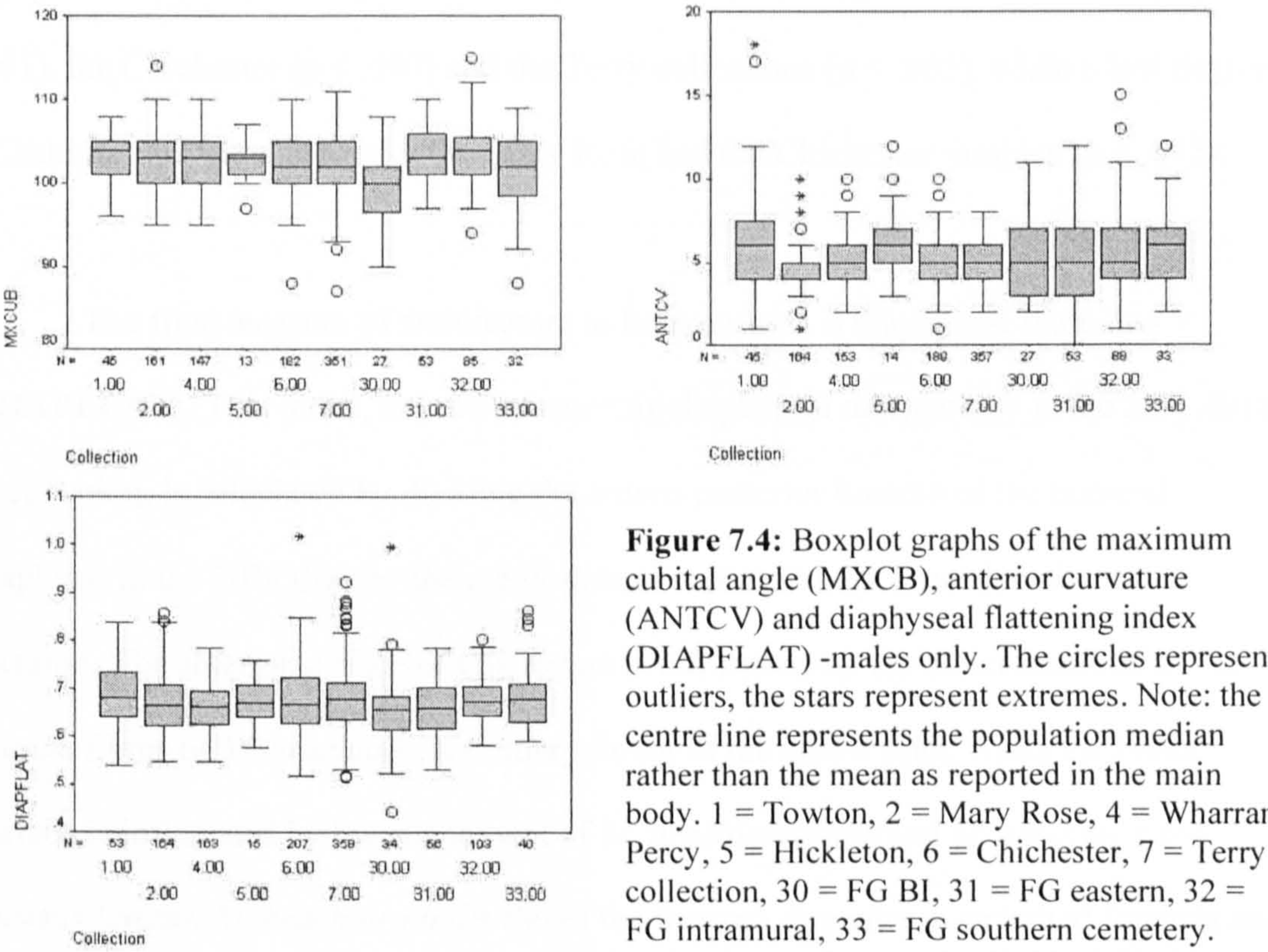

Figure 7.4: Boxplot graphs of the maximum cubital angle (MXCB), anterior curvature (ANTCV) and diaphyseal flattening index (DIAPFLAT) -males only. The circles represent outliers, the stars represent extremes. Note: the centre line represents the population median rather than the mean as reported in the main body. 1 = Towton, 2 = Mary Rose, 4 = Wharram Percy, 5 = Hickleton, 6 = Chichester, 7 = Terry collection, 30 = FG BI, 31 = FG eastern, 32 = FG intramural, 33 = FG southern cemetery. Individual outliers are detailed in Table 7.5.

Anterior curvature (**ANTCV**) is a measurement designed to quantify the degree of anterior bowing present in the distal humerus when viewed from the medial aspect. A valgus deformity creates a laterally deviated distal epiphysis, in effect, elevating the medial epicondyle when viewed from the side. This measurement is similar to the distal bowing measurement, only it describes the angle formed by the anterior bowing relative to the diaphysis, rather than a linear measurement. The humerus is oriented such that the beam of the torsiometer at 0° (origin) bisects the diaphysis from the midpoint of the humeral head and through the length of the shaft. This beam is then moved such that it bisects the distal transverse axis (midtrochlear). The angle is that formed between the two lines. The Hickleton sample displays the largest angle of anterior curvature, 6.42°,

closely followed by the Towton sample at 6.23°. The Mary Rose sample display the smallest angle of anterior curvature, 4.82°, followed by the Wharram Percy sample at 4.98° and the Chichester sample at 5.12°. The high degree of anterior curvature separates the Towton sample from the Mary Rose ($p < .000$), the Wharram Percy ($p < .001$), the Chichester ($p < .007$) and the Terry collections ($p < .005$), while a low degree of anterior curvature separates the Mary Rose and the Chichester samples ($p < .045$).

The final measure of architecture to be examined is diaphyseal flattening (**DIAPFLAT**). This index, created to ascertain diaphyseal morphology at the 20% distal slice region, is calculated by dividing the antero-posterior breadth of the humeral diaphysis at the 20% slice by the medio-lateral supracondylar breadth at the same location. The anterior surface of this region is influenced by the direct insertion of the muscle fibres of *M. brachialis*, a primary flexor of the elbow joint, while the lateral surface is influenced by the attachment of *M. brachioradialis* and *M. extensor carpi radialis longus*. *M. brachioradialis* flexes the forearm, pronates a supinated forearm and supinates a pronated forearm. *M. extensor carpi radialis longus* extends the hand at the wrist, assists in wrist abduction, as well as weakly flexing the forearm at the elbow and weakly supinates the hand

An average to high A/P breadth in combination with a narrow supracondylar breadth creates a high index value, while an average A/P breadth and a broad supracondylar breadth relates to a low index value. The range of variables of mean diaphyseal flattening index is not great. The males from the southern cemetery from Fishergate and the Towton sample display the greatest average diaphyseal flattening index, .6829 and .6827, respectively, while the lowest mean index is .6573 from the Fishergate blade-injured sample followed by the Wharram Percy sample (.6596). There

are no significant differences in the diaphyseal flattening index between any population samples.

Table 7.5: Outlying individuals in the measurements of architecture (see figure 7.4). These individuals have increased or decreased measurements in these values compared with the remaining samples. An increased diaphyseal flattening index indicates increased pilaster thickness.

Measurement	Collection	Skeleton	Side	Outlying position	Context
MXCB	Mary Rose	MR83	R	High	-
	Hickleton	HK52	L	Low	-
	Chichester	CH255	R	Low	Skeletally healthy*
	Terry collection	TR379	R	Low	-
		TR867	L	Low	Tailor
	FG intramural	FG5270	L	High	Chapter house
		FG3111	R, L	Low	Chapter house
	FG southern	FG6289	L	Low	-
ANTCV	Towton	T41	R	High	Antemortem blade trauma**
		T13	R	High	-
	Mary Rose	MRDIS39	L	Low	Disarticulated
		MR69	R	Low	-
		MRDIS66	L	High (extreme)	-
		MR12	R	High (extreme)	-
		MR27	L	High (extreme)	-
		MR8	L	High (extreme)	-
		MR92	L	High (extreme)	-
		MRDIS32	R	High (extreme)	Disarticulated
		MRDIS8	R, L	High (extreme)	Disarticulated
		MR1	R	High	-
		MR12	R	High	-
		MR76	R	High	-
		MR82	R	High	-
		MR86	R, L	High	-
		MRDIS16	L	High	Disarticulated
		MRDIS46	R	High	Disarticulated
	Wharram Percy	CN6	L	High	Church nave
		NA128	R	High	-
		CN32	L	High	Church nave
	Hickleton	HK52	R	High	-
		HK12	R	High	-
	FG intramural	FG3203	R	High	Cloister alley
		FG2178	R	High	Nave
	FG southern	FG1457	R	High	-
DIAPFLAT	Mary Rose	MRDIS11	L	High	Disarticulated
		MR63	R	High	-
	Chichester	CH141	L	High	Skeletally healthy*
	Terry collection	TR867	L	Low	Tailor
		TR1618	L	Low	-
		TR335	R, L	High	-
		TR895	L	High	-
		TR598	R, L	High	-

		TR1598	R	High	-
		TR259	R	High	-
	FG BI	FG2368	L	High	Period 4
		FG2371	R	High	Period 4
		FG6448	L	Low	Period 4
	FG intramural	FG3557	R	High	Cloister alley
		FG3111	R	High	Chapter house
	FG southern	FG6202	R, L	High	-
		FG1490	R	High	-

*(Fay, 2002); **This individual appears to have been a veteran campaigner, with 13 antemortem and perimortem weapon injuries to the cranium and nine perimortem weapon injuries to the postcranial skeleton (Novak, 2000).

Comparison of the combatant-related samples with the remaining populations grouped as a non combatant-related sample is described in Table 7.6. Significant differences between groups are found in the measurements of diaphyseal bowing and anterior curvature. Post-hoc analysis (Hochberg's GT2) identifies differences in proximal bowing (**HPBW**) between the Mary Rose sample and the non blade-injured group ($p < .000$). The amount of distal bowing (**HDBW**) found in the blade-injured group is significantly different from both the Mary Rose sample and the non blade-injured group ($p < .010$, $p < .010$). The Mary Rose sample is significantly different in the amount of medio-lateral bowing from the blade-injured and non blade-injured samples ($p < .010$, $p < .000$). The amount of anterior curvature (**ANTCV**) in all samples is unique; the blade-injured men and the Mary Rose sample both significantly vary from the non blade-injured men ($p < .004$, $p < .032$) as does the blade-injured group and the Mary Rose sample ($p < .000$). All descriptive statistics for the three groups may be found in Table 7.7, at the end of the chapter.

Table 7.6: Differences in the measurements of architecture, all blade-injured samples compared with the non blade-injured individuals. Those with direct weapon injuries are grouped together, while the Mary Rose sample, with an inferred weapons-related context, is grouped separately.

ANOVA	HPBW	HDBW	HML	MXCUB	ANTCV	DIAPFLAT
Sig.	.001**	.000**	.000**	.355	.000**	.502

*Sig. p = 0.05; **Sig. p = 0.01

7.1.2 Measurements of Architecture – Females

Six of the nine populations contain data for females. These are the Hickleton, Wharram Percy and Chichester samples, as well as the eastern, intramural and southern cemeteries at Fishergate. In the majority of these samples, females form a distinct minority and only the Hickleton material has an equal number of males and females (8). There are 95 females to the 151 males analysed from the Wharram Percy sample, 72 females to the 193 males analysed in the Chichester sample, 18 females to the 57 males analysed in the Fishergate intramural cemetery, while there are only eight females and 29 males in the southern cemetery and two females and 35 males in the eastern cemetery. Sample sizes are adequate in most samples; however, the statistics involving the eastern cemetery females are likely to be unreliable given the small sample size. Therefore, they have been eliminated from future analyses. All descriptive statistics regarding the female samples are found in Table 7.8, at the end of this chapter.

Table 7.9: Differences between sexes: Measurements of architecture.

Mann-Whitney U		HPBW	HDBW	HML	MXCB	ANTCV	DIAPFLAT
Wharram Percy	Z	-4.150	-4.554	-7.365	-1.490	-1.004	-2.896
	Sig. (2-tailed)	.000**	.000**	.000**	.136	.315	.004**
Hickleton	Z	-1.970	-3.142	-2.883	-2.440	-2.072	-.692
	Sig. (2-tailed)	.302	.114	.039*	.672	.018*	.668
Chichester	Z	-4.088	-2.471	-7.271	-2.595	-.060	-2.911
	Sig. (2-tailed)	.000**	.013**	.000**	.009**	.952	.004**
FG intramural	Z	-1.227	-1.129	-4.563	-1.528	-2.356	-2.124
	Sig. (2-tailed)	.220	.259	.000**	.126	.018*	.034*
FG southern	Z	-2.289	-2.402	-1.879	-.717	-1.849	-.750
	Sig. (2-tailed)	.022*	.016*	.060	.474	.064	.453

*Sig. p = 0.05; ** Sig. p = 0.01

Diaphyseal bowing measurements are most consistently different between males and females (Table 7.9). In all cases, the males display greater proximal, distal and M/L bowing when compared with their female counterparts. The maximum cubital angles, as well as the degree of anterior curvature, are greater in the Hickleton females in comparison with the males, although the Chichester females have a lower maximum cubital angle compared with their male counterparts. The males of the intramural

cemetery at Fishergate, though, have a higher degree of anterior curvature than their female counterparts. The males of all samples display a lower diaphyseal flattening index, indicating a flattened, M/L broad supracondylar region at 20%, significant when compared with the females in the Wharram Percy and Chichester samples. The exception to this is found within the females of the Fishergate eastern cemetery, who demonstrate increased medio-lateral breadth and decreased A/P thickness when compared with the males.

Table 7.10: Population differences in the measurements of architecture (females only).

ANOVA	HPBW	HDBW	HML	MXCB	ANTCV	DIAPFLAT
Sig.	.021*	.000**	.021*	.000**	.043*	.271

*Sig. p = 0.05; ** Sig. p = 0.01

Population differences between the female samples are similar to those found in the males. All measures of architecture differ significantly between populations, with the exception of the diaphyseal flattening index (Table 7.10). The sample with the greatest amount of proximal bowing is the intramural cemetery at Fishergate (9.47 mm), while the sample with the least (mean) amount of proximal bowing is the southern cemetery at the same site (8.5 mm). Despite the significant result in the ANOVA test, post-hoc analyses fail to identify any two female samples that differ significantly in this variable. Distal bowing is greatest in the Chichester sample, with a mean of 13.56 mm and least in the Hickleton and Fishergate southern cemetery samples (7.99 mm 9.10, respectively). Post-hoc analysis reveals these differences as significant, as the low degree of distal bowing demonstrated by the Hickleton females differs from that of the Wharram Percy females ($p < .006$), the Chichester sample ($p < .000$) and the Fishergate intramural sample ($p < .014$). The high degree of distal bowing in the Chichester females differs significantly from only those of the Fishergate southern cemetery ($p < .022$). The Hickleton females, however, display the highest degree of medio-lateral bowing (18.73 mm), while the least (mean) is found in the Chichester sample, 16.74

mm. Despite the significant result in the ANOVA, there are no individual samples that reach the level of statistical significance ($p = .05$) in this variable.

The Hickleton female sample displays a significantly higher maximum cubital angle (105.13°) than the Wharram Percy (102.12°, $p < .000$), Chichester (101.53°, $p < .000$), and intramural Fishergate samples (102.41°, $p < .010$). The degree of anterior curvature of the humeral shaft does not vary significantly between any two populations, despite a low mean value of 4.08° in the Fishergate southern cemetery sample and a high mean value of 5.12° in the Wharram Percy sample. The variation is limited in the diaphyseal flattening index, with a low of .682, found in the Wharram Percy sample and a high of .703 found in the Chichester female sample. Outlying values are not discussed for the female samples as they are few in number and females form a minority in this analysis.

7.2 Articular Robusticity

Although analysis of growth trajectories indicate that articular size may be more closely related to the general linear body growth and, as such, less affected by mechanical stimuli, significant differences in the bilateral asymmetry of radial head breadth have been identified in a sample of professional tennis players (Ruff *et al,*. 1994). Additionally, Frost (1999) found a correlation between muscle strength and joint size, as individuals with stronger muscles have larger joints when compared to subjects with less developed muscular strength. However, in a 2001 study, Lieberman and colleagues tested for increased articular surface area as a response to mechanical loading in sheep and found no increases in articular surface area (standardised by body mass) in response to mechanical loading in any age group – juvenile, sub-adult or adult. The sheep were exercised for 90 days by running on a horizontal inclination for 60 minutes at a speed of approximately 4 km/hr. While this resulted in approximately 6,000 loading cycles per

day per limb, it is not comparable to the levels found in the professional athlete. Perhaps articular surface area is responsive to increased mechanical loading, but only under hyper-loading conditions such as those found in the youthful, pre-physiologically mature professional athlete.

This analysis investigates a number of articular dimensions to identify if there is any change that might be ascribed to strenuous activity within the sample populations. Ontogenetic studies indicate the growth of the articulations levels off around the age of 17 years, although cortical area continues to increase until the age of 22 years. Therefore, any increase in joint dimension will reflect activity patterns from juvenile stages (Ruff *et al.*, 1994) The size of the articular surface may indicate muscle strength and loading during this period (Frost, 1999). As the size of the articular surface is correlated with the overall humeral size, the direct measurement of the articular surfaces, trochlear breadth (**HTBST**) and distal articular breadth (**DAB**) will be standardised by the articular length of the humerus. Additional indices employed consist of the humeral head index (**HEAD**), the articular / epicondylar index (**ARTEPI**) and, finally, the capitular index (**CAPIT**).

7.2.1 Articular Robusticity - Males

There are significant differences between populations in all articular measurements (Table 7.11). The population with the greatest mean trochlear breadth (standardised) (**HTBST**) is the Mary Rose sample (9.00), followed by the Wharram Percy (8.97) and the Terry collections (8.91). The lowest mean trochlear breadth (standardised) is found in the Fishergate southern cemetery (8.51), followed by the eastern (8.56) and intramural (8.64) cemeteries at Fishergate. The increased trochlear breadth in the Mary Rose sample distinguish it from the Chichester sample ($p < 000$), and the Fishergate

eastern ($p < .000$), intramural ($p < .000$) and southern cemeteries ($p < .001$) (Table 7.12). Equally, the increased trochlear breadth in the Terry collection distinguish it from the three cemetery areas at Fishergate; eastern ($p < .002$), intramural ($p < .004$) and the southern ($p < .007$), as well as the Chichester sample ($p < .002$). The relatively reduced trochlear breadth found in the Chichester sample is further distinguished from the Wharram Percy sample ($p < .001$).

Table 7.11: Population differences in the measurements of articular robusticity (males only).

ANOVA	HTBST	DAB	HEAD	ARTEPI	CAPIT
Sig.	.000**	.001**	.001**	.000**	.000**

*Sig. p = 0.05; **Sig. p = 0.01

The distal articular breadth index (**DAB**) is standardised using the articular length of the humerus. The average value found in a sample of recent Europeans (Serbians) is 14.2 +/- 0.8 (Vandermeersch and Trinkaus, 1995). All population values fall within this range with the exception of the Hickleton sample, which is marginally outside this range at 15.01. The Mary Rose sample displays the next highest index value, 14.74, while the lowest mean value, 14.35, is found in the Fishergate blade-injured sample, followed by the eastern cemetery sample at 14.38 and the Chichester sample at 14.39. The only significant difference between any samples is found between the Mary Rose and the Chichester samples ($p < .002$).

The humeral head index (**HEAD**) is created by dividing the transverse humeral head diameter by the maximum humeral length, effectively giving a standardised value for the proximal articular surface. The mean humeral head index values largely fall within expected limits of those of Euroamericans (13.0 +/- 0.5) (Vandermeersch and Trinkaus, 1995). The exception to this is the Hickleton population, with a high mean index value of 14.14. The Fishergate eastern and intramural cemetery samples have the

Table 7.12: ANOVA: Post-hoc analysis Hochberg's GT2. All significant relationships among external measurements of articular robusticity (males only). Each column contains the measurement variable or variables that demonstrated a significant difference between the relevant population groups.

ANOVA Post-hoc	Towton	Mary Rose	WP	HK	CH	Terry	FG BI	FG East	FG Intra
Towton	-								
Mary Rose	CAPIT .000**	-							
WP	ARTEPI .000**	ARTEPI .000** CAPIT .000**	-						
HK	CAPIT .041*	HEAD .002**		-					
CH	ARTEPI .000** CAPIT .003**	HTBST .000** DAB .002** ARTEPI .000**	HTBST .000**	HEAD .008**	-				
Terry		CAPIT .000**	ARTEPI .000** CAPIT .000**	HEAD .048* CAPIT .001**	HTBST .002** ARTEPI .000** CAPIT .000**	-			
FG BI				HEAD .002**			-		
FG Eastern	ARTEPI .000**	HTBST .000** ARTEPI .000** CAPIT .026*	HTBST .001**			HTBST .002** ARTEPI .001**		-	
FG Intra	ARTEPI .000**	HTBST .000** ARTEPI .000**	HTBST .000**			HTBST .004** ARTEPI .000** CAPIT .000**			-
FG South	ARTEPI .001**	HTBST .001** ARTEPI .006**	HTBST .002**			HTBST .007** ARTEPI .017*			

*Sig. p = 0.05; **Sig. p = 0.01

next highest mean humeral head size, both at 13.63. The sample with the lowest mean humeral head index is the blade-injured sample from Fishergate, at 13.24. This is followed by the Mary Rose sample at 13.41. Differences are significant between the

Hickleton sample and the Mary Rose ($p < .002$), the Chichester ($p < .008$), the Terry collection ($p < .048$) and the Fishergate BI samples ($p < .002$).

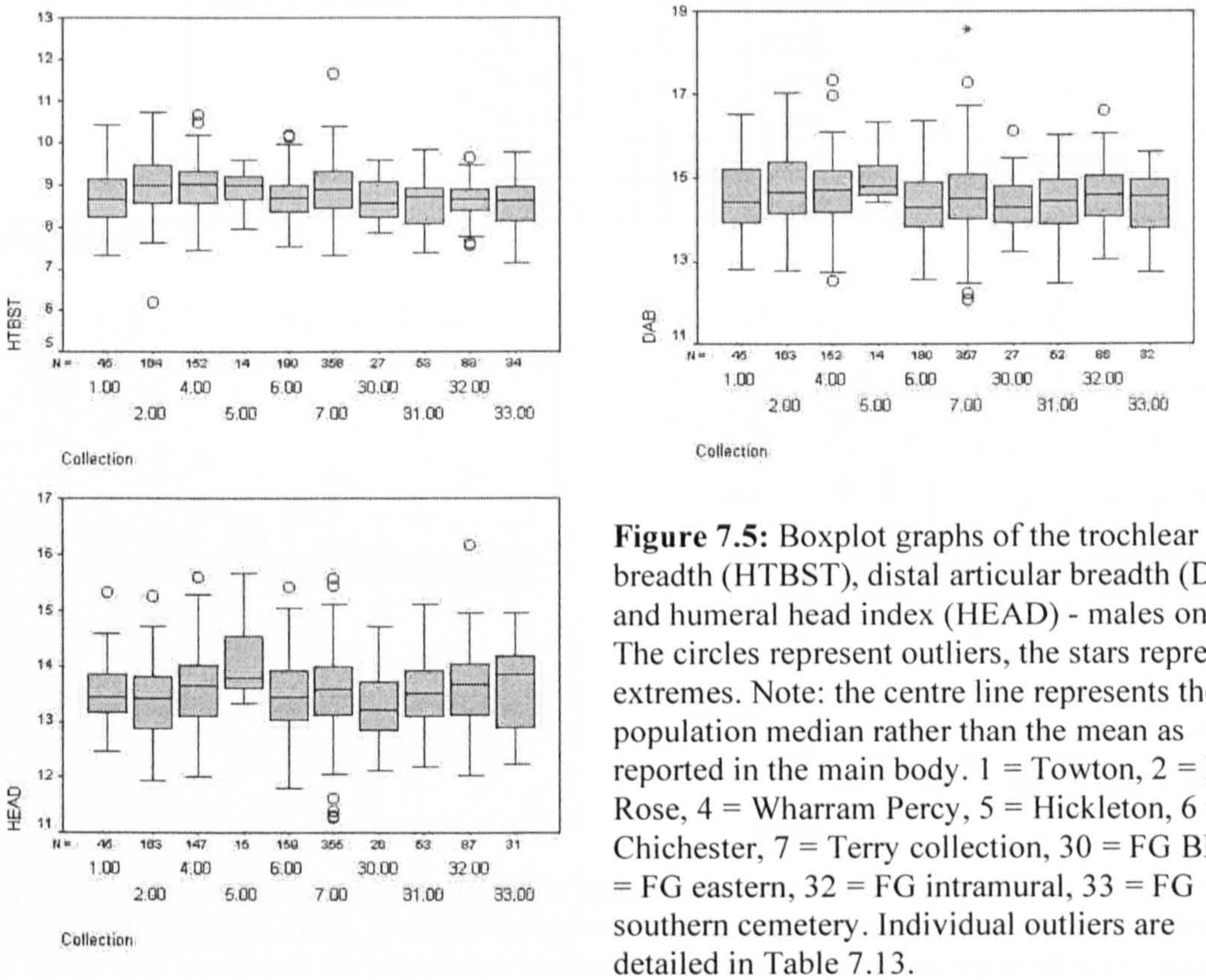

Figure 7.5: Boxplot graphs of the trochlear breadth (HTBST), distal articular breadth (DAB) and humeral head index (HEAD) - males only. The circles represent outliers, the stars represent extremes. Note: the centre line represents the population median rather than the mean as reported in the main body. 1 = Towton, 2 = Mary Rose, 4 = Wharram Percy, 5 = Hickleton, 6 = Chichester, 7 = Terry collection, 30 = FG BI, 31 = FG eastern, 32 = FG intramural, 33 = FG southern cemetery. Individual outliers are detailed in Table 7.13.

Table 7.13: Individual outliers in the measurements of articulations (see Fig. 7.5). Those individuals with outlying articular dimensions possibly indicate heightened or increased activity levels during juvenile development. Changes in articular dimensions related to activity appear to be regionalised, rather than a systemic response, as those individuals with increased or decreased proximal dimensions differ from the outliers in distal joint size in the majority of the samples.

Measurement	Collection	Skeleton	Side	Outlying position	Context
HTBST	Mary Rose	MRDIS65	L	Low	-
	Wharram Percy	CN28	R	High	Church nave
	Chichester	CH109	R	High	Skeletally healthy*
		CH199	L	High	Skeletally healthy*
	Terry collection	TR1126	R	High	Barber
	FG intramural	FG2261	L	Low	Nave
		FG2198	R	Low	Nave
		FG6082	R	High	Nave
		FG2172	L	High	Nave
DAB	Wharram Percy	CN28	R	High	Church nave
		WCO91	R	High	-
		NA102	L	Low	-
	Terry collection	TR1126	R	High	Barber
		TR1043	R	High	Labourer
		TR342	R, L	Low	Restaurateur
	FG BI	FG1931	L	High	Period 4

	FG intramural	FG6082	R	High	Nave
HEAD	Towton	T16	R	High	Antemortem blade trauma
	Mary Rose	MRDIS5	R	High	Disarticulated
	Wharram Percy	WCO162	R	High	-
	Terry collection	TR634	R	High	-
		TR598	R	High	-
		TR1618	L	Low	-
		TR1569	L	Low	-
		TR342	R, L	Low	Restaurateur
	FG intramural	FG6082	R	High	Nave

*(Fay, 2002)

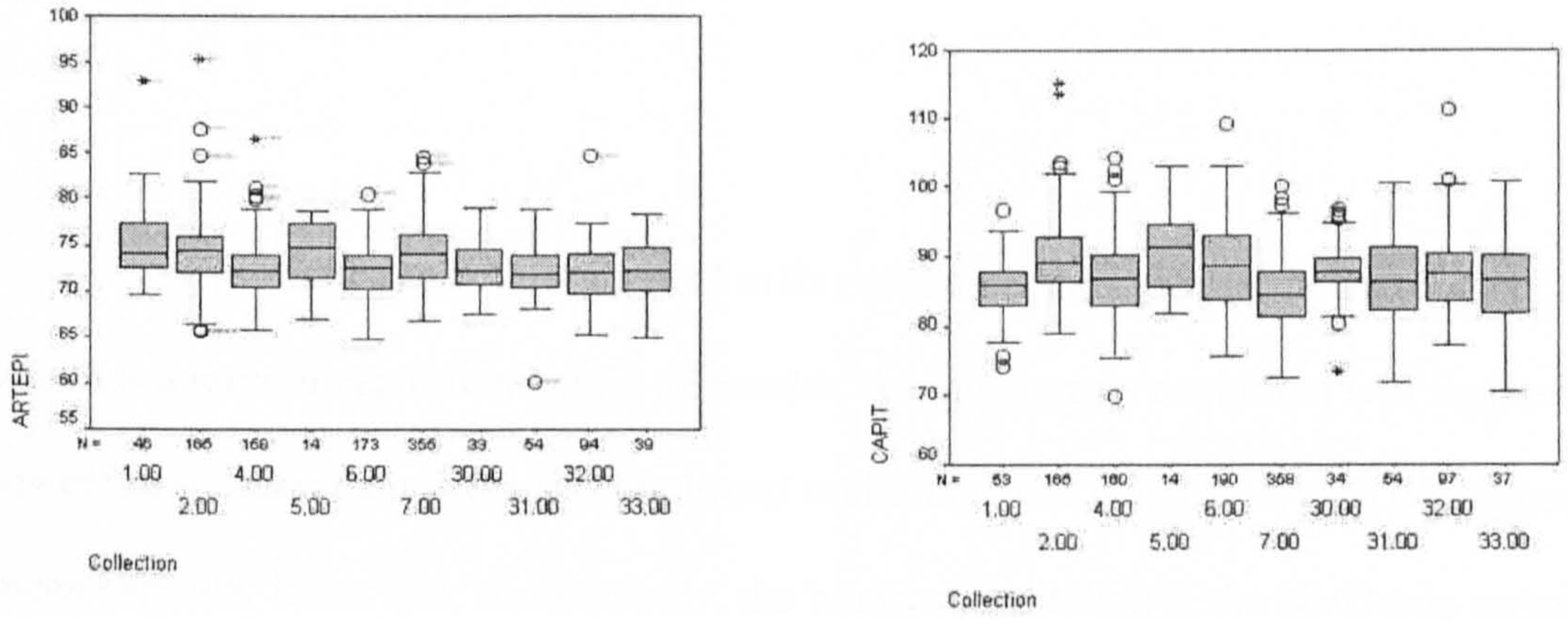

Figure 7.6: Boxplot graphs of the articular / epicondylar index (ARTEPI) and the capitular index (CAPIT) -males only. The circles represent outliers, the stars represent extremes. Note: the centre line represents the population median rather than the mean as reported in the main body. 1 = Towton, 2 = Mary Rose, 4 = Wharram Percy, 5 = Hickleton, 6 = Chichester, 7 = Terry collection, 30 = FG BI, 31 = FG eastern, 32 = FG intramural, 33 = FG southern cemetery. Individuals are discussed in Table 7.14.

The articular / epicondylar index (**ARTEPI**) measures the relationship of the distal articular surface standardised by epicondylar breadth. An increased distal articular breadth (DAB) in relation to the epicondylar breadth results in a high index value while an increased epicondylar breadth in relation to the distal articular breadth results in a low index value. The average value for recent Europeans is 72.0 +/- 2.6 (Vandermeersch and Trinkaus 1995). Again, there is one population that exceeds this average, the Towton sample, with an index of 75.06, indicating an overall increased distal articular surface in relation to the epicondylar breadth. The next highest mean index value is the Hickleton sample at 74.278, followed by the Mary Rose sample at 74.272. The lowest mean articular / epicondylar index value is found in the Fishergate intramural cemetery

(71.85) followed by the eastern cemetery (71.95). The combat-related Towton and Mary Rose samples, with the increased DAB in relation to the epicondylar breadth, are both significantly different from the Wharram Percy, Chichester, FG eastern and intramural cemetery samples ($p < .000$) and the FG southern cemetery sample ($p < .001$ Towton; $p < .006$ Mary Rose). Additionally, the high mean index value demonstrated by the Terry sample is significantly different from the Wharram Percy sample ($p < .000$) and the three Fishergate cemetery samples (eastern $p < .001$; intramural $p < .000$ and southern $p < .017$).

The last index to be investigated in this section is the capitular index (**CAPIT**), which is a ratio of capitulum height to breadth. A high, narrow capitulum will register a lower index value than will a shorter, broad capitulum. The population with the highest mean capitular index and, consequently, the broadest capitulum is the Hickleton sample at 90.90. This is followed by the Mary Rose sample at 89.79. The sample with the lowest capitular index is the Terry collection at 84.60, followed by the Towton sample (85.45). Differences in the capitular index are significant between individual population samples, both combat-related and not. Table 7.12 details the significant relationships further.

Table 7.14: Individual outliers in the indices of articular size. Those individuals with a high articular/epicondylar index (**ARTEPI**) have a large distal articular breadth relative to the epicondylar breadth. A high capitular index value (**CAPIT**) indicates a short, broad capitulum.

Measurement	Collection	Skeleton	Side	Outlying position	Context
ARTEPI	Towton	T16*	L	High	Antemortem blade trauma
	Mary Rose	MR7*	L	High	-
		MR44	R	High	-
		MRDIS39	L	High	Disarticulated
		MRDIS41	R	Low	Disarticulated
		MRDIS50	R	Low	Disarticulated
	Wharram Percy	CN28	R	High	Church nave
		CN6	R	High	Church nave
		CN5	R	High	Church nave
	Chichester	CH143	R	High	Skeletally healthy**
	Terry collection	TR271	R	High	-

		TR763	R	High	Odd job man
	FG eastern	FG5076	R	High	-
	FG intramural	FG6271	R	High	Nave
CAPIT	Towton	T9***	L	High	
		T40	L	Low	-
		T11	R	Low	-
	Mary Rose	MRDIS64	R	High	Disarticulated
		MR75	R, L	High	-
		MRDIS30	L	High	Disarticulated
	Wharram Percy	CN33	L	High	Church nave
		WCO91	R	High	
		SA3	R	High	
	Chichester	CH129	R	High	
		TR846	R, L	High	Bricklayer
		TR878	R	High	
		TR317	R	High	
	FG BI	FG2371	R	Low	Period 4
		FG1886	L	High	Period 4
		FG1874	R	Low	Period 4
		FG6191	L	Low	Period 4
		FG6448	R	Low	Period 4
	FG intramural	FG6271	R	High	Nave
		FG3203		High	Cloister alley

*These individuals both demonstrate an avulsion fracture of the medial epicondyle, reducing the epicondylar breadth.
** (Fay, 2002);
*** This individual has fused elements of the vertebral column, possibly through trauma (Coughlan and Holst, 2000).

Table 7.15: Group differences in the measurements of articulations, all blade-injured samples compared with the non blade-injured individuals. Those with direct weapon injuries are grouped together, while the Mary Rose sample, with an inferred weapons-related context is grouped separately.

ANOVA	HTBST	DAB	HEAD	ARTEPI	CAPIT
Sig.	.000**	.007**	.012*	.000**	.000**

Sig. p = 0.05; **Sig. p = 0.01

Comparison of all blade-injured individuals, the Mary Rose sample, with an implied combatant status, and the non blade-injured groups is described in Table 7.15. The groups are significantly different in all measurements of joint size, possibly indicating differences in the onset of increased activity levels. Post-hoc analysis (Hochberg's GT2) indicates that the differences in trochlear breadth (**HTBST**) are unique to the Mary Rose sample, as the increased mean value is significantly different from both the blade-injured and the non blade-injured groups ($p < .000$; $p < .001$). Distal articular breadth (**DAB**) is highest in the Mary Rose sample and lowest in the non blade-

injured group, significant at $p < .013$. However, the humeral head index (**HEAD**) is lowest in the Mary Rose sample and highest in the non blade-injured sample, significant at $p < .012$. The Mary Rose and non blade-injured samples also differ significantly in the articular / epicondylar index (**ARTEPI**) ($p < .000$). The high capitular index mean (**CAPIT**) is also significantly different in the Mary Rose sample when compared with the blade-injured ($p < .000$) and non blade-injured groups ($p < .000$).

7.2.1 Articular Robusticity – Females

The standardised trochlear breadth (**HTBST**) variable differs significantly between male and female samples in all collections, with the exception of the Fishergate southern cemetery (Table 7.16). In every sample, the males display increased trochlear breadth when compared with the females. These results parallel the distal articular breadth index (**DAB**) as, again, the males display an increased articular breadth in comparison to the females, significant in four of the five population samples (Wharram Percy, $p < .000$; Hickleton, $p < .011$; and both the Chichester and FG intramural samples, $p < .000$). The humeral head index (**HEAD**) is significantly increased in the male samples when compared with the females in the aforementioned populations (Wharram Percy, $p < .000$; Hickleton, $p < .004$; and both the Chichester and FG intramural samples, $p < .000$), as well as the southern Fishergate cemetery ($p < .000$). While there are significant differences in humeral head size between males and females, there are no significant differences in the relationship of the distal articular surface to the epicondylar breadth (articular / epicondylar index, **ARTEPI**). There are differences when considering the capitular index (**CAPIT**), as the males from Chichester demonstrate a lower index value and subsequent more narrow and vertical capitulum (88.86) when compared with that of the females (91.29) ($p < .002$).

Table 7.16: Differences between sexes: Measures of articular robusticity.

Mann-Whitney U		HTBST	HEAD	DAB	CAPIT	ARTEPI
Wharram Percy	Z	-8.909	-7.359	-7.628	-.446	-1.042
	Sig. (2-tailed)	.000**	.000**	.000**	.672	.297
Hickleton	Z	-4.280	-4.474	-4.277	-4.37	-1.920
	Sig. (2-tailed)	.000**	.000**	.011*	.662	.055
Chichester	Z	-6.405	-6.358	-6.950	-3.056	-1.200
	Sig. (2-tailed	.000**	.000**	.000**	.002**	.230
FG intramural	Z	-3.911	-4.982	-3.563	-.341	-1.943
	Sig. (2-tailed)	.000**	.000**	.000**	.733	.052
FG southern	Z	-1.526	-2.247	-1.146	-.721	-.289
	Sig. (2-tailed	.127	.025*	.252	.471	.772

*Sig. p = 0.05; **Sig. p = 0.01

Again, the females of the different populations are more uniform in the measurements of articular robusticity (Table 7.17). There are no significant differences between population in trochlear breadth (standardised), the humeral head index, the distal articular breadth index and the articular / epicondylar index. The vertical capitulum characterising the Chichester sample also differs significantly when compared with the relatively broad capitulum found in the Hickleton sample ($p < .000$). There are no significant inter-population differences between the right and left humerus in any of the measurements of articular robusticity.

Table 7.17: Population differences in measurements of articular robusticity (females only).

ANOVA	HTBST	HEAD	DAB	CAPIT	ARTEPI
Sig.	.148	.078	.241	.000**	.249

*Sig. p = 0.05; **Sig. p = 0.01

7.3 Measurements of Robusticity

Measurements of skeletal robusticity reflect levels of biomechanical stress. There are two primary methods of calculating skeletal robusticity involving internal and external measurements. The internal method of calculating cross-sectional geometric properties has been discussed in the preceding chapter. This section discusses the external measurements of robusticity.

Skeletal robusticity is influenced by long-term selective pressures such as climate and culture, as well as more immediate environmentally determined factors such as the individual's lifestyle (patterns of habitual activity). Individuals from colder regions will have a more robust skeleton than those from hotter regions (Pearson, 2000). However, the influences of climate should be minimal in this analysis as all specimens are of European origin, whether directly (all archaeological specimens) or indirectly (the Euro-American individuals from the Terry collection). Skeletal robusticity is influenced by its immediate strain environment, both in terms of frequency and force of loading. However, it must be considered that body size has an influence on the loading environment, as it takes more effort to move a large skeleton than a small one. Calculation of a body mass index such as that found in Ruff (2000b) might identify larger individuals, however, this requires measurements of bi-iliac breadth, a measurement outside the scope of this analysis.

The (external) robusticity of a skeletal element may be described by its thickness, diaphyseal or epiphyseal, relative to length or another mechanically relevant measurement of body size. Alternatively, robusticity may be determined by the degree of muscular development as inferred from muscle scars (Pearson, 2000). Therefore, a robusticity index can involve either a diaphyseal or epiphyseal variable. In this light, the aforementioned indices of defining articular size may be used as indicators of robusticity, as well as defining articulations. Long bone diaphyses, however, have been found to be more responsive to mechanical loading than the epiphyseal surfaces, as the latter appear to be under more direct genetic control (Pearson, 2000; Ruff *et al.*, 1994; Lieberman *et al.*, 2001). Changes in diaphyseal robusticity are also likely to indicate modifications to humeral form from post-adolescence periods, as cortical growth does not cease until around 22 years of age (*ibid.*).

The measurements analysed include diaphyseal and epiphyseal dimensions, as well as those reflective of muscle attachment sites. These include the greater tuberosity (**HGTST**), deltoid tuberosity (**HGBDST**) and epicondyles (**EPIC**). The diaphyseal measures of robusticity include the maximum humeral length (**HL**) and the midshaft index (**MDSHFT**). Additional indices employed include the humeral robusticity (**HROB**) index and the deltoid index (**DELT**). As measurements of robusticity will vary with humeral size, all variables are standardised by maximum humeral length.

7.3.1 Measurements of Robusticity - Males

All measurements of robusticity are significantly different between each population (Table 7.18). The two blade-injured samples, Fishergate BI and Towton, demonstrate the greatest mean humeral length (**HL**), 341.42 mm and 337.48 mm, respectively. These are followed by the Mary Rose sample, with an average humeral length of 332.48 mm. The Hickleton sample is characterised by the lowest mean humeral length, 318.60 mm, followed by Chichester (323.14 mm) and the intramural cemetery at Fishergate (327.52). The increased humeral length that characterises the Towton sample also isolates it, significantly, from the Wharram Percy ($p < .020$), Hickleton ($p < .007$), Chichester ($P < .000$) and Fishergate intramural samples ($p < .047$) (Table 7.19). The Fishergate BI sample is significantly different from the Wharram Percy ($p < .004$), Hickleton ($p < .001$) Chichester populations ($p < .000$) and Fishergate intramural cemetery sample ($p < .008$). The reduced humeral length characterising the Chichester sample also separates it from the Mary Rose ($p < .000$) and Terry collection samples ($p < .001$).

Table 7.18: Population differences in the measurements of robusticity (males only).

ANOVA	HL	HGTST	HGBDST	MDSHFT	HROB	EPIC	DELT
Sig.	.000**	.000**	.001**	.001**	.000**	.000**	.000**

*Sig. p = 0.05; **Sig. = p = 0.01

Table 7.19: Post-Hoc analysis, Hochberg's GT2. All significant relationships among external measurements of robusticity (males only). Each column contains the measurement variable or variables that demonstrated a significant difference between the relevant population groups.

	Towton	**Mary Rose**	**WP**	**HK**	**CH**	**Terry**	**FG BI**	**FG East**	**FG Intra**
Towton	-								
Mary Rose		-							
WP	HL .020* EPIC .010**		-						
HK	HL .007**			-					
CH	HL .000** HROB .049*	HL .000**			-				
Terry		HGTST .002** DELT .000**	HGTST .013** EPIC .000 DELT .003		HL .001** DELT .001**	-			
FG BI	DELT .000**	DELT .000**	HL .004** DELT .000**	HL .001**	HL .000** DELT .000**	DELT .000**	-		
FG Eastern	HROB .000** DELT .000**	HROB .004** DELT .000**	HROB .022* DELT .000**	DELT .006**	MDSHFT .002** DELT .000**	HROB .019* DELT .000**		-	
FG Intra	HL .047* EPIC .001** HROB .001** DELT .000**	EPIC .016* DELT .000**	DELT .000**		DELT .000**	EPIC .000 DELT .000**	HL .008*		-
FG South	DELT .019*					DELT .000**			DELT .007**

*Sig. p = 0.05; **Sig. p = 0.01

The breadth of the greater tuberosity (**HGTST**) will be influenced by muscle action, as it forms an insertion point for the three of the rotator cuff muscles, *M. supraspinatus*, *M. infraspinatus* and *M. teres minor*. This measurement, then, would be expected to indicate activity patterns at the shoulder. These muscles are responsible for abduction and lateral rotation of the arm, as well as being stabilisers of the shoulder. The

Hickleton sample displays the greatest standardised average breadth in the greater tuberosity, 11.07, followed by the Terry collection at 10.93. The lowest mean greater tuberosity breadth is found in one of the combatant-related samples, the blade-injured sample from Fishergate (10.54), the Chichester (10.64) and the Mary Rose (10.67). The increased breadth found in the Terry collection differs significantly from that of the Mary Rose ($p < .009$) and the Chichester ($p < .001$) samples.

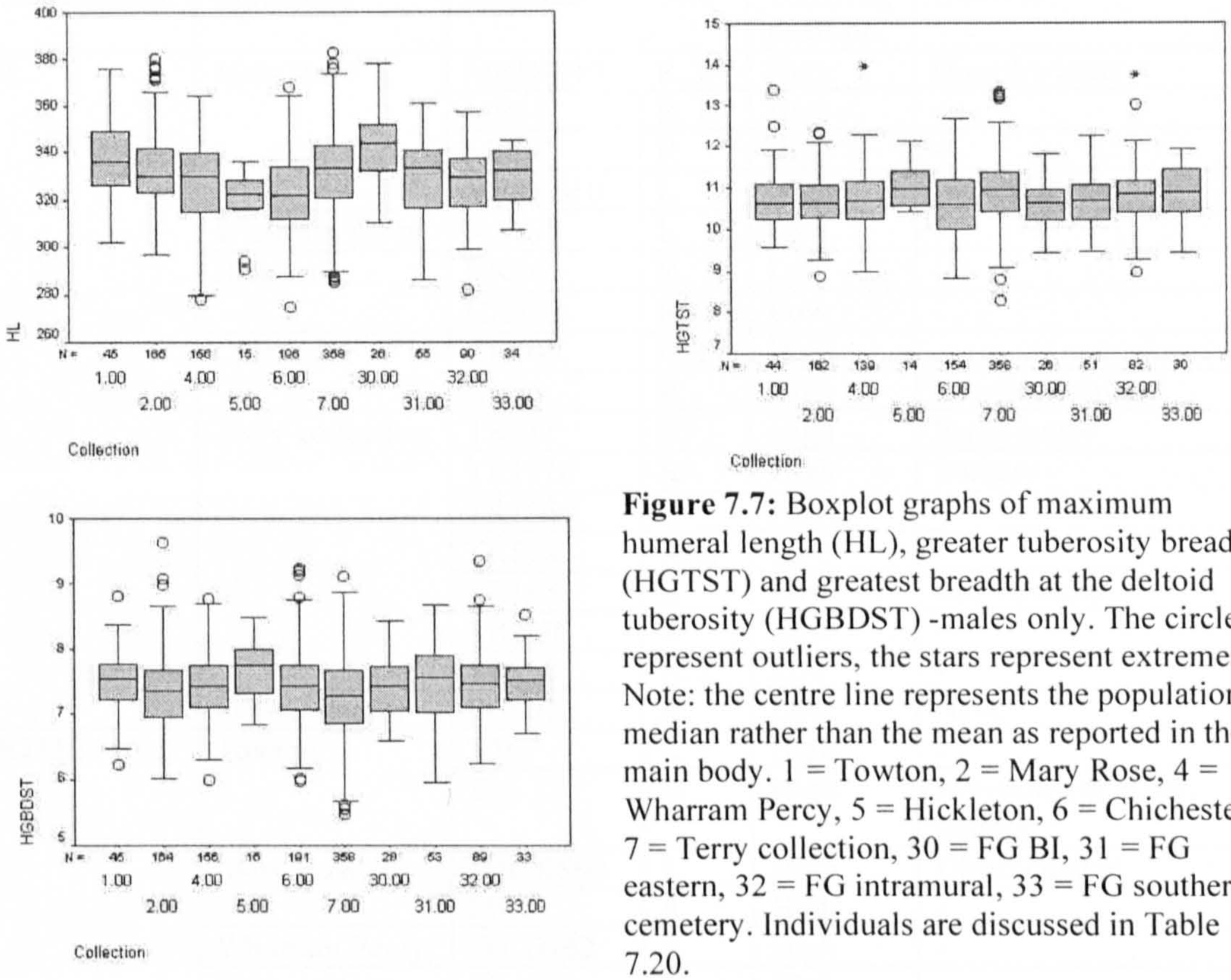

Figure 7.7: Boxplot graphs of maximum humeral length (HL), greater tuberosity breadth (HGTST) and greatest breadth at the deltoid tuberosity (HGBDST) -males only. The circles represent outliers, the stars represent extremes. Note: the centre line represents the population median rather than the mean as reported in the main body. 1 = Towton, 2 = Mary Rose, 4 = Wharram Percy, 5 = Hickleton, 6 = Chichester, 7 = Terry collection, 30 = FG BI, 31 = FG eastern, 32 = FG intramural, 33 = FG southern cemetery. Individuals are discussed in Table 7.20.

The greatest breadth at the deltoid tuberosity (**HGBDST**) is measured wherever it occurs on the tuberosity. This variable quantifies robusticity through measurement of a muscle-related feature, as this tuberosity forms an attachment point for *M. deltoideus*. This muscle has an anterior, middle and posterior portion that flexes and medially rotates the arm, abducts and extends and laterally rotates the arm. The Hickleton males also demonstrate the greatest mean standardised breadth in this variable (7.67), although the Towton sample follow with a value of 7.51. The Terry collection, in this case,

demonstrates the most reduced mean deltoid breadth, 7.26, followed by the Mary Rose at 7.35. The differences between populations do not meet the p = .05 significance level for this variable.

Table 7.20: Individual outliers in the measurements of robusticity (see Fig. 7.7). Humeral length is influenced by environmental factors such as diet and nutrition, as well as activity levels. This variable may indicate social differences within the population samples. Increased or decreased greater tuberosity breadth (HGTST) may identify individuals with different habitual movement patterns at the shoulder, while increased or decreased breadth at the deltoid tuberosity (HGBDST) may identify individuals with different habitual use patterns in the upper limb.

Measurement	Collection	Skeleton	Side	Outlying position	Context
HL	Mary Rose	MRDIS40	R, L	High	Disarticulated
		MR14	R, L	High	-
		MR57	R	High	-
		MRDIS10	L	High	Disarticulated
	Wharram Percy	NA199	L	Low	-
	Hickleton	HK36	R	Low	-
		HK103	R	Low	-
	Chichester	CH109	R, L	High	-
		CH25	R	High	Possible leprosy*
	Terry collection	TR411	L	High	Paper cutter
		TR1126	R	High	Barber
		TR1569	L	High	-
		TR598	R, L	Low	-
		TR195	L	Low	Day labourer
		TR73R	R	Low	-
		TR918	R, L	Low	-
	FG intramural	FG6082	R	Low	Nave
HGTST	Towton	T26	R	High	-
		T16	R	High	Antemortem blade trauma
	Mary Rose	MRDIS66	L	High	Disarticulated
		MR2	R	High	-
	Wharram Percy	WCO162	R	High	-
	Terry collection	TR1204	R	High	-
		TR634	R	High	-
		TR588	L	High	-
		TR342	R, L	Low	Restaurateur
	FG intramural	FG6082	R	High	Nave
		FG2086	R	High	Nave
		FG5331	L	Low	Crossing
HGBDST	Towton	T16	R	High	Antemortem blade trauma
		T8	R	Low	-
	Mary Rose	MR75	R, L	High	-
		MRDIS5	R	High	Disarticulated
	Wharram Percy	CN1	L	High	Church nave
		G710	L	Low	-
	Chichester	CH75	R	High	Diagnosed with DISH*
		CH115	R	High	Lepromatous leprosy*
		CH134	R	High	-

		CH143	R	High	-
		CH89	L	Low	-
		CH341	L	Low	-
	Terry collection	TR73R	R	High	
		TR342	R, L	Low	Restaurateur
		TR335	L	Low	-
	FG intramural	FG6082	R, L	High	Nave
		FG2185	L	High	Nave
	FG southern	FG1547	R	High	-

*(Fay, 2002)

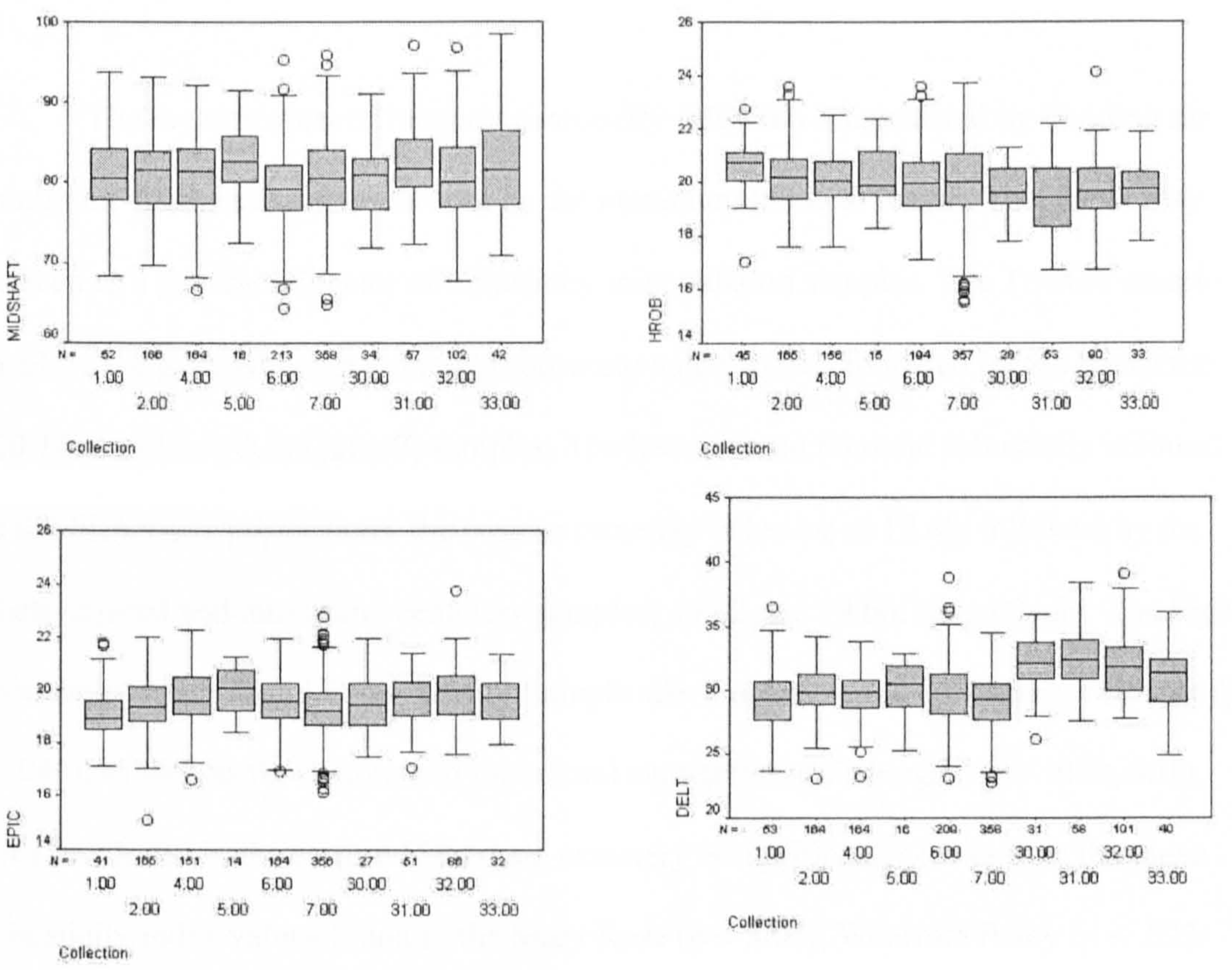

Fig 7.8: Boxplot graphs of the midshaft index (MDSHFT), the humeral robusticity index (HROB), the epicondylar index (EPIC) and the deltoid index (DELT) - males only. The circles represent outliers. Note: the centre line represents the population median rather than the mean as reported in the main body. 1 = Towton, 2 = Mary Rose, 4 = Wharram Percy, 5 = Hickleton, 6 = Chichester, 7 = Terry collection, 30 = FG BI, 31 = FG eastern, 32 = FG intramural, 33 = FG southern cemetery. Individual values are provided in Table 7.21.

The midshaft diaphyseal index (**MDSHFT**) is created by dividing the minimum diameter by the maximum diameter at midshaft. A high index value indicates a eumeric, or broad diaphysis while a lower value index a more platymeric, or flattened diaphysis. The range for recent humans, as reported by Vandermeersch and Trinkaus (1995), is

70.2 – 83.4. All population means fall within this range, with the highest average midshaft index, 82.39, found in the Hickleton sample. This is followed by the eastern cemetery at Fishergate, at 82.36. The sample displaying the greatest difference between minimum and maximum breadths at midshaft is the Chichester sample at 79.24, followed by the blade-injured sample from Fishergate at 79.59. Only the Chichester and Fishergate eastern samples differ significantly in the midshaft index ($p < .002$).

The measurement of humeral robusticity (**HROB**) is calculated by dividing the minimum diaphyseal circumference by the maximum humeral length. This index may be seen as a general indicator of robusticity in population samples. The Towton sample displays the greatest mean humeral robusticity value, 20.63, followed by the Hickleton (20.18) and Mary Rose (20.17) samples. The lowest mean humeral robusticity is found in the Fishergate populations, the eastern cemetery is lowest at 19.40, followed by the blade-injured and intramural cemetery samples, 19.62 and 19.66, respectively. The high robusticity index found in the Towton sample sets it apart from the Chichester sample ($p < .049$), as well as the eastern and intramural cemeteries at Fishergate ($p < .000, 001$). This low index in the eastern Fishergate cemetery is significantly lower than the mean robusticity index values found in the Mary Rose ($p < .004$), Wharram Percy ($p < .022$ and the Terry collections ($p < .019$).

The epicondylar index (**EPIC**) is a standardised measurement of epicondylar breadth. This measurement includes both articular and muscular components, as the lateral and medial epicondyles form an attachment point for the common extensor and common flexor muscles. This variable can be expected to thus reveal information concerning activity patterns involving the elbow, forearm, wrist and hand. However, levels of bilateral asymmetry in a sample of professional tennis players indicate that

epicondylar breadth may reflect differences in articular size rather than muscle origin and, as such, be less susceptible to plasticity (Ruff *et al.*, 1994). The Fishergate intramural cemetery demonstrates the greatest mean epicondylar index value, 19.95, followed by the Hickleton sample (19.94). The most reduced mean epicondylar breadth (in relation to maximum humeral length) is found in the Towton sample (19.06) and the Terry collection (19.28). The differences are significant when examining the Fishergate intramural cemetery and the Towton ($p < .001$), Mary Rose and Terry collections ($p < .000$), as well as the Wharram Percy group compared with the Terry collection ($p < .000$) and Towton sample ($p < .010$).

The final robusticity index to be examined is the deltoid index (**DELT**). This is formed by dividing the breadth as measured across the anterior and lateral-most crests that form the deltoid tuberosity by the deltoid circumference. This index further quantifies robusticity at the deltoid tuberosity region. The highest index values are found in the Fishergate cemeteries, the eastern cemetery sample (32.48), followed by the blade-injured sample (32.04) and the intramural cemetery sample (31.80). The Terry collection demonstrates the lowest mean deltoid index value, 28.99, followed by that of the Towton population (29.17). The three aforementioned Fishergate samples demonstrate significant differences in this index when compared with the Towton, Mary Rose, Wharram Percy, Chichester and Terry collections (all significant at $p < .000$). Additionally, the low value produced by the Terry collection is significant when compared to the Mary Rose ($p < .000$), Wharram Percy sample ($p < .003$), FG southern cemetery ($p < .000$) and the Chichester sample ($p < .001$). The eastern cemetery at Fishergate also demonstrates a significant increase in this variable when compared with the Hickleton and southern Fishergate cemetery samples ($p < .006$, $p < .007$,

respectively), while the FG southern cemetery sample also is significantly different from the Towton sample ($p < .019$).

Table 7.21: Individual outliers in the measurements of humeral robusticity (see Fig. 7.8). A high index value in the midshaft index (MDSHFT) indicates a eumeric, or rounded, diaphysis, while a low value is a more platymeric, indicative of a flattened diaphysis.

Measurement	Collection	Skeleton	Side	Outlying position	Context
MDSHFT	Wharram Percy	SA34	L	Low	-
	Chichester	CH196	L	High	-
		CH354	L	High	Lepromatous leprosy*
		CH43	R	Low	Borderline leprosy*
		CH82	L	Low	-
	Terry collection	TR369	R	Low	-
		TR901R	R	Low	-
		TR871	R	High	-
		TR73R	R	High	-
	FG eastern	FG10269	L	High	-
	FG intramural	FG6082	L	High	Nave
HROB	Towton	T32	L	High	-
		T8	R	Low	-
	Mary Rose	MR75	R, L	High	-
	Chichester	CH83	R	High	Lepromatous leprosy*
		CH373	L	High	-
	Terry collection	TR311 R	R, L	Low	-
		TR187R	L	Low	-
		TR342	R, L	Low	Restaurateur
		TR335	R	Low	-
	FG intramural	FG6082	R	High	Nave
EPIC	Towton	T32	R, L	High	-
	Mary Rose	MR7**	L	Low	-
	Wharram Percy	G604	R	Low	-
	Chichester	CH43	R, L.	Low	Borderline leprosy*
	Terry collection	TR1043	R, L	High	Labourer
		TR73R	R	High	-
		TR764	R	High	-
		TR924	R, L	High	-
		TR763	R, L	Low	Odd job man
		TR342	R, L	Low	Restaurateur
		TR187R	L	Low	-
		TR1569	L	Low	-
	FG eastern	FG5335	R	Low	-
	FG intramural	FG6082	R	High	Nave
DELT	Towton	T30	L	High	-
	Mary Rose	MR26	L	Low	-
	Wharram Percy	CN20	L	Low	Church nave
		NA199	L	Low	-
	Chichester	CH115	R	High	Lepromatous leprosy*
		CH128	L	High	Lepromatous leprosy*
		CH55	L	High	-
		CH185	L	Low	-
	Terry collection	TR721	R	Low	-

		TR216	R	Low	Farm hand
		TR167	L	Low	-
		TR573	L	Low	-
	FG BI	FG2368	L	Low	Period 4
	FG intramural	FG2274	R	High	Nave

*(Fay, 2002); **This humerus has an avulsion fracture of the medial epicondyle.

Examination of the combat-related samples reveals these groups to be most similar in the measurements of robusticity. The difference between groups is significant only in the breadth of the greater tuberosity, humeral length and the humeral robusticity index (Table 7.22). Post-hoc analysis (Hochberg's GT2) show that the non blade-injured sample is significantly different (reduced humeral length) from both the blade-injured ($p < .000$) and Mary Rose groups ($p <. 011$). The differences between sample groups in both the greater tuberosity breadth and the humeral robusticity index did not meet the $p = .05$ significance level.

Table 7.22: Group differences in the measurements of robusticity, all blade-injured samples compared with the non blade-injured individuals. Those with direct weapon injuries are grouped together, while the Mary Rose sample, with an inferred combat-related context is grouped separately.

ANOVA	HL	HGTST	HGBDST	MDSHFT	HROB	EPIC	DELT
Sig.	.000**	.030*	.391	.578	.043*	.104	.329

*Sig. p = 0.05; **Sig. p = 0.01

7.3.2 Measurements of Robusticity – Females

Humeral length (**HL**) varies significantly between male and female samples in all populations, with the males demonstrating greater humeral length in comparison with the females (Table 7.23). The two measurements involving muscle insertions, the breadth of the greater tuberosity (**HGTST**) and the greatest breadth at the deltoid tuberosity (**HGBDST**), are significantly different in four of the five populations, the Fishergate southern cemetery forming the exception. This sample has the smallest number of females, so the limited number of specimens may be a factor. The males demonstrate an increased greater tuberosity breadth in all population samples. The

female samples all demonstrate a reduced maximum breadth at the deltoid tuberosity when compared with the males.

Table 7.23: Differences between sexes, males and females: Measurements of robusticity. WP = Wharram Percy, HK = Hickleton, CH = Chichester, FG intra = Fishergate intramural cemetery, FG south = FG southern cemetery.

Mann-Whitney U		HL	HGTST	HGBDST	MDSHFT	HROB	EPIC	DELT
WP	Z	-10.305	-4.441	-4.461	-1.771	-5.996	-6.531	-1.740
	Sig. (2-tailed)	.000**	.000**	.000**	.077	.000**	.000**	.082
HK	Z	-2.843	-3.142	-3.817	-2.261	-3.546	-3.309	-3.053
	Sig. (2-tailed)	.004**	.002**	.000**	.024*	.000**	.001**	.002**
CH	Z	-7.968	-4.700	-3.314	-1.664	-4.700	-6.263	-2.847
	Sig. (2-tailed)	.000**	.000**	.001**	.096	.000**	.000**	.004**
FG intra	Z	-5.939	-3.761	-3.461	-.150	-5.804	-4.365	-2.431
	Sig. (2-tailed)	.000**	.000**	.001**	.881	.000**	.000**	.015*
FG south	Z	-3.969	-1.766	-.664	-1.407	-1.898	-1.937	-1.385
	Sig. (2-tailed)	.000**	.077	.507	.160	.058	.053	.166

*Sig. p = 0.05; **Sig. p = 0.01

Only one sample, Hickleton, demonstrates significant differences between the sexes when considering the midshaft index (**MDSHFT**). In this case, the males display a considerably broader diaphysis at this location when compared with the females. The results for the humeral robusticity index and the epicondylar index are similar, varying significantly between sexes in all populations with the exception, again, of the Fishergate southern cemetery. The deltoid index (**DELT**), unlike the other robusticity indices employing muscle insertions, differs between sexes in only the Hickleton, Chichester and Fishergate intramural samples.

Table 7.24: Population differences in the measurements of robusticity (females only).

ANOVA	HL	HGTST	HGBDST	MDSHFT	HROB	EPIC	DELT
Sig.	.275	.255	.159	.265	.000**	.133	.000**

*Sig. p = 0.05; **Sig. p = 0.01

The female samples display less inter-population variation in the measurements of robusticity when compared with the males, as the population averages differ

significantly only in two of the seven variables (Table 7.24). The Fishergate southern cemetery sample demonstrates the greatest mean humeral length, 308.41 mm, while the Wharram Percy sample demonstrates the lowest mean humeral length, 300.40 mm. The standardised breadth of the greater tuberosity (**HGTST**) is greatest in the FG southern cemetery (10.43) and least in the Chichester sample (10.04). Considering the standardised breadth of the deltoid tuberosity (**HGBDST**), the southern Fishergate cemetery demonstrates the greatest mean value, 7.32, while the Hickleton sample demonstrates the least (6.90). There are no statistically significant inter-population differences in this variable, or in the midshaft or epicondylar indices. Humeral robusticity (**HROB**) is greatest in the rural Wharram Percy sample (19.18), followed by the Chichester sample (19.15) and lowest in the urban high status, intramural cemetery from Fishergate (17.79). The low levels of humeral robusticity in the Fishergate intramural female sample differ significantly from the high levels found in both the Hickleton and Chichester female samples ($p < .000$). The deltoid index (**DELT**) is highly variable among the female samples, similar to the result for the males, although the results for this robusticity variable contrast sharply with the general robusticity index. The southern (31.69) and intramural (30.32) cemeteries from Fishergate demonstrate the greatest deltoid index values, while the Hickleton sample demonstrates the least (26.91). Inter-population differences are significant when considering the southern Fishergate cemetery and the Wharram Percy ($p < .007$), Hickleton ($p < .000$) and Chichester ($p < .001$) samples. The low deltoid index in the Hickleton sample differs significantly from the Wharram Percy ($p < .007$), Chichester ($p < .032$) and Fishergate intramural cemetery samples ($p < .000$). There are no significant inter-population differences between sides in any of the measurements of robusticity analysed.

7.4 Analysis of Asymmetry

Differences in the measures of architecture, articular robusticity, as well as robusticity have been identified and indicate differences between populations. Analyses of asymmetry can further distinguish activity differences between limbs. A select number of variables have been chosen to examine bilateral asymmetry. All populations are examined, non-human primates included, to identify any trends in asymmetry among samples.

The measurements chosen include diaphyseal and epiphyseal measurements, as well as a select number of muscle-related measurements. These are: maximum humeral length (**HL**) and minimum humeral circumference (**HC**). Bilateral asymmetries in these variables will be used to identify systemic variations in mechanical loading. The breadth of the greater tuberosity (**HGT**), the distal articular breadth (**HDAB**) and epicondylar breadth (**HEP**) are used to reveal joint asymmetries and to identity regionalised differences in mechanical loading. Asymmetry is calculated as $[(R - L) / ((R + L)/2] \times 100$. This calculation results in either a positive (right-sided) or a negative (left-sided) value, however, for SPSS analysis (ANOVA and descriptive statistics) all negative values were converted to absolute values and are thus positive.

7.4.1 Bilateral Asymmetry – Males

Asymmetry is analysed for all archaeological and modern human samples, as well as the non-human primate species, *Gorilla* sp., *Pan* sp., *Pongo* sp. and *Macaca* sp. The human samples are expected to demonstrate higher levels of asymmetry in humeral measurements due to the broader range of motion permitted in human upper limbs as a result of being released from locomotor-related functions. All descriptive statistics

regarding the measures of asymmetry are included in Table 7.25 at the end of the chapter.

Dividing the male samples into two different groups, human and non-human primate samples, reveals significant differences in the levels of bilateral asymmetry between the two groups (Table 7.26). This occurs in all variables with the exception of humeral length (**HL**) and epicondylar breadth (**HEB**). The levels of bilateral asymmetry in the human populations exceed those found in the non-human primate species in every variable with the exception of epicondylar breadth (humans: 2.04, non-human primates: 2.14).

Table 7.26: Population differences in levels of bilateral asymmetry. The samples are divided into two groups, human and non-human primate species (males only).

Mann Whitney U	HL	HGT	HC	HEB	HDAB
Z	-1.819	-2.793	-4.674	-.283	-2.798
Sig. (2-tailed)	.069	.005**	.000**	.778	.006**

*Sig. p = 0.05; **Sig. p = 0.01

Table 7.27: Population differences in bilateral asymmetry (males only, human samples only).

ANOVA	HL	HGT	HC	HEB	HDAB
Sig.	.287	.333	.749	.877	.620

*Sig. p = 0.05; **Sig. p = 0.01

Further analyses of asymmetry exclude non-human primate species, as significant differences in the levels of asymmetry between the two groups have been identified. There are no significant inter-population differences in bilateral asymmetry in any of the measurements analysed (Table 7.27). Maximum humeral length (**HL**) is the least asymmetric of the measurement variables examined. Of the human samples, the highest level of mean asymmetry is found in the Chichester sample (1.418), followed closely by the blade-injured sample from Fishergate (1.417). The most symmetric population sample is that of the *Mary Rose* (.931). This could relate to bimanual tasks, or it may be a result of its reconstruction from a largely disarticulated assemblage into

individuals. The Towton sample also displays a low mean bilateral asymmetry value, .952.

The (non-standardised) breadth of the greater tuberosity (**HGT**) is the most bilaterally asymmetric of all the variables analysed. The size of the greater tuberosity is expected to be influenced by the rotator cuff muscle attachments along its proximal and posterior surfaces, and thus relate to activity differences at the shoulder. The Fishergate intramural assemblage demonstrates the most asymmetry in greater tuberosity breadth, with a mean asymmetry score of 5.49. This is followed by the Wharram Percy (4.85) and Towton (4.38) samples. The lowest mean asymmetry is found in the Hickleton (2.68) and the Mary Rose samples (3.31).

Bilateral differences in the minimum humeral circumference (**HC**) identifies the side having a thicker diaphysis, be that through increased cortical thickness or increased total area. The Fishergate eastern cemetery displays the highest level of asymmetry in this variable (3.45), followed by the Terry collection (2.99) and the Fishergate blade-injured sample (2.89). The Towton sample falls intermediately, with an asymmetry score of 2.79. The Hickleton and Mary Rose samples, again, demonstrate the least variation between limbs, with scores of 1.55 and 2.36, respectively.

Epicondylar breadth (**EPIC**) has both epiphyseal and muscular components and is influenced by muscle attachments at the medial epicondyle, which forms part of the attachment site for the common flexor muscles, and the lateral epicondyle which forms part of the attachment site for the common extensor muscles. This variable can identify differences in activity patterns involving the elbow, forearm, wrist and hand. As would be expected from an epiphyseal measurement, this variable demonstrates low levels of

bilateral asymmetry. Asymmetry is greatest in the southern cemetery from Fishergate (2.79), followed closely by the Mary Rose sample (2.74) and the Towton population (2.43). The blade-injured sample from Fishergate, with a score of 1.60, falls towards the bottom. Bilateral asymmetry is the least in the Hickleton (1.42) and the Fishergate eastern cemetery samples (1.44). There are no significant inter-population differences in this variable.

The final variable, distal articular breadth (**DAB**), is not expected to display a high degree of asymmetry, as it is an epiphyseal measurement and thus has been found in previous analyses to be less subject to plasticity (see Ruff *et al.,* 1994; Lieberman *et al.*, 2001). However, any differences in activity levels, if identified in this variable, may identify increased activity in juvenile periods, as the endpoint of articular growth has been identified to occur around the age of 17 years, as opposed to cortical area, which has been identified to level out at 22 years of age (Ruff *et al.,* 1994). Bilateral asymmetry in distal articular breadth demonstrates higher population mean values than the epicondylar breadth. Bilateral asymmetry is greatest in the Mary Rose sample (3.30). This result may demonstrate different activity patterns between limbs at the elbow. The Hickleton and southern Fishergate cemetery samples demonstrate the next highest asymmetry values, both at 2.74, followed by the Towton population (2.47). The samples demonstrating the most symmetry are the Terry collection and the intramural cemetery at Fishergate (both at 2.08). The Fishergate blade-injured sample again falls towards the bottom, ranking seventh in this list with a score of 2.11.

7.4.2 Bilateral Asymmetry – Females

The female samples were also divided into two groups, humans and non-human primate species, to test for differences in the levels of bilateral asymmetry. Similar to the results

for the males, the results are significant for three out of the five variables analysed, although it is the breadth of the distal articular surface that does not display significant differences between female samples, while the level of bilateral asymmetry in humeral length is significantly different between the female human and non-human primate species (Table 7.28). In all variables, the levels of asymmetry in the human samples exceed those found in the non-human primates.

Table 7.28: Population differences in levels of bilateral asymmetry. The samples are divided into two groups, human and non-human primate species (females only).

Mann-Whitney U	HL	HGT	HC	HEB	HDAB
Z	-2.356	-3.977	-2.615	-1.928	-1.438
Sig. (2-tailed)	.018*	.000**	.009*	.054	.150

*Sig. p = 0.05; **Sig. p = 0.01

Despite the elevated levels of bilateral asymmetry found in the female samples when compared with those of the males, there are no significant differences between the sexes in the human populations analysed (Table 7.29). Further analyses exclude the non-human primate species.

There are no significant inter-population differences among the female samples in the levels of bilateral asymmetry in any of the variables analysed (Table 7.30). Asymmetry in humeral length is greatest in the Fishergate southern (2.59) and intramural (2.14) cemeteries and least in the Hickleton sample (1.35). Mean asymmetry in the greater tuberosity breadth is also increased in the female samples compared to the results for the males, greatest in the Fishergate southern cemetery (5.91) and the Wharram Percy sample (5.58). The Wharram Percy sample demonstrates the greatest asymmetry between limbs in the minimum diaphyseal circumference (2.27), while the most symmetric sample is the Hickleton group (1.40). Epicondylar breadth is most asymmetric in the intramural Fishergate cemetery sample (2.26), followed by the Chichester sample (2.06) and least in the Hickleton sample (1.56). The intramural

cemetery sample also displays the most asymmetric distal articular breadth (4.20), while the Hickleton sample, again, demonstrates the most symmetry between limbs in this variable (1.77).

Table 7.29: Differences between sexes: Bilateral asymmetry, all samples.

Mann-Whitney U		**HL**	**HGT**	**HC**	**HEB**	**HDAB**
Wharram Percy	Z	-.646	-.791	-.278	-.003	-.558
	Sig. (2-tailed)	.518	.429	.781	.998	.577
Hickleton	Z	-.192	-.447	-.054	-.575	-.463
	Sig. (2-tailed)	.848	.655	.957	.565	.643
Chichester	Z	-1.037	-1.507	-.738	-.754	-.402
	Sig. (2-tailed)	.300	.132	.461	.451	.688
FG intramural	Z	-1.894	-1.185	-1.570	-1.687	-1.508
	Sig. (2-tailed)	.058	.236	.116	.092	.132
FG southern	Z	-1.822	-.793	-.732	-.716	-.661
	Sig. (2-tailed)	.069	.428	.464	.474	.508
Gorilla sp.	Z	-.127	.000	-1.535	-.254	-.408
	Sig. (2-tailed)	.899	1.000	.125	.800	.683
Pan sp.	Z	-.585	-.849	-1.299	-1.872	-1.189
	Sig. (2-tailed)	.391	.396	.194	.061	.234
Pongo sp.	Z	-.592	-.092	-.896	-.085	-1.269
	Sig. (2-tailed)	.554	.926	.385	.932	.204
Macaca sp.	Z	.000	-1.937	-1.823	-1.026	-.775
	Sig. (2-tailed)	1.000	.053	.068	.383	.439

*Sig. p = 0.05; **Sig. p = 0.01

Table 7.30: Population differences in the level of bilateral asymmetry (females only).

ANOVA	**HL**	**HGT**	**HC**	**HEB**	**HDAB**
Sig.	.321	.291	.609	.118	.092

*Sig. p = 0.05; **Sig. p = 0.01

7.4.3 Limb Dominance and Hand Preference Inference

Asymmetry in humeral length is often attributed to a preferential handedness bias, with the side demonstrating the greatest length interpreted as the dominant limb. One study of children and adolescents, reported by Steele and Mays (1995), found out of 110 right-handers, 107 demonstrated quantifiably longer upper limbs (humerus and radius combined) on the right side, while 33 of 35 left-handers demonstrated greater upper limb length on the left side, as determined through radiographic analysis. In Steele and Mays' analysis of the adult specimens from Wharram Percy, hand preferences inferred from differences in mechanical loading were identified. Further support for the

identification of hand dominance comes from the sports medicine literature. In a study of professional tennis players, Krahl and colleagues (1994) found that the constant strain caused by intensive training resulted in significantly increased bone diameter and increased bone length in the stroke arm over the contralateral arm.

In a study of humeral bilateral asymmetry and bone plasticity, the levels of bilateral asymmetry in the humerus were low compared with the bilateral asymmetry found in the cross-sectional properties. While the Trinkaus and colleagues (1994) concede that it is possible that these low levels found in the humeral length are related to fluctuating (random) asymmetry related to system stress levels, they believe that any asymmetry over a baseline of a few percent is most likely from differential levels of mechanical stress.

The majority of modern populations are naturally right-handed, as only around 10% are left-handed (Calvin, 1983). In nearly every sample analysed, the percentage of left-handedness, as identified through asymmetry in the maximum humeral length, exceeds the average reported for modern humans. The Towton sample (Fig. 7.9) demonstrates a left-handed ratio of 21% that exceeds the modern average. The greatest bilateral asymmetry in maximum humeral length was found in an individual with left-side dominance (T16 – an individual with healed weapon trauma). This individual appeared as an outlier in a number of variables. These include increased values in the right proximal articular surface, although the distal articular surface is enlarged in relation to the epicondylar breadth in the contralateral, left humerus. This, though, is due to an avulsion fraction of the medial epicondyle and non-union of the fragment. The right humerus of T16 also has increased breadth of the greater tuberosity and increased deltoid tuberosity breadth. The level of bilateral asymmetry in the majority of the

Towton sample is low – less that that determined by Trinkaus *et al.*, (1994) to identify directional asymmetry as opposed to fluctuating asymmetry. However, this low level of asymmetry may occur through an activity involving elevated strains on both limbs. The Mary Rose sample (Fig. 7.10) demonstrates a similar percentage of left-side dominant individuals (22%), although there are five individuals from this sample that demonstrate no asymmetry in humeral length.

Figure 7.9: Side dominance in the Towton population. This is calculated from asymmetry in maximum humeral length. A negative value is left-side dominant, while a positive value is right-side dominant. Those spaces with no bar represent symmetry between limbs.

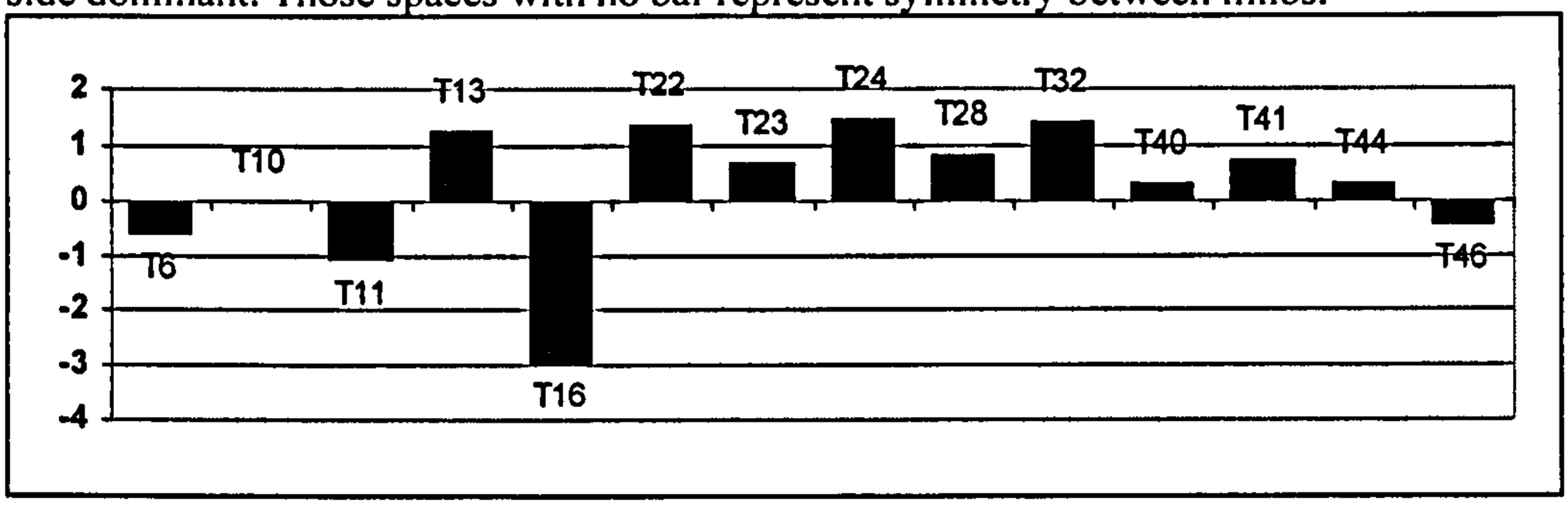

The Wharram Percy male sample has eight left-sided individuals that form a total of 11%, while the left-sided females make up 9% of the population (Figs. 7.11, 7.12). Twenty-eight percent of both male and female samples from the Hickleton population appear left-side dominant (Fig. 7.13). The percentage of left-side dominant individuals in the Chichester male sample far exceeds that found in the females, 20% compared with 4% (Figs. 7.14 and 7.15). Nearly one-fourth of the individuals from the Terry collection (Fig. 7.16) demonstrate a left-side dominance (24%), while 21% of the Fishergate blade-injured sample is identified as left-side dominant (Fig. 7.17). This percentage is similar for the eastern cemetery at Fishergate, who demonstrate a 20% ratio of left-side dominance (Fig. 7.18). The intramural and southern cemeteries are both composed of 15% left-side dominant males, while the intramural sample has 25% of the females identified as left-side dominant (Figs. 7.19 and 7.20). The three females from the Fishergate southern cemetery are all identified as right-side dominant.

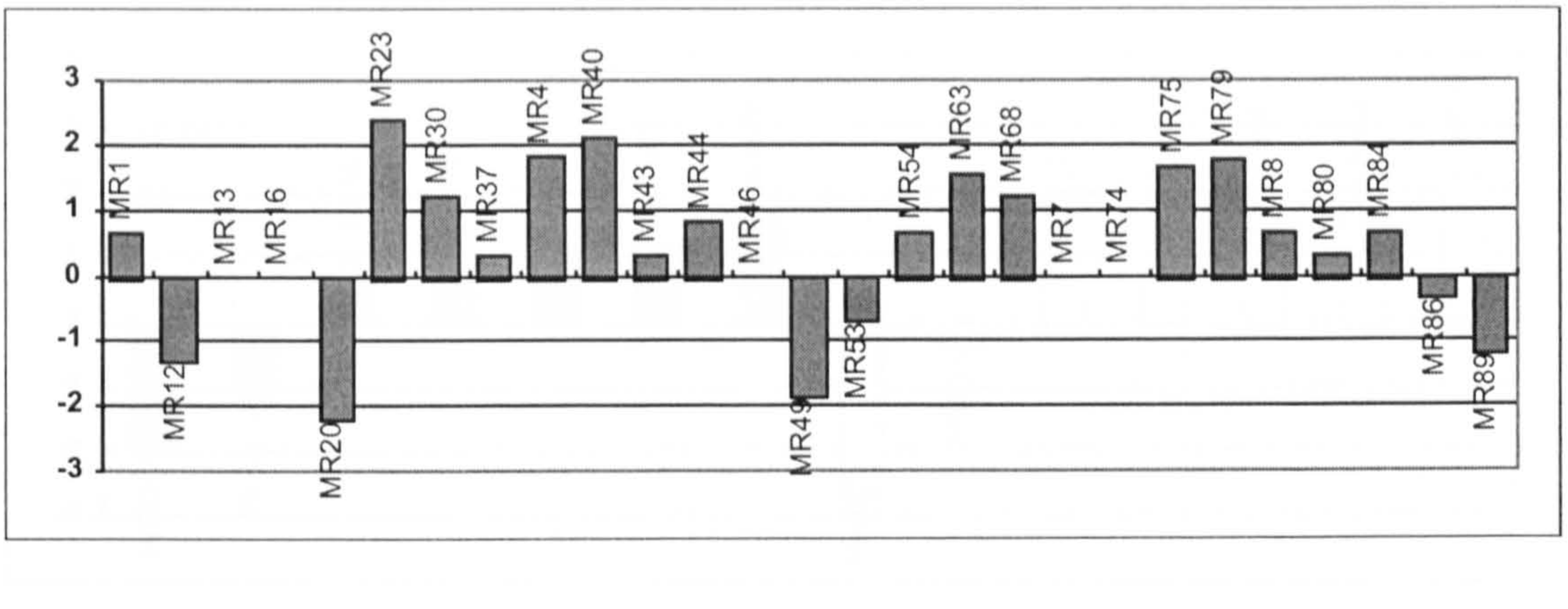

Figure 7.11: Side dominance in the Wharram Percy population: Males. This is calculated from asymmetry in maximum humeral length. A negative value is left-side dominant, while a positive value is right-side dominant. Those spaces with no bar represent symmetry between limbs.

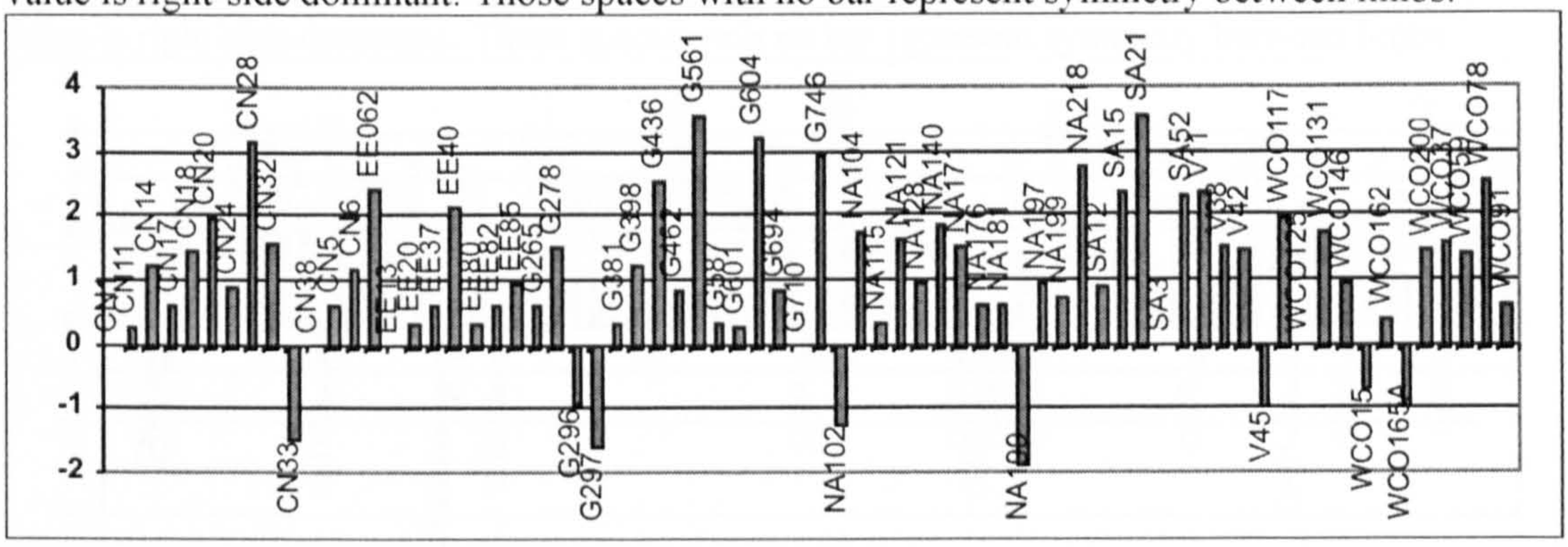

Figure 7.12: Side dominance in the Wharram Percy population: Females. This is calculated from asymmetry in maximum humeral length. A negative value is left-side dominant, while a positive value is right-side dominant. Those spaces with no bar represent symmetry between limbs.

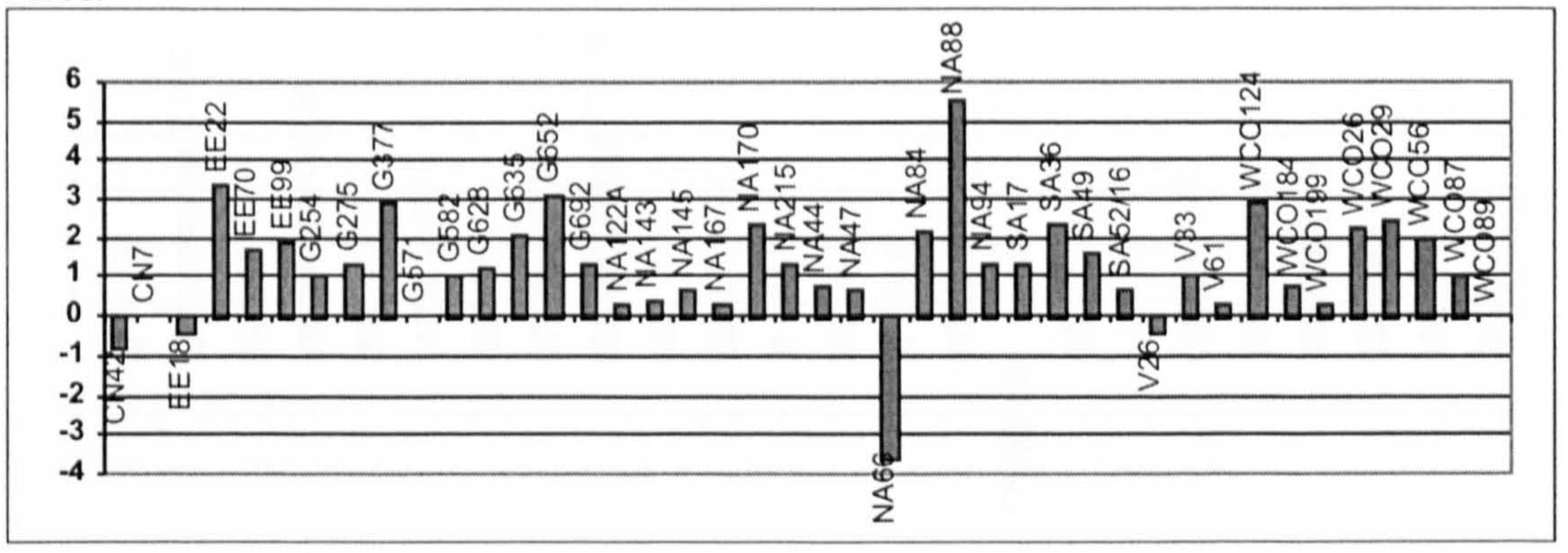

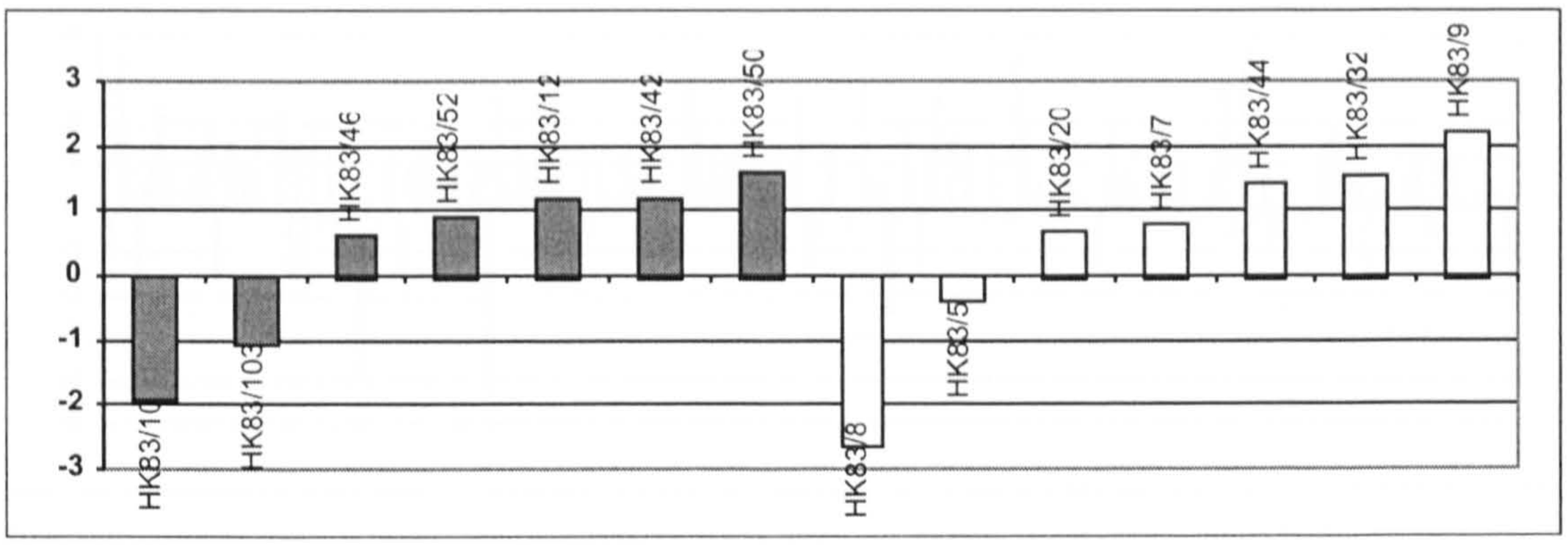

Figure 7.14: Side dominance in the Chichester population: Males. This is calculated from asymmetry in maximum humeral length. A negative value is left-side dominant, while a positive value is right-side dominant. Those spaces with no bar represent symmetry between limbs.

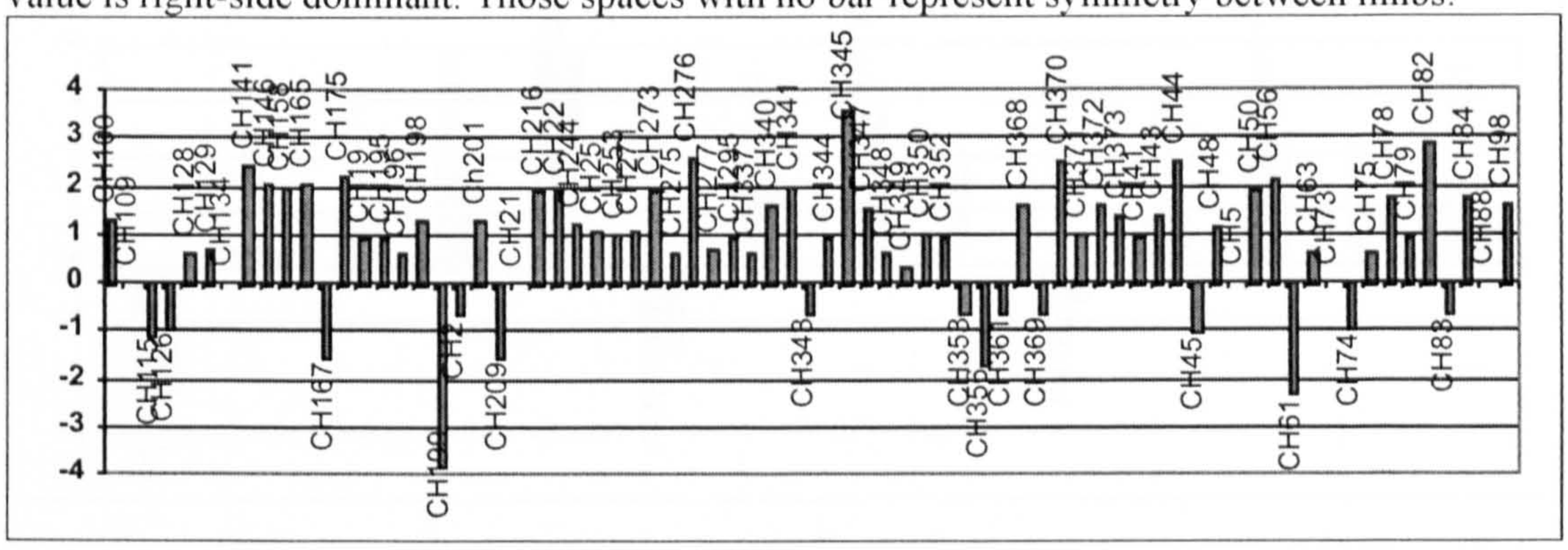

Figure 7.15: Side dominance in the Chichester population: Females. This is calculated from asymmetry in maximum humeral length. A negative value is left-side dominant, while a positive value is right-side dominant. Those spaces with no bar represent symmetry between limbs.

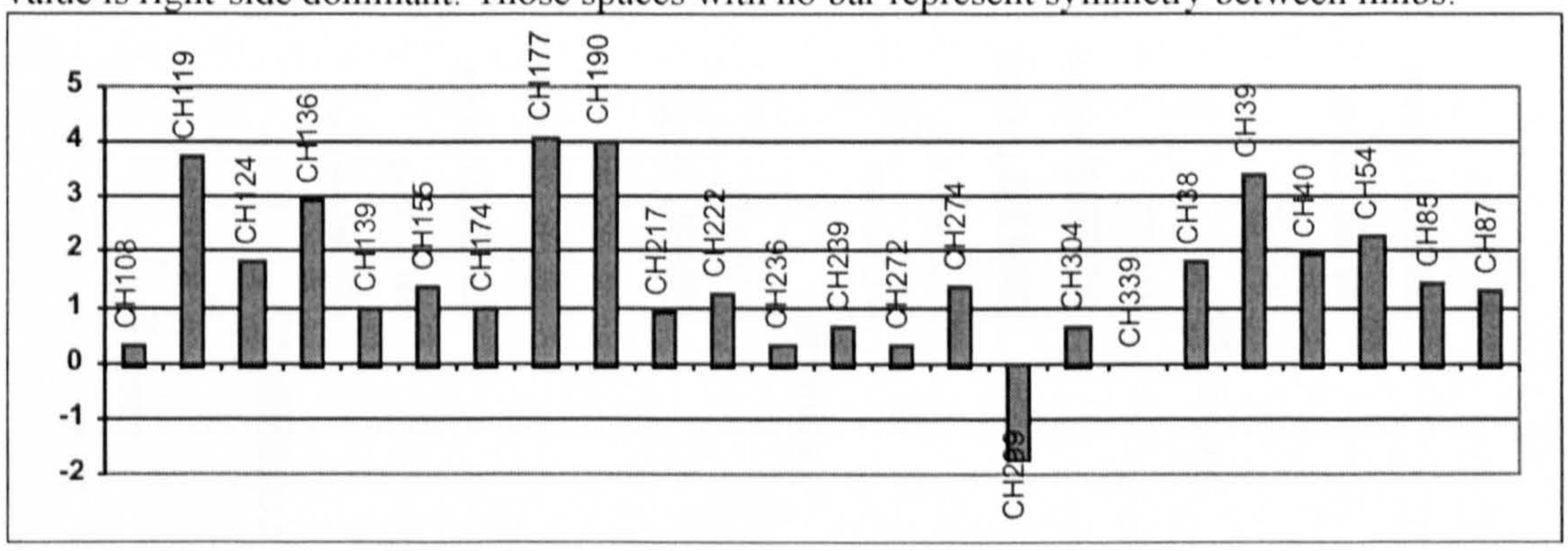

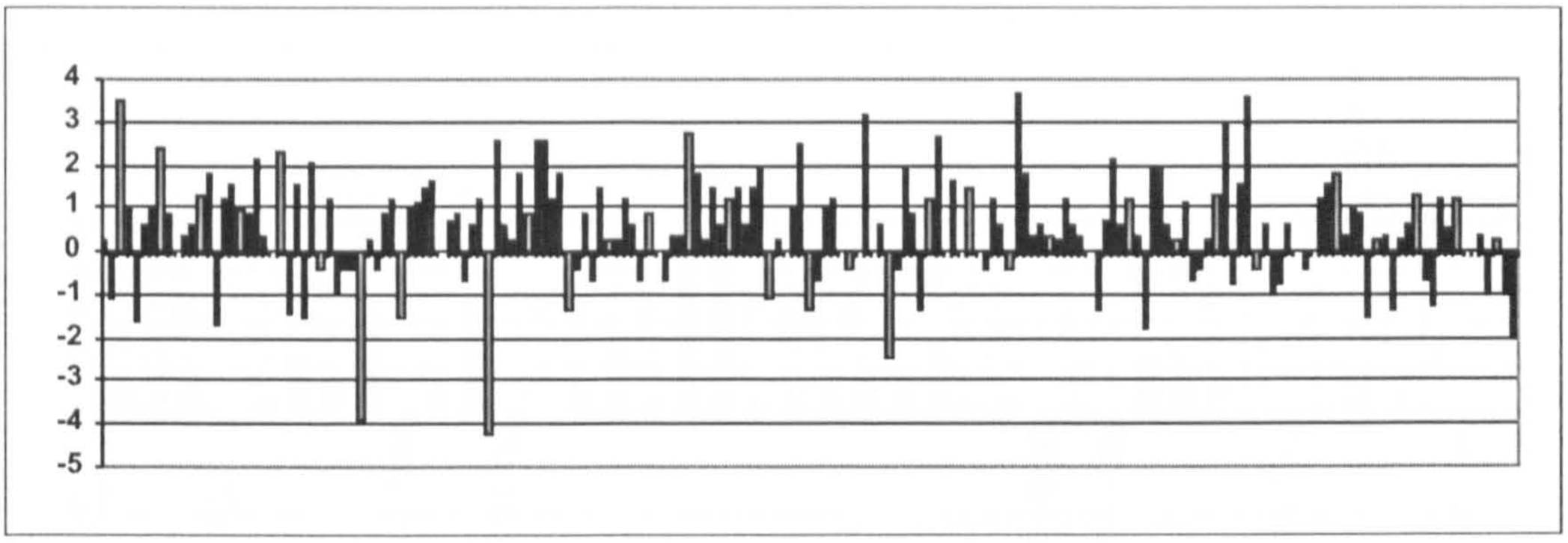

Figure 7.17: Side dominance in the Fishergate blade-injured sample. This is calculated from asymmetry in maximum humeral length. A negative value is left-side dominant, while a positive value is right-side dominant. Those spaces with no bar represent symmetry between limbs.

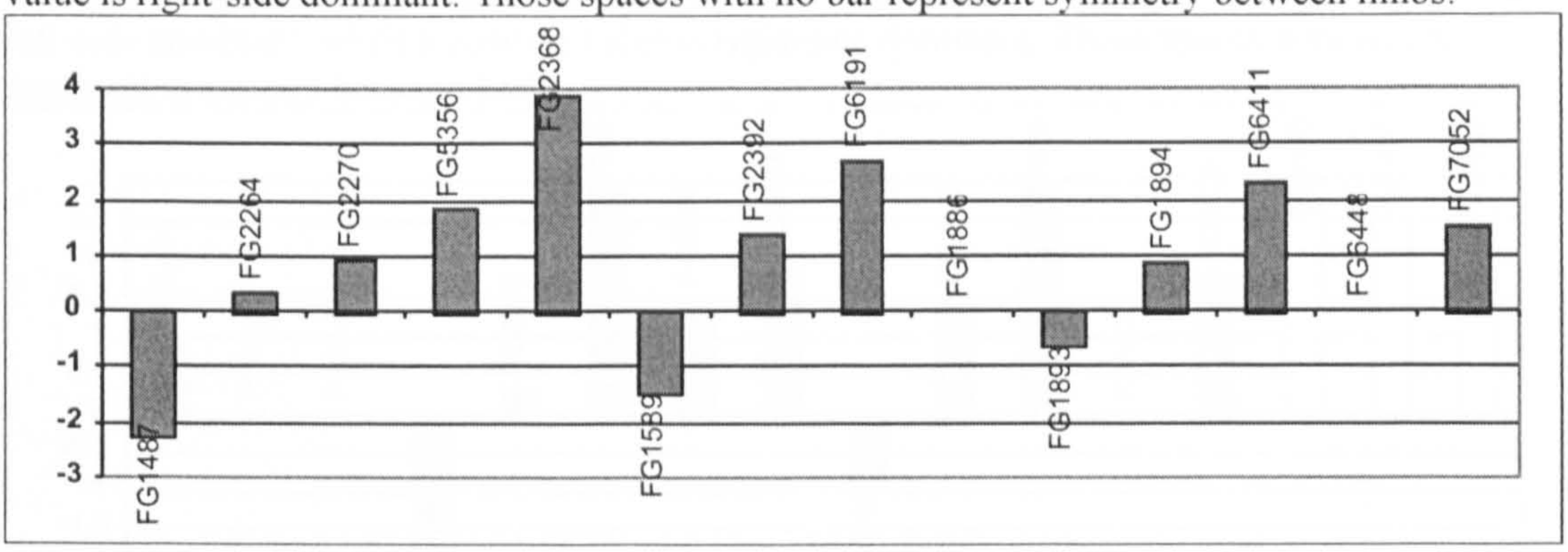

Figure 7.18: Side dominance in the Fishergate eastern cemetery. Males are dark grey, females are white. This is calculated from asymmetry in maximum humeral length. A negative value is left-side dominant, while a positive value is right-side dominant. Those spaces with no bar represent symmetry between limbs.

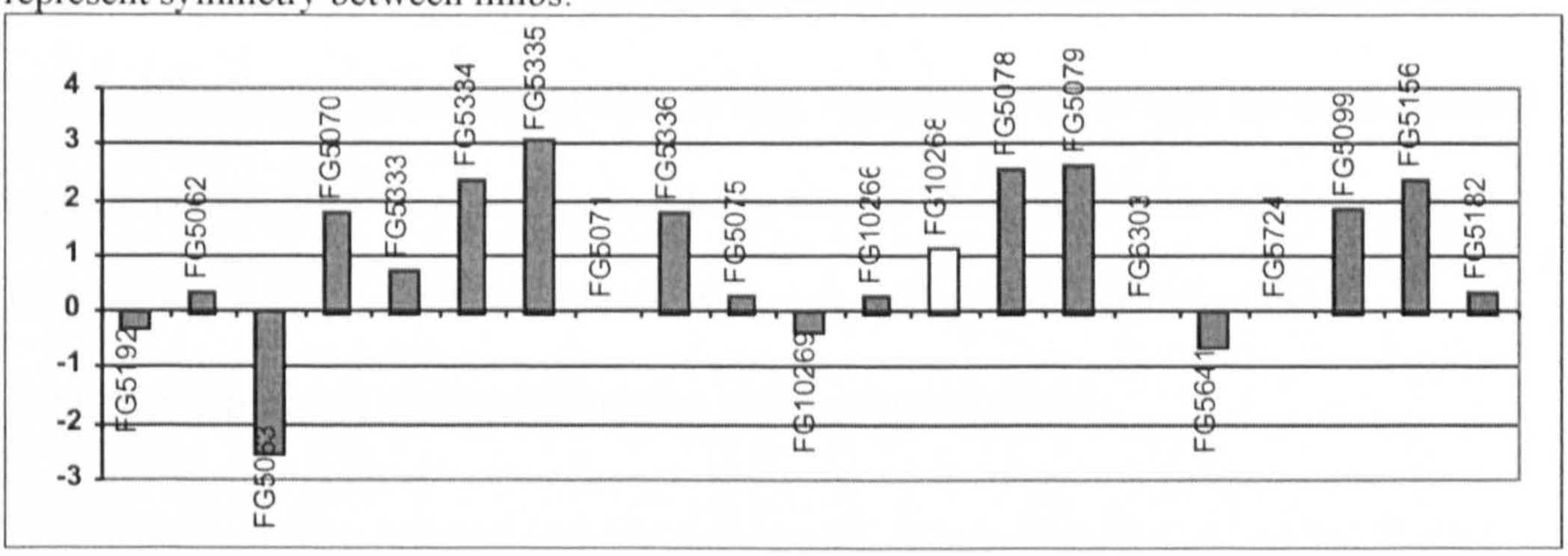

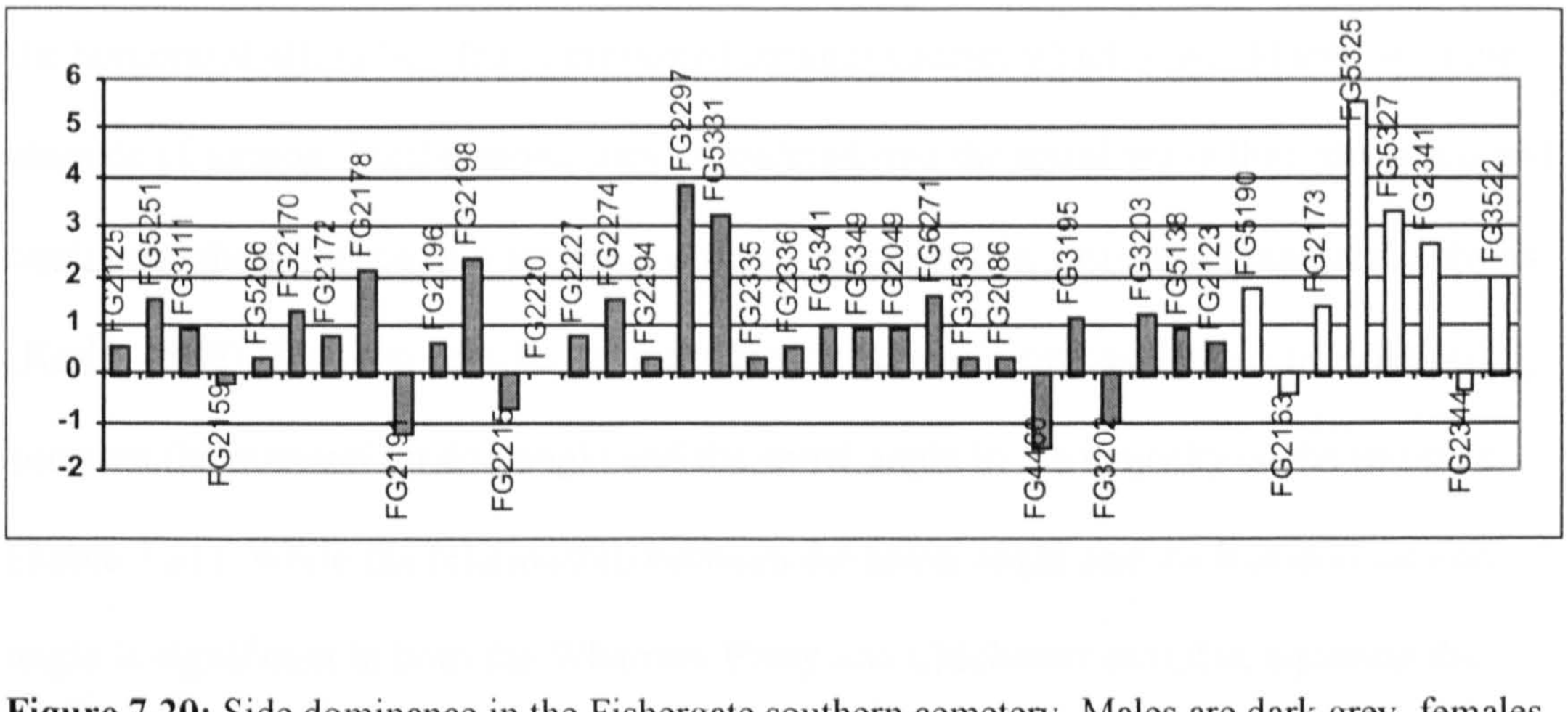

Figure 7.20: Side dominance in the Fishergate southern cemetery. Males are dark grey, females are white. This is calculated from asymmetry in maximum humeral length. A negative value is left-side dominant, while a positive value is right-side dominant. Those spaces with no bar represent symmetry between limbs.

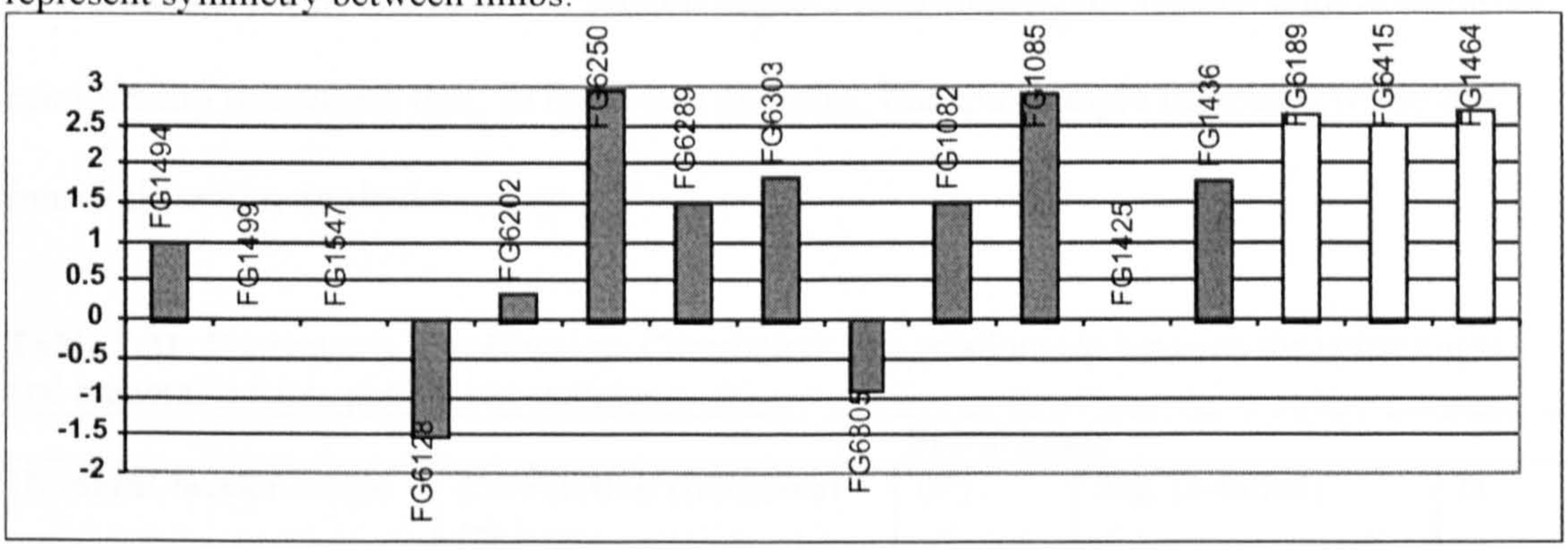

7.5 Bivariate Correlation Analysis: Spearman's Rho

Humeral torsion, although discussed separately in another chapter, is included in the correlation analysis to determine what, if any, relationship it has with the other humeral measurements. Specific questions involving humeral torsion involve its relationship with the spiral angle and humeral robusticity, as well as whether there is any relationship between diaphyseal bowing and the torsion angle.

A question raised in Chapter 6, Humeral Torsion, involved the assumed correlation between the spiral angle, a measurement of the direction of the bicipital

groove, and humeral torsion. Early anatomists considered that torsion occurred in the proximal epiphysis, twisting the bicipital groove such that it follows a curved path down the humeral shaft, rather than a presumed straight course, which it would follow in the absence of torsion. Furthermore, they considered that the spiral angle thus identified and confirmed the presence of a torsional process involving the proximal humeral diaphysis (Krahl, 1948). This can now be demonstrated to be inaccurate as there is no relationship between the humeral torsion angle and the spiral angle in the majority of the samples (Table 7.31). While the relationship between the spiral angle and the humeral torsion angle is significant in both the Wharram Percy and Chichester samples, squaring the correlation coefficient shows that only 5% or less of the variation in the spiral angle can be accounted for by the humeral torsion angle. Additionally, the relationship is negative relationship indicating that, in these two samples, the spiral angle increases while the humeral torsion angle decreases.

Table 7.31: Spearman's Rho Bivariate Correlation: The relationship between the spiral angle and humeral torsion, pooled sex samples.

	Spiral angle			
Humeral torsion angle	**Correlation coefficient (r)**	**(r^2)**	**Sig. (2-tailed)**	**N**
Towton	.027	.054	.862	43
Mary Rose	.022	.0004	.777	162
Wharram Percy	-.225	.05	.000**	240
Hickleton	-.130	.016	.508	28
Chichester	-.139	.019	.028*	249
Terry	-.034	.001	.517	357
FG blade-injured	.042	.001	.840	26
FG eastern	.200	.04	.152	53
FG intramural	-.009	.0000	.923	106
FG southern	-.151	.022	.351	40

*Sig. p = 0.05; **Sig. p = 0.01

Another question raised in the humeral torsion chapter regarded the relationship between humeral torsion and humeral robusticity. Martin (1933) identified decreased torsion angles with a less robust humerus, as the gracile element was assumed to have an inherent weakness in its structure which made it susceptible to increased torsion. An aim

of this project was to identify the relationship between the humeral torsion angle and humeral robusticity. Following the primary hypothesis that increased humeral torsion is related to strenuous activity, increased torsion angles are expected to correlate with increased humeral robusticity and both should occur in the dominant limb. This hypothesis further detailed that the non-dominant limb should have a decreased torsion angle and decreased humeral robusticity. The analysis is conducted presuming the majority of the individuals as right-side dominant, as it is impossible to identify side dominance in every skeleton, as not all have paired humeri.

Table 7.32: Population averages for right and left side humeral robusticity and humeral torsion angles. The measure of significant is from a Spearman's Rho correlation analysis of humeral torsion and humeral robusticity (both limbs) conducted for a pooled sex population.

	Right humerus				Left humerus				
	Humeral rob.	**N**	**Humeral torsion angle**	**N**	**Humeral rob.**	**N**	**Humeral torsion angle**	**N**	**Sig.**
Towton	20.45	25	14.96°	26	20.83	20	16.76°	21	.708
Mary Rose	20.22	77	16.11°	77	20.11	88	18.12°	87	.018*
WP (males)	20.17	77	17.25°	74	19.98	79	17.94°	79	.011*
WP (females)	19.22	49	14.06°	49	19.14	48	15.12°	48	
Hickleton (males)	20.35	8	17.37°	8	19.98	7	15.85°	7	.130
Hickleton (females)	18.36	8	13.06°	8	18.30	7	11.85°	7	
Chichester (males)	20.02	101	19.63°	99	19.87	93	18.60°	92	.993
Chichester (females)	19.10	32	17.03°	32	19.20	36	17.55°	36	
Terry	20.23	179	23.68°	179	19.83	178	21.73°	178	.118
Fishergate BI	19.89	15	25.14°	14	19.44	13	22.76°	13	.577
FG eastern (males)	19.78	22	23.00°	22	18.05	31	16.80°	31	.001**
FG intra (males)	19.88	47	16.41°	47	19.42	43	14.92°	40	.482
FG intra (females)	17.69	13	18.41°	12	17.82	11	19.00°	11	
FG south (males)	19.73	19	17.81°	19	19.74	14	18.42°	14	.001**
FG south (females)	18.76	6	11.42°	7	18.65	5	9.4°	5	

*Sig. p = 0.05; **Sig. p = 0.01

The Towton sample demonstrate greater humeral robusticity and a higher mean humeral torsion angle on the left side, while the Mary Rose and Wharram Percy (both male and females) demonstrate greater humeral robusticity on the right side and a greater mean torsion angle on the left side (Table 7.32). Both males and females from the Hickleton sample demonstrate greater humeral robusticity on the right side, as well as an increased torsion angle on this side. The Chichester male sample follows this pattern, although the females demonstrate greater mean robusticity and torsion angle on the left side. The Terry collection, Fishergate blade-injured, Fishergate eastern cemetery (males only) and Fishergate intramural cemetery samples all demonstrate greater humeral robusticity and a higher mean torsion angle on the right side, although the female sample from the Fishergate intramural cemetery displays greater robusticity and torsion angles on the left side. The Fishergate southern cemetery displays the opposite pattern, with the males demonstrating left-side dominance in humeral robusticity and humeral torsion angles, while the females display right-side dominance in both of these variables.

Only the Mary Rose ($p < .018$), Wharram Percy (combined sex) ($p < .011$), Fishergate eastern (combined sex) ($p < .001$) and the Fishergate southern cemetery samples ($p < .001$) have a significant (positive) relationship between humeral torsion angles and the humeral robusticity index (Table 7.33). The square of the correlation coefficient shows the variation in humeral robusticity accounts for only 3.5% or less of the humeral torsion angle in the first two samples, but 19.7% and higher in the last two samples. The Fishergate blade-injured and intramural cemeteries demonstrate a negative, non-significant correlation between the humeral torsion angle and the humeral robusticity index while all other samples demonstrated a positive correlation.

Questions regarding the relationship of the humeral torsion angle and a valgus deformity were raised previously. It is believed that an accurate measurement of the valgus deformity should identify what role it plays in humeral torsion. The anterior curvature measurement was designed to quantify the valgus deformity. A valgus deformity results in the distal-most shaft deviating away from the midline. Therefore, this will result in an elevated angle between the humeral shaft and the (medially viewed) mid-trochlear surface (an increased anterior curvature measurement). There is a significant positive correlation between the degree of anterior curvature and the humeral torsion angle in six of the 10 populations. These are the Mary Rose ($p < .000$), Wharram Percy ($p < .034$), Chichester ($p < .000$), Terry ($p < .000$), Fishergate eastern ($p < .005$) and southern cemetery ($p < .006$) samples (Table 7.24). In these populations, the degree of anterior curvature is significantly correlated with an increased humeral torsion angle. This is logical, as a lateral twist of the distal epiphysis would be expected to affect the humeral torsion angle. The question is what is occurring in those samples that do not demonstrate a correlation between these two variables (Towton, Hickleton, Fishergate blade-injured, and the Fishergate intramural cemetery)? These samples, with the exception of the Fishergate blade-injured group, all display relatively low humeral torsion angles when compared with the rest of the samples. They also demonstrate the highest degree of anterior curvature. Therefore, there appears to be a separate process occurring in the proximal humerus that is counter-acting the increased anterior curvature angle in these samples. Perhaps this is a further increased torsional process regionalised to the proximal humerus, such that were the anterior curvature of a lesser degree, the humeral torsion angle would fall even lower.

The humeral torsion angle is also correlated with the other measures of diaphyseal bowing, indicating that humeral torsion is perhaps not exclusive to the

proximal or distal articular surfaces (Table 7.33). Rather, it is being influenced by or actively influencing other architectural measures of bowing. Interestingly, the amount of bowing in the distal shaft (**HDBW**) is significantly correlated with the humeral torsion angle in every population sample with the exception of the Towton group. This sample demonstrates the lowest amount of distal bowing, possibly counter-acting the torsional architectural modifications of the humerus and thus reducing the humeral torsion angle.

Table 7.33: The correlation (Spearman's Rho) between the measures of bowing, anterior (ANTCV), proximal (HPBW), distal (HBDW) and medio-lateral (HML), and the humeral torsion angle, all populations, pooled sexes. T = Towton, MR = Mary Rose, WP = Wharram Percy, HK = Hickleton, CH = Chichester, TR = Terry, FG BI = Fishergate blade-injured, FG E = Fishergate eastern cemetery, FG I = Fishergate intramural cemetery, FG S = Fishergate southern cemetery.

	T	MR	WP	HK	CH	TR	FG BI	FG E	FG I	FG S
ANTCV										
Correlation coefficient	-.004	.278	.134	.304	.285	.193	-.037	.369	.071	.401
Sig. (2-tailed)	.982	.000**	.034*	.109	.000**	.000**	.853	.005**	.460	.006**
N	45	164	250	29	254	357	27	56	110	45
HPBW										
Correlation coefficient	.543	.226	.320	.243	.251	.278	.338	.043	.077	.227
Sig. (2-tailed)	.000**	.004**	.000**	.195	.003**	.000**	.084	.751	.431	.134
N	44	163	235	30	195	356	27	56	108	45
HDBW										
Correlation coefficient	-.124	.673	.697	.530	.630	.754	.543	.559	.611	.537
Sig. (2-tailed)	.418	.000**	.000**	.003**	.000**	.000**	.003**	.000**	.000**	.000**
N	45	161	235	29	188	356	27	56	108	45
HML										
Correlation coefficient	-.057	-.286	-.157	.040	-.129	-.112	-.207	-.090	-.300	-.098
Sig. (2-tailed)	.714	.000**	.015*	.832	.048*	.035*	.300	.509	.002**	.532
N	44	163	241	30	234	358	27	56	109	43

*Sig. p = 0.05; **Sig. p = 0.01

7.6 Discussion

Significant inter-population differences have been identified among the males in the measurements of diaphyseal bowing, in proximal, distal and medio-lateral directions, as well as the degree of anterior curvature, although there is no one population that

proximal or distal articular surfaces (Table 7.33). Rather, it is being influenced by or actively influencing other architectural measures of bowing. Interestingly, the amount of bowing in the distal shaft (**HDBW**) is significantly correlated with the humeral torsion angle in every population sample with the exception of the Towton group. This sample demonstrates the lowest amount of distal bowing, possibly counter-acting the torsional architectural modifications of the humerus and thus reducing the humeral torsion angle.

Table 7.33: The correlation (Spearman's Rho) between the measures of bowing, anterior (ANTCV), proximal (HPBW), distal (HBDW) and medio-lateral (HML), and the humeral torsion angle, all populations, pooled sexes. T = Towton, MR = Mary Rose, WP = Wharram Percy, HK = Hickleton, CH = Chichester, TR = Terry, FG BI = Fishergate blade-injured, FG E = Fishergate eastern cemetery, FG I = Fishergate intramural cemetery, FG S = Fishergate southern cemetery.

	T	MR	WP	HK	CH	TR	FG BI	FG E	FG I	FG S
ANTCV										
Correlation coefficient	-.004	.278	.134	.304	.285	.193	-.037	.369	.071	.401
Sig. (2-tailed)	.982	.000**	.034*	.109	.000**	.000**	.853	.005**	.460	.006**
N	45	164	250	29	254	357	27	56	110	45
HPBW										
Correlation coefficient	.543	.226	.320	.243	.251	.278	.338	.043	.077	.227
Sig. (2-tailed)	.000**	.004**	.000**	.195	.003**	.000**	.084	.751	.431	.134
N	44	163	235	30	195	356	27	56	108	45
HDBW										
Correlation coefficient	-.124	.673	.697	.530	.630	.754	.543	.559	.611	.537
Sig. (2-tailed)	.418	.000**	.000**	.003**	.000**	.000**	.003**	.000**	.000**	.000**
N	45	161	235	29	188	356	27	56	108	45
HML										
Correlation coefficient	-.057	-.286	-.157	.040	-.129	-.112	-.207	-.090	-.300	-.098
Sig. (2-tailed)	.714	.000**	.015*	.832	.048*	.035*	.300	.509	.002**	.532
N	44	163	241	30	234	358	27	56	109	43

*Sig. p = 0.05; **Sig. p = 0.01

7.6 Discussion

Significant inter-population differences have been identified among the males in the measurements of diaphyseal bowing, in proximal, distal and medio-lateral directions, as well as the degree of anterior curvature, although there is no one population that

demonstrates a consistently increased or decreased amount of diaphyseal bowing when compared with the others. Inter and intra-population differences have been identified in the maximum cubital angle. The Fishergate blade-injured sample demonstrates a low cubital angle compared with the other populations, possibly identifying differences in the carrying angle. The lack of correlation between the maximum cubital angle and the anterior curvature measurement indicate the former has little relationship with *cubitus valgus*. Direct measurement of the carrying angle using the ulna, as well as the humerus might be able to clarify the identification of a valgus deformity. A measurement of diaphyseal flattening, a measurement thought to be related to elbow hypertrophy was created to identify any differences in humeral morphology at 20% of the maximum length, however, no significant population differences were identified.

There are a large number of individuals with outlying values in the measurements of architecture. However, there do not appear to be any consistent patterns within the samples. The Mary Rose and the Terry collection are the most heterogeneous of the samples analysed, with the greatest number of outlying values in all measurements. Both combatant-related samples, Towton and the Fishergate blade-injured, are more homogenous in their make-up, with the least outlying values in the measures of architecture similar in this regard to the Hickleton and Fishergate eastern cemetery samples. The blade-injured men from both the intramural and southern cemeteries do not differ enough to occur as outliers within their population groups. In the individuals with known occupations from Terry collection, those performing manual labour tend to have increased values, while those with less physical jobs tend to have decreased values.

The results of the articular robusticity measurements are also mixed among males. The Hickleton sample demonstrates the greatest standardised proximal and distal articular dimensions, however, this sample falls intermediately in the trochlear breadth measurement, and demonstrates the highest, most narrow capitulum of the samples analysed. Despite falling intermediately in the standardised measurement of distal articular breadth, the Towton sample demonstrates the largest distal articular breadth when standardised against the epicondylar breadth. The Mary Rose sample displays increased trochlear breadth (standardised), but decreased humeral head diameter. These results indicate that articular size is localised, rather than being a systemic response to increased activity.

A number of individuals produce outlying values in more than a single articular measurement. The right humeri of CN28 and WCO91 (Wharram Percy), but not the left, possess increased trochlear and distal articular breadths when compared with the rest of the group. Furthermore, WCO91 has an increased capitular index value, indicating a short, broad capitulum, while CN28 demonstrates an increased DAB in relation to epicondylar breadth. T16 demonstrates an (outlying) increased right proximal articulation but an outlying left distal articular / epicondylar index value – indicating increased DAB, although the latter outlying result is more likely to occur from an avulsion fracture to the medial epicondyle that reduces epicondylar breadth. A man identified as a restaurateur from the Terry collection is an outlier with reduced measurements of trochlear breadth, distal articular breadth and the transverse humeral head breadth. This individual further demonstrates outlying reduced values for the greater tuberosity breadth, greatest breadth at the deltoid tuberosity and the humeral robusticity index, indicating reduced activity levels in this individual relative to the remaining population.

The Mary Rose and the Terry collections, again, appear most heterogeneous in the measurements of robusticity, with many individuals displaying increased and decreased outlying values. The number of individuals diagnosed with leprosy from the Chichester sample with outlying increased robusticity measurements demonstrates that this disease does not necessarily reduce activity levels, although the increased robusticity could have originated from activity levels prior to falling prey to the disease. There is one individual from the Fishergate intramural cemetery, FG6082, a male buried in the nave that has consistently increased values in most measurements of the articulations, as well as greater tuberosity breadth, deltoid tuberosity breadth and humeral robusticity. Unfortunately, this individual does not have a complete left limb to identify whether this is the result of unimanual activity patterns, or a general increased activity level in comparison to the rest of the sample. This man does have an outlying value in humeral length, as he is shorter of limb than the remaining sample. It is possible that this could be influencing those measurements that are standardised by humeral length as a low humeral length may inflate robusticity values (see Pearson, 2000 for more).

Examination of the combatant-related groups compared with the remaining populations indicates that significant differences between these samples are more likely to occur in humeral architecture and articular size rather than humeral robusticity. The Mary Rose sample is significantly different than the non blade-injured group in all measures of articular size, indicating increased activity patterns at a young age in this group. Of the robusticity measurements, only humeral length demonstrated significant differences between both the blade-injured sample and the Mary Rose sample when compared with the non blade-injured men. The increased humeral length typifying these samples implies that these men may have been pre-selected on the basis of their size

(but not their muscularity) to serve in combat. It also may indicate that these men could have originated from a higher social class than the remaining populations (when considered as a whole) or had access to a more nutritional diet.

Greater tuberosity breadth is most bilaterally asymmetric in this analysis, with mean asymmetry scores ranging from 5.49 to 2.68. These results indicate unimanual activity patterns at the shoulder. The next highest levels of asymmetry are found in the minimum humeral circumference measurement, ranging from 3.45 to 1.55. The results may indicate two things. Firstly, those populations with high bilateral asymmetry in this variable indicate a systemic response from increased mechanical loading (from a unimanual activity). Secondly, this may indicate increased activity patterns in post-adolescence. Those populations with high asymmetry in minimum humeral circumference (Fishergate eastern cemetery, Terry collection and Fishergate blade-injured sample) demonstrate low bilateral asymmetry in the distal articular breadth, a measurement most influenced by pre-adolescent activity levels. Those populations with increased bilateral asymmetry in distal articular breadth (Mary Rose, Fishergate southern cemetery, Hickleton and the Towton sample) all fall within the lowest ranks in the level of asymmetry of minimum humeral circumference, indicating increased activity patterns from a pre-adolescent stage.

The measurements of bilateral asymmetry that indicate systemic differences in activity patterns (humeral length and minimum humeral circumference) confirm the unimanual activity pattern in the Fishergate blade-injured sample, as identified in the biomechanical analysis (see Chapter 6). However, in the Towton and Mary Rose populations, the men appear to be using both limbs in a similarly strenuous manner or to a similar extent. A right proximal - left distal cross-over pattern to humeral robusticity

characterises the Towton sample and is identifiable in the asymmetry of the greater tuberosity breadth and the epicondylar breadth.

7.6.1 External vs. Internal Measurements of Robusticity

The results for the measures of robusticity are mixed depending upon the variables used. If the humeral diaphysis is more responsive over a longer period to plastic change than the epiphysis, then the general robusticity index [(min. humeral circumference / max. humeral length) x 100] should be the most accurate of the external robusticity variables. But how does this compare with the previously reported cross-sectional robusticity measurements? According to Trinkaus and colleagues (1994), the clearest patterns of asymmetry indicating behavioural differences between limbs have been identified in the polar moments of area, with J demonstrating the most marked asymmetry in the upper limb (Trinkaus *et al.*, 1994). Therefore, comparison of robusticity will be made using this variable.

Table 7.34: Internal vs. external measurements of robusticity in those specimens from the biomechanical analysis.

	J	Hum Rob	Max. length		J	Hum Rob	Max. length		J	Hum Rob	Max. length
T06	L	L	L	FG1589	R	R	L	FG1425	R	S**	S**
T11	L	L	L	FG1886	R	L	S**	FG1436	L*	L	R
T13	L	L	L	FG1893	R	R	L	FG2178	L*	L	R
T16	R	R	R	FG2270	L*	R	R	FG3195	L*	L	R
T22	R	R	R	FG2392	R	R	R	FG3202	R	R	L
T23	L*	L	R	FG5356	R	L	R	FG5071	R	R	R
T24	L*	L	R	FG6191	R	R	R	FG5138	R	R	R
T32	L	L	L	FG6411	R	L	R	FG5336	R	R	R
T40	L	L	R	FG6448	R	R	S**	FG6128	L	L	L
T41	L	L	R	FG7052	R	R	R	--			
T44	R	R	R	--				--			
T46	L*	L	R	--				--			

*If the J values are mixed between sides, the side dominant at 35% was used; **S = symmetry between sides

Analysis of the cross-sectional properties from the Towton sample seems to indicate that increased total area, rather than cortical area is linked with increased

strength properties, as defined by J, torsional rigidity. Certainly increased total area (sub-periosteal expansion) will result in an increased general robusticity score, as the minimum circumference will be increased. The increased total area (TA) found in the Towton sample could explain why this sample was most robust only in the general robusticity index [(hum length / min. circ.) x 100]. But is this general index a reliable indicator of robusticity? Identification of increased robusticity via standardised J values, the humeral robusticity index and limb dominance as defined by maximum humeral length indicate variable results (Table 7.34).

In the Towton sample, humeral robusticity as indicated by the J values and the robusticity index all suggest the same side dominance. However, four individuals, T23, T24, T40 and T46, indicate a divergence between limb dominance as indicated by humeral length asymmetry (which favours the left-side) and robusticity scores (favouring the right-side). It is possible that these individuals were habitually right-handed, but practiced an activity that requires more strength or subjects the left limb to greater strain levels. Based upon the robusticity values, 75% of this sample are left-side dominant for length, but only 33% appear to be left-side dominant as indicated by the robusticity index.

In the blade-injured sample from Fishergate, there are a number of individuals who have contradictory robusticity indicators. Standardised measures of J indicate a predominately right-limb dominant group (90%), with only FG2270 demonstrating a left-side dominance in robusticity. However, when considering the external measurements of robusticity, only 70% appear right-limb dominant. Three individuals, FG1886, FG5356 and FG6411, appear to be more robust on the left side in this variable. This may be a result of a similar humeral circumference between sides, but a reduced

humeral length on the left that artificially increases humeral robusticity. Sixty percent of the sample is right-side dominant, with two individuals demonstrating symmetry between limbs. In the comparative sample, all humeral robusticity measurements match the side dominance as denoted by the J values, however, there is one individual, FG3202, that demonstrates right-side dominance in robusticity, but left-side dominance in J. Sixty-six percent of this sample demonstrates right-limb dominance, while only 55% demonstrate right-side dominance in the robusticity values. Therefore, it appears that hand preference and limb dominance as indicated by robusticity indices are not necessarily connected.

7.7 Conclusions

The results of this study indicate significant differences in measurements of humeral morphology both between and within samples. The Towton population stands out because of the architectural modifications to the distal humerus, most likely resulting from long-term training with weapons. The longbow appears likely or a pole weapon, as the use of these requires both arms but also requires each limb to perform different motions and results in differential strain between sides at the shoulder and elbow. However, the results from the Fishergate blade-injured and Mary Rose samples fail to identify any typical signature from presumed weapon use, as each combatant-related sample demonstrates its own suite of architectural modifications. In the case of the blade-injured men from Fishergate, this would appear to have been a unimanual weapon, while the men from the *Mary Rose* demonstrate a mixed pattern, not consistent with either sample. If the men from the *Mary Rose* included longbowmen, as indicated by Stirland (2000), they cannot be confidently identified as such in this analysis. It is possible that the high number of individuals with outlying measurement values could

identify longbowmen as opposed to sailors, but the results indicate a more heterogeneous sample than one composed simply of longbowmen and sailors.

Significant differences have been identified in humeral measurements between males and females and between, as well as within, population samples. The Towton sample is characterised by architectural modifications of the distal humerus with a significantly lower degree of distal bowing in the diaphysis, but a significantly higher degree of anterior curvature, a lateral deviation of the distal end. Articular dimensions are comparatively reduced, while humeral length is increased. This sample falls intermediately in breadth at the greater tuberosity, but has an increased maximum breadth at the deltoid tuberosity when standardised by humeral length, but interestingly, it has a reduced robusticity value for the deltoid tuberosity when this measurement is standardised by the deltoid tuberosity circumference. It also demonstrates a narrow epicondylar breadth, indicating reduced attachment sites of the common flexor and extensor muscle groups. There appear to be differential activity patterns at the shoulder and elbow, as indicated by a higher level of asymmetry in the greater tuberosity breadth and epicondylar breadth, but asymmetry in the humeral length is minimal.

The Mary Rose sample is characterised by increased diaphyseal bowing in all measurements, proximal, medio-lateral and distal, but decreased anterior curvature at the distal epiphyseal region. This sample has increased distal articular dimensions, but relatively reduced proximal dimensions. Humeral length and humeral robusticity are high, but measurements of the greater tuberosity and deltoid tuberosity indicate relatively reduced robusticity at these muscle sites. Asymmetry is low in humeral length, the breadth of the greater tuberosity and humeral circumference, but high in the distal

epicondylar breadth and articular breadth. These results indicate variations in the loading patterns of the distal humerus from a young age.

The Wharram Percy (male) sample is characterised by increased proximal and M/L bowing of the humeral diaphysis, but reduced anterior curvature of the distal epiphyseal region. It demonstrates increased trochlear breadth in comparison with the other populations and significant differences in the size of the humeral head. Humeral length and breadth of the greater tuberosity are highly asymmetrical which may relate to different activity patterns between limbs at the shoulders. The female sample, in contrast, demonstrates relatively high anterior curvature and increased robusticity when compared with the other samples (females only). High bilateral asymmetry in the greater tuberosity breadth indicates localised differences in the activity patterns of the shoulder. The high bilateral asymmetry in the minimum diaphyseal circumference further identifies the systemic response of preferential mechanical loading from unimanual activity.

The Hickleton (male) sample is characterised by increased M/L bowing in conjunction with an increased anterior curvature angle. Articular dimensions are relatively increased, as are greater tuberosity breadth, greatest breadth at the deltoid tuberosity and epicondylar breadth. The sample demonstrates a rounder diaphyseal midshaft section and increased humeral robusticity. Asymmetry is low in greater tuberosity breadth and epicondylar breadth but high in the distal articular surface. The female sample is characterised by reduced distal diaphyseal bowing, but increased medio-lateral diaphyseal bowing. The maximum cubital angle is significantly increased. Both robusticity indicators at the deltoid tuberosity, the greatest breadth and the deltoid index, indicate reduced activity involving this muscle when compared with the other

samples. Finally, asymmetry is also reduced in minimum humeral circumference, indicating little activity variation between limbs, as well as little regionalised variation related to differential joint function.

The Chichester male sample is characterised by reduced measurements of bowing, including the anterior curvature angle. It has a relatively reduced distal articular region. Maximum humeral length is reduced as is the midshaft index, indicating a flattened diaphysis at 50%. The Chichester female sample, in contrast, demonstrates increased distal diaphyseal bowing, although it has a reduced greater tuberosity breadth. Humeral robusticity is high in this sample as is the extent of asymmetry at the epicondyles, indicating differential use patterns between limbs at the elbow.

The Terry collection is characterised by reduced proximal and M/L diaphyseal bowing, but increased distal bowing of the humeral diaphysis. This sample demonstrates regionalised differences in articular dimensions, with an increased trochlear breadth, but reduced capitular index, indicating a broad capitulum. The distal articular surface is increased when standardised by the epicondylar breadth. Robusticity measurements related to muscle insertions vary inversely. The breadth of the greater tuberosity is significantly increased, but the two measurements of the deltoid tuberosity, the greatest breadth and the deltoid index, are reduced in comparison with the other samples. Asymmetry in humeral length is high, but reduced in the distal articular surface when compared with the other populations.

The Fishergate blade-injured sample demonstrates increased proximal and distal bowing, but decreased medio-lateral bowing. The size of the humeral head is reduced in this sample when compared with the others. Humeral length is increased, but the breadth

at the greater tuberosity is decreased when compared with the other samples. The deltoid index, however, is increased and the midshaft morphology is flattened compared with other samples. Asymmetry is high in the maximum humeral length and in the minimum humeral circumference, a systemic response to increased mechanical loading indicating a strong limb dominance bias. These results possibly indicate increased mechanical loading from post-adolescent periods.

The Fishergate eastern cemetery sample demonstrates high proximal bowing, but falls intermediately in the other diaphyseal bowing measurements. The trochlear breadth is reduced, as is the distal articular surface when standardised against epicondylar breadth. Humeral robusticity is increased in this sample, as is deltoid robusticity. Asymmetry is high in humeral length, but low in epicondylar breadth. The females, though, demonstrate low distal and medio-lateral diaphyseal bowing, as well as a low degree of anterior curvature. Humeral length is reduced, as is the asymmetry of this value, while the breadth of the greater tuberosity is increased.

The males from the intramural cemetery at Fishergate fall intermediately in the most variables, although they do demonstrate a moderately high amount of M/L diaphyseal bowing. Trochlear breadth is reduced, as is the distal articular surface when standardised by the epicondylar breadth. Humeral robusticity is low, although the epicondylar and deltoid tuberosity measurements are increased. Asymmetry is high in the greater tuberosity, indicating differential activity patterns across the shoulder, but low in the distal articular breadth. The females demonstrate high proximal diaphyseal bowing in this sample, but have a low humeral robusticity index value. The deltoid robusticity index is also increased. Asymmetry is high in humeral length, epicondylar

breadth and the distal articular breadth, indicating different activity patterns involving the elbow and forearm.

The males from the Fishergate southern cemetery are characterised by low proximal diaphyseal bowing, as well as a reduced trochlear breadth and distal articular breadth, whether standardised by humeral articular length or epicondylar breadth. The maximum humeral length is low, and the midshaft diaphysis is more rounded compared with the other samples. Asymmetry is high in the epicondylar breadth and distal articular breadth, indicating different use patterns at the elbow. The females also demonstrate low proximal diaphyseal bowing, but have increased maximum humeral length, as well as increased dimensions in both measurements of the deltoid tuberosity. Asymmetry is high in both the humeral length and greater tuberosity breadth.

Significant differences in the levels of asymmetry between human and non-human primate species have been identified. The males differ significantly in the levels of asymmetry in the maximum humeral length, breadth of the greater tuberosity, minimum diaphyseal circumference and distal articular breadth, but not epicondylar breadth. The females differ significantly in the maximum humeral length, breadth of the greater tuberosity, minimum diaphyseal circumference and epicondylar breadth, but not the distal articular breadth. There were no significant differences identified in the levels of asymmetry between males and females of the human samples analysed, although the females demonstrated elevated asymmetry levels when compared with the males. Analysis of side dominance identified more individuals with a left-side bias than would be expected given current population averages for right-handedness. Most samples averaged around 20% of left-side dominance compared with an average of around 10% for modern populations. This may suggest that modern values of right-handedness

reveal a proportion increased either ontogenetically or one that is culturally motivated. Comparisons of humeral robusticity as indicated by J values and the humeral torsion index with side dominance identify increased strength of the left humerus, but a right-side preferential handedness as interpreted by limb asymmetry in the Towton population.

Examination of humeral torsion and the spiral angle was unable to consistently determine a relationship between these two variables. A significant (negative) correlation was identified in the Wharram Percy and Chichester samples. These results indicate that the spiral angle increases as the humeral head becomes more medially directed in these samples. Examination of the humeral torsion angle and its relationship with humeral robusticity was also unable to identify any consistent relationship. Following the identification of increased humeral torsion angles in professional athletes, indicating that increased angles are correlated with increased robusticity, a hypothesis was formed seeking to identify increased humeral torsion angles with increased humeral robusticity in the archaeological populations. Despite a significant positive correlation identified in the Mary Rose, Wharram Percy, Fishergate eastern and Fishergate southern cemeteries, the results in this analysis are not consistent enough to fully support this hypothesis. The degree of anterior curvature, quantifying a valgus deformity - a laterally deviated distal end - appears to directly influence humeral torsion angles, although the Towton sample appears to indicate a separate phenomenon occurs that acts to reduce the humeral torsion angle.

The results of this study indicate that differences in morphology and robusticity may be used to identify differences in habitual activity patterns between archaeological and modern populations. The heterogeneous nature of the samples, with no consistent

patterns, indicates, though, that the population samples are not consistently drawn from similar backgrounds. There is no clear morphological pattern associated with or isolated to the blade-injured or combat-related samples. The Towton population appears largely unique its suite of humeral modifications. These changes likely result from pre-adolescent activity patterns, as do those occurring in the Mary Rose sample, while those changes characterising the Fishergate blade-injured sample likely come from post-adolescent stages.

Comparison of the combatant-related samples with the remaining populations as a whole identifies diaphyseal shape and articular size – especially at the distal end of the humerus - rather than robusticity as most dissimilar between groups. It is the Mary Rose sample, however, and not the blade-injured group that demonstrate the greatest differences in humeral morphology when compared with the non blade-injured group. All combat-related samples have significantly increased humeral length compared with the non blade-injured group, indicating that these men may have been intentionally selected for combat, based on physical size. The high number of outliers in each population sample indicates that individuals, rather than groups, may have been behaving in a manner similar to that associated with professional athletes, with increased levels of strenuous activity.

Table 7.2: Descriptive statistics, all measurements of skeletal variation (males only).

Collection	Measurement	N	Min	Max	Mean	S.D.
Towton	HPBW	44	4.42	18.59	9.99	3.17
	HDBW	45	.06	21.72	9.25	6.05
	HML	44	15.03	26.78	20.39	2.92
	MXCB	45	96.00	108.00	102.92	2.97
	ANTCV	45	1.00	18.00	6.23	3.35
	DIAPFLAT	53	.538	.839	.683	.07
	HTBST	45	7.32	10.42	8.70	.65
	HEAD	45	12.46	15.33	13.54	.62
	DAB	45	12.81	16.52	14.58	.86
	CAPIT	53	47.21	96.56	85.46	4.31
	ARTEPI	46	69.64	92.94	75.06	4.11
	HL	45	302.00	376.00	337.49	17.39
	HGTST	44	9.55	13.39	10.73	.76
	HGBDST	45	6.23	8.82	7.51	.51
	MIDSHAFT	52	68.30	93.81	80.86	5.48
	HROB	45	17.02	22.73	20.63	.97
	EPIC	41	17.12	21.80	19.06	1.07
	DELT	53	23.59	36.49	29.17	2.78
Mary Rose	HPBW	163	6.92	14.68	10.55	1.53
	HDBW	161	2.62	33.00	16.56	4.65
	HML	162	13.86	31.88	21.23	3.00
	MXCB	161	95.00	114.00	102.60	3.61
	ANTCV	164	1.00	10.00	4.82	1.30
	DIAPFLAT	164	.546	.858	.668	.06
	HTBST	164	6.19	10.73	9.00	.66
	HEAD	163	11.95	15.27	13.41	.61
	DAB	163	12.78	17.04	14.75	.84
	CAPIT	165	79.01	115.12	89.80	5.66
	ARTEPI	165	65.59	95.31	74.27	3.75
	HL	165	297.00	380.00	332.48	15.91
	HGTST	162	8.85	12.34	10.67	.65
	HGBDST	164	6.02	9.63	7.35	.58
	MIDSHAFT	166	69.67	93.09	80.90	4.79
	HROB	165	17.58	23.55	20.17	1.16
	EPIC	165	15.09	22.03	19.45	1.08
	DELT	164	23.07	34.25	29.91	1.83
Wharram Percy	HPBW	144	4.57	14.53	10.29	1.70
	HDBW	142	1.61	32.81	15.45	5.65
	HML	149	12.68	26.95	20.49	2.88
	MXCB	147	95.00	110.00	102.73	3.04
	ANTCV	153	2.00	10.00	4.99	1.39
	DIAPFLAT	163	.548	.786	.660	.05
	HTBST	152	7.45	10.67	8.98	.54
	HEAD	147	12.07	15.61	13.60	.65
	DAB	152	12.53	17.34	14.67	.74
	CAPIT	160	69.90	104.23	87.00	5.30
	ARTEPI	158	65.86	86.68	72.50	3.13
	HL	156	278.00	364.00	327.57	16.63
	HGTST	139	9.00	13.96	10.67	.71
	HGBDST	156	6.00	8.77	7.43	.52
	MIDSHAFT	164	66.52	92.12	80.92	5.00
	HROB	156	17.56	22.54	20.08	1.06
	EPIC	151	16.63	22.28	19.75	1.03
	DELT	164	23.24	33.80	29.80	1.89

Hickleton	HPBW	15	7.45	13.85	9.99	1.87
	HDBW	14	3.86	20.73	13.80	4.40
	HML	15	18.23	24.90	21.23	2.02
	MXCB	13	97.00	107.00	102.46	2.55
	ANTCV	14	3.00	12.00	6.43	2.44
	DIAPFLAT	15	.577	.759	.673	.05
	HTBST	14	7.96	9.60	8.95	.43
	HEAD	15	13.33	15.67	14.15	.77
	DAB	14	14.42	16.33	15.02	.57
	CAPIT	14	81.80	103.02	90.90	5.58
	ARTEPI	14	67.09	78.78	74.28	3.63
	HL	15	291.00	336.00	318.60	14.94
	HGTST	14	10.43	12.12	11.08	.56
	HGBDST	15	6.83	8.50	7.67	.46
	MIDSHAFT	16	72.34	91.44	82.39	5.64
	HROB	15	18.24	22.36	20.18	1.23
	EPIC	14	18.40	21.26	19.94	.90
	DELT	16	25.25	32.88	30.13	2.38
Chichester	HPBW	157	5.15	14.37	9.77	1.49
	HDBW	150	3.05	28.22	15.66	4.70
	HML	179	12.70	27.66	19.82	2.75
	MXCB	182	88.00	110.00	102.60	3.12
	ANTCV	189	1.00	10.00	5.12	1.61
	DIAPFLAT	207	.517	1.018	.676	.07
	HTBST	190	7.52	10.19	8.70	.53
	HEAD	159	11.81	15.42	13.46	.70
	DAB	180	12.55	6.36	14.40	.75
	CAPIT	190	75.47	109.13	88.87	6.30
	ARTEPI	173	64.87	80.45	72.41	2.86
	HL	196	275.00	368.00	323.14	17.00
	HGTST	154	8.79	12.69	10.64	.77
	HGBDST	191	5.97	9.23	7.43	.59
	MIDSHAFT	213	64.24	95.21	79.24	5.05
	HROB	194	17.12	23.58	19.95	1.29
	EPIC	164	16.91	21.95	19.57	1.02
	DELT	209	23.07	38.82	29.80	2.38
Terry collection	HPBW	356	5.84	16.00	9.94	1.67
	HDBW	356	1.97	34.94	18.55	5.48
	HML	358	11.70	28.45	19.67	2.97
	MXCB	351	87.00	111.00	102.11	3.37
	ANTCV	357	2.00	8.00	5.16	1.26
	DIAPFLAT	358	.516	.924	.678	.06
	HTBST	358	7.32	11.67	8.92	.64
	HEAD	355	11.28	15.59	13.57	.68
	DAB	357	12.08	18.58	14.59	.86
	CAPIT	358	72.52	100.11	84.60	4.91
	ARTEPI	355	66.82	84.61	74.00	3.23
	HL	358	285.00	383.00	331.91	17.51
	HGTST	358	8.29	13.32	10.93	.75
	HGBDST	358	5.47	9.12	7.26	.60
	MIDSHAFT	358	64.68	95.94	80.40	5.16
	HROB	357	15.51	23.72	20.04	1.38
	EPIC	356	16.13	22.79	19.28	1.07
	DELT	358	22.78	34.48	28.99	2.05
Fishergate blade-injured	HPBW	25	7.07	12.81	10.22	1.53
	HDBW	25	6.87	32.06	18.88	7.03
	HML	25	13.42	24.88	19.11	3.38

	MXCB	25	90.00	108.00	99.68	3.70
	ANTCV	25	2.00	11.00	5.48	2.49
	DIAPFLAT	32	.444	.997	.657	.10
	HTBST	25	7.86	9.60	8.64	.52
	HEAD	24	12.13	14.72	13.24	.60
	DAB	25	13.23	16.13	14.36	.72
	CAPIT	32	73.41	96.53	87.68	4.80
	ARTEPI	31	67.62	79.00	72.71	2.74
	HL	26	310.00	378.00	341.42	16.27
	HGTST	24	9.40	11.78	10.54	.58
	HGBDST	26	6.59	8.44	7.39	.46
	MIDSHAFT	32	71.68	88.63	79.59	4.31
	HROB	26	17.76	21.29	19.62	1.01
	EPIC	25	17.50	21.99	19.39	1.21
	DELT	31	26.15	35.91	32.04	2.26
Fishergate eastern cemetery	HPBW	55	6.68	13.71	10.20	1.62
	HDBW	55	5.77	26.06	15.48	4.69
	HML	55	14.33	26.13	20.16	2.91
	MXCB	55	92.00	110.00	103.24	3.95
	ANTCV	55	.00	12.00	5.31	2.71
	DIAPFLAT	58	.532	.785	.662	.06
	HTBST	55	7.37	9.85	8.57	.58
	HEAD	54	12.18	15.13	13.63	.71
	DAB	56	12.47	16.05	14.38	.84
	CAPIT	56	72.00	100.55	86.89	6.31
	ARTEPI	55	60.16	78.85	71.96	2.95
	HL	55	286.00	361.00	328.82	18.05
	HGTST	53	9.43	12.26	10.74	.69
	HGBDST	55	5.95	8.68	7.45	.65
	MIDSHAFT	59	72.24	97.06	82.36	5.50
	HROB	55	16.71	22.19	19.40	1.37
	EPIC	53	17.08	21.42	19.67	.96
	DELT	58	27.58	38.42	32.48	2.33
Fishergate intramural cemetery	HPBW	86	7.08	13.46	9.99	1.40
	HDBW	86	4.16	25.78	13.58	4.66
	HML	87	14.34	28.01	21.27	2.67
	MXCB	85	94.00	115.00	103.66	3.63
	ANTCV	88	1.00	15.00	5.45	2.30
	DIAPFLAT	103	.582	.804	.676	.05
	HTBST	88	7.55	9.67	8.64	.44
	HEAD	87	12.03	16.18	13.63	.69
	DAB	86	13.05	16.63	14.60	.72
	CAPIT	97	77.21	111.21	87.73	5.50
	ARTEPI	94	65.24	84.70	71.85	2.99
	HL	90	282.00	357.00	327.53	14.40
	HGTST	82	8.94	13.74	10.85	.73
	HGBDST	89	6.24	9.35	7.48	.55
	MIDSHAFT	102	67.68	96.87	80.47	5.63
	HROB	90	16.72	24.11	19.66	1.19
	EPIC	86	17.58	23.74	19.95	1.16
	DELT	101	27.76	39.09	31.80	2.51
Fishergate southern cemetery	HPBW	34	6.97	12.84	9.85	1.72
	HDBW	34	4.72	25.14	13.68	6.00
	HML	32	15.73	28.79	20.07	2.43
	MXCB	32	88.00	109.00	101.59	4.58
	ANTCV	33	2.00	12.00	5.79	2.57
	DIAPFLAT	40	.589	.861	.683	.07

	HTBST	34	7.13	9.78	8.51	.65
	HEAD	31	12.24	14.97	13.60	.75
	DAB	32	12.75	15.63	14.40	.74
	CAPIT	37	70.43	100.82	86.65	6.10
	ARTEPI	39	65.02	78.43	72.04	3.32
	HL	34	307.00	345.00	329.21	11.45
	HGTST	30	9.41	11.93	10.84	.65
	HGBDST	33	6.69	8.53	7.48	.426
	MIDSHAFT	42	70.84	98.54	82.02	.33
	HROB	33	17.75	21.90	19.74	1.03
	EPIC	32	17.96	21.39	19.66	.86
	DELT	40	24.91	36.13	30.78	2.46

Table 7.7: Descriptive statistics, all measurements of skeletal variation, martial-related samples.

Collection	N	N	Min	Max	Mean	S.D.
Non blade-injured	HPBW	840	4.57	16.00	9.98	1.63
	HDBW	830	1.61	24.94	16.53	5.56
	HML	869	11.70	28.79	20.04	2.89
	MXCUB	859	87.00	115.00	102.52	3.41
	ANTCV	883	.00	15.00	5.20	1.69
	DIAPFLAT	934	.516	1.018	.674	.06
	HTBST	884	7.13	11.67	8.82	.60
	HEAD	842	11.28	16.18	13.58	.69
	DAB	868	12.08	18.58	14.55	.81
	CAPIT	907	69.90	111.21	86.54	5.78
	ARTEPI	878	60.16	86.68	73.00	3.23
	HL	897	275.00	383.00	328.31	17.10
	HGTST	824	8.29	13.96	10.81	.75
	HGBDST	890	5.47	9.35	7.38	.58
	MIDSHAFT	946	64.24	98.54	80.47	5.31
	HROB	893	15.51	24.11	19.95	1.29
	EPIC	849	16.13	23.74	19.53	1.07
	DELT	937	22.78	39.09	29.91	2.42
Mary Rose	HPBW	163	6.92	14.68	10.55	1.53
	HDBW	161	2.62	33.00	16.56	5.65
	HML	162	13.86	31.88	21.23	3.00
	MXCUB	161	95	114.00	102.60	3.61
	ANTCV	164	1.00	10.00	4.82	1.30
	DIAPFLAT	164	.546	.858	.668	.06
	HTBST	164	6.19	10.73	9.00	.66
	HEAD	163	11.95	15.27	13.41	.61
	DAB	163	12.78	17.04	14.75	.84
	CAPIT	165	79.01	115.12	89.80	5.66
	ARTEPI	165	65.59	95.31	74.27	3.75
	HL	165	297.00	380.00	332.48	15.91
	HGTST	162	8.85	12.34	10.67	.65
	HGBDST	164	6.02	9.63	7.35	.58
	MIDSHAFT	16	69.67	93.09	0.90	4.79
	HROB	165	17.58	23.55	20.17	1.16
	EPIC	165	15.09	22.03	19.45	1.08
	DELT	164	23.07	34.25	29.91	1.83
Blade-injured	HPBW	76	4.42	18.59	10.10	2.58
	HDBW	77	.06	32.06	12.83	7.68
	HML	75	13.42	26.78	20.02	305
	MXCUB	76	90.00	108.00	101.95	3.52
	ANTCV	76	1.00	18.00	5.89	3.02
	DIAPFLAT	95	.444	.997	.672	.08
	HTBST	77	7.32	10.42	8.69	.59
	HEAD	76	12.03	15.33	13.45	.64
	DAB	77	12.81	16.52	14.50	.79
	CAPIT	96	73.41	96.56	86.55	4.50
	ARTEPI	88	65.39	92.94	73.88	3.75
	HL	78	302.00	378.00	338.00	16.84
	HGTST	74	9.40	13.39	10.66	.71
	HGBDST	78	6.23	8.82	7.46	.49
	MIDSHAFT	92	68.30	93.81	80.35	5.02
	HROB	78	17.02	22.73	20.19	1.10
	EPIC	73	17.12	21.99	19.27	1.17
	DELT	93	23.59	37.91	30.29	2.96

Table 7.8: Descriptive statistics, all measurements of skeletal variation (females only).

Collection	Measurement	N	Min	Max	Mean	S.D.
Wharram Percy	HPBW	92	5.98	12.96	9.40	1.35
	HDBW	93	2.36	25.04	12.25	4.41
	HML	92	12.66	25.11	17.56	2.51
	MXCB	93	95.00	109.00	102.13	2.58
	ANTCV	97	3.00	8.00	5.12	1.24
	DIAPFLAT	100	.562	.831	.683	.06
	HTBST	94	6.92	9.72	8.24	.52
	DAB	90	11.63	15.63	13.83	.75
	HEAD	90	11.49	14.13	12.93	.57
	ARTEPI	92	66.77	79.75	72.14	2.79
	CAPIT	92	75.10	99.29	87.13	5.07
	HGTST	91	8.44	11.71	10.23	.61
	HGBDST	96	6.03	8.90	7.13	.55
	EPIC	90	16.97	21.26	18.78	.95
	HL	97	262.00	331.00	300.40	14.71
	MIDSHAFT	102	64.89	88.96	79.45	5.24
	HROB	97	16.62	22.26	19.19	1.26
	DELT	101	22.36	35.21	29.23	2.38
Hickleton	HPBW	15	7.26	11.94	8.81	1.32
	HDBW	15	2.06	19.97	8.00	4.43
	HML	15	15.65	22.20	18.74	2.02
	MXCB	15	101.00	109.00	105.13	2.53
	ANTCV	15	2.00	11.00	4.80	2.18
	DIAPFLAT	16	.95	.785	.689	.05
	HTBST	15	7.42	8.40	7.94	.28
	DAB	15	12.66	14.72	13.63	.57
	HEAD	14	12.62	13.51	12.99	.28
	ARTEPI	15	67.14	76.21	71.86	2.73
	CAPIT	16	73.56	96.59	89.19	5.66
	HGTST	15	9.51	11.65	10.26	.64
	HGBDST	15	6.06	7.64	6.90	.42
	EPIC	14	18.01	19.46	18.67	.53
	HL	15	281.00	322.00	304.73	12.62
	MIDSHAFT	16	67.17	84.89	77.70	4.64
	HROB	15	17.19	20.79	18.34	1.06
	DELT	16	22.50	32.81	26.91	2.60
Chichester	HPBW	43	5.64	11.79	8.75	1.33
	HDBW	41	4.66	23.04	13.57	4.43
	HML	60	11.49	21.29	16.75	2.08
	MXCB	64	96.00	107.00	101.53	2.36
	ANTCV	66	2.00	9.00	5.12	1.70
	DIAPFLAT	78	.561	.998	.703	.07
	HTBST	67	6.67	9.38	8.18	.50
	DAB	62	12.38	14.92	13.56	.67
	HEAD	46	11.48	13.79	12.68	.56
	ARTEPI	58	67.38	81.06	73.10	3.27
	CAPIT	67	76.90	103.10	91.29	5.55
	HGTST	48	8.71	11.21	10.04	.56
	HGBDST	68	6.04	8.53	7.14	.56
	EPIC	55	15.79	20.36	18.33	1.17
	HL	68	273.00	334.00	302.98	13.43
	MIDSHAFT	80	64.19	91.69	77.80	6.38
	HROB	68	16.62	22.94	19.16	1.15
	DELT	79	24.97	33.71	28.89	2.19

Fishergate intramural cemetery	HPBW	24	6.49	12.03	9.48	1.60
	HDBW	23	5.81	23.82	12.71	4.59
	HML	24	12.76	23.38	18.00	2.65
	MXCB	23	98.00	107.00	102.41	2.57
	ANTCV	23	1.00	8.00	4.22	2.07
	DIAPFLAT	29	.568	.812	.702	.07
	HTBST	21	6.67	9.05	7.99	.67
	DAB	22	11.79	15.65	13.79	.94
	HEAD	24	11.81	13.91	12.75	.61
	ARTEPI	26	65.98	84.29	73.13	3.32
	CAPIT	24	80.31	98.73	87.89	4.56
	HGTST	22	8.93	11.03	10.14	.66
	HGBDST	23	5.56	8.40	6.92	.69
	EPIC	21	17.13	20.60	18.59	.97
	HL	24	281.00	325.00	303.92	11.99
	MIDSHAFT	29	63.12	88.82	79.87	6.03
	HROB	24	15.63	20.13	17.80	1.04
	DELT	28	24.42	38.13	30.33	3.06
Fishergate southern cemetery	HPBW	12	7.30	9.83	8.52	.88
	HDBW	12	4.41	15.00	9.10	3.50
	HML	11	10.98	21.66	18.14	2.89
	MXCB	12	100.00	105.00	102.92	1.56
	ANTCV	12	1.00	8.00	4.08	2.19
	DIAPFLAT	14	.572	.808	.694	.07
	HTBST	12	6.61	8.92	8.14	.69
	DAB	12	11.75	15.28	13.87	1.05
	HEAD	10	12.09	14.03	12.99	.63
	ARTEPI	13	67.78	78.64	72.33	3.15
	CAPIT	12	80.11	100.87	89.14	7.25
	HGTST	11	9.31	11.17	10.43	.58
	HGBDST	11	6.55	7.87	7.33	.49
	EPIC	12	16.05	20.38	18.80	1.33
	HL	12	283.00	326.00	308.42	12.44
	MIDSHAFT	13	67.74	87.69	78.65	6.77
	HROB	11	15.91	20.14	18.72	1.39
	DELT	13	26.30	35.40	31.70	2.38

Table 7.25: Descriptive statistics, bilateral asymmetry (all populations).

Sex	Collection	Measurement	N	Min	Max	Mean	S.D.
Males	Towton	HL	14	.00	2.92	.95	.73
		HGT	17	.34	12.62	4.38	3.65
		HC	22	.00	6.71	2.80	2.13
		HEB	17	.06	14.90	2.43	3.37
		HDAB	21	.33	9.67	2.47	1.97
	Mary Rose	HL	27	.00	2.38	.93	.75
		HGT	26	.45	8.95	3.32	2.44
		HC	28	.00	6.25	2.37	1.86
		HEB	28	.17	20.42	2.75	4.00
		HDAB	28	.02	18.06	3.30	3.56
	Wharram Percy	HL	70	.00	3.57	1.26	.91
		HGT	59	.25	13.88	4.85	3.22
		HC	78	.00	9.09	2.68	1.84
		HEB	73	.02	6.32	1.69	1.33
		HDAB	75	.00	17.97	2.41	2.79
	Hickleton	HL	7	.63	1.85	1.20	.41
		HGT	7	.06	7.45	2.69	2.91
		HC	8	.00	3.28	1.55	1.44
		HEB	7	.22	3.50	1.42	1.06
		HDAB	7	.32	9.98	2.74	3.55
	Chichester	HL	74	.00	12.70	1.42	1.55
		HGT	53	.03	13.38	3.91	3.56
		HC	93	.00	20.90	2.84	2.71
		HEB	62	.02	10.72	2.37	2.36
		HDAB	71	.04	6.77	2.09	1.53
	Terry	HL	177	.00	4.12	1.03	.83
		HGT	177	.00	12.46	4.34	3.12
		HC	177	.00	13.89	3.00	2.72
		HEB	176	.02	84.88	2.28	6.43
		HDAB	176	.02	10.15	2.09	1.73
	Gorilla sp.	HL	12	.00	3.60	1.24	1.07
		HGT	11	.10	5.92	2.09	1.77
		HC	12	.00	6.12	1.29	1.71
		HEB	12	.05	10.17	1.75	2.82
		HDAB	11	.10	1.83	.79	.54
	Pan sp.	HL	8	.00	1.39	.51	.49
		HGT	8	.09	5.23	2.77	1.83
		HC	8	.00	1.60	.75	.80
		HEB	8	.77	3.81	2.10	1.00
		HDAB	8	.41	2.65	1.42	.79
	Pongo sp.	HL	10	.00	1.31	.73	.44
		HGT	9	.33	4.42	2.60	1.44
		HC	10	.00	3.08	1.32	1.08
		HEB	10	.10	3.73	1.30	1.19
		HDAB	10	.20	2.95	1.48	.98
	Macaca sp.	HL	7	.00	3.64	1.13	1.38
		HGT	7	.15	36.49	7.47	12.92
		HC	7	.00	3.08	1.82	1.33
		HEB	7	1.86	7.95	4.10	2.18
		HDAB	6	.75	3.35	2.01	1.03
	Fishergate blade-injured	HL	14	.00	3.84	1.42	1.09
		HGT	11	.24	10.29	3.91	2.94
		HC	20	.00	5.88	2.89	1.72
		HEB	18	.11	4.73	1.60	1.31

		HDAB	18	.20	6.10	2.11	1.65
	Fishergate eastern cemetery	HL	20	.00	3.09	1.20	1.09
		HGT	21	.09	9.58	4.20	2.93
		HC	23	1.46	9.09	3.46	1.94
		HEB	21	.07	3.85	1.45	1.16
		HDAB	22	.41	4.19	2.17	1.30
	Fishergate intramural cemetery	HL	32	.00	3.86	1.07	.85
		HGT	29	.22	15.88	5.49	3.97
		HC	41	.00	8.33	2.80	1.92
		HEB	35	.10	3.88	1.47	1.01
		HDAB	36	.09	11.50	2.09	2.06
	Fishergate southern cemetery	HL	13	.00	2.97	1.24	1.01
		HGT	13	.18	9.19	4.36	3.10
		HC	19	.00	8.70	2.65	2.40
		HEB	17	.14	12.88	2.79	3.05
		HDAB	16	.45	6.49	2.74	2.13
Females	Wharram Percy	HL	42	.00	5.52	1.44	1.16
		HGT	38	.23	16.54	5.59	4.04
		HC	47	.00	9.07	2.27	1.82
		HEB	38	.14	4.88	1.62	1.13
		HDAB	39	.03	9.27	2.03	1.88
	Hickleton	HL	7	.33	2.58	1.36	.83
		HGT	7	.29	4.56	2.69	1.55
		HC	8	.00	3.23	1.41	1.26
		HEB	7	.37	3.06	1.56	.97
		HDAB	8	.38	3.17	1.78	.88
	Chichester	HL	24	.00	4.05	1.64	1.20
		HGT	13	1.61	9.37	4.88	2.67
		HC	37	.00	6.78	2.06	1.82
		HEB	21	.27	12.55	3.09	3.48
		HDAB	27	.08	9.02	2.44	2.13
	Gorilla sp.	HL	7	.00	1.81	.98	.70
		HGT	6	.57	2.84	1.71	.90
		HC	7	.00	2.74	1.57	.92
		HEB	7	.20	2.07	.82	1.82
		HDAB	7	.26	1.88	.91	.69
	Pan sp.	HL	4	.00	1.98	.93	.82
		HGT	4	.62	3.51	2.05	1.40
		HC	4	1.40	1.65	1.51	.12
		HEB	4	.51	1.74	1.09	.52
		HDAB	4	.33	1.87	.94	.66
	Pongo sp.	HL	3	.29	.96	.52	.38
		HGT	3	2.01	3.62	2.78	.81
		HC	3	.00	1.68	.56	.97
		HEB	3	12	1.75	1.15	.90
		HDAB	3	1.49	3.21	2.33	.86
	Macaca sp.	HL	3	.00	2.03	.97	1.02
		HGT	3	.09	.43	.23	.18
		HC	3	.00	.00	.00	.00
		HEB	3	1.10	3.89	2.53	1.40
		HDAB	3	1.04	4.35	2.87	1.68
	Fishergate intramural cemetery	HL	8	.31	5.56	2.14	1.72
		HGT	9	.56	11.94	4.05	3.34
		HC	13	.00	3.77	1.68	1.53
		HEB	11	.10	5.07	2.26	1.47
		HDAB	11	.55	14.98	4.20	4.32

	Fishergate southern cemetery	HL	3	2.49	2.69	2.60	.10
		HGT	4	4.13	8.43	5.92	2.0
		HC	4	.84	2.02	1.60	.53
		HEB	4	.61	3.37	1.64	1.23
		HDAB	4	.09	3.78	2.04	1.79

CHAPTER EIGHT

CONCLUSIONS

This thesis has examined humeral torsion as an osteogenic response to mechanical loading and has attempted to identify its role in the behavioural morphology of the upper limb. It has investigated how the differences in biomechanical forces alter shape and size (robusticity) in relation to habitual behaviour patterns in the humerus among the populations sampled. The results of this analysis identify significant differences in humeral morphology between later medieval and modern human population samples. It has also examined humeral morphology in a group of non-human primates to establish that the level of plasticity in these traits – alterations in size, shape and asymmetry - are unique to humans. The results identify adaptations to humeral form that may be inferred to result from differences in habitual use-patterns related to lifestyle.

8.1 Project Aims and Their Conclusions

This project integrated historical and biological data to identify the nature of morphological variation in humeral form in the context of activity and movement patterns. It has also investigated the physical results of participation in medieval warfare before the historically recorded advent of standing armies in the Late Medieval period (see Keen, 1999). This was addressed through four primary project aims.

Aim 1: The first aim of this project was to examine skeletal tissue dynamics and establish plasticity as an active phenomenon that adapts the shape and size of skeletal elements in response to physical activity (Chapter Two: Skeletal Tissue Dynamics). It was the objective of this chapter to discuss how both external and internal skeletal morphology is influenced by activity patterns. The focus of this project are changes between populations and individuals resulting from differences in functional

morphology brought about by differences in the individual's skeletal loading history. Specific questions included how the skeleton adapts to various loading and movement patterns, the validity of Wolff's Law of Bone Remodelling in bioarchaeological research and whether functional inferences drawn from adult human bone variation reflect patterns established in childhood or, later, in adulthood.

Conclusions: The skeleton adapts its structure to mechanical loading through the processes of modelling and remodelling. These processes adapt bone size and shape to meet the needs of typical peak mechanical loads. Modelling occurs during growth and increases bone strength to reduce high-level strains and to maintain bone strength in the face of typical peak strains. Mechanically-induced modelling is triggered when strains reach a set-point (1,500 – 2,500 microstrain). Remodelling is episodic and serves to replace bone or tissue. It appears to be triggered by smaller microstrain levels, around 100-300 microstrain (Frost 1987a).

The modelling process may be seen to adapt the skeleton to the specific loading patterns of the individual while remodelling is a process that fine-tunes the element to the mechanical demands placed upon it. These processes enable a causal relationship between skeletal architecture and functional loading. In limb bones, only the general form is developed and the process of functional loading adapts the architecture – the breadth, cortical thickness, cross-sectional geometry, curvature, mass and trabecular orientation all develop as an adaptive response to functional loading.

Recent debate has questioned the validity of Wolff's Law of Bone Remodelling. Wolff's Law recognises that skeletal tissue is dynamic and that elements have the ability to sense mechanical loading and to modify their structure to adapt to these loads. There

are a number of questions that have been raised regarding Wolff's Law, from whether it is truly a mathematical 'law' to the nature of trabecular bone organisation. However, the most relevant point for this discussion regards the nature of bone hypertrophy. One viewpoint holds that any increase in bone from experimental analyses results not from cortical expansion, but as a periosteal reaction to an irritant in the form of a strain gauge or other surgical device. In professional athletes, increased bone formation is attributed to an underlying injury (see Bertram and Swartz, 1991 for more). This project has examined the humerus directly, thus any periosteal reaction may be confidently identified and those elements have been excluded from the study. Therefore, any bone change identified is not from reactive periosteal bone formation, but through changes in cortical bone thickness. This work, then, refutes the claims that limb hypertrophy arises from periosteal reaction or other pathological conditions and supports the principle tenant of Wolff's Law regarding the mechanical adaptability of the human skeleton.

The last point to conclude regards the nature of the bone response from activity patterns established in childhood versus those established as an adult. Modelling in adult bone is reduced due to epiphyseal fusion and physiological maturity, while the level of remodelling slows down in adulthood. This raises the question of whether humeral form is adapted to loading patterns established in childhood. Growing bone is more responsive to fluctuations in mechanical loading (strains), therefore, any increases in the individual's activity level in pre-adolescence will have a greater effect on the bone than those incurred post-adolescence. The juvenile response to an increased strain environment is to increase cortical thickness via the periosteal envelope. Endosteal dimensions remain static, thus maintaining medullary canal size. The adult bone response to increased strains is the opposite, expanding the cortical thickness via the endosteal envelope. The total area of the bone will be largely static, but the medullary

canal dimension is reduced (Ruff *et al.*, 1994). Biomechanical analysis of the Towton sample has identified a different pattern, one of periosteal expansion, but the medullary canal appears to have responded with endosteal resorption, rather then remaining static. This pattern does not fit either age-related model. Historical and social information about these men indicates it is most likely that they were participating in weapon training from an early age, but these results indicate that the humeral form may have continued to adapt to its loading environment throughout the individual's lifetime. It is also possible that hyperactivity in youth leading to architectural change permanently alters the bone such that later responses in bone thickness and distribution are affected henceforth. Therefore, skeletal adaptation from the strain environment may not simply reflect activity levels and patterns during juvenile stages, but may be altered throughout the individual's lifetime.

Aim 2: The second aim of this project was to examine variability and asymmetry in humeral torsion and identify any patterns in the torsional angle related to inferred habitual movement patterns (Chapter 5: Humeral Torsion). The primary hypothesis was that the humeral torsion angle may be modified during the individual's lifetime by mechanical forces. The sports medicine literature links increased humeral torsion angles in the professional athlete to throwing. The hypothesis, then, is that an increased humeral torsion angle will be correlated with other indicators of increased activity in the same limb. Specific issues regarding humeral torsion include its relationship with robusticity. If an increased torsion angle is related to higher levels of activity in the humerus, are increased angles found in the more robust limb? Does the humeral torsion angle relate to largely static ontogenetic change, or is it influenced by mechanical processes as indicated by the clinical literature? Early anatomists believed the torsional process to be limited to the proximal humeral diaphysis. However, if humeral torsion is

related to the functional use of the limb, there is no reason to assume that it relates exclusively to the proximal humeral diaphysis, as both the proximal and distal axes may undergo modification due to biomechanical forces.

More general questions about the humeral torsion angle include whether there are differences between archaeological samples and how the humeral torsion angle and the levels of bilateral asymmetry found between limbs compares between the archaeological samples and the more recent Terry collection and the non-human primate species groups. Are there differences between sex and between right and left limbs? Is the size of the humeral torsion angle reflected in the spiral angle, a measure of the extension of the bicipital groove?

Conclusions: This analysis has identified significant differences both between and within population samples in the humeral torsion angle. The comparative samples of the Terry collection and the non-human primates demonstrate significant differences in the humeral torsion angle when compared to the archaeological populations. While the level of standardised asymmetry in humeral torsion angles was primarily non-significant between human and non-human primate samples, the level of bilateral asymmetry is lower in all non-human primate species when compared with the human samples. This indicates more homogeneous activity patterns, with little variation between limbs in the non-human primate samples due to locomotor constraints and restricted manipulative capacities when compared with those of humans. The remaining human samples indicate morphological variability which may indicate greater heterogeneity in activity patterns. Therefore, the humeral torsion angle does not appear to be ontogenetically constrained, but is highly variable between populations.

Within the archaeological and modern populations, there were no clear patterns identified according to inferred lifestyle as the rural Wharram Percy sample, for example, had one of the highest levels of bilateral asymmetry in the humeral torsion angle, while the similarly rural Hickleton sample had the lowest level of bilateral asymmetry. Neither were there consistent differences identified between sexes or between sides. Only three of the seven archaeological populations (the Wharram Percy, Fishergate eastern cemetery and Fishergate southern cemetery samples) demonstrated a significant difference between sexes and only one of the ten human samples (Fishergate eastern cemetery) demonstrated a significant difference between sides in the humeral torsion angle. This analysis indicates, then, that the humeral torsion angle is adaptive on the individual rather than the population level. This is in keeping with the findings in sports medicine studies that demonstrate significant differences between those accustomed to certain movements as opposed to those who are not.

This analysis investigated the relationship between the spiral angle, a measure of the direction of the bicipital groove and the humeral torsion angle. It was believed that torsion occurred in the proximal epiphysis, twisting the bicipital groove such that it follows a curved path down the humeral shaft rather than a presumed straight course that would result in the absence of a torsional process. The results from this analysis indicate that there is no consistent relationship between the humeral torsion angle and the spiral angle, as a significant relationship was only identified in two of the ten population samples (the Wharram Percy and Chichester samples).

The primary hypothesis that humeral torsion is adapted through strenuous activity can neither be demonstrated, nor refuted. The results indicate a complex relationship between humeral shape and robusticity. The hypothetical relationship

between increased humeral robusticity and humeral torsion has not been demonstrated in the majority of the samples. Analyses of external measurements identify a significant (positive) relationship, but in only four of the ten populations analysed (the Mary Rose, Wharram Percy, Fishergate eastern cemetery and Fishergate southern cemetery samples). One sample (Fishergate blade-injured) demonstrated a non-significant, negative correlation between humeral robusticity and the humeral torsion angle. This occurs because this sample, as a whole, has high humeral torsion angles, but low humeral robusticity values.

This project has attempted to identify the nature of adaptation in the humeral torsion angle, whether an increased or decreased angle is an acquired trait or one of genetic origin. The results of this analysis indicate that the humeral torsion angle does not appear to be ontogenetically constrained, but is adapted through biomechanical forces. One movement pattern that has been correlated with an increased humeral torsion angle is overhand throwing with force among high-level athletes. This creates a movement pattern in which the arm is abducted to an angle of at least 90° with the forearm and hand flexed and then rapidly extended. The inconsistencies in results do not refute the hypothesis that humeral torsion is an adaptive response to physical activity. Even though population samples may have similar social conditions, they are made up of individuals. It is likely that there are simply not enough individuals practicing a movement pattern within a population sample to register a significant difference. Or, equally, the lack of a statistically significant difference between some populations of different social standings may demonstrate an intrinsic similarity in movement patterns that disguises individual differences.

Further support for the argument that torsion is an acquired condition comes with the consideration of torsion and other architectural features of the humerus. The humeral torsion angle is correlated with the other measures of diaphyseal bowing, indicating that humeral torsion is perhaps not exclusive to the proximal or distal articular surfaces. Rather, it is influenced by or is actively influencing other architectural measures of bowing. A significant positive correlation between the degree of anterior curvature and the humeral torsion angle in six of the 10 populations (The Mary Rose, Wharram Percy, Chichester, Terry, Fishergate eastern cemetery and Fishergate southern cemetery) has been identified. Those samples that do not demonstrate a correlation between these variables (Towton, Hickleton, Fishergate blade-injured, and the Fishergate intramural cemetery) appear to be under the influence of a separate process occurring in the proximal humerus that counter-acts the increased anterior curvature angle in these samples. Interestingly, the amount of anterior bowing of the distal diaphysis (**HDBW**) is significantly correlated with the humeral torsion angle in every population sample with the exception of the Towton group. This sample demonstrates the lowest extent of distal bowing, possibly counter-acting the torsional architectural modifications in the humerus and thus reducing the humeral torsion angle.

Aim 3: The third aim of this project was to examine variations in diaphyseal robusticity, diaphyseal shape and bilateral asymmetry through analysis of humeral cross-sectional geometric properties (Chapter 6: Biomechanics). This involved examination of a subset of data from two blade-injured samples (Towton and Fishergate samples) and a comparative sample chosen to represent the normal range of variation found in the medieval period. The specific research question addresses the identification of movement patterns repeatedly performed during training for and involvement in armed conflict. A further goal was to identify what role architectural adaptations play in

mechanical competence. The biomechanical analysis may also help to identify any link between variation in humeral torsion angles and internal measurements of increased activity (total area, cortical thickness and diaphyseal robusticity) in these samples.

Conclusions: Differences have been identified in the patterns and levels of mechanical loading between blade-injured populations, as well as a representative sample of medieval society. Significant differences have been identified between blade-injured populations in the measurement of area, percent cortical area, and the measure of diaphyseal shape, Ix/Iy. While the Fishergate blade-injured and Fishergate comparative samples do not differ significantly in cross-sectional properties, the comparative sample has the most reduced measurements of area and second moments of area. The Towton and Fishergate comparative samples are significantly different in J and Imax. A pattern of fluctuating asymmetry in cross-sectional properties has been identified in the humerus where increased cortical area or greater robusticity (J) is found in the left distal slices. The increased CA and J then crosses-over to the right proximal slices in the same individual. This pattern has been identified in a few individuals from all population samples, although it is found most commonly in the Towton sample.

Significant differences in movement patterns have been identified through analyses of diaphyseal shape and appear to relate to differences between blade-injured samples in habitual behaviour at the shoulder and elbow. A single signature related to weapon-training has not been identified, although this most likely relates to changes in training or technology through time or simply individual preference in weapon use. The men of the Towton sample appear to have been engaged in a habitual movement pattern that preferentially loaded the left humerus when compared with the right. The greatest strains occur in the left distal humerus and the right proximal humerus. This pattern may

relate to a type of weapon requiring both hands, possibly a longbow, a weapon that gained increasing prominence in the Late Medieval period but was not employed earlier in the Medieval period. The blade-injured sample from Fishergate appears to have been engaged in a habitual movement pattern that creates right-side dominance. This pattern may relate to a unimanual weapon, held in the right hand, most likely a sword. This sword use is also reflected in the types of injuries sustained in this group, the grand majority coming from bladed weapons (Stroud and Kemp, 1993).

The role of architecture and mechanical competence has been identified in this project. The results of the biomechanical analysis in the Towton population indicate a two-stage process of humeral plasticity, one in which humeral shape is modified to accommodate powerful motions, initially, during the juvenile period when bone is most responsive. Normally, cortical thickness increases as these movements continue. If the shape is modified previously, however, such that it adequately compensates for increased force, there is no need for increased cortical thickness. Therefore, the men of the Towton sample appear to have an adapted architectural arrangement to their humeri that functions to more efficiently distribute strain. The results from this analysis imply that biomechanical adaptations may be life-long processes reflecting the biomechanical environment (or behaviours) of the key juvenile development period when architectural patterns become fixed. These architectural alterations then influence the extent and pattern of further bone modification.

Internal measurements of cross-sectional properties indicate that humeral torsion is correlated with strenuous activity as identified through limb hypertrophy. Hypertrophy is defined as increased total area (TA), cortical thickness (CA) and diaphyseal robusticity (J). However, this relationship is different depending upon the

sample analysed. In the blade-injured samples, there is a significant *negative* correlation between humeral torsion angles and all three measurements of hypertrophy. In the Towton and the Fishergate blade-injured samples, decreased humeral torsion angles, rather than the increased humeral torsion angles identified in the professional throwing athlete, are related to limb hypertrophy. The comparative sample, contrary to the blade-injured groups, does follow the model identified in professional throwing athletes. A significant *positive* correlation has been identified between increased TA, CA and J and humeral torsion angles. These results indicate that humeral torsion may be modified by strenuous activity, as identified by limb hypertrophy (increased total area, cortical area and diaphyseal robusticity), although the nature of the adaptation (i.e. increased or decreased humeral torsion angles) varies in relation to movement patterns that may not relate solely to rotational movements at the shoulder. In other words, the movement patterns here are not comparable to those of a professional, throwing athlete or those long-habituated to throwing.

Aim 4: The fourth and final aim of this project was to identify and examine osteometric differences in humeral morphology within and between population groups (Chapter 7: Analysis of Skeletal Variation). This was conducted through external measurements of architecture, articular size and robusticity, as well as analyses of bilateral asymmetry in these measurements. Unilateral limb asymmetry (limb dominance) was inferred through asymmetry in humeral length.

Conclusions: The results of this study indicate significant differences in measures of humeral morphology – architecture, articular size and robusticity - between and within sample groupings, as well as between sexes. Significant differences in the levels of asymmetry between human and non-human primate species have been identified. There

were no significant differences identified in the levels of asymmetry between males and females of the human samples analysed, although the females demonstrated elevated asymmetry levels when compared with those of the males. Analysis of side dominance identified more individuals with a left-side bias than found in current population averages, around 20% for most samples analysed, compared with an average of around 10% for modern populations.

The results of the external measurements confirm those identified in the biomechanical analysis. The Towton population stands out because of the architectural modifications to the distal humerus, most likely resulting from long-term training with weapons. The results are consistent with what may be expected from the use of a longbow, which exerts strain on the right shoulder (drawing limb) and the left elbow (of the bow-holding limb) as it stabilises the bow while drawing the arrow back in a right-handed individual (Fig. 8.1). The changes to humeral form in this population likely occur from pre-adolescent activity (up to 17 years of age, when epiphyseal growth ceases), although the unusual patterning of the biomechanical properties (periosteal expansion with endosteal resorption) indicates that humeral morphology may have been continually modified in adulthood or was never required due to previously acquired architectural features.

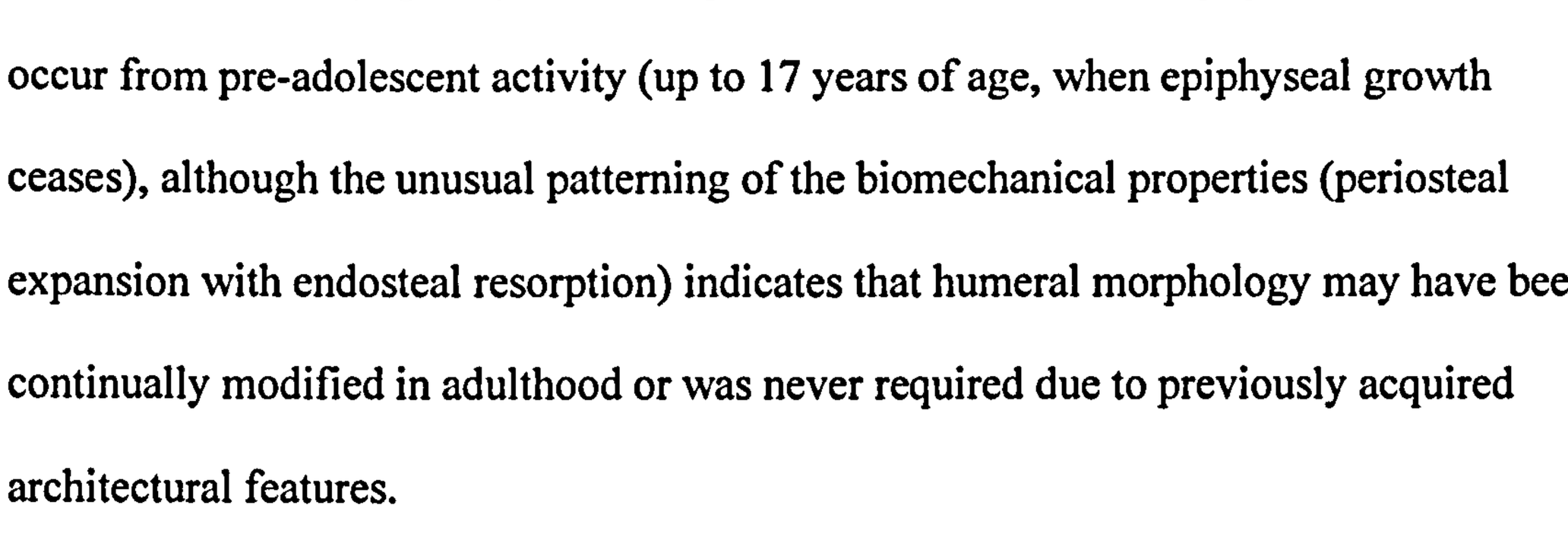

Figure 8.1: An archer in the shooting position. Drawing the string back brings the right arm from an internally rotated to an externally rotated position at the shoulder. The draw weight is transferred back to the shoulders in this position (image modified from Axford, 1995).

The results from the Fishergate blade-injured and Mary Rose samples do not identify any typical signature from presumed weapon use, as each combatant-related sample demonstrates its own suite of architectural modifications, although these results appear to identify the use of a unimanual weapon in the blade-injured men from Fishergate. Social and historical records indicate this would have been a sword. The changes in humeral form, including decreased bilateral asymmetry in distal articular breadth, likely originate from post-adolescent stages (17 years to 22 years, when diaphyseal growth ceases) in the Fishergate blade-injured sample, while the opposite is indicated in the Mary Rose sample. This sample demonstrates increased bilateral asymmetry in the distal articular breadth, indicating increased activity levels from a pre-adolescent stage, up to 17 years of age. The men from the *Mary Rose* demonstrate a mixed pattern of humeral morphology, not consistent with either the Towton or Fishergate blade-injured samples. If the men from the *Mary Rose* included longbow men, as indicated by Stirland (2000), they cannot be confidently identified as such in this analysis.

Combat-related individuals were investigated as a model for adaptations in humeral form in response to suspected strenuous activity patterns and weapon use. The activity patterns differ in all three samples (Towton, Fishergate blade-injured and Mary Rose), although biomechanical analysis identified limb hypertrophy in both the Towton and Fishergate blade-injured men when compared with a comparative sample. The increased humeral length found in all of these groups indicates that these men may have been selected based upon their size, or may have had access to better nutrition while training in youth. In seeking similar adaptations to humeral form from strenuous activity, this project has demonstrated the need for individual rather than population-based analyses. This study has demonstrated the heterogeneous nature of the population

samples, which obscures individual variation. Even those groups with a similar social make-up possess significant differences in humeral shape or robusticity, and most have individuals who stand out from the remaining population through increased or decreased values in mechanically relevant measurements. This analysis further demonstrates the information that may be gained by integrating the biological data with the social and historical record for a more complete picture of activity patterns in the past.

This research has contributed both to the field of biological anthropology, as well as having increased our knowledge of the combatant within medieval warfare. This work has created a baseline of population-specific information typical within the Middle Ages. From this, it is possible to identify individual differences as they relate to increased or even decreased activity levels. It has identified humeral torsion as an adaptation to strenuous movement patterns, as the level of variation within this trait indicates that it is not ontogenetically constrained. Significant differences in humeral torsion angles have been identified between species (human and non-human primates), between sexes and between sides. There appears to be no non-overlapping species-specific range of variation, as the Fishergate blade-injured and the Gorilla samples have similar values, for example. Humeral torsion appears to be a complex process, as it is not exclusive to the proximal shaft and is correlated with other measurements of diaphyseal bowing.

Biomechanical analyses indicate that humeral architecture may be adapted to more efficiently distribute increased strain. Furthermore, the results from the Towton population indicate that humeral morphology may continue to adapt to the strain environment throughout the individual's lifetime. Contributions to the field of medieval warfare include the identification of a pattern of biomechanical properties and external

morphology that likely relates to weapon-use, specifically, the longbow. Sword use is indicated in the Fishergate blade-injured sample, and the Mary Rose population appears to be made up of a more diverse group of men. There are no indications that longbowmen made up a significant part of this sample. This project has also identified the possible selection of individuals for combat based upon increased humeral size (indicating overall larger body size or increased height), or perhaps indicates that individuals who became involved in combat benefited from a better socio-economic environment during growth and development.

8.2 Recommendations for Future Work

The potential for continued research into the behavioural morphology of the humerus is limitless. There is the scope for a number of projects based upon this work. Differences in the behavioural morphology of the humerus may be investigated at key social transitions, or to identify differences in habitual behaviour in any culture. It may be used to build a model to identify changes to the humerus that might arise with throwing behaviour in hominids. Experimental analysis may be conducted to identify biomechanical signatures specific to weapon use. The pattern of skeletal change from weapon use may be further examined through a number of other non-pathological and pathological conditions. A limited study was conducted in this analysis.

There are a number of pathological alterations to the humerus that may be associated with weapon use. These include a medial epicondylar avulsion injury and lesions at the ulnar collateral ligament (UCL) at the elbow. An avulsion injury is a type of traction fracture that occurs at the insertion of a tendon or ligament that, when occurring in juvenile stages, results in a complete separation of the apophysis (Resnick *et al.*, 1995). The fracture may originate from either a single violent episode, or may

result from persistent stress or traction on an apophysis (Pavlov, 1995). Medial epicondylar avulsion fractures, such as those identified in this analysis, have been identified in youth "little league" baseball players aged 8 to 12 years and are caused by forceful termination of wrist flexion while pitching a baseball (Gugenheim *et al.*, 1976). This type of injury has been associated with archery in the Towton population (Knüsel, 2000) and may be a reliable indicator of weapon training.

There are three cases of medial epicondyle avulsions identified. The first is in the Towton sample, T16, left humerus. This specimen is a prime example of the modifications possible from strenuous activity patterns in the humerus. The left humerus has a low humeral torsion angle of 5° in the left humerus, but 27° in the right humerus. The avulsion injury is a complete separation of the apophysis, indicating that the fracture occurred during adolescence, before the epiphysis was fused. Additionally, this man has extensive antemortem blade trauma to the mandible indicating previous campaign experience. Fluctuating asymmetry has been identified in this individual in both the cross-sectional properties and the external measurements, with increased right proximal measurements and, in the contralateral limb, increased left distal measurements. If a suite of changes in any individual may indicate habitual longbow use, it would be these.

The second case of a medial epicondyle avulsion injury is found in the Mary Rose sample, MR7, left humerus. This case also involves full separation of the apophysis, indicating that the injury occurred during adolescence. The humeral torsion angle in the right humerus is 12°, the left is 9°, so the high level of asymmetry characterising T16 is not found in this individual, nor are the suite of changes to humeral morphology similar between individuals. The last specimen is CH136, right humerus,

from the *leprosarium* and almshouse at Chichester. This has been identified only as a probable case of a medial epicondyle avulsion injury, and occurs in a female with no skeletal signs of ill-health (Fay, 2002). There are no further distinguishing characteristics in this individual.

Strenuous or repetitive activity at the elbow may be identified through lesions or enthesophytes at the ulnar collateral ligament (UCL). This ligament is responsible for elbow stabilisation against valgus stress. Injuries to the ulnar collateral ligament are associated with overhead throwing with force, and are commonly found in baseball pitchers, javelin throwers and tennis players (Pavlov, 1995). From the data analysis, the Towton sample would be expected to exhibit pathological signs of a medial stress syndrome, however, there is a frequency of only 3.44% of this lesion in the left humerus (one out of 28 individuals, a disarticulated specimen) and none in the right. The Mary Rose sample has a frequency of 9.21% in the right humerus and 4.65% in the left. The Fishergate blade-injured sample only has one occurrence of this pathological condition, 5.26% of the sample. The highest frequency of lesions at the UCL is found in the Chichester female sample (right humerus 37.5%, left humerus 17.54%), although the males from this sample also have an increased frequency; 16.07% right, 8.40% left. The Wharram Percy sample also has elevated frequencies, 13.75% in the right humerus (males), 20.6% females, and in the left humerus, 1.2% (males), 11.11% females. The Hickleton sample, though, has no occurrence of this condition. Therefore, the presence of this lesion does not appear related to habitual weapon use.

Further identification of movement patterns may be inferred from pathological alterations to the skeleton related to strenuous or repetitive activity. A slipped humeral capital epiphysis (Salter-Harris Type I fracture) occurs from chronic stress related to

activity and has been linked to adolescent tennis players and gymnasts (Gregg and Torg, 1988; Dalldorf and Bryan, 1994). The presence of rotator cuff disease from an early age can help identify habitual movement patterns in the upper limb. Rotator cuff disease in younger individuals may indicate strenuous activity patterns at the shoulder (see Connell, 1994; Resnick, 1995 for more). Impingement syndrome of the shoulder may also be examined as a pathological record of habitual movement patterns (see Miles, 1999). This occurs when *M. supraspinatus* and *M. infraspinatus* are impinged as the arm is placed in 90° of abduction and maximal external rotation (Paley *et al.*, 2000). Humeral impingement has four known aetiologies: vascular insufficiencies, degenerative change, and most relevant, mechanical or shape problems, as well as trauma or overuse (Nevasier and Nevasier, 1990).

The biomechanical analysis may be expanded to include other population samples with a weapon-related context. This may either be through direct skeletal evidence of antemortem or perimortem weapon trauma, or through the archaeological context of weapon burials. The 'warrior' is archaeologically visible through inhumation with weapon inclusions across a broad temporal spectrum, from the Bronze Age to the Early Medieval period in Europe. Previously, such individuals have often been considered separate genetic or ethnic groups, as well as a physically active social stratum. Further application of biomechanical analyses may address the question of whether these and other 'warrior graves' represent symbolism in death related to the individual's social status in life or if the weapons relate to the physical reality of weapon use. It is thus possible to examine the individual for changes in activity patterns related to weapon use, rather than concentrating on the weapon itself.

APPENDIX I

MEASUREMENT DESCRIPTIONS

Measurement	Description	Instrument
Humerus: Maximum length (HL)	The direct distance from the most superior point on the humeral head to the most inferior point on the trochlea (Buikstra and Ubelaker, 1994).	Osteometric board
Humerus: Articular length (HAL)	The distance from the proximal surface of the humeral head to the distal most point on the lateral trochlear margin (Churchill, 1994).	Osteometric board
Humerus: Proximal bowing (HPBW)	This can be measured by placing the bone flat resting on the posterior surface and measuring the maximum height from the flat surface to the proximal posterior shaft.	Sliding callipers / depth gauge
Humerus: Distal bowing (HDBW)	Place the bone flat on the posterior surface and measure the height to the posterior margin of the trochlea.	Sliding callipers / depth gauge
Humerus: M/L bowing (HML)	A height measurement is taken with the bone lying stabilised on its lateral surface, with the greater tuberosity and lateral epicondyle supporting the bone. The maximum distance to the shaft is measured.	Sliding callipers / depth gauge
Humerus: Transverse head diameter (HTH)	The distance between the medial and lateral aspects of the humeral head (Knußmann, 1988).	Sliding callipers
Humerus: Greater tuberosity breadth (HGT)	The maximum distance between the anterior margin as marked by the bicipital groove and the posterior limit of the greater tubercle (Stirland, 1993).	Sliding callipers
Humerus: Deltoid tuberosity breadth (HDB)	After Endo (1971). The distance between the apices of the delimiting crests of the tuberosity taken at its maximum width location, approximately 5/12ths of humeral maximum length (Churchill, 1994).	Sliding callipers
Humerus: Deltoid tuberosity circumference (HDC)	Greatest circumference at the deltoid tuberosity, where it occurs.	Tape
Humerus: Greatest breadth at deltoid tuberosity (HGBD)	Greatest breadth, where it occurs, at the deltoid tuberosity (Knüsel, 2000a).	Sliding callipers
Humerus: Maximum diameter at midshaft (HMXM)	The maximum diameter of the humeral shaft occurring at the midshaft mark (Buikstra and Ubelaker, 1994).	Sliding callipers
Humerus: Minimum diameter midshaft (HMNM)	The minimum diameter of the humeral shaft occurring at the midshaft mark (Buikstra and Ubelaker, 1994).	Sliding callipers
Humerus: Minimum circumference (HC)	Minimum circumference where it occurs on the humeral shaft (Buikstra and Ubelaker, 1994).	Tape
Humerus: Distal diaphyseal	Breadth of the diaphysis in an A/P plane measured at 20% of the length from the distal	Sliding callipers

breadth (HDT)	articular surface.	
Humerus: Supracondylar breadth (HSB)	Supracondylar breadth taken at 20% from the distal articular surface.	Sliding callipers
Humerus: Epicondylar breadth (HEB)	The distance from the most laterally protruding point on the lateral epicondyle to the corresponding point on the medial epicondyle (Bass, 1987).	Sliding callipers
Humerus: Articular breadth of trochlea (HTB)	The distance from the medial margin of the trochlea to the groove between the capitulum and the trochlea (Carretero *et al.*, 1997).	Sliding callipers
Humerus: Capitulum height (HCH)	The direct distance between the most distal and most proximal points on the capitulum (Carretero *et al.*, 1997).	Sliding callipers
Humerus: Capitulum breadth (HCB)	Taken in the transverse axis of the capitulum, this is the direct distance between the most lateral point on the capitulum and the groove separating the capitulum and the trochlea (Carretero *et al.*, 1997).	Sliding callipers
Humerus: Distal articular breadth (HDAB)	The distance from the medial border of the trochlea to the lateral border of the capitulum as measured across the anterior aspect of the humerus (Knußmann, 1988).	Sliding callipers
Angles		
Torsion	Proximally, the point measured is the centre of the head. This can be measured distally in terms of the tangent elbow axis, or the transepicondylar axis (Boileau and Walch, 1997). Larson (1996) and Krahl and Evans (1945) measure the transverse articular axis for the distal plane.	Torsiometer
Maximum cubital angle	Stabilise bone on the posterior surface, with the distal articular surface against the rim of the board. The angle measured is that formed between the diaphyseal axis and the rim of the osteometric board. (Knußmann, 1988)	Osteometric table
Spiral angle	The angle between the proximal origin and the distal margin of the bicipital groove (Krahl, 1948)	Torsiometer
Anterior curvature	This angle is measured with the humerus placed in a holding device exposing the medial surface to the laser. The bone is oriented such that the beam at 0° (origin) bisects the diaphyseal axis through the midpoint of the humeral head and through the length of the shaft. The beam is then moved such that it bisects the distal transverse axis (midtrochlear) and the angle is read from the torsiometer.	Torsiometer
Pathological analysis		

Avulsion	A type of fracture relating to an attachment site of a tendon or ligament. In children or adolescence, this may be an entire apophysis (Resnick *et al.*, 1995). Note the location when occurring.	Visual identification
Ulnar collateral ligament (UCL)	Lesions or fossae may occur in the insertion of the ulnar collateral ligament on the medial epicondyle of the humerus. These are recorded when occurring.	Visual identification
Indices		
Humeral robusticity index	Least circumference of shaft X 100 / maximum length of the humerus (Bass, 1987).	
Diaphyseal flattening	Distal diaphyseal breadth of the humerus (taken at 20%) / Supracondylar breadth at same location.	
Humeral head	(Transverse humeral head diameter / Maximum length) X 100 (Vandermeersch and Trinkaus, 1995).	
Distal articular breadth	Distal articular breadth / Articular length X 100 (Vandermeersch and Trinkaus, 1995).	
Midshaft diaphyseal	Minimum diameter at midshaft / maximum diameter at midshaft (Vandermeersch and Trinkaus, 1995).	
Articular / epicondylar breadth	(Distal articular breadth / epicondylar breadth) X 100 (Vandermeersch and Trinkaus, 1995).	
Epicondylar	(Epicondylar breadth / humeral maximum length) X 100 (Carretero *et al.*, 1995).	
Capitular	(Capitulum breadth / capitulum height) X 100 (Carretero *et al.*, 1995).	
Deltoid Index	100 X (Deltoid tuberosity breadth / Deltoid tuberosity circumference) (Churchill & Smith 2000).	

APPENDIX 2

GLOSSARY OF TERMS

GLOSSARY OF TERMS

Abduction: the movement of a limb away from the body (Anderson and Anderson, 1995).

Adduction: the movement of a limb towards the body (Anderson and Anderson, 1995).

Anteversion: the position of an organ in which the organ is tilting forward (Anderson and Anderson, 1995).

Lateral rotation: movement turning away from the midline of the body (Anderson and Anderson, 1995).

Medial rotation: movement turning towards the midline of the body (Anderson and Anderson, 1995).

Osteoblast: a cell responsible for the formation of bone tissue (Anderson and Anderson, 1995).

Osteoclast: a multinucleated cell responsible for growth and repair. It functions by tunnelling through the surrounding tissue (Anderson and Anderson, 1995).

Pronation: the rotational movement of the forearm so that the palm faces downwards (Anderson and Anderson, 1995).

Retroversion: A condition where an organ is tipped backwards (Anderson and Anderson, 1995).

Supination: the rotational movement of the forearm so that the palm faces upwards (Anderson and Anderson, 1995).

REFERENCES CITED

Abbott S, Trinkaus E and Burr DB. 1996. Dynamic bone remodeling in Later Pleistocene Fossil hominids. Am J Phys Anthropol 99: 585-601.

Aiello L and Dean C. 1990. An introduction to human evolutionary anatomy. San Diego: Academic Press.

Anderson KN and Anderson LE. 1995. Mosby's pocket dictionary of nursing, medicine and professions allied to medicine. London: Mosby.

Ankel-Simons F. 2000. Primate anatomy. San Diego: Academic Press.

Ayton A. 1999. Arms, armour, and horses. In: Keen M, editor. Medieval warfare: a history. Oxford: Oxford University Press. p 86-208.

Axford R. 1995. Archery anatomy: an introduction to techniques for improved preformance. London: Souvenier Press.

Bass SL. 2000. The prepuberal years: a uniquely opportune stage of growth when the skeleton is most responsive to exercise. Sports Med 30: 73-78.

Bass WM. 1987. Human osteology: a laboratory and field manual (3rd edition). Columbia: Missouri Archaeological Society.

Ben-Itzhak S, Smith P and Bloom RA. 1988. Radiographic study of the humerus in Neandertals and *Homo sapiens sapiens*. Am J Phys Anthropol 77: 231-242.

Bertram JE and Swartz SM. 1991. The 'law of bone transformation': a case of crying Wolff? Biol Rev 66: 245-273.

Bigliani LU, Codd TP, Connor PM, Levine WN, Littlefield MA and Hershon SJ. 1997. Shoulder motion and laxity in the professional baseball player. Am J Sports Med 25: 609-613.

Bock WJ and Von Wahlert G. 1965. Adaptation and the form-function complex. Evolution 19: 269-299.

Boileau P and Walch G. 1997. The three-dimensional geometry of the proximal humerus: Implications for surgical technique and prosthetic design. J Bone Joint Surg 79-B: 857-865.

Boardman AW. 1998. The medieval soldier in the Wars of the Roses. Phoenix Mill: Sutton Publishing Ltd.

Boardman AW. 2000. The historical background to the battle and the documentary evidence. In: Fiorato V, Boylston A and Knüsel C, editors. Blood red roses: the archaeology of a mass grave from the Battle of Towton AD 1461. Oxford: Oxbow. p 15 – 28.

Boule M. 1911-1913. L'homme fossile de La Chapelle-aux-Saints. Ann. Palaeontol 6:111-172; 7:21-56, 85-192; 8: 1-70.

Bouvier M. 1985. Application of in vivo bone strain measurement techniques to problems of skeletal adaptations. Yearb Phys Anthropol 28: 237-248.

Bridges PS. 1989. Changes in activities with the shift to agriculture in the southeastern United States. Curr Anthropol 30: 385-394.

Broca P. 1881. La torsion de l'humerus at le tropometre. (Redige par L. Manouvrier.) Revue d'Anthrop. T. 4 p 193-210, 385–423.

Buikstra JE and Ubelaker DH. 1994. Standards for data collection from human skeletal remains: proceedings of a seminar at the Field Museum of Natural History. Fayetteville: Arkansas Archaeological Survey Press.

Burgess A. 2000. The excavation and finds. In: Fiorato V, Boylston A and Knüsel C, editors. Blood red roses: the archaeology of a mass grave from the Battle of Towton AD 1461. Oxford: Oxbow. p 29-36.

Burr DB. 1985. Symposium on current theoretical and experimental perspectives on bone remodeling mechanisms: introductory comments. Yearb Phys Anthropol 28: 207-209.

Burr DB and Martin RB. 1989. Errors in bone remodeling: toward a unified theory of metabolic bone disease. Am J Anat 186: 186-216.

Burr DB, Robling AG, Turner CH. 2002. Effects of biomechanical stress on bones in animals. Bone 30: 781-786.

Calvin WH. 1983. The throwing Madonna: essays on the brain. New York: McGraw Hill.

Carretero JM, Arsuaga JL and Lorenzo C. 1997. Clavicles, scapulae and humeri from the Sima de los Huesos site (Sierra de Atapuerca, Spain). J Hum Evol 33: 357-408.

Carter DR and Beaupré GS. 2001. Skeletal Function and Form: Mechanobiology of skeletal development, aging, and regeneration. Cambridge: Cambridge University Press.

Carter DR, Orr TE, Fyhrie DP and Schurman DJ. 1987. Influences of mechanical stress on prenatal and postnatal skeletal development. Clin Orthop and Rel Res 291: 237-250.

Churchill SE. 1994. Human upper body evolution in the Eurasian Later Pleistocene. PhD thesis, University of New Mexico.

Churchill SE. 1996. Particulate versus integrated evolution of the upper body in late Pleistocene humans: a test of two models. Am J Phys Anthropol 100: 559-583.

Churchill SE and Smith F. 2000. A modern human humerus from the Early Aurignacian of Vogelherdhöhle (Stetten, Germany). Am J Phys Anthropol 112: 251-273.

Cohn MJ and Bright PE. 2000. Development of vertebrate limbs: insights into pattern, evolution and dysmorphogenesis. In: Development, Growth and Evolution: Implications for the study of the hominid skeleton, Ohiggens, P and Cohn MJ, editors. London: Academic Press.

Connell BF. 1994. Enthesopathies of the rotator cuff and related structures. MSc dissertation, University of Bradford.

Contamine P. 1984. War in the Middle Ages. New York: Basil Blackwell.

Coughlan J and Holst M. 2000. Health status. In: Fiorato V, Boylston A and Knüsel C, editors. Blood red roses: the archaeology of a mass grave from the Battle of Towton AD 1461. Oxford: Oxbow. p 60–76.

Cowin SC. 2001. The false premise in Wolff's Law. In: Bone mechanics handbook, Cowin SC, editor. Boca Raton: CRC. p 30-1 – 30-15.

Crockett HC, Gross LB, Wilk KE, Schwartz ML, Reed J, O'Mara J, Reilly MT, Dugas JR, Meister K, Lyman S and Andrews JR. 2002. Osseous adaptation and range of motion at the glenohumeral joint in professional baseball pitchers. Am J Sp Med 30: 20-26.

Currey JD and Butler G. 1975. The mechanical properties of bone tissue in children. J Bone Joint Surg 57-A: 810-814.

Daegling DJ. 2002. Estimation of torsional rigidity in primate long bones. J Hum Evol 42: 229-239.

Dalldorf PG and Bryan WJ. 1994. Displaced Salter-Harris type I injury in a gymnast. Ortho Rev 23: 538-541.

Daniell C. 1998. Death and burial in Medieval England 1066 – 1550. London: Routledge.

Dias JJ, Mody BS, Finlay DBL and Richardson RA. 1993. Recurrent anterior glenohumeral joint dislocation and torsion of the humerus. Injury 24: 329-332.

Dobzhansky T. 1941. Genetics and the origin of the species. New York: Columbia University Press.

Dunlap K, Shands AR, Hollister LC, Gaul JS and Streit HA. 1953. A new method for determination of torsion of the femur. J Bone Joint Surg 35A: 289-311.

Dyer C. 1989. Standards of living in the Later Middle Ages. Cambridge: Cambridge University Press.

Dyer C. 2002. Making a living in the Middle Ages: the people of Britain 850 – 1520. New Haven: Yale University Press.

Eckhardt RB. 2000. Human Paleobiology. Cambridge: Cambridge University Press.

Edelson G. 1999. Variations in the retroversion of the humeral head. J Shoulder Elbow Surg 8: 142-145.

Edelson G. 2000. The development of humeral head retroversion. J Shoulder Elbow Surg 9: 316-318.

Endo B. 1971 . Some characteristics of the deltoid tuberosity of the humerus in the West Asian and European "classic" Neandertals. J Anthrop Soc Nippon 79: 249-258.

Evans FD and Krahl VE. 1945. The torsion of the humerus: a phylogenetic survey from fish to man. Am J Anat 193: 303-337.

Fay IHH. 2002. The experience of leprosy in the Middle Ages: the cemetery of SS. James and Mary Magdalene, Chichester. MSc dissertation, University of Bradford.

Field A. 2000. Discovering statistics using SPSS for Windows. London: Sage.

Fiorato V, Boylston A and Knüsel C. 2000. Blood red roses: the archaeology of a mass grave from the Battle of Towton AD 1461. Oxford: Oxbow.

Fleagle JG. 1999 Primate adaptation and evolution. San Diego: Academic Press.

Fresia AE, Ruff CB and Larsen CS. 1990. Temporal decline in bilateral asymmetry of the upper limb on the Georgia coast. Larsen CS, editor. The archaeology of Mission Santa Catalina De Gaule 2: biocultural interpretations of a population in transition. Anthropol Pap Am Mus Nat His 68: 121-135.

Frost HM. 1985. The "new bone": some anthropological potentials. Yearb Phys Anthropol 28: 211-226.

Frost HM. 1987a. Bone "mass" and the "mechanostat": a proposal. Anat Rec 219: 1-9.

Frost HM. 1987b. Secondary osteon populations: an algorithm for determining mean bone tissue age. Yearb Phys Anthroplo 30: 221-238.

Frost HM. 1999. An approach to estimating bone and joint loads and muscle strength in living subjects and skeletal remains. Am J Hum Bio 11: 437-455.

Frost HM. 2000. Muscle, bone and the Utah paradigm: a 1999 overview. Med Sci Sports Exerc 32: 911-917.

Frost HM. 2001. From Wolff's law to the Utah paradigm: insights about bone physiology and its clinical applications. Anat Rec 262: 398-419.

Gjerdrum T, Walker P and Andrushko V. 2003. Humeral retroversion: an activity pattern index in prehistoric Southern California [abstract]. Am J Phys Anthropol (suppl 34) p 100-101.

Golding B. 1995. Gilbert of Sempringham and the Gilbertine order c. 1130- c.1300. Oxford: Clarendon Press.

Graham R. 1901. St. Gilbert of Sempringham and the Gilbertines: a history of the only English monastic order. London: E. Stock.

Gravlee CC, Bernard HR and Leonard WR. 2003a. Heredity, environment and cranial form: A re-analysis of Boas's immigrant data. Am Anthropol. 105: 125-138.

Gravlee CC, Bernard HR and Leonard WR. 2003b. Boas's Changes in bodily form: the immigrant study, cranial plasticity, and Boas's physical anthropology. Am Anthropol 105: 326-332.

Gugenheim JJ, Stanley RF, Woods GW and Tullos HS. 1976. Little league survey: the Houston study. Am J Sports Med 4: 189-200.

Gregg JR and Torg E. 1988. Upper extremity injuries in adolescent tennis players. Clinics in Sports Med 7: 371-385.

Haapasalo H, Sievanen H, Kannus P, Heinonen A, Oja P and Vuori I. 1996. Dimensions and estimated mechanical characteristics of the humerus after long-term tennis loading. J Bone Min Res 11: 864-872.

Hardy R. 1992. Longbow: a social and military history. Sparkford: Patrick Stephens Ltd.

Herring S. 1994. Development of functional interactions between skeletal and muscular systems. In: Hall BK, editor. Bone - a treatise: differentiation and morphogenesis of bone. Boca Raton: CRC Press. p 165-191.

Herrington L. 1998. Glenohumeral joint: internal and external rotation range of motion in javelin throwers. Br J Sports Med 32: 226-228.

Holloway RL. 2002. Head to head with Boas: did he err on the plasticity of head form? PNAS 99: 14622-14623.

Hsieh YF, Robling AG, Ambrosius WT, Burr DB and Turner CH. 2001. Mechanical loading of diaphyseal bone in vivo: the strain threshold for an osteogenic response varies with location. J Bone Min Res 16: 2291-2297.

http://rsb.info.nih.gov/nih-image/. National Institutes of Health (NIH) Image Programme.

Hunt DR. 2000. The Robert J. Terry anatomical skeletal collection. www.nmnh.si.edu/anthro/Collmgt/terry.htm.

Hulse FS. 1981. Habits, habitats, and heredity: A brief history of studies in human plasticity. Am J Phys Anthropol 56: 495-501.

Jaworski ZFG and Uhtoff HK. 1986. Reversibility of nontraumatic disuse osteoporosis during its active phase. Bone 7: 431-439.

Jaworski ZFG, Liskova-Kiar M and Uhtoff HK. 1980. Effect of long-term immobilization on the pattern of bone loss in older dogs. J Bone Joint Surg 62-B: 104-110.

Jones HH, Priest JB, Hayes WC, Tichenor CC and Nagel DA. 1977. Humeral hypertrophy in response to exercise. J Bone Joint Surg 59-A: 204-208.

Kannus P, Haapsalo H, Sankelo M, Sievänen H, Pasanen M, Heinonen A, Oja P and Vuori I. 1995. Effect of starting age of physical activity on bone mass in the dominant arm of tennis and squash players. Ann Intern Med 123: 27-31.

Kate BR. 1968. The torsion of the humerus in Central India. J Indian Anthrop Soc 3: 17-30.

Keen, M. 1990. English society in the Later Middle Ages. London: Penguin Books.

Keen, M. 1999. Guns, gunpowder and permanent armies. In: Keen M, editor. Medieval warfare: a history. Oxford: Oxford University Press. p 273-292.

Kemp RL and Graves C.P. 1996. The church and Gilbertine priory of St Andrew, Fishergate. York Archaeological Trust for Excavation and Research, Council for British Archaeology, York (published by CBA for YAT).

Kibler WB, Chandler TJ, Livingston BP and Roetert EP. 1996. Shoulder range of motion in elite tennis players. Am J Sports Med 24: 279-285.

King JW, Brelsford HJ and Tullos HS. 1969. Analysis of the pitching arm of the professional baseball pitcher. Clin Ortho 67: 116-123.

Knüsel CJ. 2000a. Activity-related skeletal change. In: Fiorato V, Boylston A and Knüsel C, editors. Blood red roses: the archaeology of a mass grave from the Battle of Towton AD 1461. Oxford: Oxbow. p 103-118.

Knüsel CJ. 2000b. Bone adaptation and its relationship to physical activity in the past. In: Cox M and Mays S, editors. Human osteology in archaeology and forensic science. London: Greenwich Medical Media. p 381-402.

Knüsel CJ and Göggel S. 1993. A cripple from the medieval Hospital of Sts. James and Mary Magdalene, Chichester, England. Intl J Osteoarchaeol 3: 155-166.

Knüsel CJ and Boylston A. 2000. How has the Towton project contributed to our knowledge of medieval and later warfare? In: Fiorato V, Boylston A and Knüsel C, editors. Blood red roses: the archaeology of a mass grave from the Battle of Towton AD 1461. Oxford: Oxbow. p 169-188.

Knußmann R. 1988. Wesen Und Methoden Der Anthropologie Band 1 Wissenschafts Throrie, Geschicte, Morphologische Methoden. Stuttgart: Gustav Fischer, Verlag.

Krahl H, Michaelis U, Pieper HG, Quack G and Montag M. 1994. Stimulation of bone growth through sports: a radiologic investigation of the upper extremities in professional tennis players. Am J Sports Med 22: 751-757.

Krahl VE. 1947. The torsion of the humerus: its localization, cause and duration in man. Am J Anat 80: 275-319.

Krahl VE. 1948. The bicipital groove: a visible record of humeral torsion. Anat Rec 101: 319-331.

Krahl VE. 1976 . The phylogeny and ontogeny of humeral torsion. Am J Phys Anthrop 45: 595-600.

Krahl VE and Evans FG. 1945. Humeral torsion in man. Am J Phys Anthropol 3: 229-253.

Kronberg M, Broström LÄ and Söderlund V. 1990. Retroversion of the humeral head in the nomral shoulder and its relationship to the normal range of motion. Clin Orth and Rel Res 253: 113-117.

Lanyon LE. 1987. Functional strain in bone tissue as an objective, and controlling stimulus for adaptive bone remodelling. J Biomech 20: 1083-1093.

Lanyon LE. 1990. The relationship between functional loading and bone architecture. In: DeRousseau CJ, editor. Primate life history and evolution. New York: Wiley-Liss. p 269-284.

Lanyon LE. 1996. Using functional loading to influence bone mass and architecture: objectives, mechanisms, and relationship with estrogen of the mechanically adaptive process in bone. Bone 18: 37S-43S.

Lanyon LE and Rubin CT. 1984. Static vs dynamic loads as an influcence on bone remodeling. J Biomech 17: 897-905.

Lanyon LE, Goodship AE, Pye CJ and MacFie JH. 1982. Mechanically adaptive bone remodeling. J Biomech 15: 141-154.

Larson SG. 1988. Subscapularis function in gibbones and chimpanzees: implications for interpretation of humeral head torsion in hominoids. Am J Phys Anthropol 76: 449 – 462.

Larson SG. 1996. Estimating humeral torsion on incomplete fossil anthropoid humeri. J Hum Evol 31: 239-257.

Lasker GW. 1969. Human biological adaptability. Science 166: 1480-1486.

Lieberman DE. 1996. How and why humans grow thin skulls: experimental evidence for systemic cortical robusticity. Am J Phys Anthropol 101: 217-236.

Lieberman DE. 1997. Making behavioural and phylogenetic inferences from hominid fossils: considering the developmental influence of mechanical forces. Ann Rev Anthropol 26: 185-210.

Lieberman DE, Devlin MJ and Pearson OM. 2001. Articular area responses to mechanical loading: effects of exercise, age, and skeletal location. Am J Phys Anthropol 116: 266-277.

Lieberman D, Pearson O and Polk J. 2002. Growth versus repair responses to loading in the limb [abstract]. Am J Phys Anthropol (suppl 34) p 102.

Magilton J and Lee F. 1989. The leper hospital of St James and St Mary Magdalene, Chichester. In: Roberts CA, Lee F and Bratliff J, editors. Burial Archaeology Current Research, Methods and Developments. British Archaeoloigcal Reports 211: 249-265.

Mallet M. 1999. Mercenaries. In: Keen, M (editor) Medieval warfare. Oxford: Oxford University Press.

Martin CP. 1933. The cause of torsion of the humerus and of the notch on the anterior edge of the glenoid cavity of the scapula. J Anat 67: 572-582.

Martin RB, Burr DB, and Sharkey NA. 1998. Skeletal Tissue Mechanics. Springer: New York.

Mays S, Steele J and Ford M. 1999. Directional asymmetry in the human clavicle. Intl J Osteoarchaeol 9: 18-28.

Miles AEW. 1999. Observations on the undersurface of the skeletalised human acromion in two populations. Intl J Osteoarchaeol 9: 131-145.

Murdock GP and Provost C. 1973. Factors in the division of labor by sex: a cross-cultural analysis. Ethnology 12: 203-225.

Nevasier RJ and Nevasier TJ. 1990. Observations on impingement. Clin Ortho and Rel Res. 254: 60-63.

Nicholson GP and Lintner SA. 1997. Tissues and their structures. In: Norris TR, editor. Orthopaedic knowledge update: shoulder and elbow. Rosemont: American Academy of Orthopaedic Surgeons. p 3-10.

Nishida S, Endo N, Yamagiwa H, Tanizawa T and Tkahashi HE. 1999. Number of osteoprogenitor cells in human bone marrow markedly decreases after skeletal maturation. J Bone Min Res 17: 171-177.

Novak SA. 2000. Case studies. In: Fiorato V, Boylston A and Knüsel C, editors. Blood red roses: the archaeology of a mass grave from the Battle of Towton AD 1461. Oxford: Oxbow. p 240–268.

Ohman JC, Krochta TJ, Lovejoy CO, Mensforth RP and Latimer B. 1997. Cortical bone distribution in the femoral neck of hominoids: implications for the locomotion of *Australopithecus afarensis*. Am J Phys Anthropol 104:117-131.

Osbahr DC, Cannon DL and Speer KP. 2002. Retroversion of the humerus in the throwing shoulder of college baseball pitchers. Am J Sp Med 30: 347-353.

Öztuna V, Öztürk H, Eskandari MM and Kuyurtar F. 2002. Measurement of the humeral head retroversion angle: a new radiographic method. Arch Orthop Trauma Surg 122: 406-409.

Paley KJ, Jobe FW, Pink MM, Kvitne RS and ElAttrache NS. 2000. Arthroscopic findings the the overhand throwing athlete: evidence for posterior internal impingement of the rotator cuff. Arthroscopy 16: 35-40.

Parsons PA. 1990. Fluctuating asymmetry: an epigenetic measure of stress. Biol Rev 65: 131-145.

Pavlov H. 1995. Physical injury: sports related abnormalities. In: Resnick D, editor. Diagnosis of bone and joint Disorders. Philadelphia: W.B. Saunders. p 3229-3263.

Pearl ML and Volk AG. 1995. Retroversion of the proximal humerus in relationship to prosthetic replacement arthroplasty. J Shoulder Elbow Surg 4: 286-289.

Pearson OM. 2000. Activity, climate and postcranial robusticity: implications for modern human origins and scenarios of adaptive change. Curr Anthropol 41: 569-607.

Pearson O and Lieberman D. 2002. Effects of age and exercise on long bone modelling and remodeling [abstract]. Am J Phys Anthropol (suppl 34) p 123.

Pieper H-G. 1985. Shoulder dislocation in skiing: choice of surgical method depending on the degree of humeral retroversion. Int J Sports Med 6: 155-160.

Pieper H-G. 1998. Humeral torsion in the throwing arm of handball players. Am J Sports Med 26: 247-253.

Qu X. 1992. Morphological effects of mechanical forces on the human humerus. Br J Sp Med 26:51-53.

Reagan KM, Meister K, Horodyski MB, Werner DW, Carruthers C and Wilk K. 2002. Humeral retroversion and its relationship to glenohumeral rotation in the shoulder of college baseball players. Am J Sp Med 30: 354-360.

Resnick D. 1995. Internal derangements of joints, In: Resnick D, editor. Diagnosis of bone and joint disorders. Philadelphia: W.B. Saunders. p 2899-3228.

Resnick D, Goergen TG and Niwayama G. 1995. Physical injury: concepts and terminology. In: Resnick D, editor. Diagnosis of bone and joint disorders. Philadelphia: W.B. Saunders. p 2561-2692.

Rhodes J. 2002. A humerus tale: humeral torsion and activity-related change in the upper limb [abstract]. Am J Phys Anthropol (suppl 34) p 130.

Richardson T. 2000. Armour. In: Fiorato V, Boylston A and Knüsel C, editors. Blood red roses: the archaeology of a mass grave from the Battle of Towton AD 1461. Oxford: Oxbow. p 137-147.

Rimer G. 2000. Weapons. In: Fiorato V, Boylston A and Knüsel C, editors. Blood red roses: the archaeology of a mass grave from the Battle of Towton AD 1461. Oxford: Oxbow. p 119-129.

Roberts DF. 1995. The pervasiveness of plasticity. In: Mascie-Taylor CGN and Bogin B., editors. Human variability and plasticity. Cambridge: Cambridge University Press. p 1-17.

Robling AG, Hinant FM, Buff DB and Turner CH. 2002. Improved bone structure and strength after long-term mechanical loading is greatest if loading is separated into short bouts. J Bone Miner Res 17: 1545-1554.

Rubin CT and Lanyon LE. 1984. Regulation of bone formation by applied dynamic loads. J Bone Joint Surg 66-A: 397-402.

Ruff CB. 1992. Biomechanical analyses of archaeological human skeletal samples. In: Saunders SR and Katzenberg AK, editors. Skeletal biology of past peoples: research methods. New York: Wiley-Liss. p 37-58.

Ruff CB. 2000a. Biomechanical analyses of archaeological human skeletons. In: Katzenberg MA and Saunders SR, editors. Biological anthropology of the human skeleton. New York: Wiley-Liss. p 71-102.

Ruff CB. 2000b. Body mass prediction from skeletal frame size in elite athletes. Am J Phys Anthropol 113: 507-517.

Ruff CB and Larsen CS. 1990. Postcranial biomechanical adaptations to subsistence strategy changes on the Georgia coast. Larsen CS, editor. The archaeology of Mission Santa Catalina De Gaule 2: biocultural interpretations of a population in transition. Anthropol Pap Am Mus Nat His 68:121-135.

Ruff CB and Larsen CS. 2001. Reconstructing behaviour in Spanish Florida: the biomechanical evidence. In: Larsen CS, editor. Bioarchaeology of Spanish Florida: the impact of colonialism. Gainesville: University Press of Florida. p. 113-145.

Ruff CB, Trinkaus E, Walker A and Larsen CS. 1993. Postcranial robusticity in *Homo*: I: temporal trends and mechanical interpretations. Am J Phys Anthropol 91: 21-53.

Ruff CB, Walker A and Trinkaus E. 1994. Postcranial robusticity in *Homo*. III: ontogeny. Am J Phys Anthropol 93: 35-54.

Schell LM. 1995. Human biological adaptability with special emphasis on plasticity: history, development and problems for future research. In: Mascie-Taylor CGN and Bogin B, editors. Human variability and plasticity. Cambridge: Cambridge University Press. p 213-237.

Schmitt D, Churchill SE and Hylander WL. 2003. Experimental evidence concerning spear use in Neandertals and early modern humans. J Archaeol Sci 30: 103-114.

Söderlund V, Kronberg M and Broström LÄ. 1989. Radiologic assessment of humeral head retroversion: description of a new method. Acta Radiol 30: 501-505.

Sparks CS and Jantz RL. 2002. A reassessment of human cranial plasticity: Boas revisited. PNAS 99: 14636-14639.

Steele J and Mays S. 1995. Handedness and directional asymmetry in the long bones of the human upper limb. Intl J Osteoarchaeol 5: 39-49.

Stock J and Pfeiffer S. 2001. Linking structural variability in long bone diaphyses to habitual behaviours: foragers from the Southern Africa Later Stone Age and the Andaman Islands. Am J Phys Anthropol 115:337-348.

Stirland AJ. 1992. Asymmetry and activity-related change in selected bones of the male skeleton. PhD thesis, University College London.

Stirland AJ. 1993. Asymmetry and activity-related change in the male humerus. Intl J Osteoarchaeol 3: 105-113.

Stirland AJ. 2000. Raising the dead: the skeleton crew of Henry VIII's great ship, the Mary Rose. Chichester: John Wiley and Sons.

Stroud G and Kemp RL 1993. Cemeteries of the church and priory of St Andrew, Fishergate. York Archaeological Trust for Excavation and Research, Council for British Archaeology, York (published by CBA for YAT).

Stout SD and Lueck R. 1995. Bone remodeling rates and skeletal maturation in three archaeological skeletal populations. Am J Phys Anthropol 98: 161-171.

Sutherland T. 2000. Recording the grave. In: Fiorato V, Boylston A and Knüsel C, editors. Blood red roses: the archaeology of a mass grave from the Battle of Towton AD 1461. Oxford: Oxbow. p 36-44.

Sydes B. 1984. The excavation of St. Wilfrid's church, Hickleton: an interim report, September 1984. Unpublished report. Sheffield: South Yorkshire County Council Archaeology Service.

Trinkaus E. 1983. Neandertal postcrania and the adaptive shift to modern humans. In: Trinkaus E, editor. The Mousterian legacy. British Archaeology Reports Intl. 164. p 165-200.

Trinkaus E. 1997. Appendicular robusticity and the paleobiology of modern human emergence. PNAS 94: 13367-13373.

Trinkaus E, Churchill SE, Villemeur I, Riley KG, Heller JA and Ruff CB. 1991. Robusticity *versus* shape: the functional interpretation of Neandertal appendicular morphology. J Anthropol Soc Nippon 99: 257-278.

Trinkaus E, Churchill SE and Ruff CB. 1994. Postcranial robusticity in *Homo*. II: humeral bilateral asymmetry and bone plasticity. Am J Phys Anthropol 93: 1-34.

Trinkaus E and Churchill SE. 1999. Diaphyseal cross-sectional geometry of Near Eastern Middle Palaeolithic humans: the humerus. J Archaeol Sci 26: 173-184.

Uhtoff HK and Jaworski ZFG. 1978. Bone loss in response to long-term immobilization. J Bone Joint Surg 60-B: 420-429.

Vandermeersch B and Trinkaus E. 1995. The postcranial remains of the Régourdou 1 Neandertal the shoulder and arm remains. J Hum Evol 28: 439-476.

Waller J. 2000a. Archery. In: Fiorato V, Boylston A and Knüsel C, editors. Blood red roses: the archaeology of a mass grave from the Battle of Towton AD 1461. Oxford: Oxbow. p 130-137.

Waller J. 2000b. Combat techniques. In: Fiorato V, Boylston A and Knüsel C, editors. Blood red roses: the archaeology of a mass grave from the Battle of Towton AD 1461. Oxford: Oxbow. p 148-154.

Waugh SL. 1991. England in the reign of Edward III. Cambridge: Cambridge University Press.

Woo SL-Y, Kuei SC, Amiel D., Gomex MA, Hayes WC, White FC and Akeson WH. 1981. The effect of prolonged physical training on the properties of long bone: a study of Wolff's law. J Bone Joint Surg 63-A: 780-787.

Wrathmell S. 1997. Wharram Percy: Yorkshire. London: English Heritage.

Zuckerman JD and Matsen FA. 1989. Biomechanics of the shoulder. In: Nordin M and Frankel VH, editors. Basic biomechanics of the musculoskeletal system, 2nd edition. Philadelphia: Lippincott, Williams and Wilkins.